Supporting Information

Catalytic Activation of Glycosyl Phosphates for Stereoselective Coupling Reactions

Samuel M. Levi, Qiuhan Li, Andreas R. Rötheli, and Eric N. Jacobsen*

Department of Chemistry and Chemical Biology, Harvard University,
12 Oxford Street, Cambridge, Massachusetts 02138, United States

jacobsen@chemistry.harvard.edu

Table of Contents for the Supporting Information

List of Figures

List of Schemes

List of Tables

1. Procedures, Materials and Instrumentation

1.1 General experimental procedures

Unless otherwise described, all reactions were performed in standard, oven- or flame-dried glassware equipped with PTFE-coated magnetic stir bars and fit with rubber septa under an inert atmosphere of nitrogen. Stainless steel syringes or cannulae were used to transfer air- and moisture-sensitive liquids. Reported concentrations refer to solution volumes at room temperature. Evaporation and concentration *in vacuo* were performed using house vacuum (~ 40 mm Hg). Column chromatography (using a Biotage® Isolera Four™) was performed using reusable cartridges filled with ZEOprep® 60 (40–63 micron) silica gel from American Scientific. Thin layer chromatography (TLC) using pre-coated glass plates covered with 0.20 mm silica gel with fluorescent indicator visualized upon UV irradiation (λ = 254 nm) or anisaldehyde stain, was used for reaction monitoring and product detection.

1.2 Materials

Reagents were purchased in reagent grade from commercial suppliers and used without further purification, unless otherwise described. Anhydrous solvents (*tert*-butyl methyl ether, dichloromethane, *N,N*-dimethylformamide, ethyl ether, methanol, tetrahydrofuran, toluene) were prepared by passing the solvent through an activated alumina column.[1] Triethylamine, *N,N*-diisopropylethylamine, and pyridine were distilled from CaH_2 at atmospheric pressure.

Compounds **Schreiner's Thiourea**, **3a**, **3b**, **3c**, **3d**, **3h**, **3i**, **3l**, **3n**, **3j** and **S7** were commercially available.

Compounds **1**, ***ent*-1**,[2] **2a**,[3] **2b**,[4] **2c**,[5] **2d**, **2e**,[6] **2l**,[6] **3e**,[7] **3f**,[8] **3k**,[9] **3m**,[10] **4j**,[11] **4k**,[12] **4l**,[13] **4r**,[14] **S10**,[15] **S11**,[16] **S12a**,[17] and **S12c**,[18] have been reported previously.

1.3 Instrumentation

Proton nuclear magnetic resonance (^{1}H NMR) spectra and proton-decoupled carbon nuclear magnetic resonance (^{13}C NMR) spectra were recorded at 25 °C (unless stated otherwise) on Varian-Mercury-400 (400 MHz), Varian Unity/Inova 500 (500 MHz), or Varian Unity/Inova 600 (600 MHz) spectrometers at the Harvard University nuclear magnetic resonance facility. Chemical shifts for protons are reported in parts per million downfield from tetramethylsilane and are referenced to residual protium in the NMR solvent according to values reported in the literature.[24] Chemical shifts for carbon are reported in parts per million downfield from tetramethylsilane and are referenced to the carbon resonances of the solvent. The solvent peak was referenced to 7.26 ppm for ^{1}H and 77.16 ppm for ^{13}C for $CDCl_3$. Data are represented as follows: chemical shift, integration, multiplicity (br = broad, s = singlet, d = doublet, t = triplet, q = quartet, qn = quintet, sp = septet, m = multiplet), coupling constants in Hertz (Hz).

Optical rotations were measured using a 1 mL cell with a 5 cm path length on a Jasco P-2000 digital polarimeter.

Infrared spectra were recorded using a Bruker Tensor 27 FT-IR spectrometer. Data are represented as follows: frequency of absorption (cm^{-1}), intensity of absorption (s = strong, m = medium, w = weak, br = broad). In-situ IR kinetic experiments were carried out using a Mettler Toledo ReactIR™ iC 10 ATR FTIR spectrometer and a 9 mm AgX probe with a SiComp (silicon-based) window.

Low-resolution mass spectrometry was measured using an Agilent 6120 Quadrupole LC/MS, samples were injected in 0.1% formic acid in methanol and bypassed the LC column en route to the MS detector. High-resolution mass spectrometry was measured using a Bruker micrOTOF-QII™ ESI-Qq-TOF mass spectrometer calibrated using an aqueous sodium formate solution (prepared via adding 1 mL of 1 M aq. NaOH in 100 mL of 1% aq. formic acid). Additional high-resolution mass spectrometry was measured at the Small Molecule Mass Spectrometry Facility at Harvard University within the Faculty of Arts and Sciences using an Agilent 6220 Electrospray Time-of-Flight LC/MS.

Chiral stationary phase high performance liquid chromatography (HPLC) analysis was performed using an Agilent 1200 quaternary HPLC system with a commercially available AD-H chiral column.

X-ray crystallographic data was collected at the Harvard X-ray Laboratory. The structural refinement details for the X-ray crystallographic data are described in the individual CIFs. X-ray crystallographic data for catalyst **1** and galactosyl phosphate (**2a**) have been deposited at the Cambridge Crystallographic Data Centre (CCDC), 12 Union Road, Cambridge CB21EZ, UK; fax: (+44)122-333-6033. These data can be obtained free of charge via the Internet at www.ccdc.cam.ac.uk/data_request/cif using the CCDC numbers given above.

1.4 Software

All curve fitting presented in this paper was carried out using MatLab.[19] NMR spectra were processed with iNMR.[20] X-ray crystallographic and computed structures were rendered with CYLview[21] and MacPyMOL.[22]

1.5 Abbreviations

aq = aqueous, atm = atmosphere, 9-BBN = 9-borabicyclo[3.3.1]nonane, Boc = *tert*-butyl carbamate, CSP = chiral stationary phase, DFB = 1,2 difluorobenzene, DIPEA = diisopropylethylamine, DMAP = 4-dimethylaminopyridine, DMPU = 1,3-dimethyl-3,4,5,6-tetrahydro-2(1*H*)-pyrimidinone, EDC•HCl = 1-3(dimethylamino)propyl)-3-ethyl-carbodiimide hydrochloride, ee = enantiomeric excess, ESI = electrospray ionization, HBTU = *O*-benzotriazol-1-yl-*N*,*N*,*N*',*N*'-tetramethyluronium hexafluorophosphate, HPLC = high performance liquid chromatography, HR = high-resolution, LC = liquid chromatography, LDA = lithium diisopropylamide, LR = low-resolution, MS = mass spectrometry, NA = not applicable, ND = not determined, NOESY = nuclear Overhauser effect spectroscopy, PTFE = polytetrafluoroethylene, rt = room temperature, TBME = *tert*-butyl methyl ether, TCDI = 1,1'-thiocarbonyldiimidizole, Tf = trifluoromethanesulfonate, TFA = trifluoroacetic acid, THF = tetrahydrofuran, TMAC = tetramethylammonium chloride, TLC = thin-layer chromatography, TOF = time-of-flight, v/v = volume/volume, w/v = weight/volume, XRD = X-ray diffraction.

2. Synthetic Procedures and Characterization Data

2.1 General Procedure for Glycosylation Reactions

To a flame-dry 5 mL round bottom flask with a stir bar was charged 0.250 mmol **donor**, 250 mg flame-dry 4 Å molecular sieves, 0.0125 mmol **catalyst**, and 0.500 mmol **acceptor**. 2.50 mL diisopropyl ether was added to the reaction mixture open to air and the flask was closed with a plastic cap and parafilm was used to seal the cap tightly. The mixture was then heated with efficient stirring at 40 ˚C in an oil bath for 19 hours over which time the mixture thickened. After 19 hours, the mixture is cooled to room temperature and 100 μL aliquot is diluted with diethyl ether and filtered to remove the molecular sieves. This solution is concentrated and ^{1}H NMR analysis on the crude mixture is used to determine the anomeric selectivity. The mixture was then chromatographed directly with 50 g SiO_2 using an ether/hexanes gradient on a Biotage MPLC.

Note: Donor is added as a solution in diisopropyl ether when stated. Phosphate donors have been found to be stable and remain pure for >6 months as solutions in ethereal solvents.

2.2 Synthetic Procedures and Characterization Data for Previously Unreported Compounds

Preparation of 4a

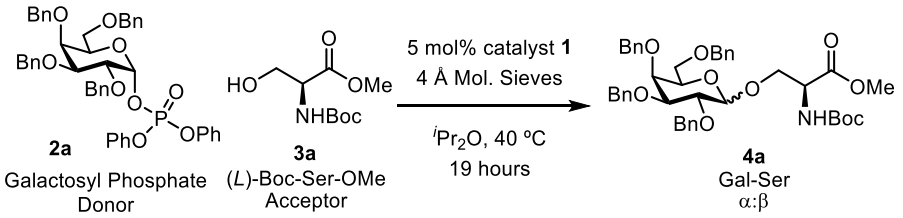

To a flame-dry 5 mL round bottom flask with a stir bar was charged 193 mg (0.250 mmol) galactosyl phosphate donor (**2a**), 250 mg flame-dry 4 Å molecular sieves, 14 mg (0.0125 mmol) catalyst **1**, and 110 mg (0.500 mmol) *L*-Boc-Ser-OMe (**3a**). 2.50 mL diisopropyl ether was added to the reaction mixture open to air and the flask was closed with a plastic cap and parafilm was used to seal the cap tightly. The mixture was then heated with efficient stirring at 40 ˚C in an oil bath for 19 hours over which time the mixture thickened. After 19 hours, the mixture is cooled to room temperature and 100 µL aliquot is diluted with diethyl ether and filtered to remove the molecular sieves. This solution is concentrated and ^{1}H NMR analysis on the crude mixture is used to determine the anomeric selectivity (97:3 β:α). The mixture was then chromatographed directly with 50 g SiO_2 using an ether/hexanes gradient on a Biotage MPLC to yield the product (**4a**) in quantitative yield (180 mg pure-β and 11 mg as an α:β mixture).

^{1}H-NMR (600 MHz; $CDCl_3$): δ 7.41-7.26 (m, 20H), 5.48 (d, *J* = 8.2 Hz, 1H), 4.93 (d, *J* = 11.6 Hz, 1H), 4.85 (d, *J* = 10.8 Hz, 1H), 4.72 (m, 3H), 4.61 (d, *J* = 11.6 Hz, 1H), 4.46-4.40 (m, 3H), 4.32 (d, *J* = 7.8 Hz, 1H), 4.30 (dd, *J* = 10.6, 2.8 Hz, 1H), 3.89 (s, 1H), 3.80-3.76 (m, 2H), 3.72 (s, 3H), 3.57 (m, 2H), 3.52-3.50 (m, 2H), 1.42 (s, 9H).

^{13}C-NMR (126 MHz, $CDCl_3$): δ 170.79, 155.57, 138.56, 138.50, 138.40, 137.90, 128.50, 128.44, 128.41, 128.38, 128.33, 128.28, 127.93, 127.88, 127.68, 127.59, 104.53, 82.19, 79.93, 79.11, 77.41, 77.16, 76.90, 75.39, 74.69, 73.60, 73.45, 73.04, 70.14, 68.62, 54.13, 52.56, 28.38.

HRMS-ESI (m/z): calculated for $C_{43}H_{51}NO_{10}$ [M+H]+: 742.3586, found: 742.3572 .

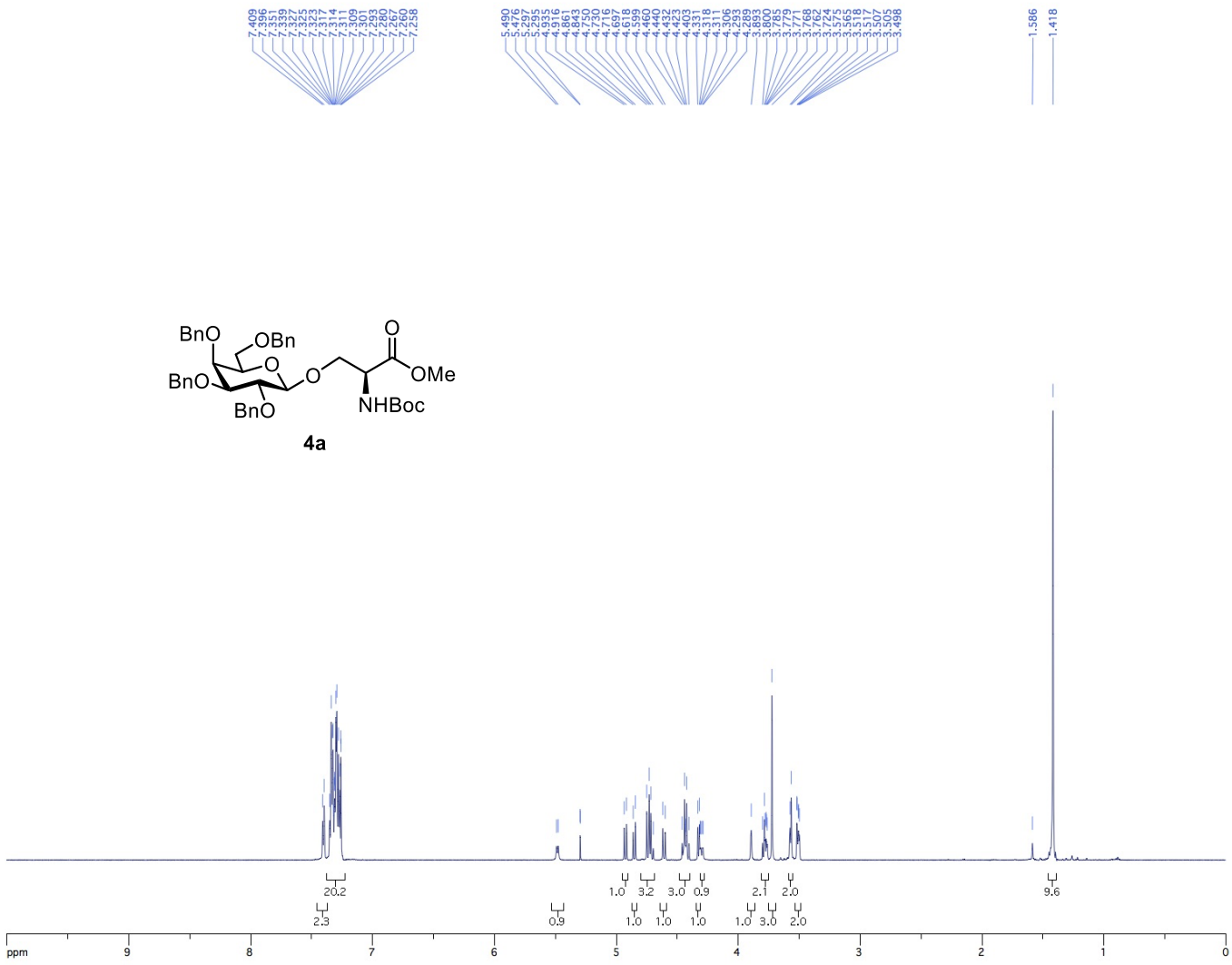

^{1}H NMR (600 MHz) spectrum of **4a** in $CDCl_3$.

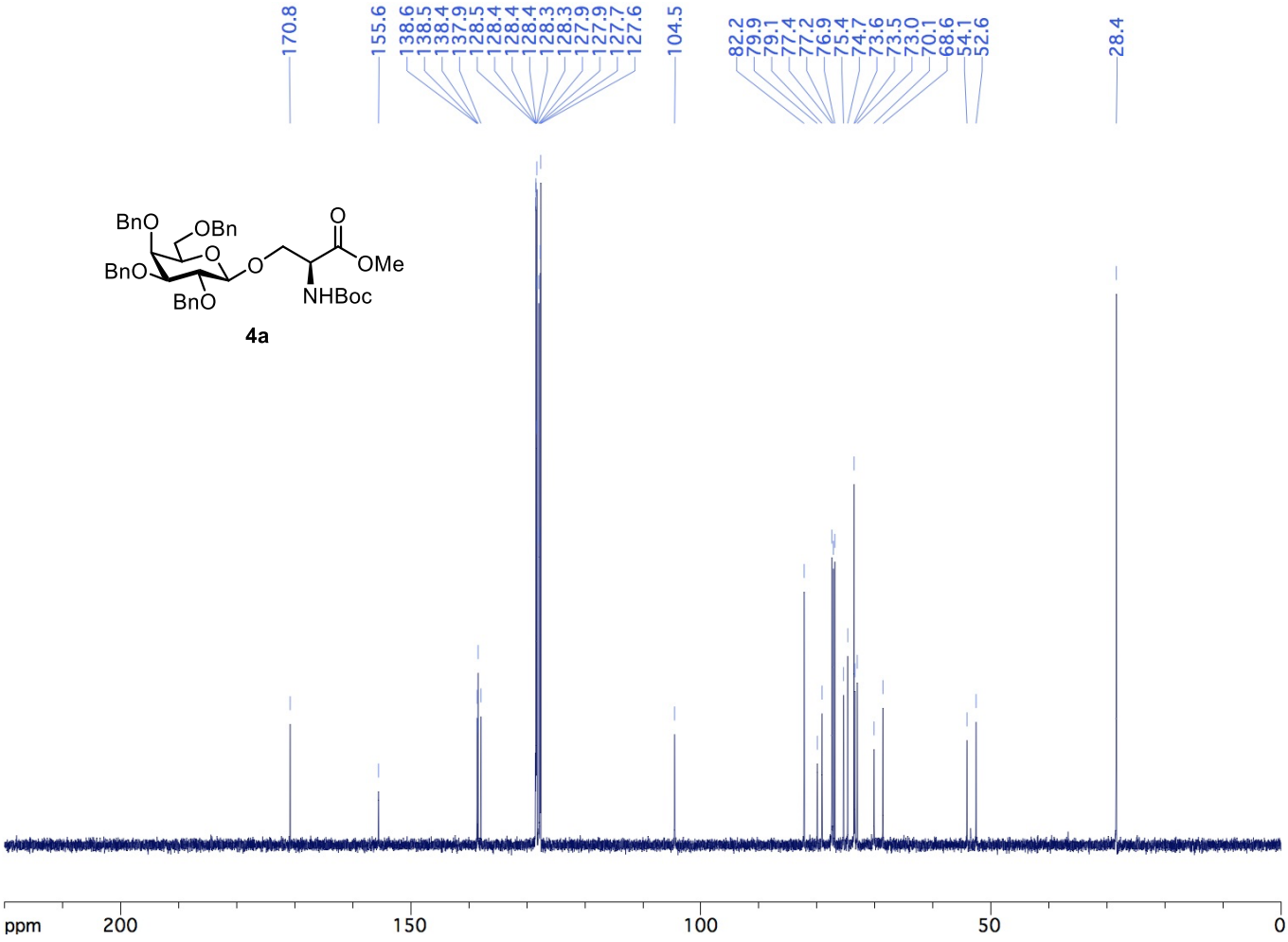

^{13}C NMR (126 MHz) spectrum of **4a** in $CDCl_3$.

Preparation of 4b

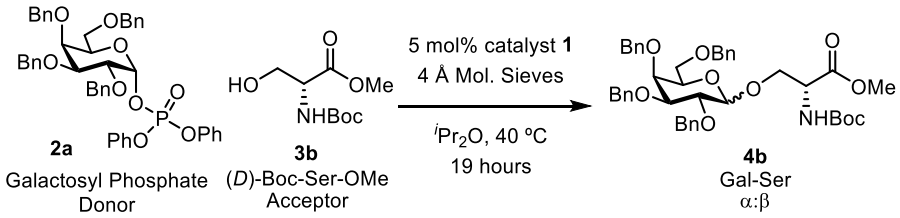

To a flame-dry 5 mL round bottom flask with a stir bar was charged 193 mg (0.250 mmol) galactosyl phosphate donor (**2a**), 250 mg flame-dry 4 Å molecular sieves, 14 mg (0.0125 mmol) catalyst **1**, and 110 mg (0.50 mmol) *D*-Boc-Ser-OMe (**3b**). 2.5 mL diisopropyl ether was added to the reaction mixture open to air and the flask was closed with a plastic cap and parafilm was used to seal the cap tightly. The mixture was then heated with efficient stirring at 40 ˚C in an oil bath for 19 hours over which time the mixture thickened. After 19 hours, the mixture is cooled to room temperature and 100 µL aliquot is diluted with diethyl ether and filtered to remove the molecular sieves. This solution is concentrated and ^{1}H NMR analysis on the crude mixture is used to determine the anomeric selectivity (96:4 β:α). The mixture was then chromatographed directly with 50 g SiO_2 using an ether/hexanes gradient on a Biotage MPLC to yield the product (**4b**) in 91% yield (169 mg, 0.228 mmol) as a mixture of anomers (163 mg pure β– and 6 mg purified α-product).

^{1}H-NMR (500 MHz, $CDCl_3$): δ 7.35-7.25 (m, *J* = 7.5 Hz, 20H), 5.60 (d, *J* = 8.9 Hz, 1H), 4.91 (d, *J* = 11.6 Hz, 1H), 4.78-4.60 (m, *J* = 12.7 Hz, 5H), 4.46-4.38 (m, 3H), 4.30 (d, *J* = 7.6 Hz, 1H), 4.08-4.03 (m, 2H), 3.87 (s, 1H), 3.78-3.75 (t, *J* = 9.6 Hz, 1H), 3.60-3.45 (m, 7H), 1.44 (s, 9H).

^{13}C-NMR (126 MHz, $CDCl_3$): δ 171.03, 155.61, 138.58, 138.47, 138.39, 137.85, 128.48, 128.41, 128.29, 128.11, 127.91, 127.87, 127.72, 127.65, 127.58, 104.19, 82.10, 79.89, 79.00, 77.41, 77.15, 76.90, 75.02, 74.66, 73.65, 73.60, 73.37, 73.14, 70.38, 68.67, 53.85, 52.46, 28.40.

HRMS-ESI (m/z): calculated for $C_{43}H_{51}NO_{10}$ [M+H]+: 742.3586, found: 742.3579 .

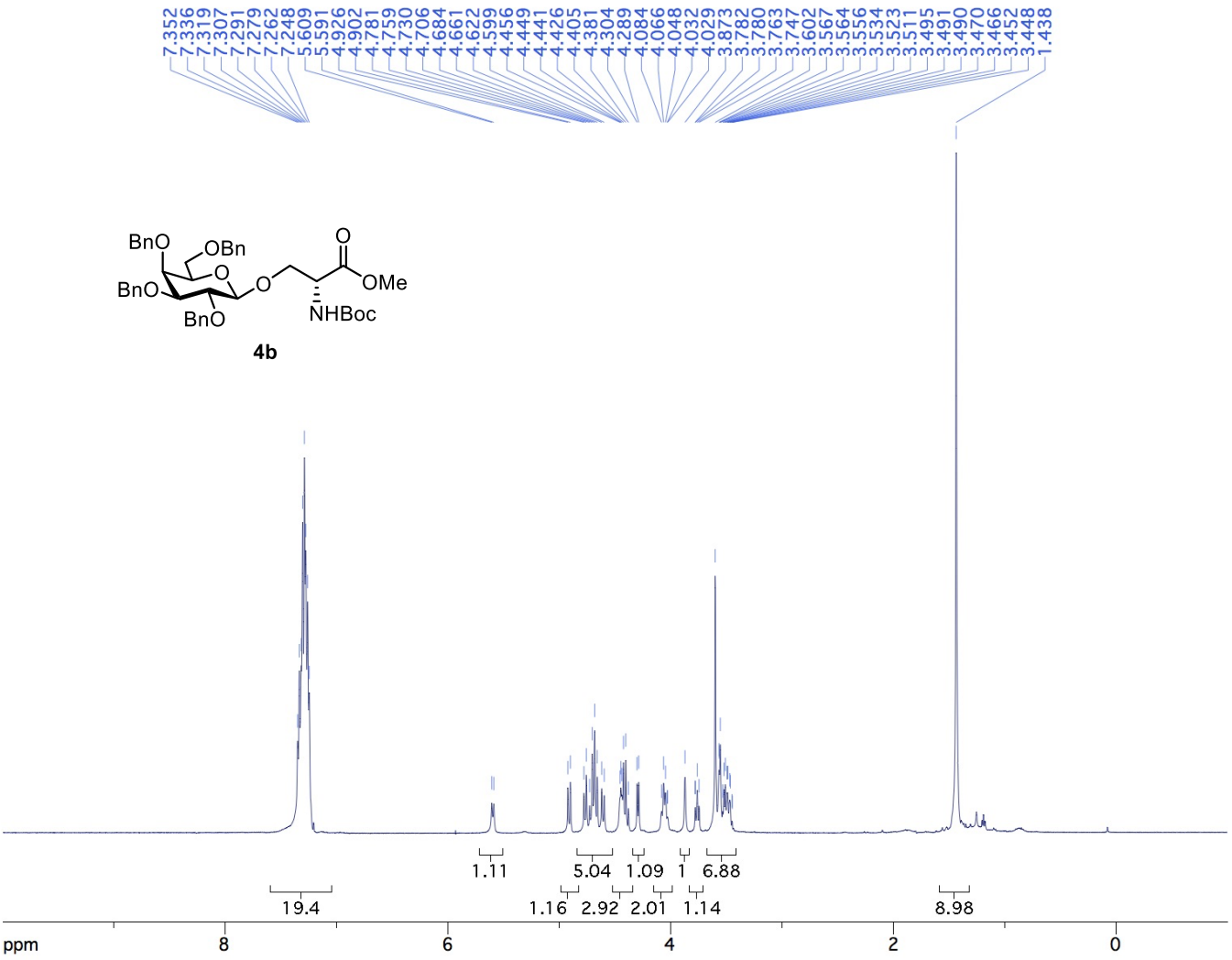

^{1}H NMR (500 MHz) spectrum of **4b** in $CDCl_3$.

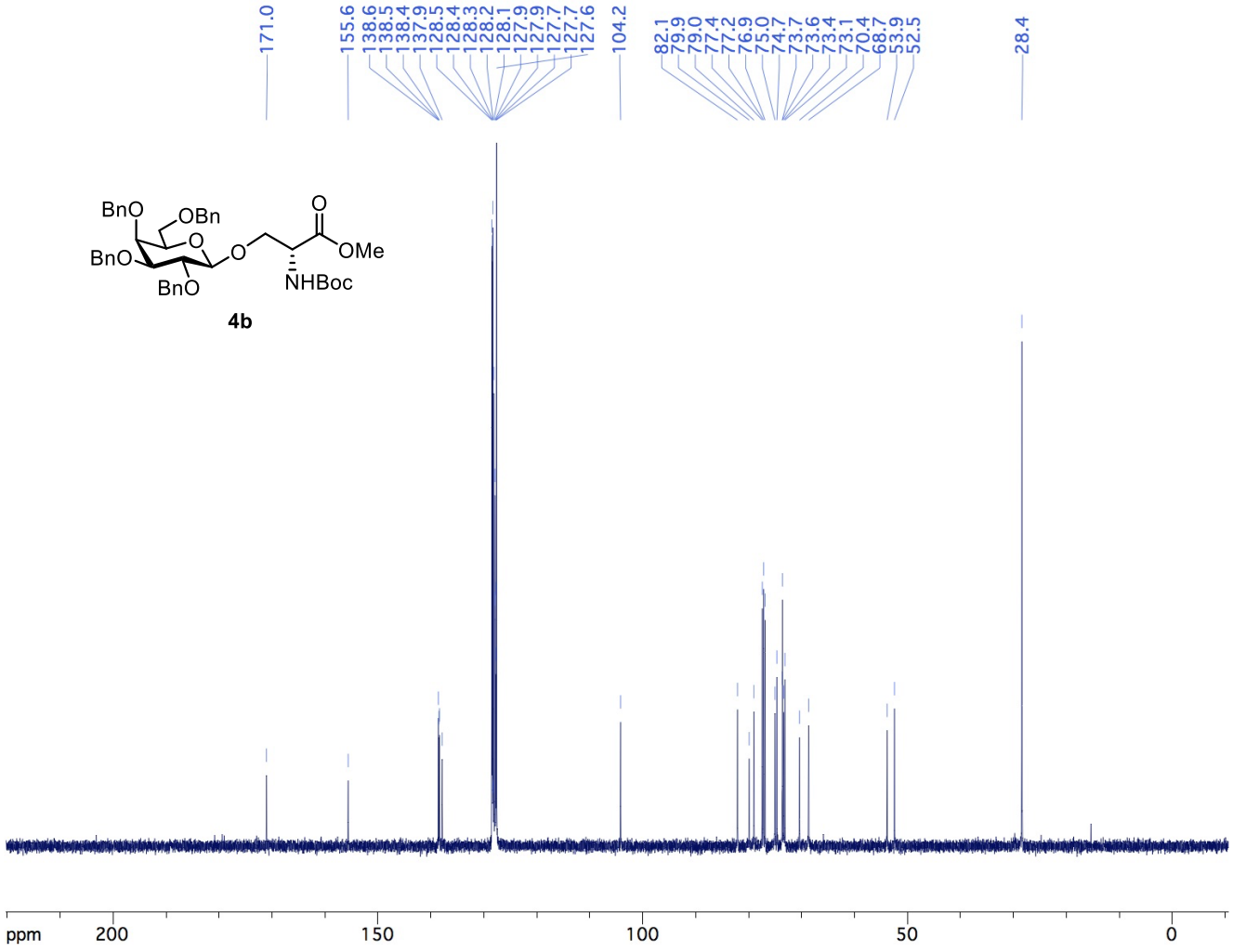

^{13}C NMR (126 MHz) spectrum of **4b** in $CDCl_3$.

Preparation of 4c

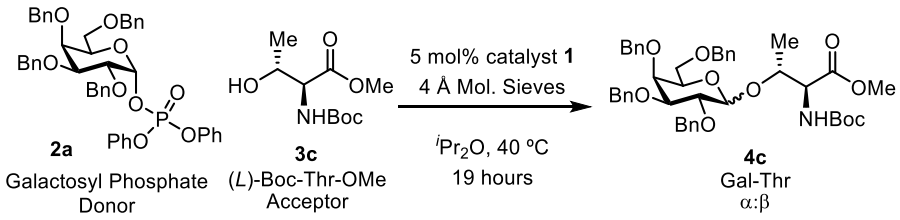

To a flame-dry 5 mL round bottom flask with a stir bar was charged 193 mg (2.50 mmol) galactosyl phosphate donor (**2a**), 250 mg flame-dry 4 Å molecular sieves, 14 mg (0.0125 mmol) catalyst **1**, and 110 mg (0.50 mmol) *L*-Boc-Thr-OMe (**3c**). 2.5 mL diisopropyl ether was added to the reaction mixture open to air and the flask was closed with a plastic cap and parafilm was used to seal the cap tightly. The mixture was then heated with efficient stirring at 40 ˚C in an oil bath for 19 hours over which time the mixture thickened. After 19 hours, the mixture is cooled to room temperature and 100 µL aliquot is diluted with diethyl ether and filtered to remove the molecular sieves. This solution is concentrated and ^{1}H NMR analysis on the crude mixture is used to

determine the anomeric selectivity (96:4 β:α). The mixture was then chromatographed directly with 50 g SiO_2 using an ether/hexanes gradient on a Biotage MPLC to yield the product (**4c**) in 92% yield (173 mg, 0.229 mmol) as a mixture of anomers.

^{1}H-NMR (600 MHz, $CDCl_3$): δ 7.36-7.26 (m, 20H), 5.55 (d, *J* = 8.2 Hz, 1H), 5.29 (d, *J* = 1.1 Hz,), 4.95 (d, *J* = 11.6 Hz, 1H), 4.84 (d, *J* = 10.8 Hz, 1H), 4.76-4.69 (m, 3H), 4.60 (d, *J* = 11.6 Hz, 1H), 4.42 (q, *J* = 9.8 Hz, 2H), 4.35-4.32 (m, 2H), 4.22 (dd, *J* = 8.2, 3.4 Hz, 1H), 3.90 (d, *J* = 2.2 Hz, 1H), 3.74 (dd, *J* = 9.7, 7.8 Hz, 1H), 3.65 (s, 3H), 3.61 (t, *J* = 8.4 Hz, 1H), 3.54 (dd, *J* = 8.9, 5.2 Hz, 1H), 3.50-3.46 (m, 2H), 1.45 (s, 9H), 1.26 (d, *J* = 6.4 Hz, 3H).

^{13}C-NMR (126 MHz, $CDCl_3$): δ 171.24, 156.21, 138.74, 138.57, 138.46, 137.86, 128.47, 128.39, 128.35, 128.23, 128.15, 128.09, 127.88, 127.61, 127.53, 102.23, 82.20, 79.72, 79.15, 77.35, 77.10, 76.84, 75.35, 75.27, 74.70, 73.66, 73.56, 73.25, 73.03, 68.35, 58.52, 28.37, 17.74.

HRMS-ESI (m/z): calculated for $C_{44}H_{53}NO_{10}$ [M+H]+: 756.3742, found: 742.3741

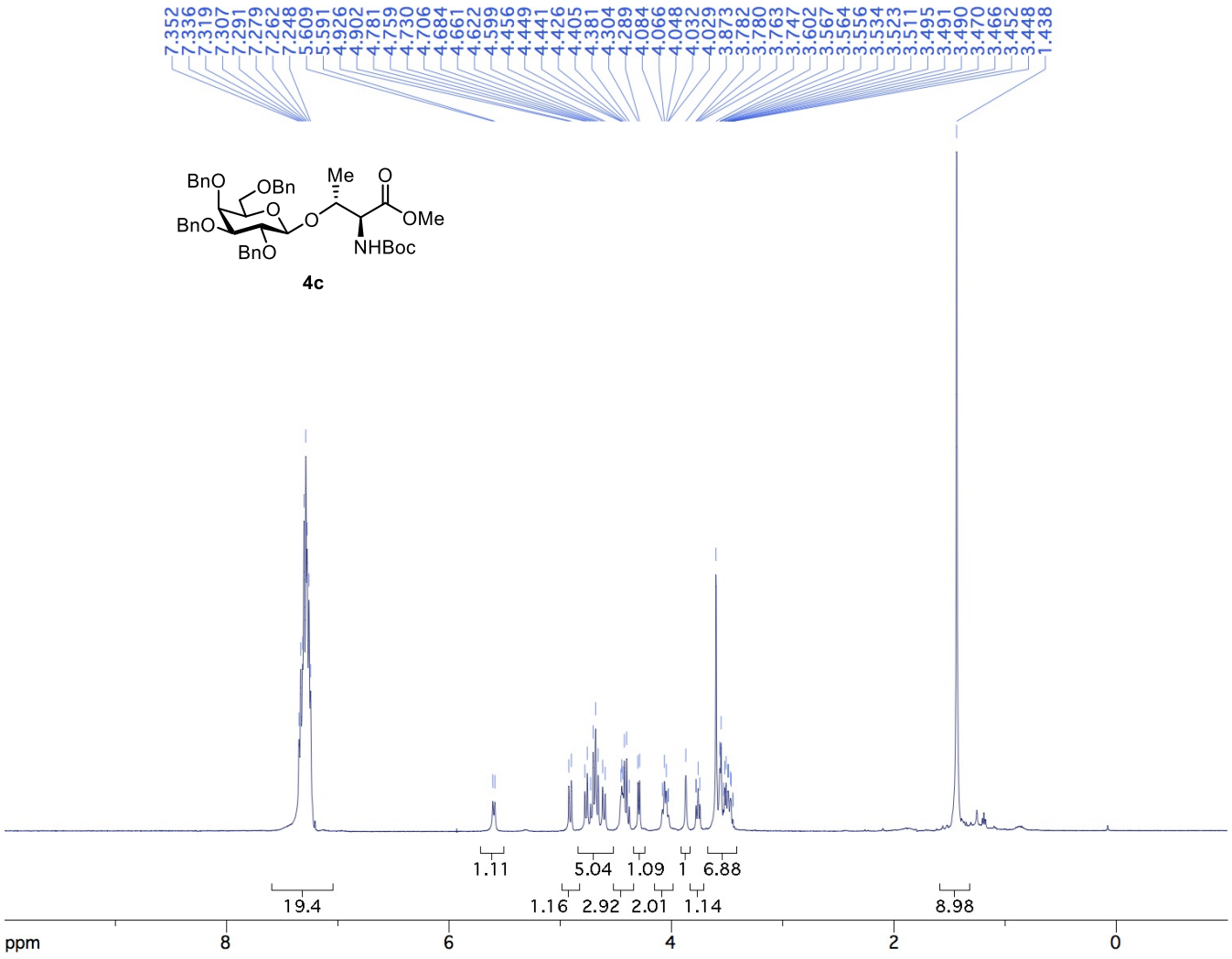

^{1}H NMR (600 MHz) spectrum of **4c** in $CDCl_3$

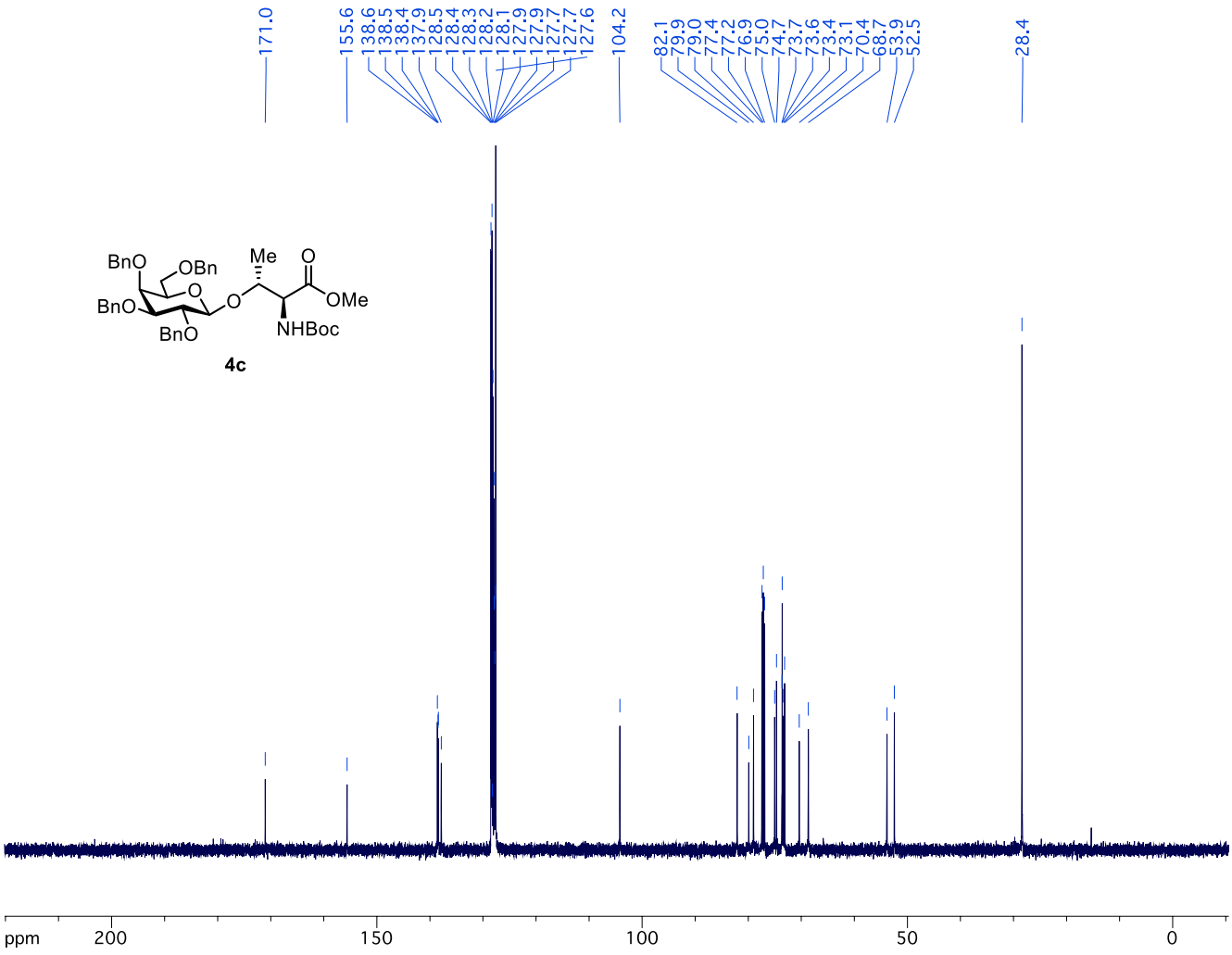

^{13}C NMR (126 MHz) spectrum of **4c** in $CDCl_3$.

Preparation of 4f

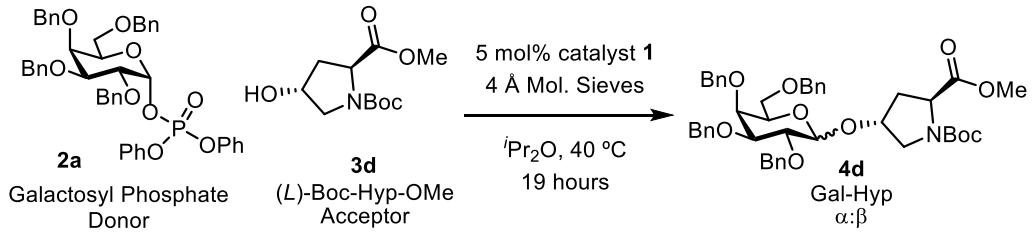

To a flame-dry 5 mL round bottom flask with a stir bar was charged 250 mg flame-dry 4 Å molecular sieves, 14 mg (0.125 mmol) catalyst **1**, and 112 mg (0.500 mmol) (*L*)-Boc-Hyp-OMe (**3d)**. 2.5 mL of a 0.1 M solution of galactosyl phosphate donor (**2a**) in diisopropyl ether was added to the reaction mixture open to air and the flask was closed with a plastic cap and parafilm was used to seal the cap tightly. The mixture was then heated with efficient stirring at 40 ˚C in an oil bath for 19 hours over which time the mixture thickened. After 19 hours, the mixture is cooled to room temperature and 100 µL aliquot is diluted with diethyl ether and filtered to remove the molecular sieves. This solution is concentrated and ^{1}H NMR analysis on the crude mixture is used to determine the anomeric selectivity (95:5 β:α). The mixture was then chromatographed directly with 50 g SiO_2 using

an ether/hexanes gradient on a Biotage MPLC to yield the product (**4d**) in 80% yield (154 mg, 0.218 mmol) as a mixture of anomers.

^{1}H-NMR (500 MHz, $CDCl_3$): δ 7.38-7.27 (m, 20H), 4.98-4.95 (m, 1H), 4.87-4.84 (m, 1H), 4.82-4.73 (m, 3H), 4.66 (d, J = 11.7 Hz, 1H), 4.48-4.34 (m, 5H), 3.93 (s, 1H), 3.86-3.82 (m, 1H), 3.78-3.70 (m, 5H), 3.62-3.53 (m, 4H), 2.44-2.36 (m, 1H), 2.08-2.04 (m, 1H), 1.48-1.43 (m, 9H).

^{13}C-NMR (126 MHz, $CDCl_3$): δ 173.51, 173.29, 154.47, 153.54, 138.52, 138.49, 138.40, 138.38, 137.83, 128.57, 128.47, 128.40, 128.35, 128.31, 128.26, 128.23, 128.12, 128.07, 128.06, 127.98, 127.91, 127.84, 127.79, 127.70, 127.66, 127.63, 127.56, 127.49, 127.47, 102.51, 102.36, 82.29, 82.24, 80.13, 79.16, 77.37, 77.32, 77.12, 76.86, 76.62, 75.85, 75.47, 75.37, 74.57, 73.69, 73.61, 73.31, 73.26, 73.12, 72.99, 68.83, 68.69, 57.81, 57.38, 53.07, 52.75, 52.24, 52.02, 36.00, 35.31, 28.40, 28.28.

HRMS-ESI (m/z): calculated for $C_{45}H_{53}NO_{10}$ [M+H]+: 768.3742, found: 742.3740.

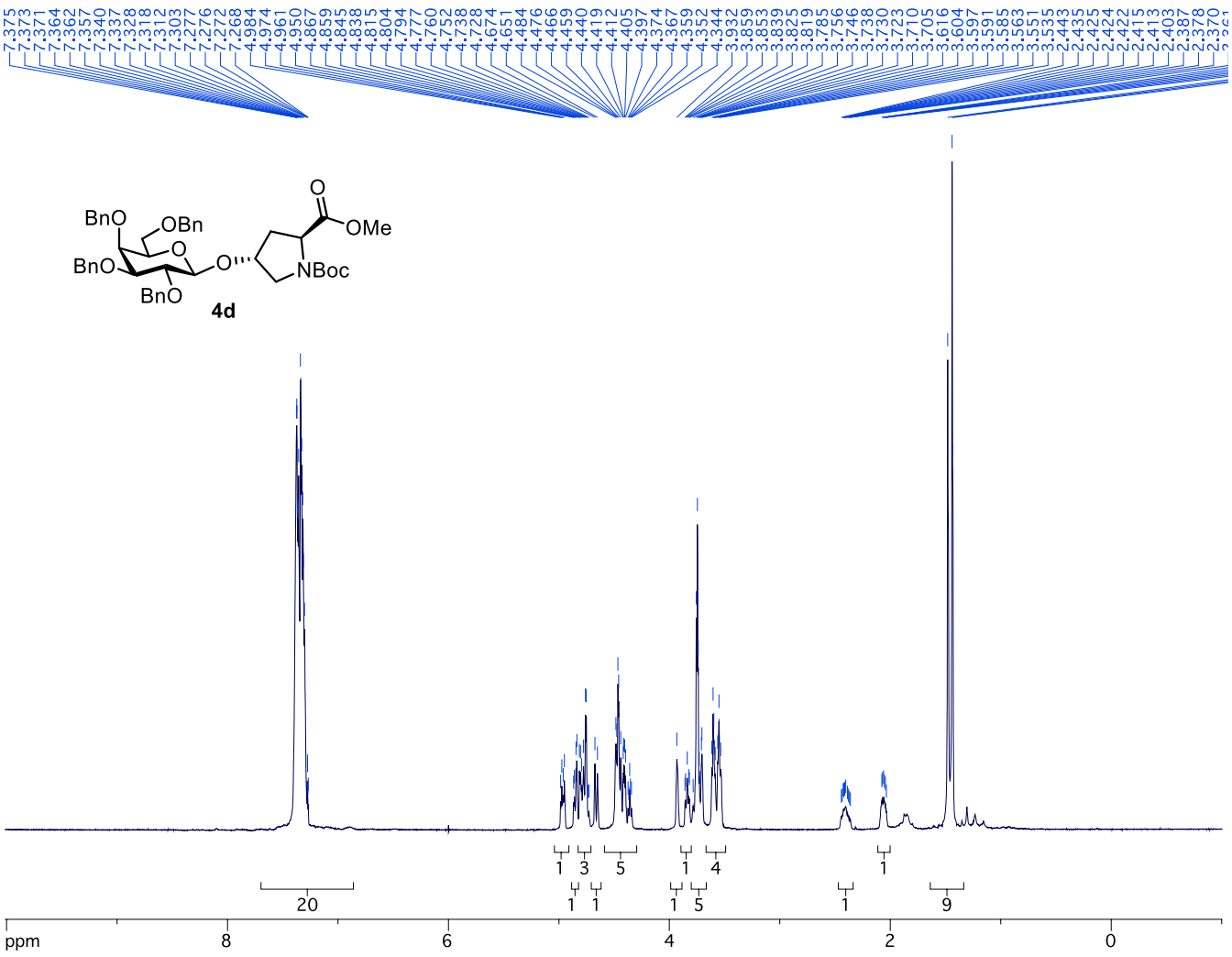

^{1}H NMR (500 MHz) spectrum of **4d** in $CDCl_3$

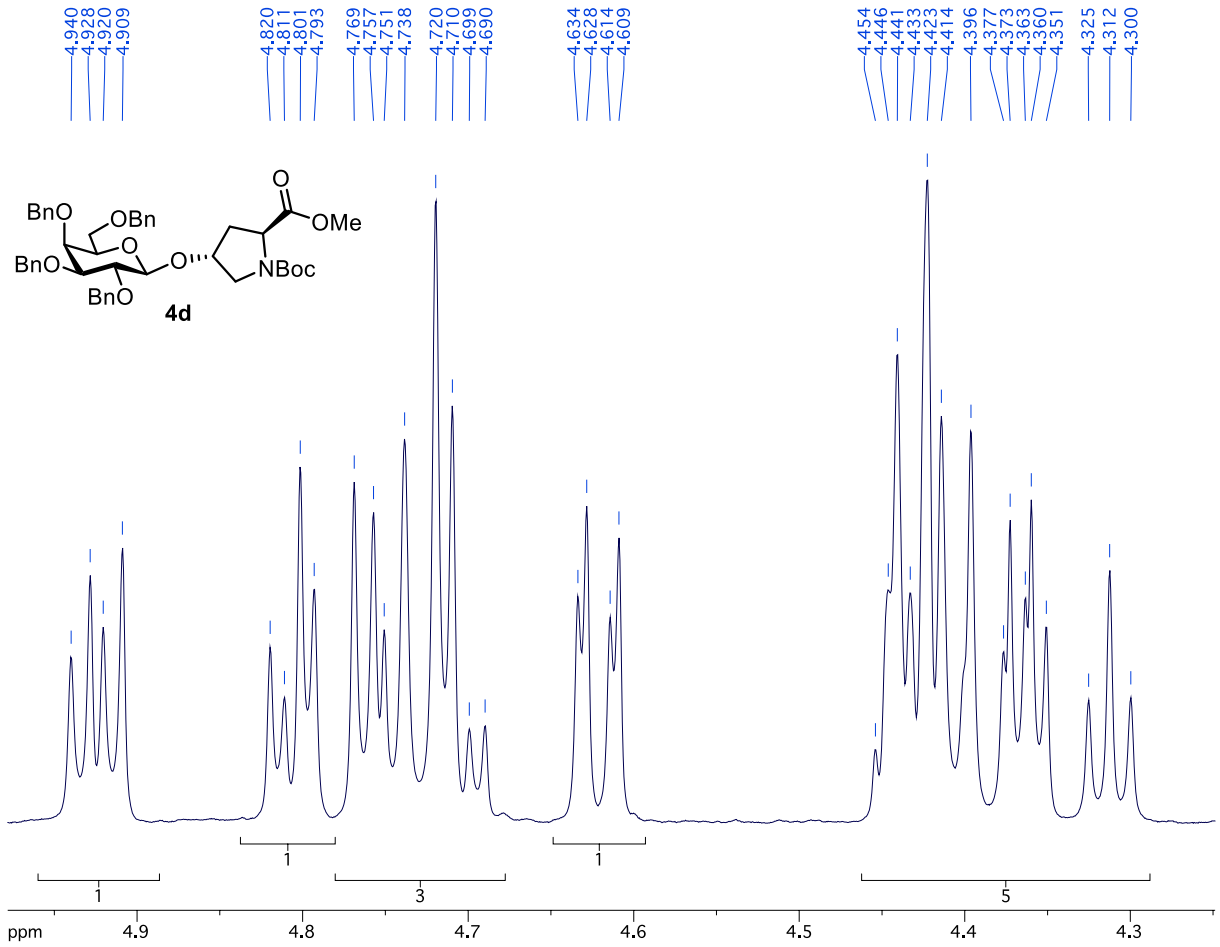

^{1}H NMR (500 MHz) spectrum of **4d** in $CDCl_3$ (4.2-5.1 ppm)

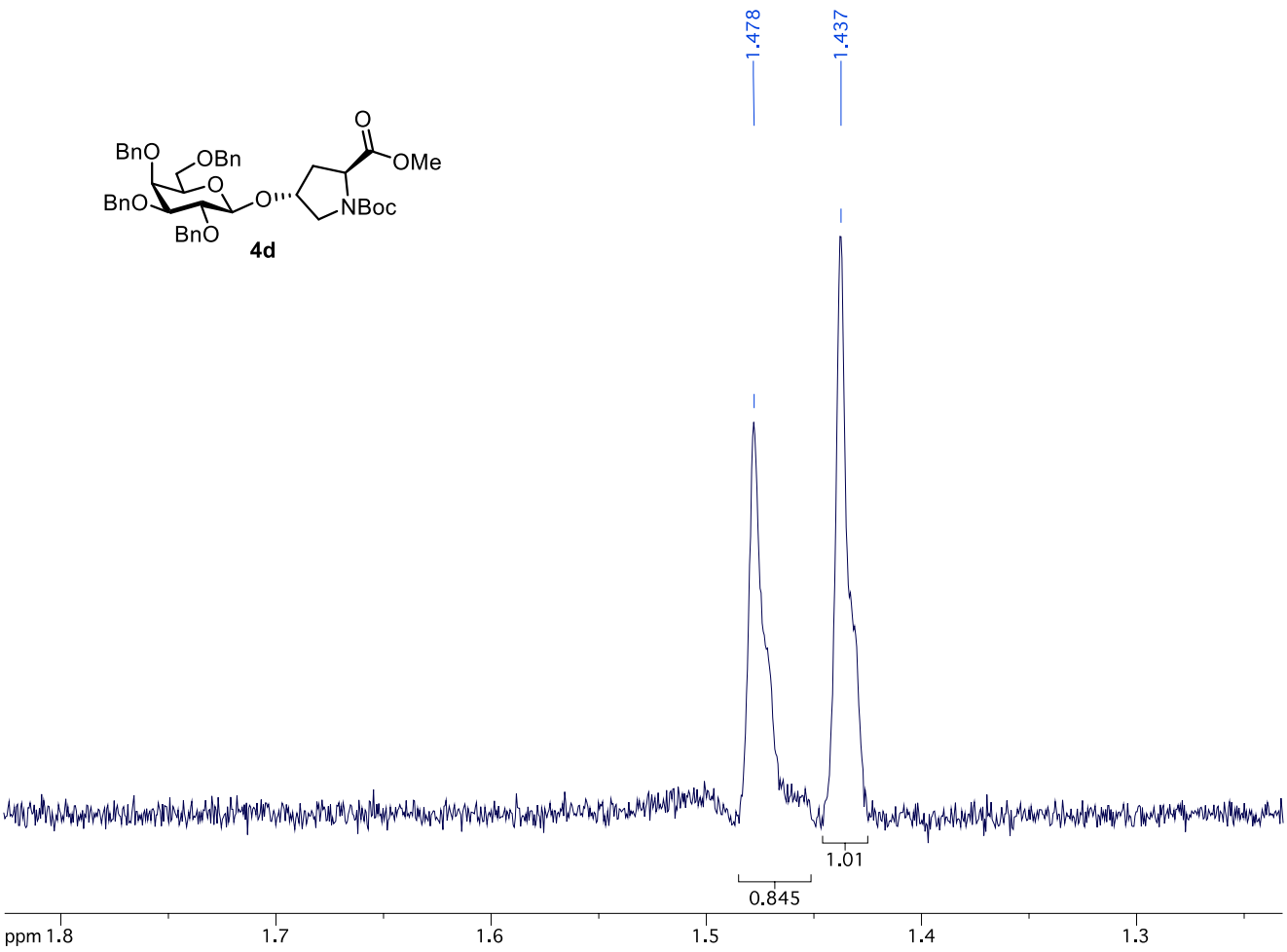

^{1}H 1D NOE NMR (500 MHz) spectrum of **4d** in $CDCl_3$ irradiated at 1.437 ppm

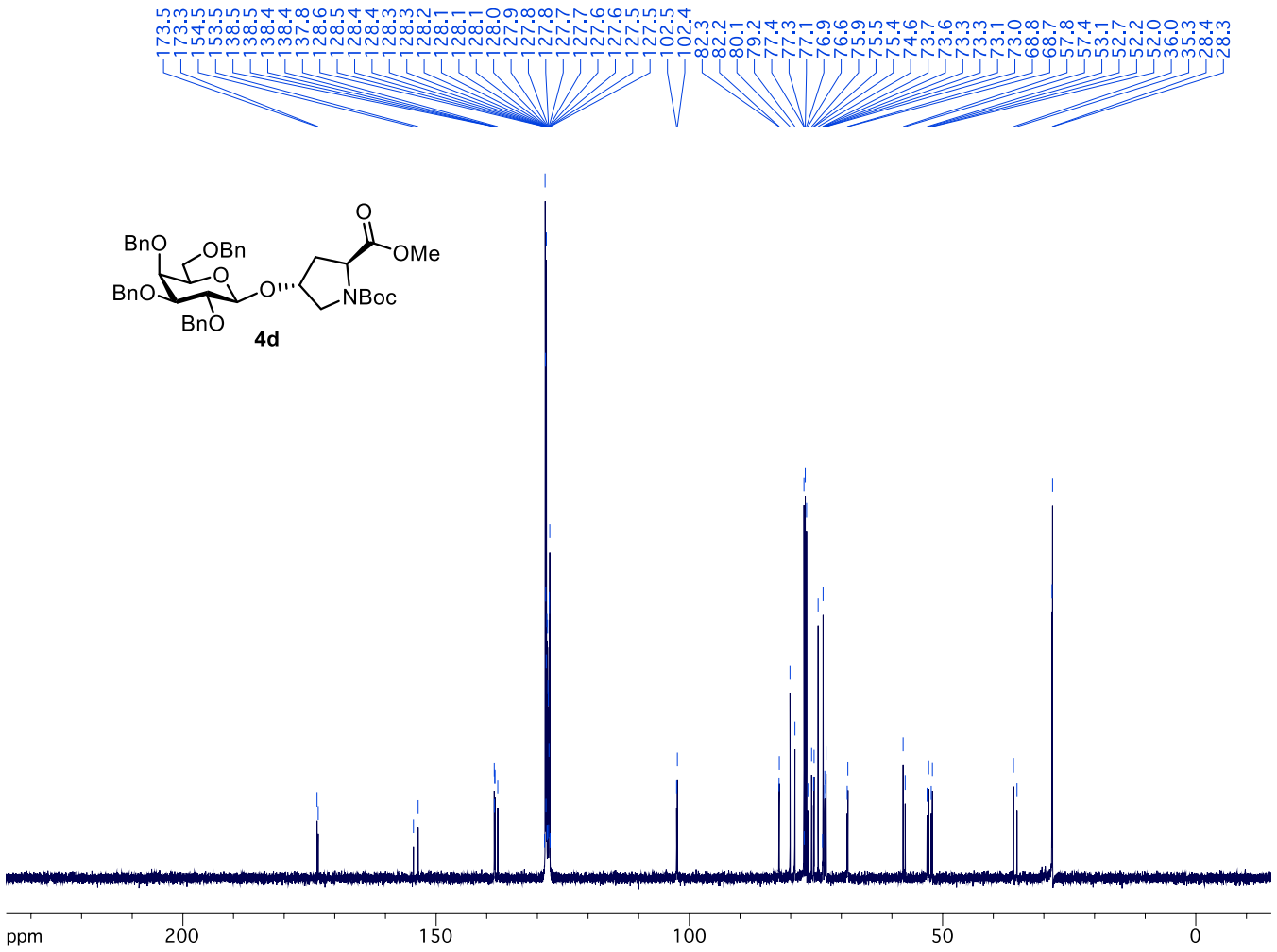

^{13}C NMR (126 MHz) spectrum of **4d** in $CDCl_3$.

Preparation of 4e

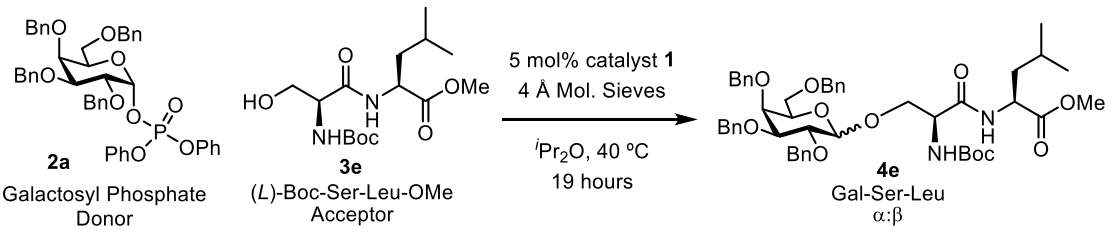

To a flame-dry 5 mL round bottom flask with a stir bar was charged 250 mg flame-dry 4 Å molecular sieves, 14 mg (0.0125 mmol) catalyst **1**, and 166 mg (0.500 mmol) (*L*)-BocSerLeuOMe (**3e**), and 2.5 mL of a 0.1 M solution of galactosyl phosphate (**2a**) donor in diisopropyl ether. Open to air, the flask was closed with a plastic cap and parafilm was used to seal the cap tightly. The mixture was then heated with efficient stirring at 40 ˚C in an oil bath for 19 hours over which time the mixture thickened. After 19 hours, the mixture is cooled to room temperature and 100 µL aliquot is diluted with diethyl ether and filtered to remove the molecular sieves. This solution is concentrated and ^{1}H NMR analysis on the crude mixture is used to determine the anomeric

selectivity (96:4 β:α). The mixture was then chromatographed directly with 50 g SiO_2 using an ether/hexanes gradient on a Biotage MPLC to yield the product (**4e**) in 84% yield (180 mg, 0.210 mmol) as a mixture of anomers.

^{1}H-NMR (600 MHz, $CDCl_3$): δ 7.36-7.25 (m, 20H), 7.01 (s, 1H), 5.52 (s, 1H), 4.95 (d, *J* = 11.4 Hz, 1H), 4.84 (d, *J* = 11.0 Hz, 1H), 4.77 (d, *J* = 11.0 Hz, 1H), 4.76-4.71 (m, 2H), 4.58 (d, *J* = 11.4 Hz, 1H), 4.54-4.40 (m, 5H), 4.02 (s, 1H), 3.91 (d, *J* = 2.6 Hz, 1H), 3.85 (dd, *J* = 9.7, 7.7 Hz, 1H), 3.80 (dd, *J* = 11.0, 7.9 Hz, 1H), 3.64-3.58 (m, 6H), 3.54 (dd, *J* = 9.8, 2.9 Hz, 1H), 1.56-1.37 (m, 2H), 1.43-1.37 (m, 10H), 0.83 (dd, *J* = 15.8, 6.3 Hz, 6H).

^{13}C-NMR (126 MHz, $CDCl_3$): δ 172.65, 169.77, 155.47, 138.64, 138.59, 138.38, 137.79, 128.49, 128.42, 128.37, 128.22, 128.16, 128.15, 127.87, 127.67, 127.60, 127.57, 104.85, 82.10, 79.97, 79.29, 75.32, 74.74, 73.61, 73.53, 73.46, 73.02, 70.42, 68.52, 53.84, 52.10, 50.96, 41.23, 28.34, 24.68, 22.82, 21.88.

HRMS-ESI (m/z): calculated for $C_{49}H_{62}N_2O_{11}$ [M+H]+: 855.4426, found: 855.4426.

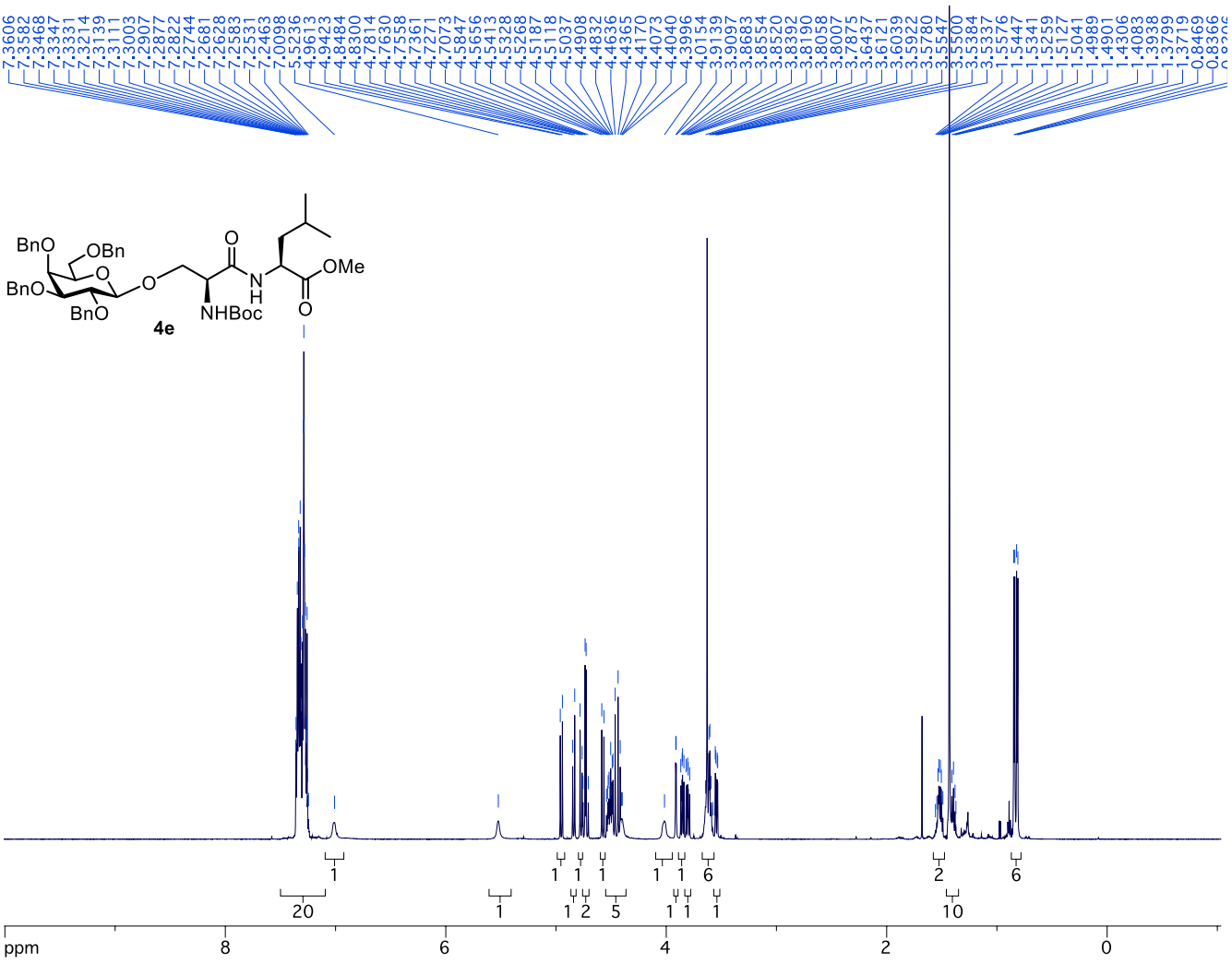

^{1}H NMR (600 MHz) spectrum of **4e** in $CDCl_3$

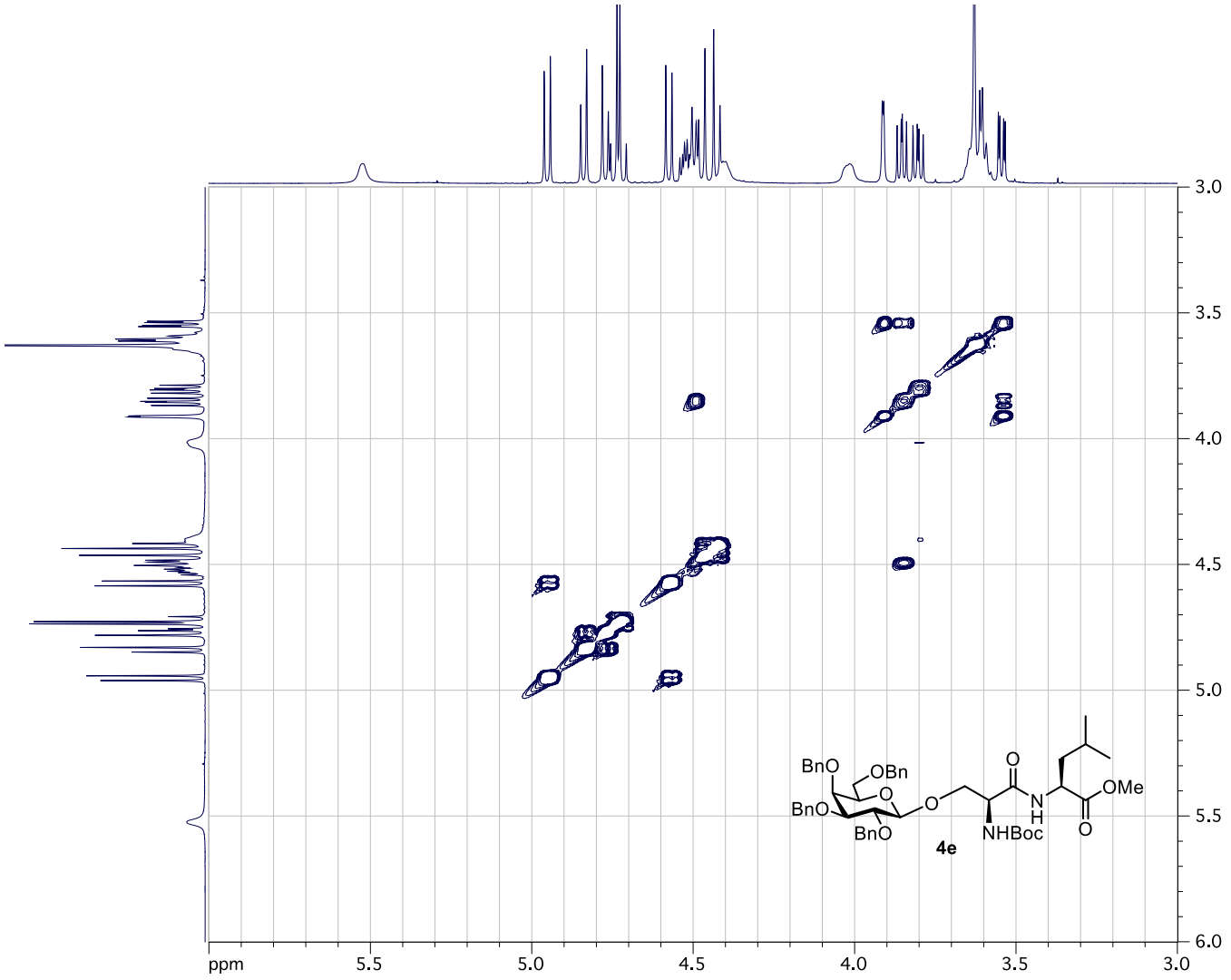

^{1}H-^{1}H COSY NMR (600 MHz) spectrum of **4e** in $CDCl_3$

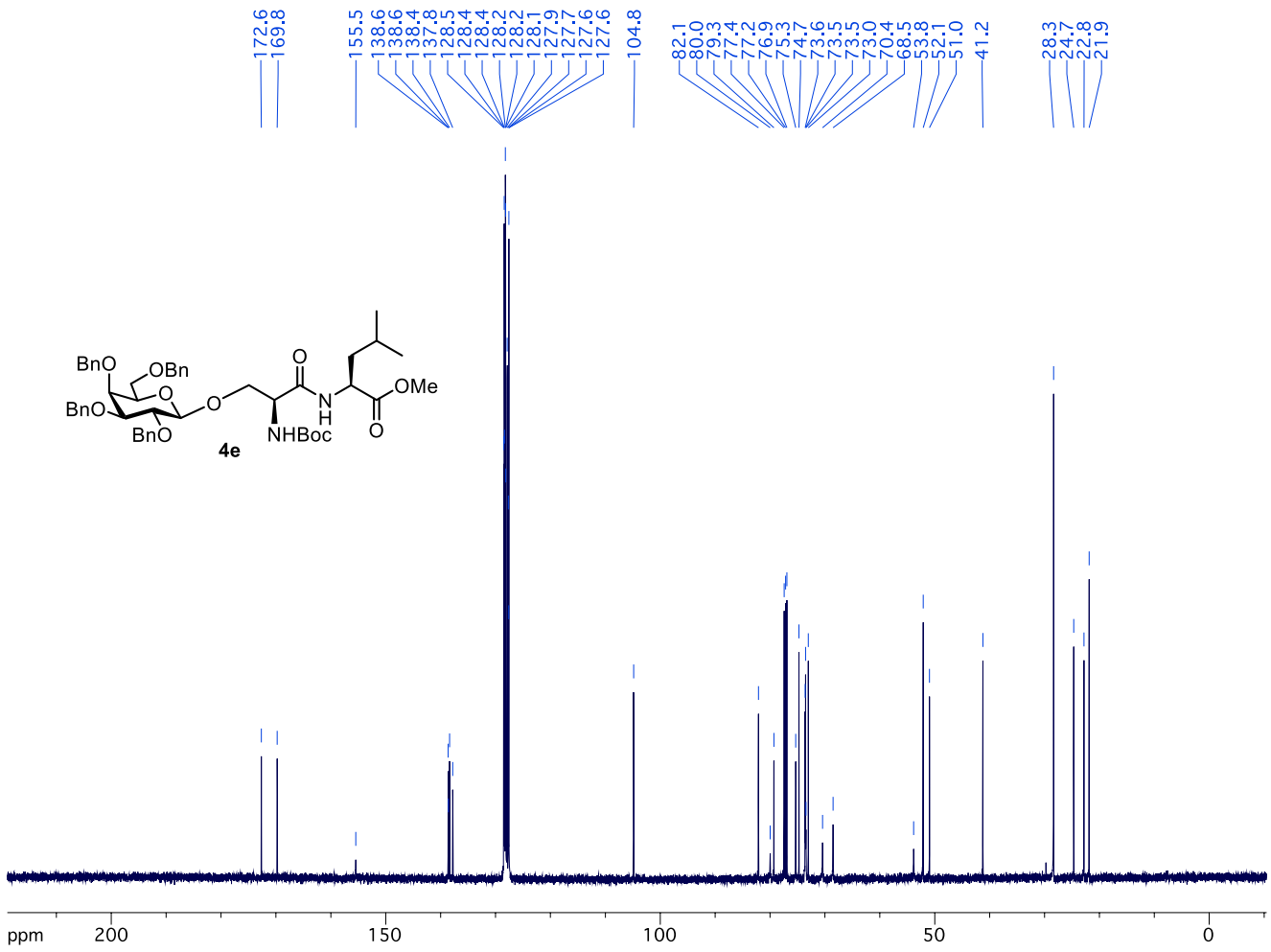

^{13}C NMR (126 MHz) spectrum of **4e** in $CDCl_3$.

Preparation of 4f

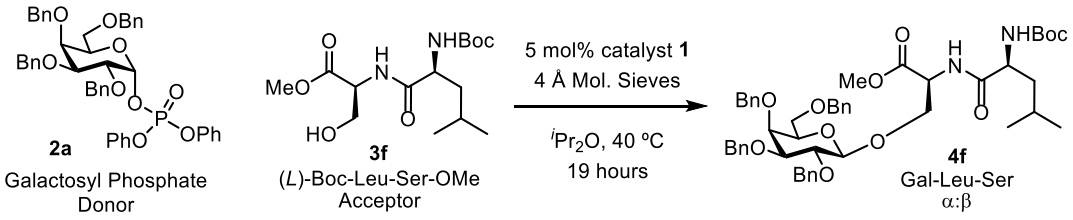

To a flame-dry 5 mL round bottom flask with a stir bar was charged 250 mg flame-dry 4 Å molecular sieves, 14 mg (0.0125 mmol) catalyst **1**, and 166 mg (0.500 mmol) BocLeuSerOMe (**3f**), and 2.5 mL of a 0.1 M solution of galactosyl phosphate donor (**2a**) in diisopropyl ether. Open to air, the flask was closed with a plastic cap and parafilm was used to seal the cap tightly. The mixture was then heated with efficient stirring at 40 ˚C in an oil bath for 19 hours over which time the mixture thickened. After 19 hours, the mixture is cooled to room temperature and 100 µL aliquot is diluted with diethyl ether and filtered to remove the molecular sieves. This solution is concentrated and ^{1}H NMR analysis on the crude mixture is used to determine the anomeric selectivity (88:12 β:α). The mixture was then chromatographed directly with 50 g SiO_2 using an ether/hexanes gradient on a Biotage MPLC to yield the product (**4f**) in 77% yield (165 mg, 0.193 mmol) product as a mixture of anomers.

^{1}H-NMR (500 MHz, $CDCl_3$): δ 7.50-7.31 (m, 20H), 6.95-6.93 (m, 1H), 4.97 (d, *J* = 11.6 Hz, 1H), 4.94 (d, *J* = 11.8 Hz, 1H), 4.84 (d, *J* = 11.1 Hz, 1H), 4.82-4.76 (m, 2H), 4.74 (td, *J* = 5.0, 2.3 Hz, 1H), 4.66 (d, *J* = 11.5 Hz, 1H), 4.56 (d, *J* = 6.1 Hz, 1H), 4.53-4.47 (m, 2H), 4.40 (d, *J* = 7.1 Hz, 1H), 4.37 (d, *J* = 11.8 Hz, 1H), 4.05 (s, 1H), 3.95-3.92 (m, 2H), 3.84 (t, *J* = 8.7 Hz, 1H), 3.81 (s, 3H), 3.66-3.57 (m, 4H), 1.55-1.48 (m, 11H), 0.89 (dd, *J* = 17.0, 5.9 Hz, 6H).

^{13}C-NMR (126 MHz, $CDCl_3$): δ 172.80, 170.33, 155.40, 138.88, 138.67, 138.47, 137.99, 128.56, 128.50, 128.40, 128.32, 128.07, 127.96, 127.93, 127.74, 127.70, 104.88, 82.32, 79.96, 79.05, 74.98, 74.75, 73.60, 73.55, 73.15, 69.65, 68.61, 53.53, 53.06, 52.77, 41.26, 29.83, 28.46, 24.72, 23.08, 21.67.

HRMS-ESI (m/z): calculated for $C_{49}H_{62}N_2O_{11}$ [M+H]+: 855.4426, found: 855.4426.

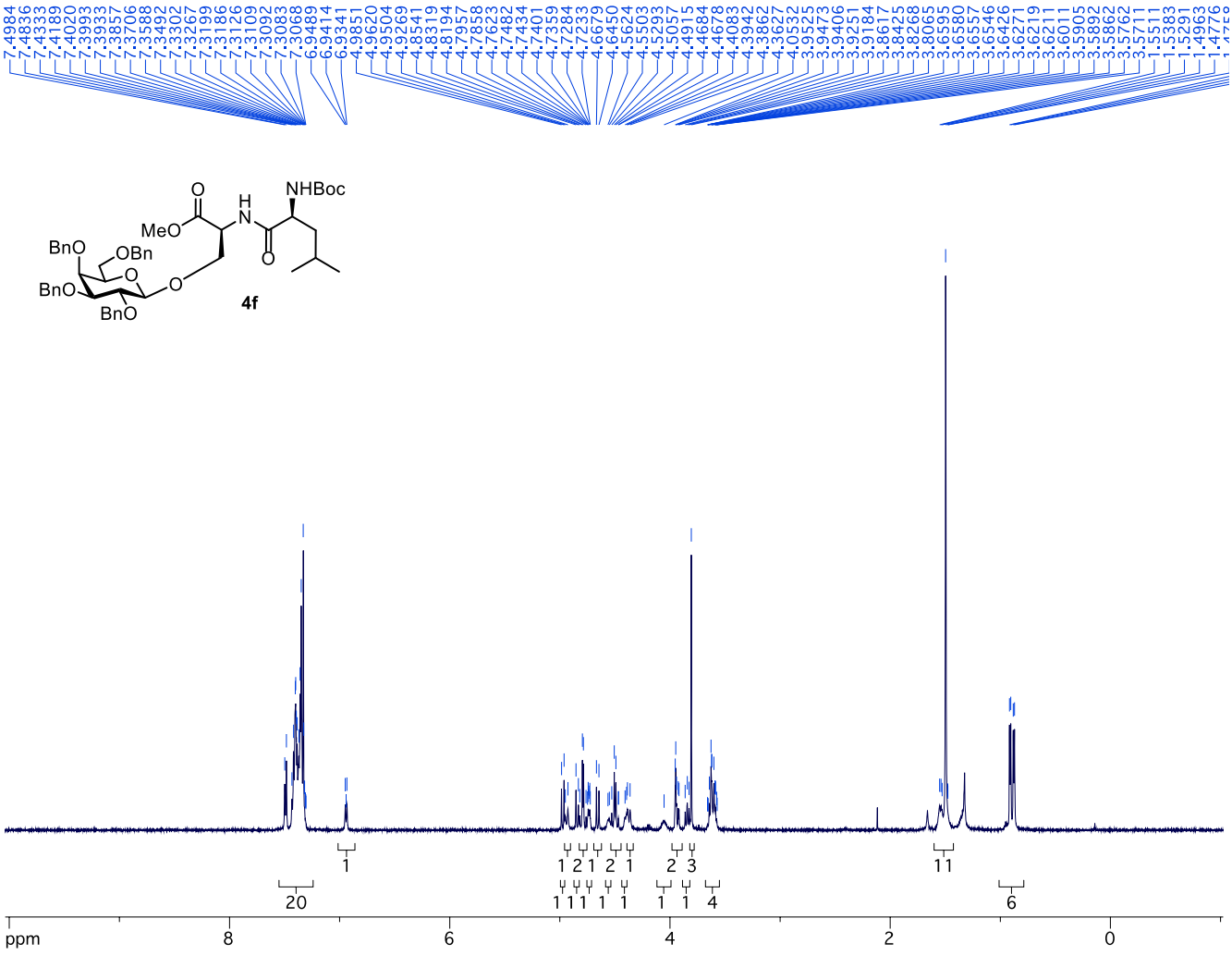

^{1}H NMR (500 MHz) spectrum of **4f** in $CDCl_3$

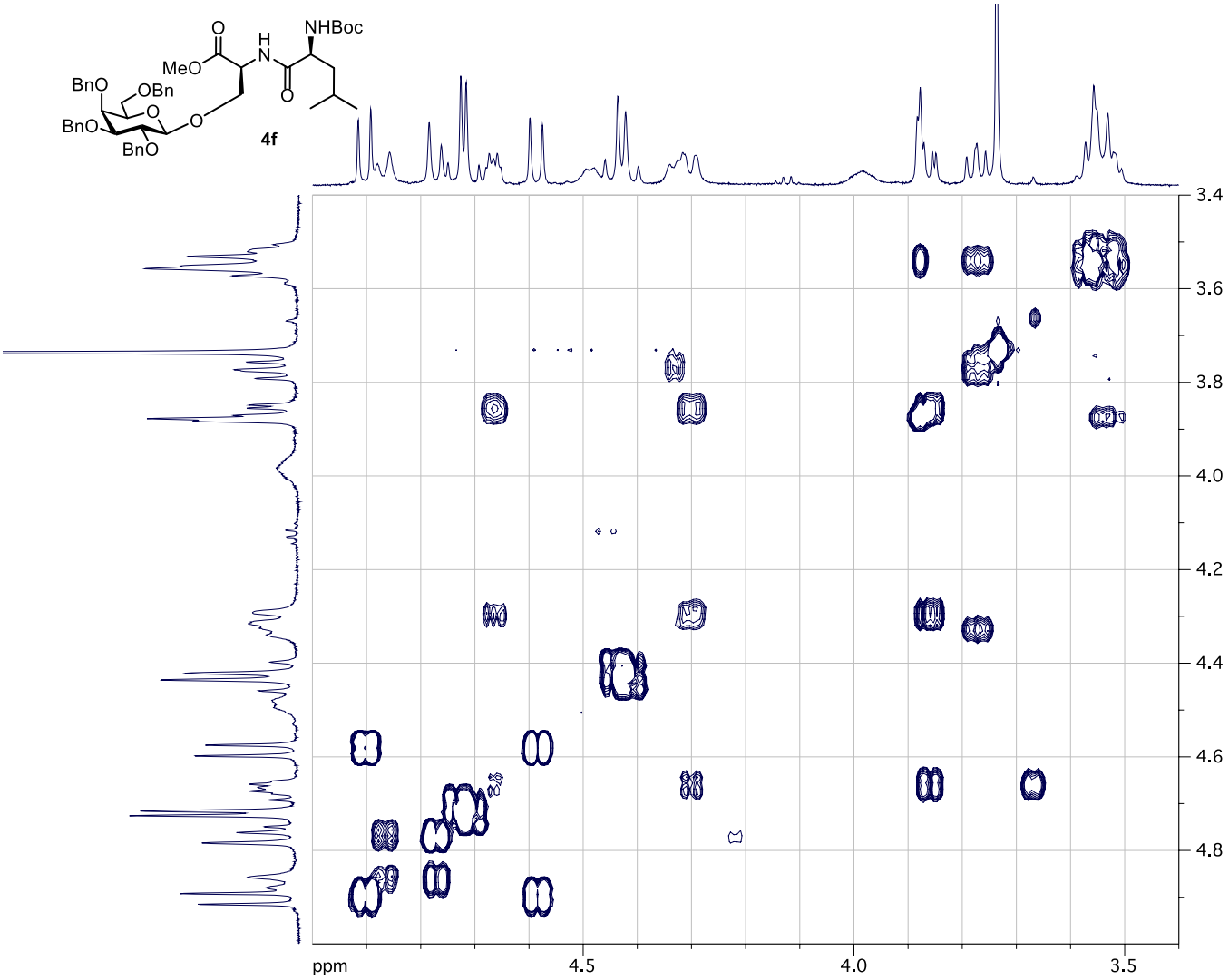

^{1}H-^{1}H COSY NMR (500 MHz) spectrum of **4f** in $CDCl_3$

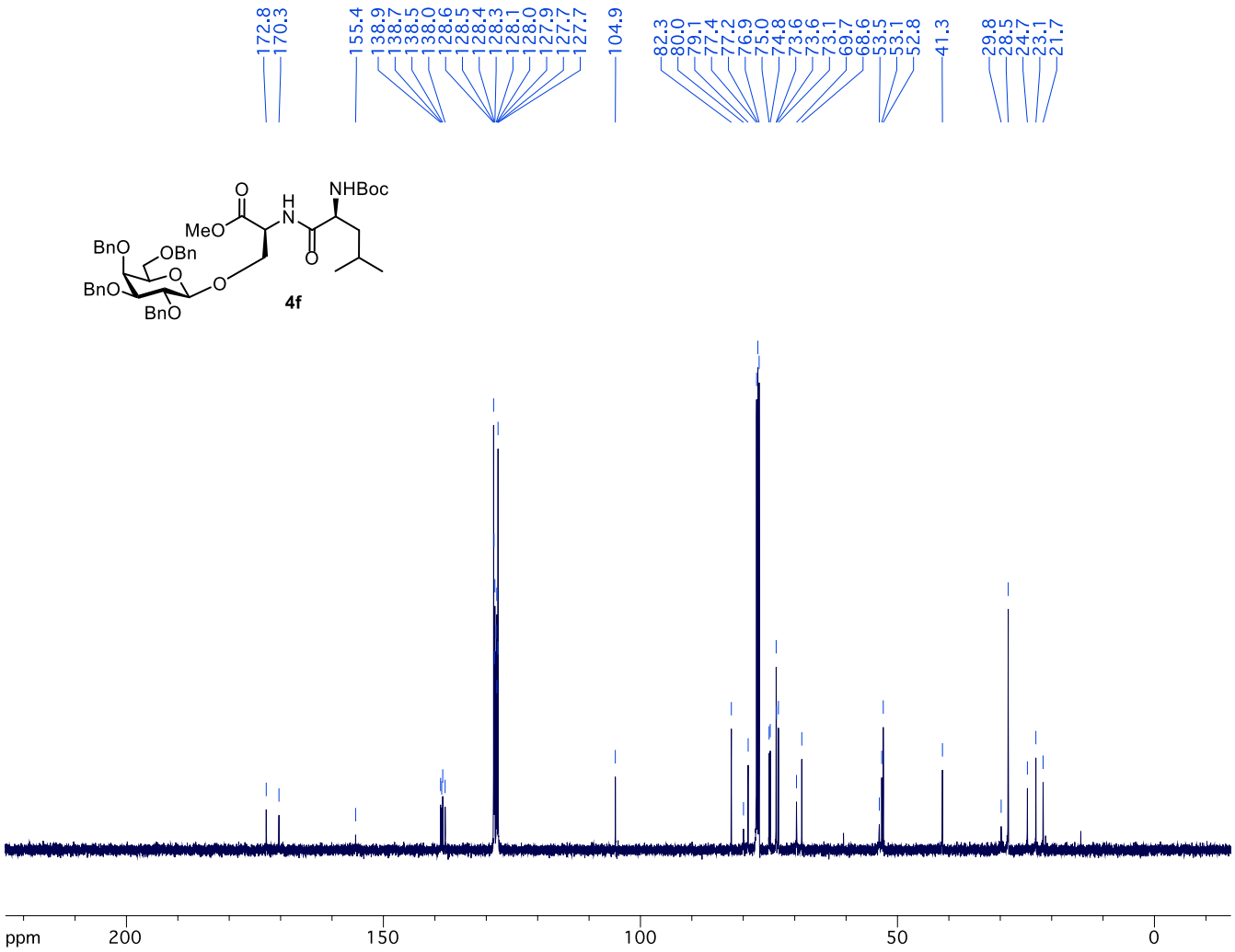

^{13}C NMR (126 MHz) spectrum of **4e** in $CDCl_3$.

Preparation of 3g

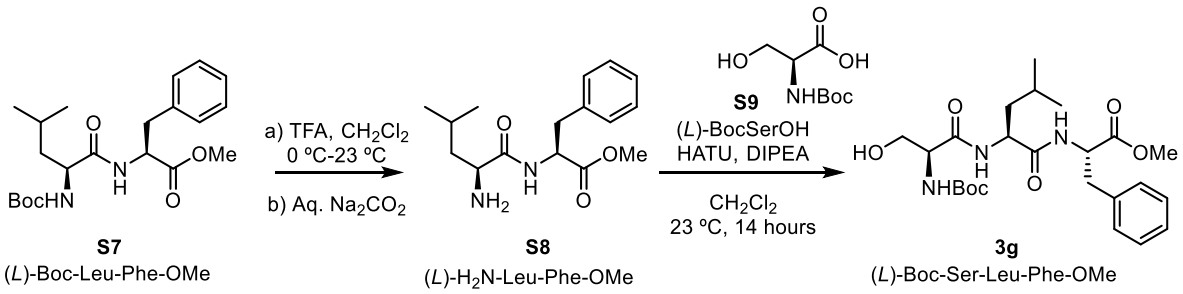

To a 25 mL round bottom flask was added (*L*)-Boc-Leu-Phe-OMe (**S7**) (0.226 g, 0.58 mmol, 1 equiv.) and 4 mL dry dichloromethane. The reaction was cooled to 0 °C, and to the cooled reaction was added 1.2 mL trifluoroacetic acid dropwise. The reaction was stirred at 0 °C for 15 min and warmed to rt. The reaction was stirred at rt for 1.5 hours. The reaction was cooled back to 0 °C and diluted with 8 mL dichloromethane. The reaction was quenched with sat. Na_2CO_3 solution until pH is 12. The organic layer was separated, and the aqueous layer was extracted with dichloromethane twice. The combined organic layers were washed with brine and dried over Na_2SO_4. The organic layer was concentrated to afford the free amine, which was directly used without purification.

To a flame-dried 25 mL round bottom flask equipped with a stir bar was added (*L*)-Boc-Ser-OH (**S9**) (0.119 g, 0.58 mmol, 1 equiv.), 3.5 mL dry dichloromethane, and HATU (0.221 g, 0.58 mmol, 1 equiv.). To the reaction mixture was added DIPEA (0.30 mL, 1.74 mmol, 3 equiv.) dropwise. To the reaction was added a solution of (*L*)-H_2N-Leu-Phe-OMe (**S8**) (0.170 g, 0.58 mmol, 1 equiv.) in 3.5 mL dry DCM. The reaction was stirred at rt overnight. The yellow solution was diluted with diethyl ether and washed with 1 M HCl, sat $NaHCO_3$, and brine. The organic layer was dried over Na_2SO_4 and concentrated. The yellow oil was concentrated and purified by column chromatography to afford (*L*)-Boc-Ser-Leu-Phe-OMe (**3g**) as a foamy white solid.

^{1}H-NMR (600 MHz, $CDCl_3$): δ 7.28-7.21 (m, 3H), 7.10 (d, *J* = 7.0 Hz, 2H), 6.89-6.85 (m, 2H), 5.55 (s, 1H), 4.82 (q, *J* = 6.9 Hz, 1H), 4.42-4.38 (m, 1H), 4.17 (s, 1H), 3.91 (s, 1H), 3.69-3.56 (m, 5H), 3.14-3.02 (m, 2H), 2.00 (s, 1H), 1.65-1.59 (m, 2H), 1.53-1.43 (m, 10H), 0.88 (dd, *J* = 15.8, 5.9 Hz, 6H).

^{13}C-NMR (126 MHz, $CDCl_3$): δ 172.01, 171.78, 171.73, 171.55, 155.85, 135.77, 129.32, 129.26, 128.54, 127.10, 80.41, 77.45, 77.23, 62.90, 54.72, 53.27, 52.39, 52.30, 40.44, 37.82, 24.68, 22.95, 21.58.

HRMS-ESI (m/z): calculated for $C_{24}H_{37}N_3O_7$ [M+H]+: 480.2704, found: 480.2704.

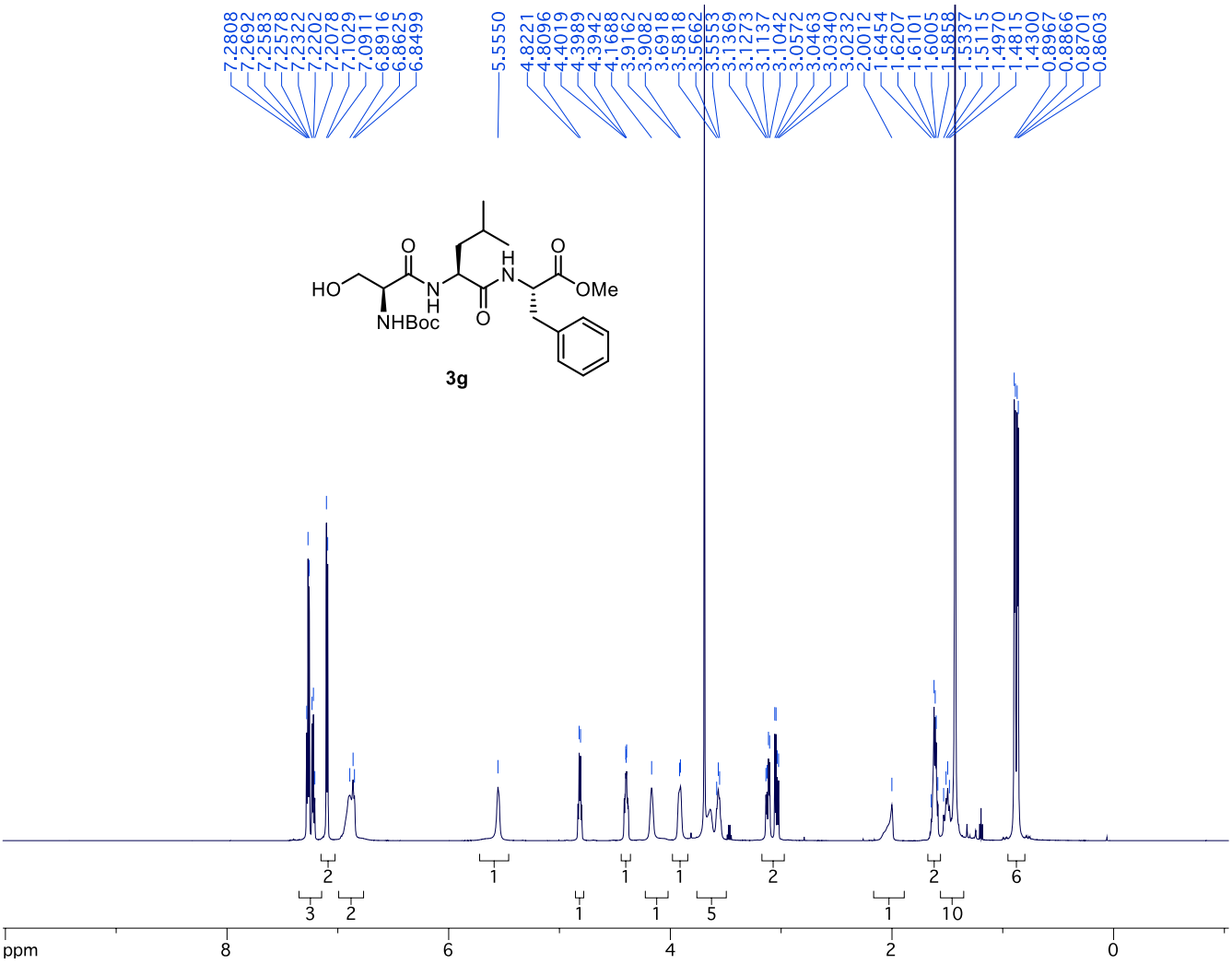

^{1}H NMR (600 MHz) spectrum of **3g** in $CDCl_3$

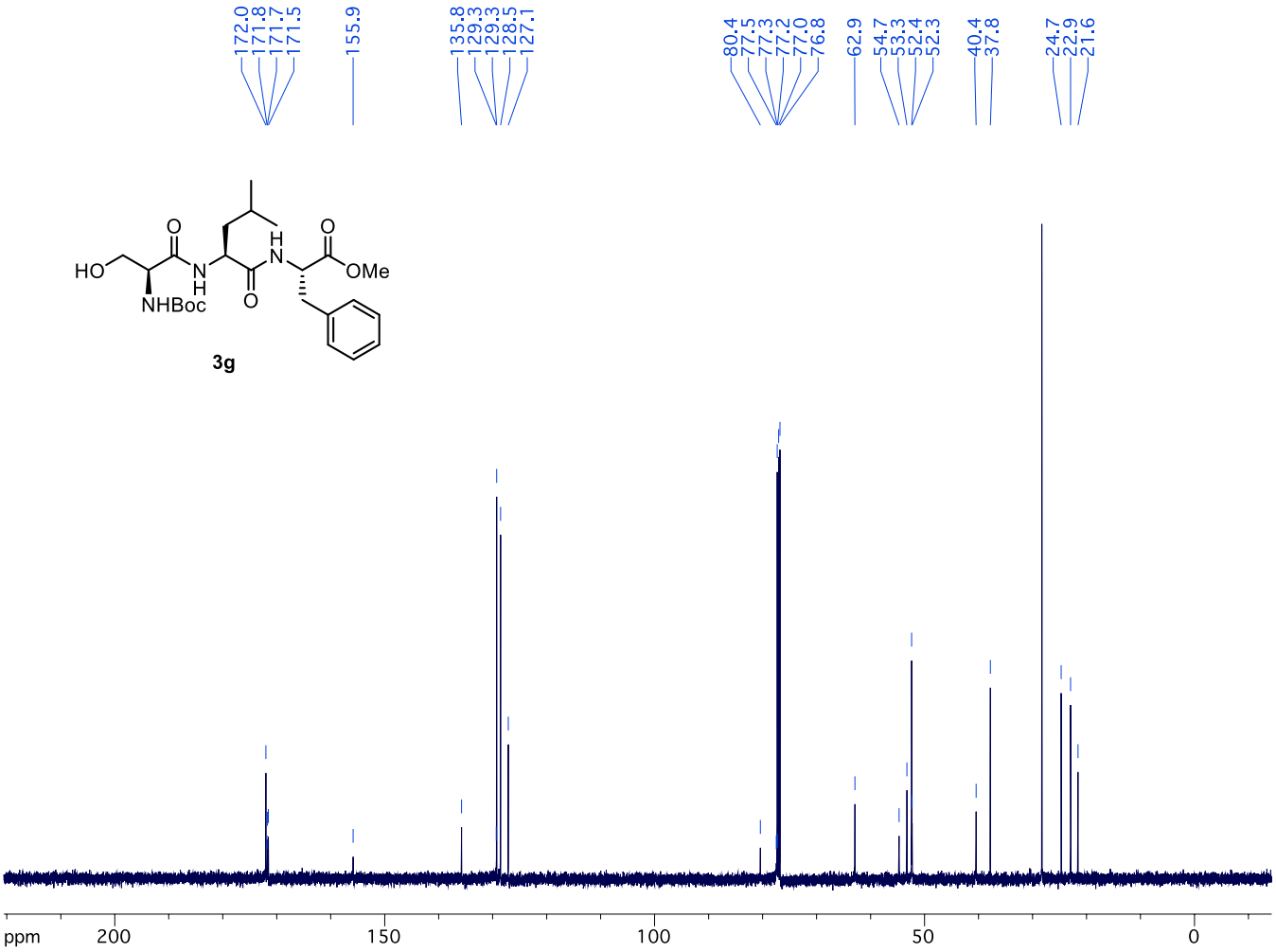

^{13}C NMR (126 MHz) spectrum of **3f** in $CDCl_3$.

Preparation of 4g

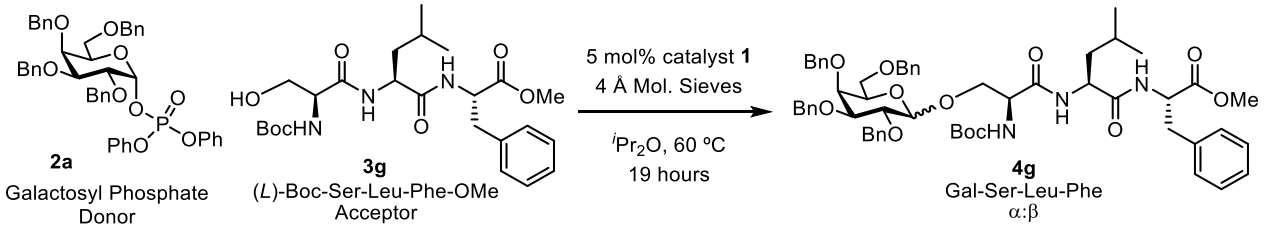

To a flame-dry 25 mL round bottom flask with a stir bar was charged 1.0 g flame-dry 4 Å molecular sieves, 14 mg (0.0125 mmol) catalyst **1**, and 120 mg (0.250 mmol) (*L*)-BocSerLeuPheOMe (**3g**), and 2.5 mL of a 0.1 M solution of galactosyl phosphate donor (**2a**) in diisopropyl ether. An additional 7.5 mL diisopropyl ether was added, bringing the total volume to 10.0 mL. Open to air, the flask was closed with a plastic cap and parafilm was used to seal the cap tightly. The mixture was then heated with efficient stirring at 60 ˚C in an oil bath for 19 hours over which time the mixture thickened. After 19 hours, the mixture is cooled to room temperature and 100 µL aliquot is diluted with diethyl ether and filtered to remove the molecular sieves. This solution is concentrated and ^{1}H NMR analysis on the crude mixture is used to determine the anomeric selectivity (89:11 β:α). The mixture

was then chromatographed directly with 50 g SiO_2 using an ether/hexanes gradient on a Biotage MPLC to yield the product (**4g**) in 30% yield (75 mg, 0.075 mmol) as a mixture of anomers.

^{1}H-NMR (600 MHz, $CDCl_3$): δ 7.37-6.98 (m, 28H), 5.53 (d, *J* = 6.0 Hz, 1H), 4.96 (d, *J* = 11.5 Hz, 1H), 4.77-4.62 (m, 5H), 4.55-4.53 (m, 2H), 4.46-4.42 (m, 3H), 4.36-4.32 (m, 1H), 3.95-3.85 (m, 3H), 3.73-3.66 (m, 3H), 3.61 (s, 3H), 3.54 (dd, *J* = 9.7, 2.9 Hz, 2H), 3.11 (dd, *J* = 13.7, 5.8 Hz, 1H), 2.96 (dd, *J* = 13.7, 7.0 Hz, 1H), 1.61-1.56 (m, *J* = 4.7 Hz, 1H), 1.53-1.47 (m, 1H), 1.43 (s, 9H), 1.37-1.31 (m, *J* = 4.6 Hz, 1H), 1.26 (s, 1H), 0.81 (t, *J* = 6.0 Hz, 6H).

^{13}C-NMR (126 MHz, $CDCl_3$): δ 171.63, 171.57, 169.76, 155.34, 138.72, 138.44, 138.39, 137.63, 136.38, 129.46, 128.61, 128.58, 128.53, 128.47, 128.42, 128.34, 128.01, 127.96, 127.86, 127.80, 127.66, 126.99, 106.01, 82.04, 80.13, 79.58, 75.22, 74.89, 73.72, 73.67, 73.54, 73.48, 73.43, 73.31, 71.76, 68.54, 53.59, 53.24, 52.52, 52.18, 40.56, 38.08, 28.42, 24.77, 23.07, 21.53.

HRMS-ESI (m/z): calculated for $C_{58}H_{71}N_3O_{12}$ [M+H]+: 1002.5111, found: 1002.5109.

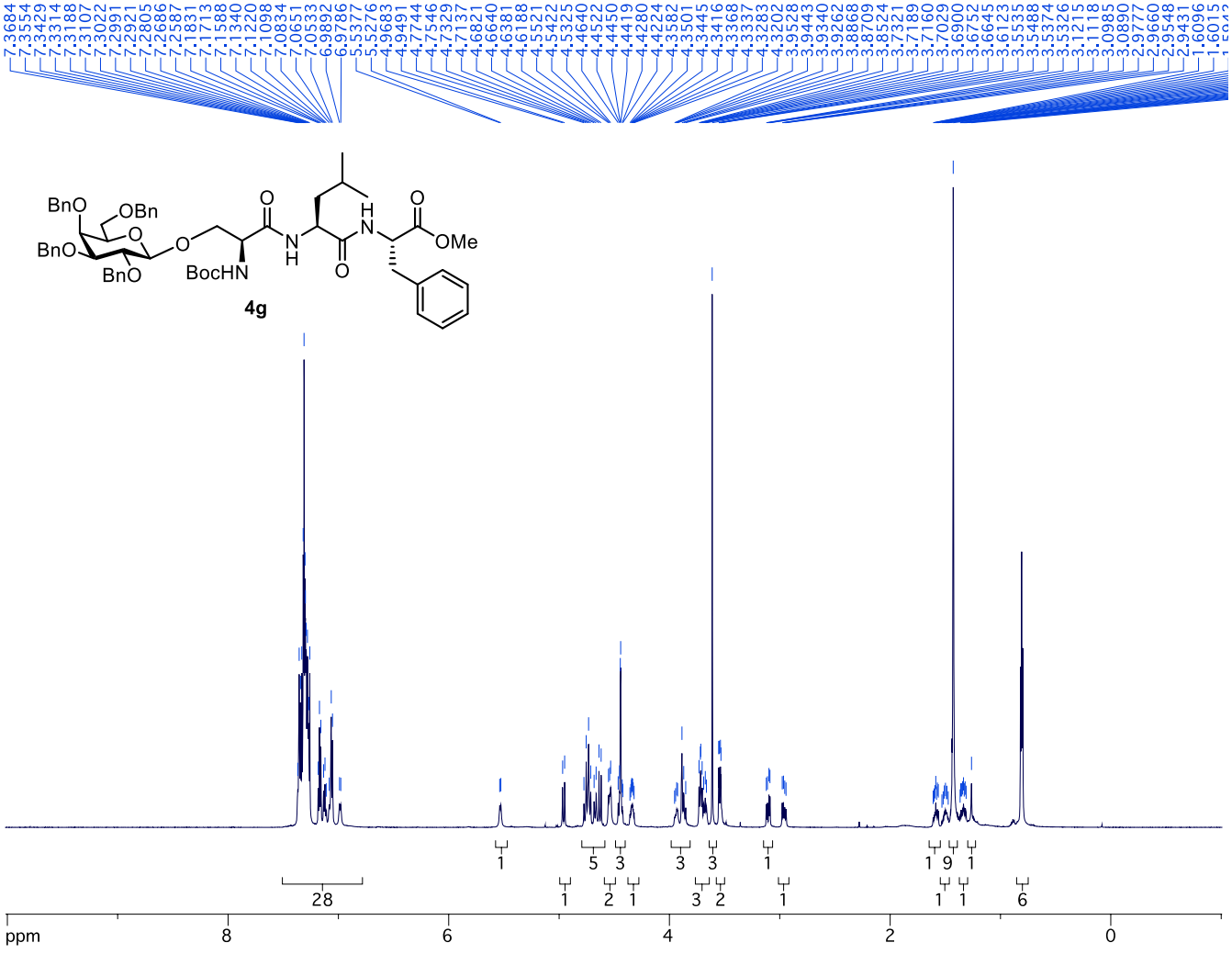

^{1}H NMR (600 MHz) spectrum of **4g** in $CDCl_3$

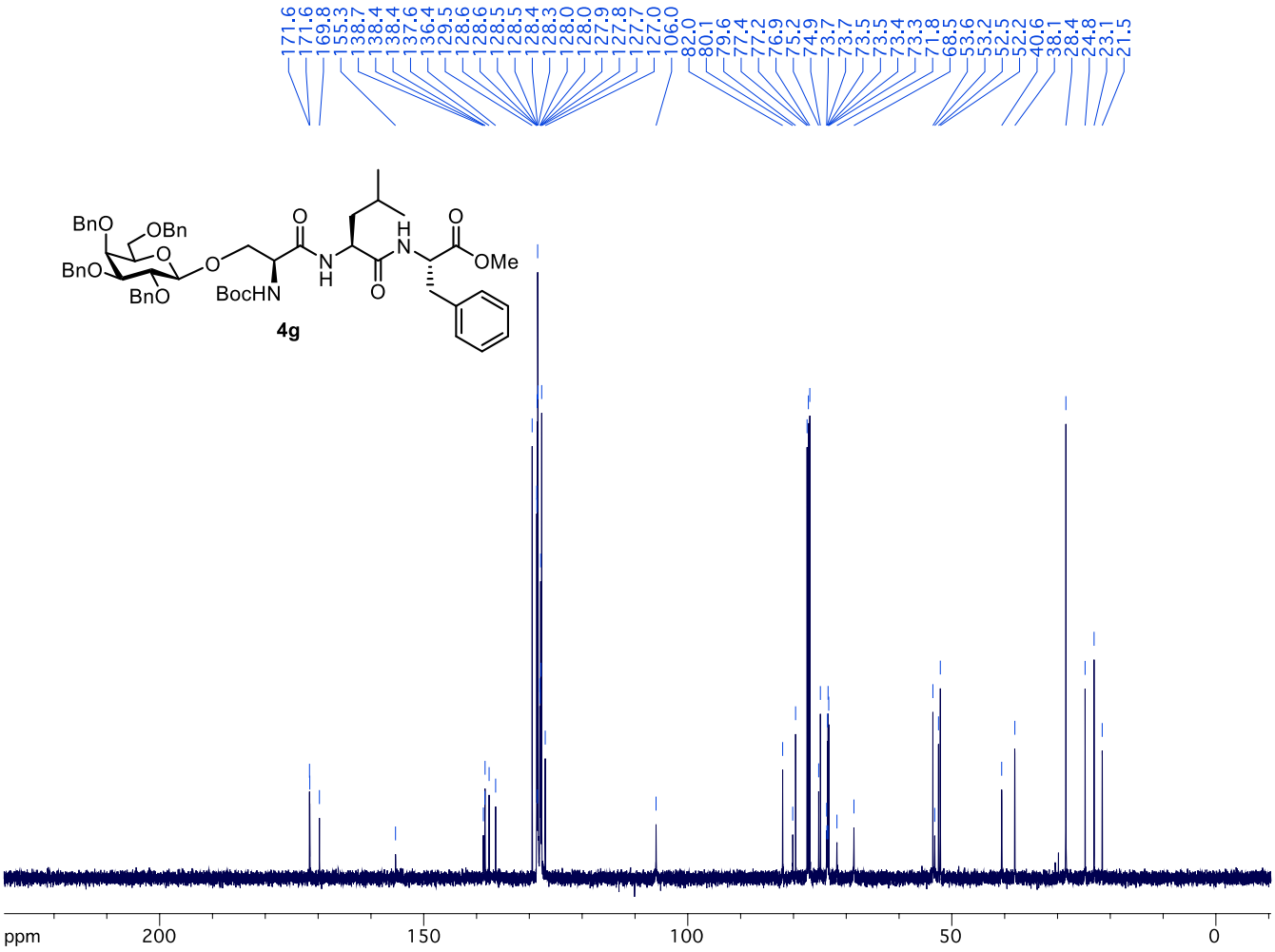

^{13}C NMR (126 MHz) spectrum of **4g** in $CDCl_3$.

Preparation of 4h

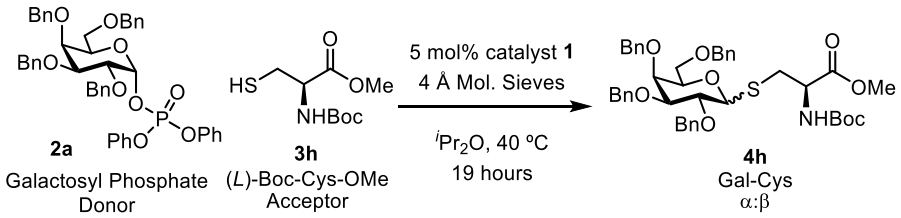

To a flame-dry 5 mL round bottom flask with a stir bar was charged 193 mg (0.250 mmol) galactosyl phosphate donor (**2a**), 250 mg flame-dry 4 Å molecular sieves, 14 mg (0.0125 mmol) catalyst **1**, and 110 mg (0.500 mmol) *L*-Boc-Cys-OMe (**3h**). 2.50 mL diisopropyl ether was added to the reaction mixture open to air and the flask was closed with a plastic cap and parafilm was used to seal the cap tightly. The mixture was then heated with efficient stirring at 40 ˚C in an oil bath for 19 hours over which time the mixture thickened. After 19 hours, the mixture is cooled to room temperature and 100 µL aliquot is diluted with diethyl ether and filtered to remove the molecular sieves. This solution is concentrated and ^{1}H NMR analysis on the crude mixture is used to determine the anomeric selectivity (β-only). The mixture was then chromatographed directly with 50 g SiO_2 using an ether/hexanes gradient on a Biotage MPLC to yield the product (**4h)** in 91% yield (172 mg, 0.227 mmol) as a single anomer.

^{1}H-NMR (600 MHz, $CDCl_3$): δ 7.38-7.26 (m, 20H), 5.89 (d, *J* = 7.3 Hz, 1H), 4.95 (d, *J* = 11.7 Hz, 1H), 4.81 (q, *J* = 8.4 Hz, 2H), 4.73-4.68 (m, 2H), 4.63 (d, *J* = 11.7 Hz, 1H), 4.47-4.45 (m, 2H), 4.41-4.39 (m, 2H), 3.99 (d, *J* = 2.0 Hz, 1H), 3.81 (t, *J* = 9.4 Hz, 1H), 3.77 (s,), 3.69 (s, 3H), 3.66 (d, *J* = 6.5 Hz, 2H), 3.56 (td, *J* = 11.6, 3.7 Hz, 2H), 3.16 (dd, *J* = 14.3, 4.1 Hz, 1H), 3.05 (dd, *J* = 14.3, 6.3 Hz, 1H), 1.45 (s, 1H), 1.41 (s, 9H).

^{13}C-NMR (126 MHz, $CDCl_3$): δ 171.49, 155.59, 138.71, 138.23, 138.07, 137.86, 128.48, 128.42, 128.38, 128.29, 127.93, 127.90, 127.84, 127.75, 127.58, 85.28, 83.95, 79.78, 77.85, 77.45, 77.41, 77.20, 76.95, 75.79, 74.58, 73.57, 73.38, 72.72, 68.34, 53.88, 52.44, 32.17, 28.44, 28.38.

HRMS-ESI (m/z): calculated for $C_{43}H_{51}NO_9S$ [M+H]+: 758.3357, found: 758.3354.

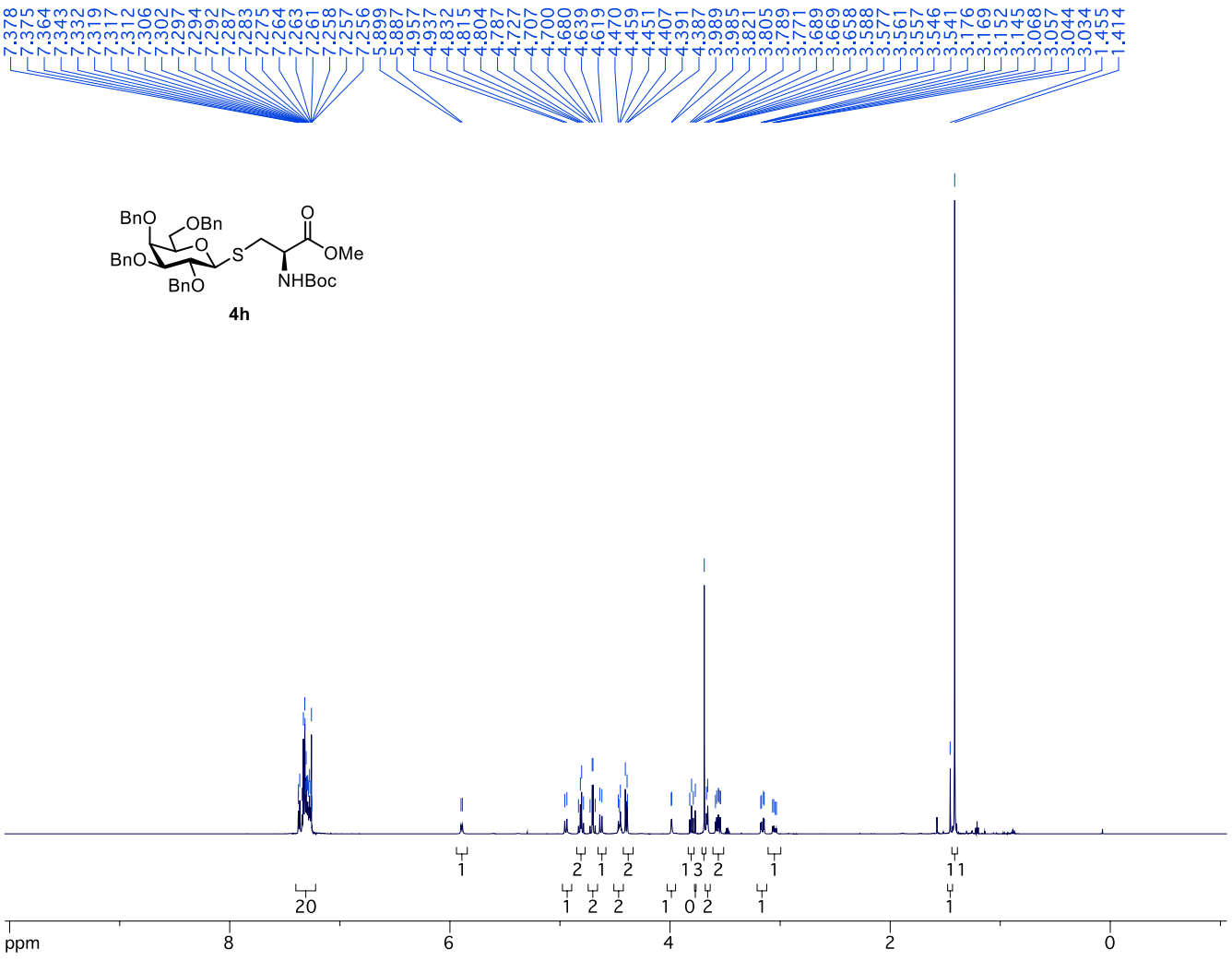

^{1}H NMR (600 MHz) spectrum of **4h** in $CDCl_3$

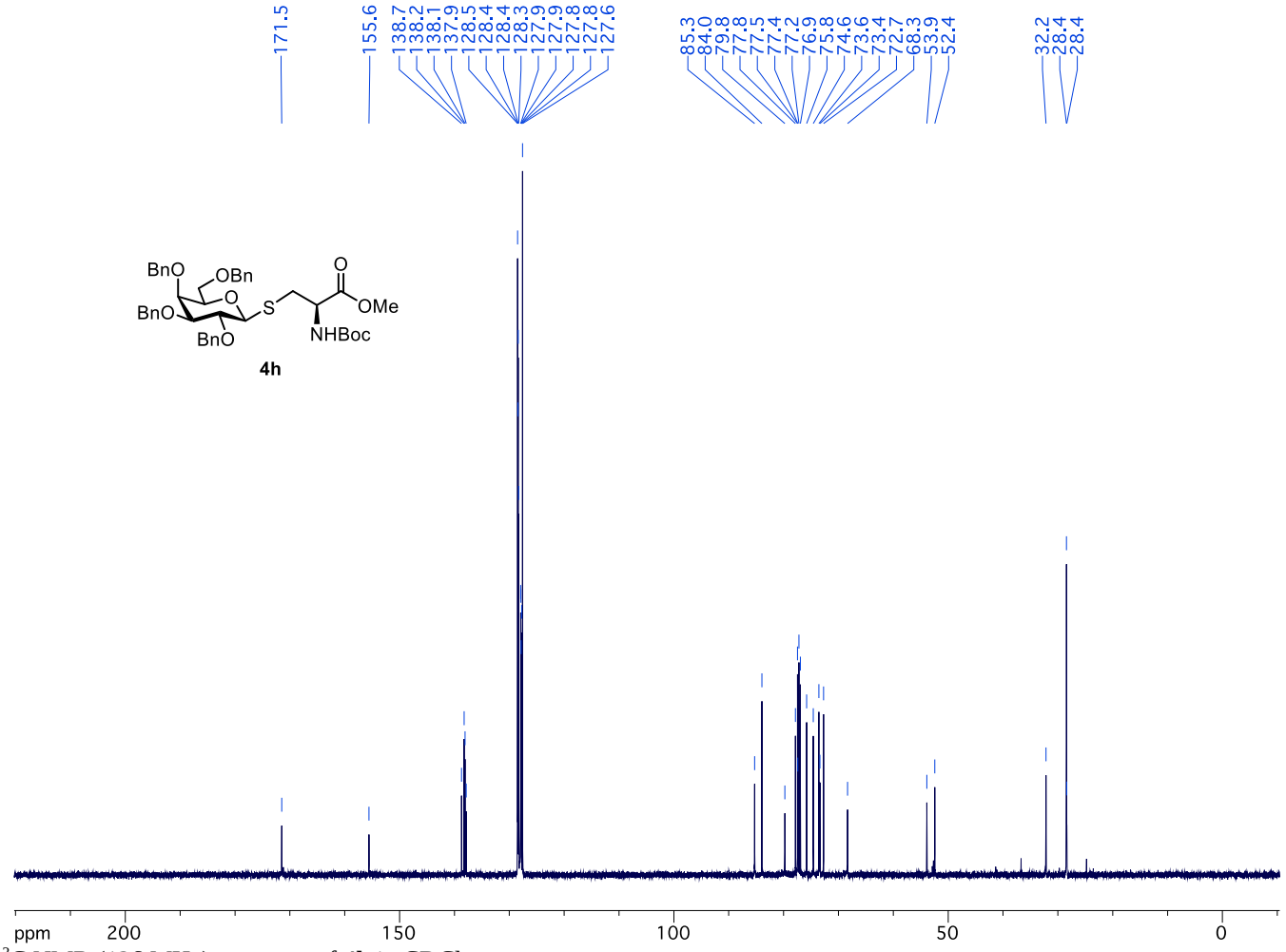

^{13}C NMR (126 MHz) spectrum of **4h** in $CDCl_3$.

Preparation of 4i

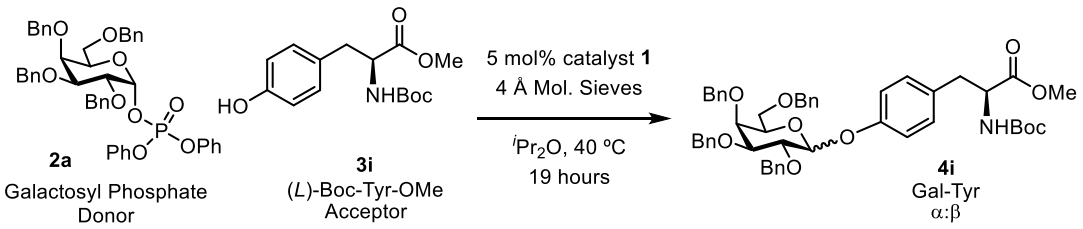

To a flame-dry 25 mL round bottom flask with a stir bar was charged 1.0 g flame-dry 4 Å molecular sieves, 14 mg (0.0125 mmol) catalyst **1**, 7.5 mL of diisopropyl ether, and 74 mg (0.250 mmol) (*L*)-BocTyrOMe (**3i**), and 2.5 mL of a 0.1 M solution of galactosyl phosphate donor (**2a**) in diisopropyl ether. Open to air, the flask was closed with a plastic cap and parafilm was used to seal the cap tightly. The mixture was then heated with efficient stirring at 40 ˚C in an oil bath for 19 hours over which time the mixture thickened. After 19 hours, the mixture is cooled to room temperature and 100 µL aliquot is diluted with diethyl ether and filtered to remove the molecular sieves. This solution is concentrated and ^{1}H NMR analysis on the crude mixture is used to determine the anomeric selectivity (86:14 β:α). The mixture was then chromatographed directly with 50 g SiO_2 using an ether/hexanes gradient on a Biotage MPLC to yield the product (**4i**) in 32% yield (65 mg, 0.080 mmol) as a mixture of anomers.

4i-β anomer:

^{1}H-NMR (600 MHz, $CDCl_3$): δ 7.37-7.25 (m, 20H), 6.99 (q, *J* = 7.3 Hz, 4H), 4.99-4.92 (m, 4H), 4.85 (d, *J* = 10.8 Hz, 1H), 4.76 (q, *J* = 11.1 Hz, 2H), 4.64 (d, *J* = 11.6 Hz, 1H), 4.56-4.54 (m, 1H), 4.43 (q, *J* = 15.1 Hz, 2H), 4.10 (t, *J* = 8.3 Hz, 1H), 3.95 (s, 1H), 3.68-3.66 (m, 4H), 3.63-3.60 (m, 3H), 3.06-2.98 (m, 2H), 1.42 (s, 9H).

^{13}C-NMR (126 MHz, $CDCl_3$): δ 172.52, 156.73, 155.23, 138.68, 138.62, 138.51, 137.99, 130.37, 130.00, 128.57, 128.54, 128.47, 128.43, 128.36, 128.32, 128.14, 128.00, 127.95, 127.91, 127.77, 127.72, 127.70, 127.64, 117.18, 102.15, 82.24, 79.34, 75.54, 74.70, 73.95, 73.75, 73.49, 73.22, 68.96, 54.60, 52.33, 37.70, 28.46.

HRMS-ESI (m/z): calculated for $C_{49}H_{55}NO_{10}$ [M+H]+: 818.3899, found: 818.3878.

4i-α anomer:

^{1}H-NMR (600 MHz, $CDCl_3$): δ 7.43-7.20 (m, 20H), 7.01 (s, 4H), 5.46 (d, *J* = 3.1 Hz, 1H), 4.99-4.95 (m, 2H), 4.90 (d, *J* = 11.6 Hz, 1H), 4.82 (dd, *J* = 20.5, 11.8 Hz, 2H), 4.71 (d, *J* = 12.0 Hz, 1H), 4.60 (d, *J* = 11.4 Hz, 1H), 4.56 (q, *J* = 6.6 Hz, 1H), 4.40 (d, *J* = 11.6 Hz, 1H), 4.35 (d, *J* = 11.6 Hz, 1H), 4.20-4.13 (m, 2H), 4.09-4.07 (m, 2H), 3.71 (s, 3H), 3.59 (t, *J* = 8.3 Hz, 1H), 3.48 (dd, *J* = 9.2, 5.6 Hz, 1H), 3.03 (qd, *J* = 15.7, 5.7 Hz, 2H), 1.43 (s, 9H).

^{13}C-NMR (126 MHz, $CDCl_3$): δ 172.54, 156.43, 155.25, 138.90, 138.75, 138.52, 138.02, 130.38, 129.84, 128.51, 128.48, 128.38, 128.33, 128.06, 127.88, 127.83, 127.80, 127.72, 127.65, 127.59, 117.40, 96.75, 80.07, 79.08, 76.34, 75.07, 75.01, 73.54, 73.51, 73.34, 70.12, 68.70, 54.61, 52.33, 37.66, 28.45.

HRMS-ESI (m/z): calculated for $C_{49}H_{55}NO_{10}$ [M+H]+: 818.3899, found: 818.3889.

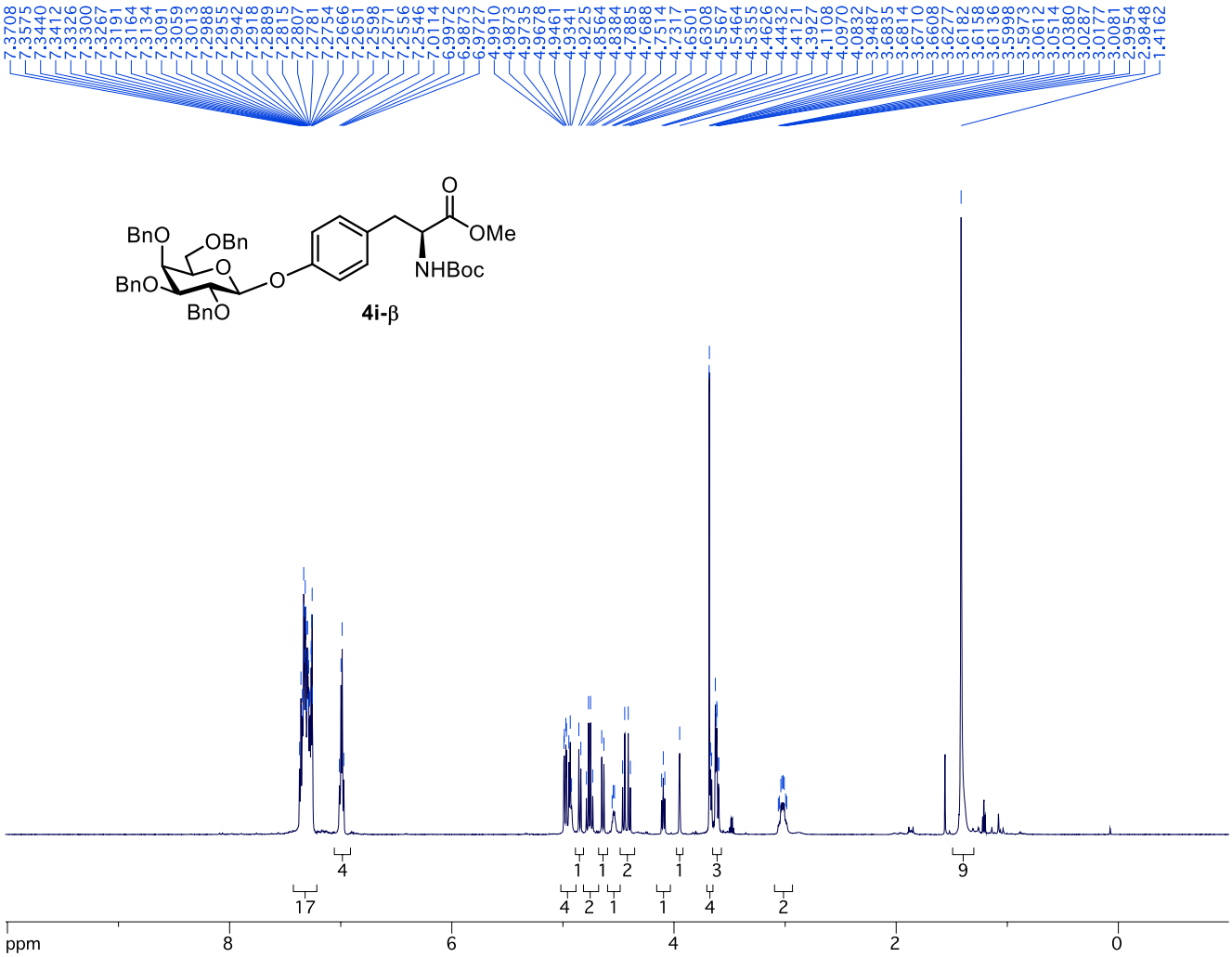

^{1}H NMR (600 MHz) spectrum of **4i-β** in $CDCl_3$

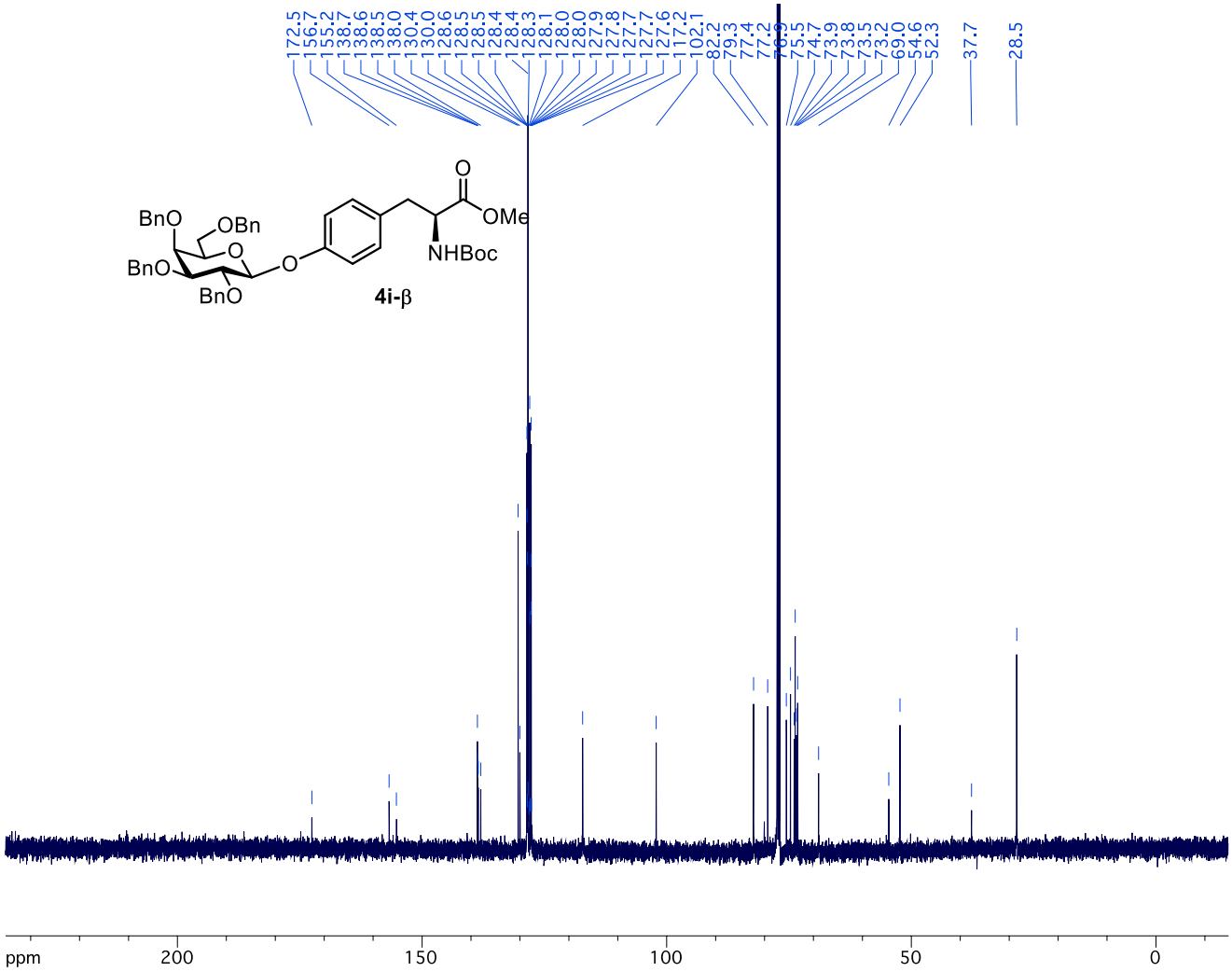

^{13}C NMR (126 MHz) spectrum of **4i-β** in $CDCl_3$.

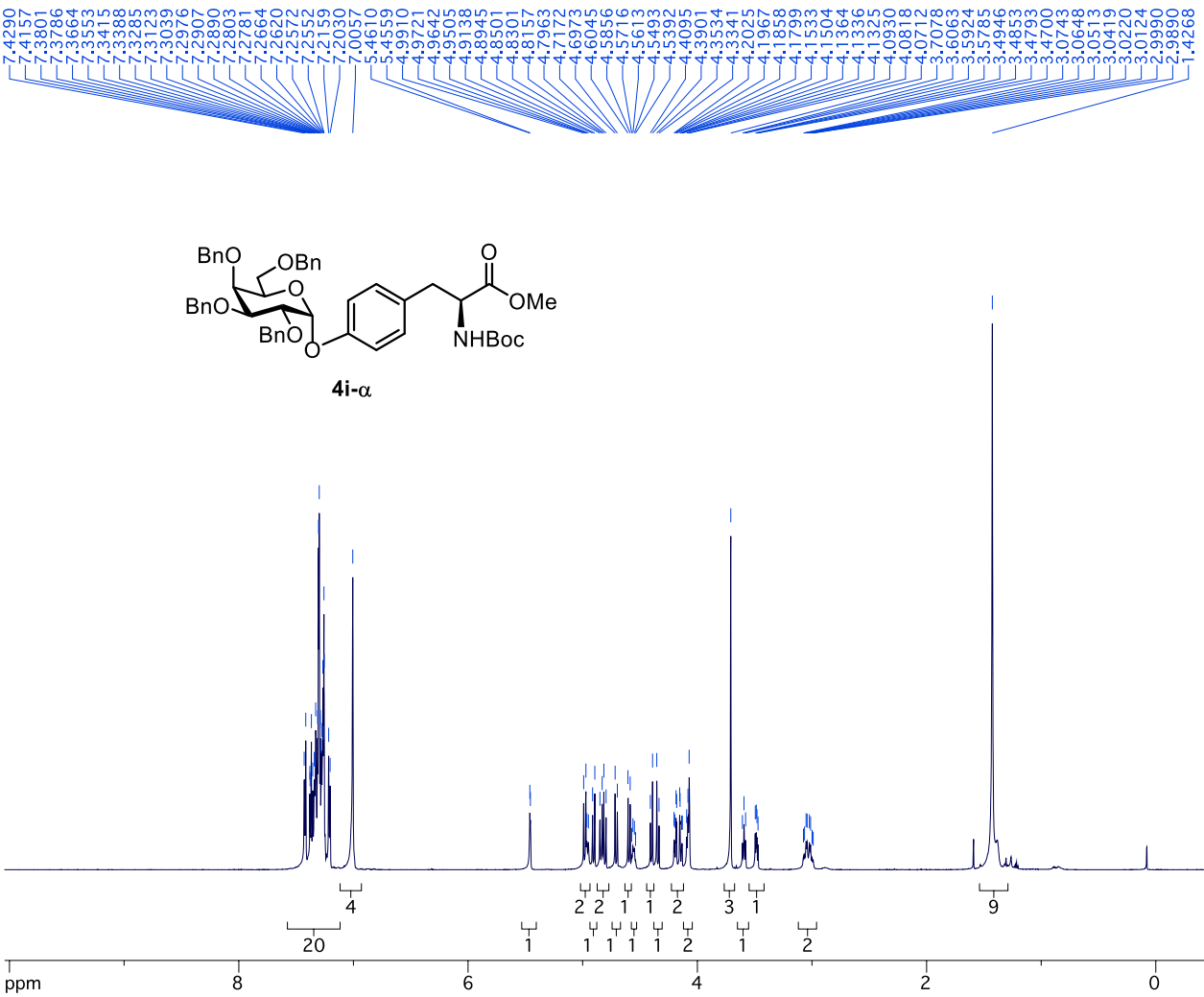

^{1}H NMR (600 MHz) spectrum of **4i-α** in $CDCl_3$

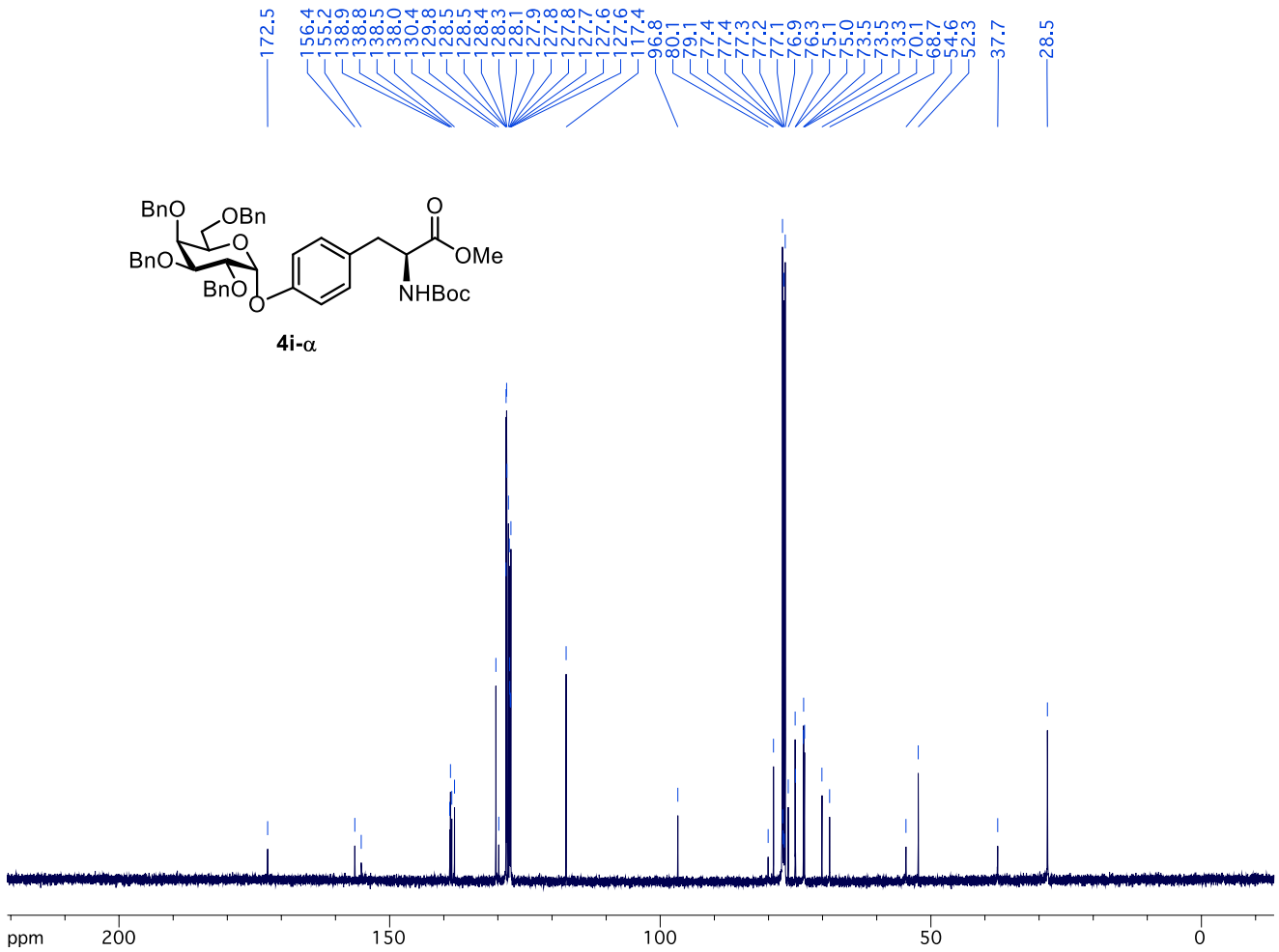

^{13}C NMR (126 MHz) spectrum of **4i-α** in $CDCl_3$.

Preparation of 4m

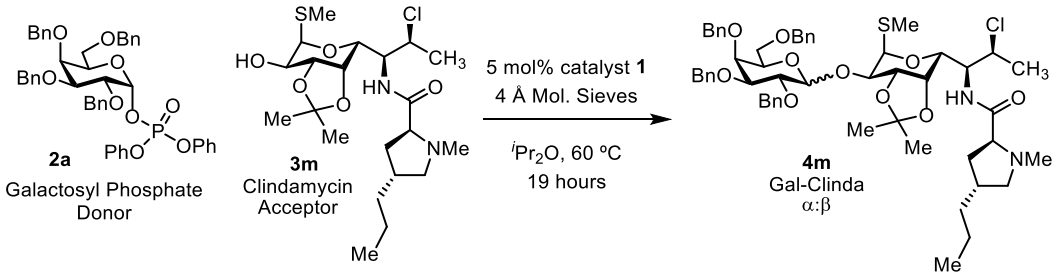

To a flame-dry 25 mL round bottom flask with a stir bar was charged 1.0 g flame-dry 4 Å molecular sieves, 14 mg (0.0125 mmol) catalyst **1**, 7.5 mL of diisopropyl ether, and 116 mg (0.250 mmol) clindamycin acetonide (**3m**), and 2.5 mL of a 0.1 M solution of galactosyl phosphate donor (**2a**) in diisopropyl ether. Open to air, the flask was closed with a plastic cap and parafilm was used to seal the cap tightly. The mixture was then heated with efficient stirring at 60 ˚C in an oil bath for 19 hours over which time the mixture thickened. After 19 hours, the mixture is cooled to room temperature and 100 µL aliquot is diluted with diethyl ether and filtered to remove the molecular sieves. This solution is concentrated and ^{1}H NMR analysis on the crude mixture is used to determine the anomeric selectivity (82:18 β:α). The mixture was then chromatographed directly with 50 g SiO_2 using an ether/hexanes gradient on a Biotage MPLC to yield the product (**4m**) in 34% yield (84 mg, 0.085 mmol) as a mixture of anomers. Further purification of anomeric mixture was conducted with reverse-phase HPLC using a C_{18} Sunfire preparatory

column and an acetonitrile/water mobile phase (0.1% formic acid added) on a 30% to 80% gradient to provide the formate salt of the β-product (**4m•HCOOH**)

^{1}H-NMR (600 MHz, CD_3OD): δ 8.46 (s, 1H), 7.41-7.23 (m, 20H), 5.33 (d, *J* = 5.0 Hz, 1H), 5.01 (d, *J* = 10.9 Hz, 1H), 4.84 (d, *J* = 11.3 Hz, 1H), 4.79 (d, *J* = 7.7 Hz, 1H), 4.73-4.67 (m, 3H), 4.61-4.57 (m, 2H), 4.53 (d, *J* = 11.5 Hz, 2H), 4.45 (q, *J* = 9.0 Hz, 2H), 4.22 (qd, *J* = 9.2, 5.0 Hz, 2H), 4.17 (dd, *J* = 4.9, 2.5 Hz, 1H), 3.90 (d, *J* = 2.9 Hz, 1H), 3.68 (dd, *J* = 9.7, 7.8 Hz, 1H), 3.62 (t, *J* = 6.1 Hz, 1H), 3.59-3.55 (m, 2H), 3.52 (dd, *J* = 9.5, 5.7 Hz, 1H), 3.33 (dd, *J* = 8.8, 6.1 Hz, 1H), 3.25 (dd, *J* = 10.3, 5.3 Hz, 1H), 2.50 (s, 3H), 2.27-2.18 (m, 3H), 2.10 (s, 3H), 2.02-1.91 (m, 2H), 1.43 (d, *J* = 5.7 Hz, 7H), 1.40-1.29 (m, 5H), 1.28-1.25 (m, 4H), 0.91 (t, *J* = 7.1 Hz, 3H).

^{13}C-NMR (126 MHz, CD_3OD): δ 175.04, 140.22, 139.97, 139.90, 139.43, 129.46, 129.41, 129.38, 129.34, 129.24, 129.21, 129.12, 129.00, 128.85, 128.76, 128.66, 128.61, 128.50, 110.32, 104.78, 86.84, 83.00, 80.38, 77.23, 77.21, 75.88, 75.77, 75.60, 74.80, 74.56, 74.34, 74.16, 70.28, 69.71, 67.80, 63.35, 59.76, 54.38, 49.51, 49.34, 49.17, 49.00, 48.83, 48.66, 48.49, 41.70, 38.88, 38.26, 36.75, 28.58, 26.87, 22.98, 22.49, 14.57, 13.33.

HRMS-ESI (m/z): calculated for $C_{55}H_{71}ClN_2O_{10}S$ [M+H]+: 987.4591, found: 987.4590.

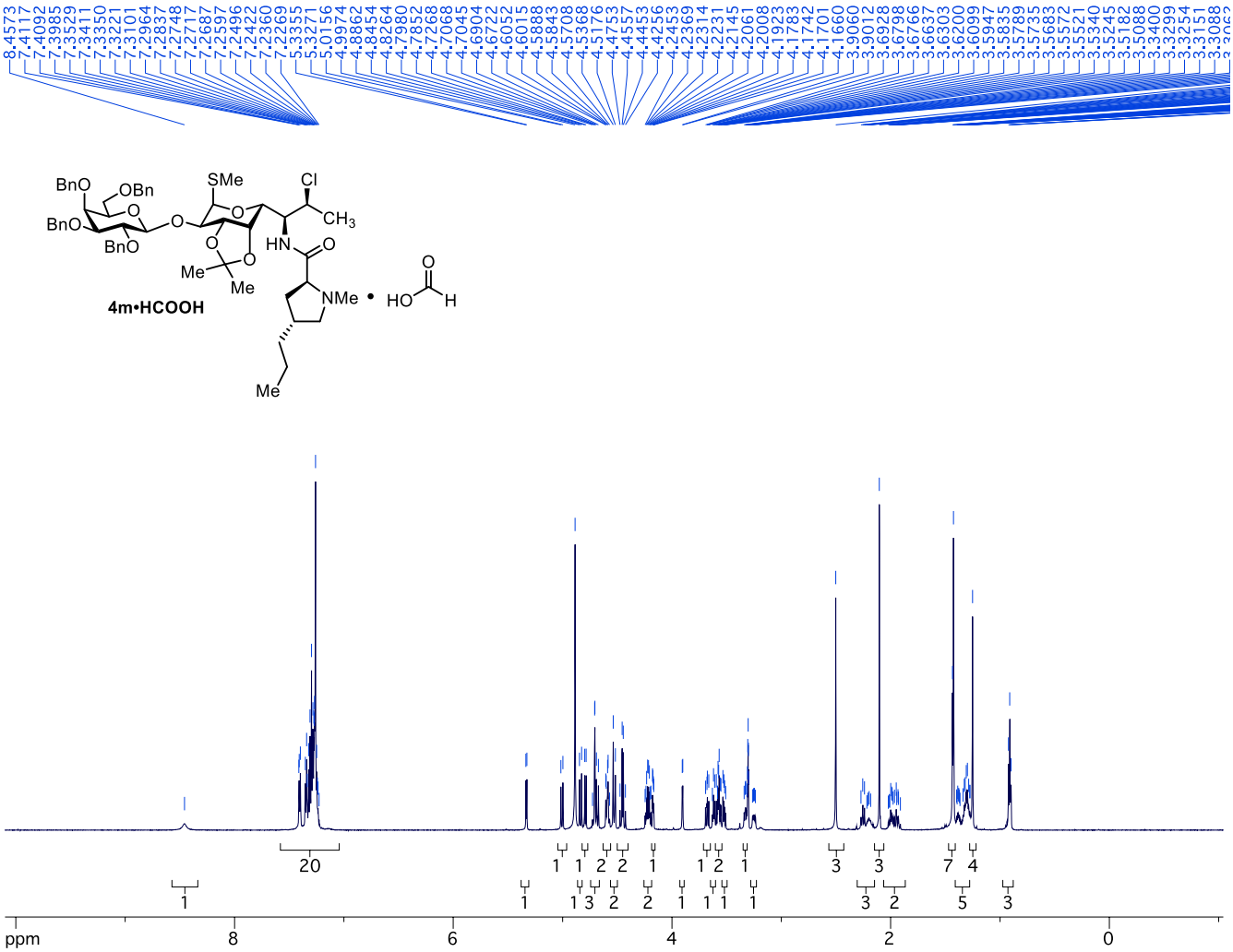

^{1}H NMR (600 MHz) spectrum of **4m•HC(O)OH** in CD_3OD

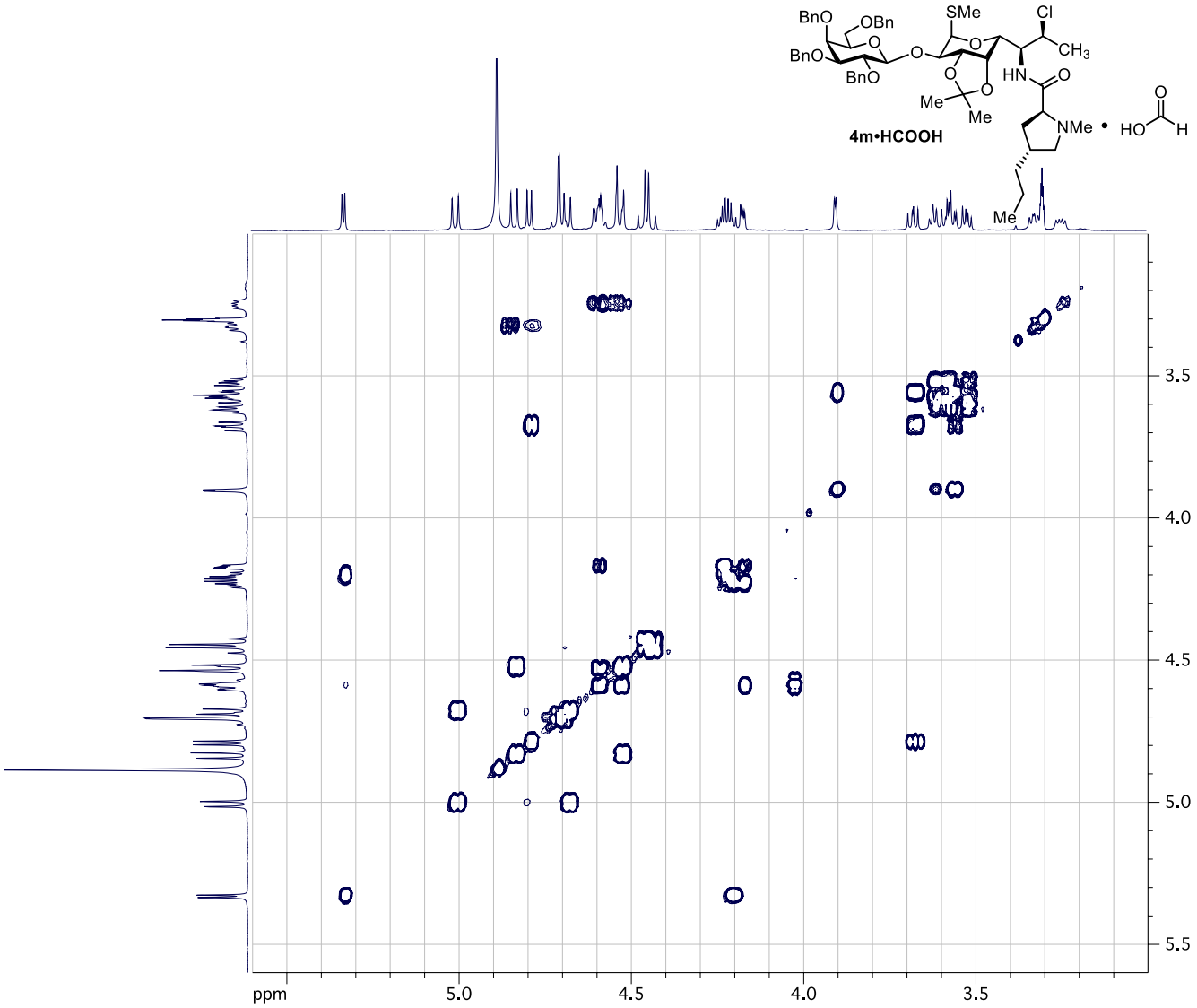

^{1}H-^{1}H COSY NMR (600 MHz) spectrum of **4m•HCOOH** in CD_3OD

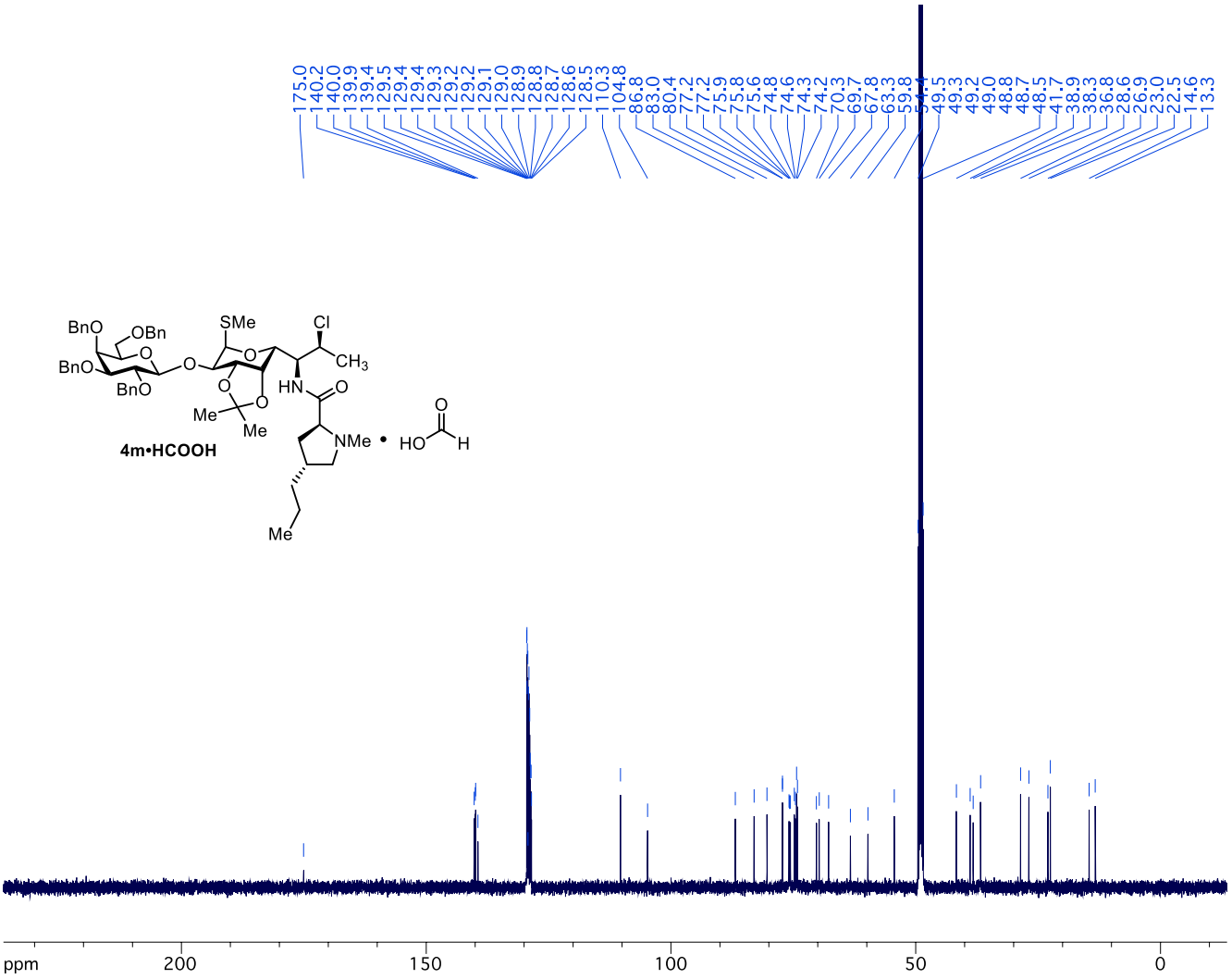

^{13}C NMR (126 MHz) spectrum of **4m•HCOOH** in CD_3OD.

Preparation of 5i

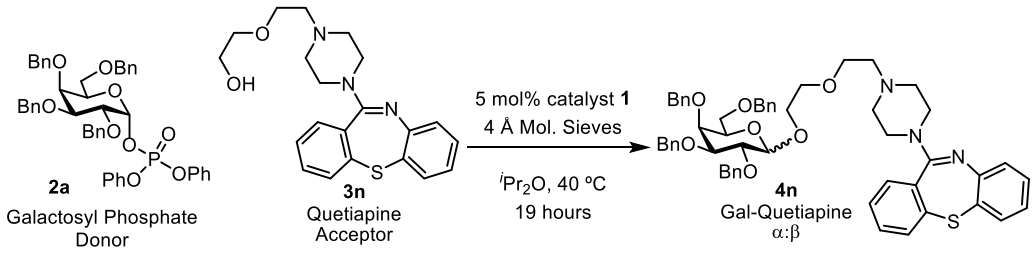

To a flame-dry 25 mL round bottom flask with a stir bar was charged 1.0 g flame-dry 4 Å molecular sieves, 14 mg (0.0125 mmol) catalyst **1**, and 96 mg (0.25 mmol) quetiapine (**3n**), and 2.5 mL of a 0.1 M solution of galactosyl phosphate donor (**2a**) in diisopropyl ether. 7.5 mL diisopropyl ether was additionally added to the reaction mixture (10 mL total volume, 0.025 M) open to air and the flask was closed with a plastic cap and parafilm was used to seal the cap tightly. The mixture was then heated with efficient stirring at 40 ˚C in an oil bath for 19 hours over which time the mixture thickened. After 19 hours, the mixture is cooled to room temperature and 100 μL aliquot is diluted with diethyl ether and filtered to remove the molecular sieves. This solution is concentrated and ^{1}H NMR analysis on the crude mixture is used to determine the anomeric selectivity (98:2 β:α). The mixture

was then chromatographed directly with 50 g SiO_2 using an ether/hexanes gradient on a Biotage MPLC to yield the product (**4n**) in 72% yield (166 mg, 0.183 mmol) as a mixture of anomers.

^{1}H-NMR (600 MHz, $CDCl_3$): δ 7.49 (d, *J* = 7.6 Hz, 1H), 7.39-7.24 (m, 24H), 7.17-7.14 (m, 1H), 7.06 (d, *J* = 8.0 Hz, 1H), 6.87 (td, *J* = 7.5, 1.4 Hz, 1H), 4.93 (m, *J* = 3.0 Hz, 2H), 4.75-4.69 (m, 3H), 4.61 (dd, *J* = 11.7, 1.4 Hz, 1H), 4.45-4.38 (m, 3H), 4.02-3.99 (m, 1H), 3.88 (t, *J* = 1.4 Hz, 1H), 3.81 (dd, *J* = 9.7, 7.7 Hz, 1H), 3.73 (m, *J* = 4.3, 2.2 Hz, 1H), 3.69-3.64 (m, 2H), 3.62 (t, *J* = 5.8 Hz, 2H), 3.58-3.57 (m, 2H), 3.53-3.49 (m, 3H), 2.58 (t, *J* = 5.8 Hz, 3H), 2.48 (s, 2H).

^{13}C-NMR (126 MHz, $CDCl_3$): δ 160.75, 160.74, 149.00, 139.92, 138.89, 138.66, 138.56, 137.94, 134.18, 132.20, 132.15, 130.74, 129.10, 129.03, 128.46, 128.38, 128.36, 128.28, 128.26, 128.20, 128.17, 128.00, 127.91, 127.82, 127.57, 125.37, 122.76, 104.13, 82.18, 79.50, 75.05, 74.54, 73.57, 73.53, 73.43, 73.11, 70.29, 68.98, 68.96, 68.88, 57.94, 53.42, 53.38.

HRMS-ESI (m/z): calculated for $C_{55}H_{59}N_3O_7S$ [M+H]+: 906.4146, found: 906.4148.

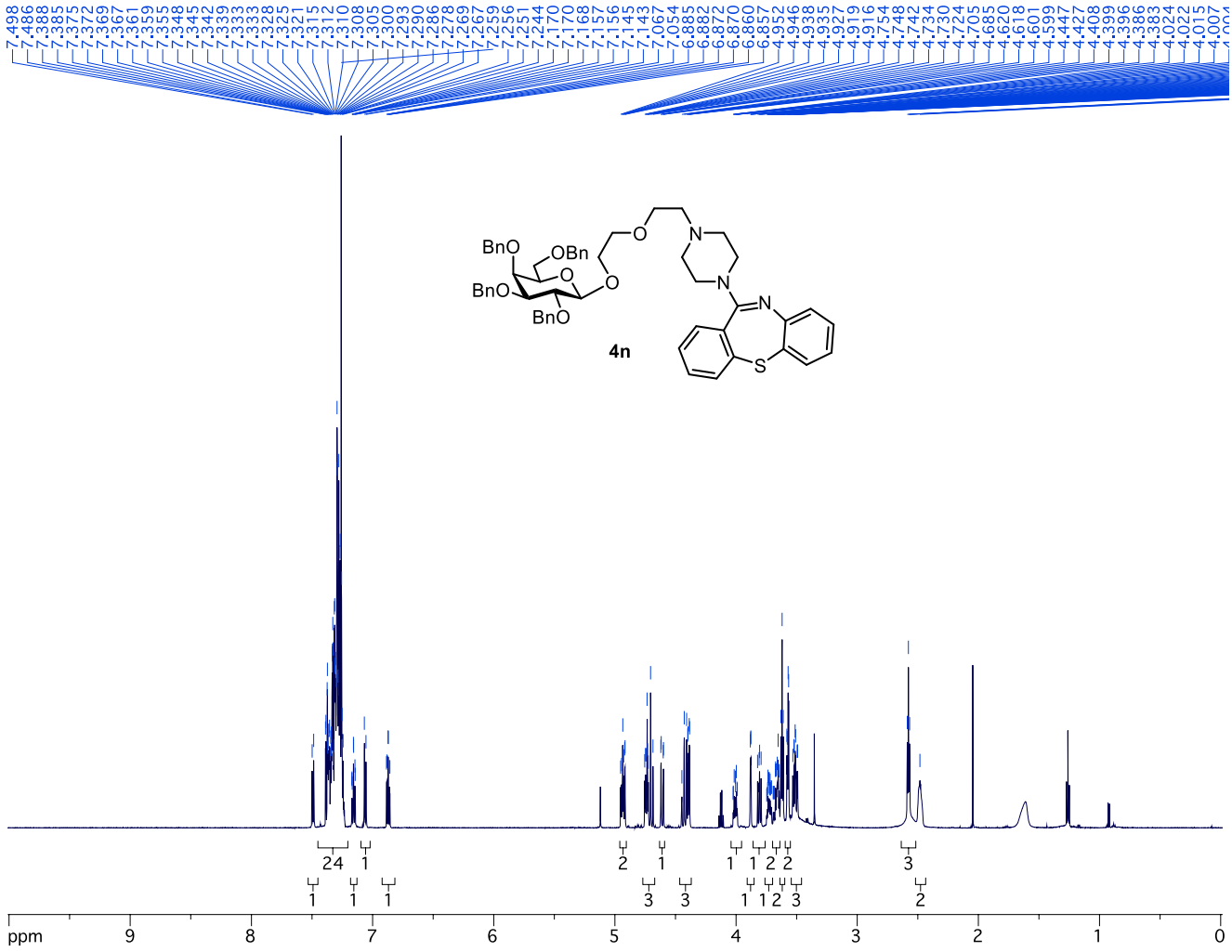

^{1}H NMR (600 MHz) spectrum of **4n** in $CDCl_3$

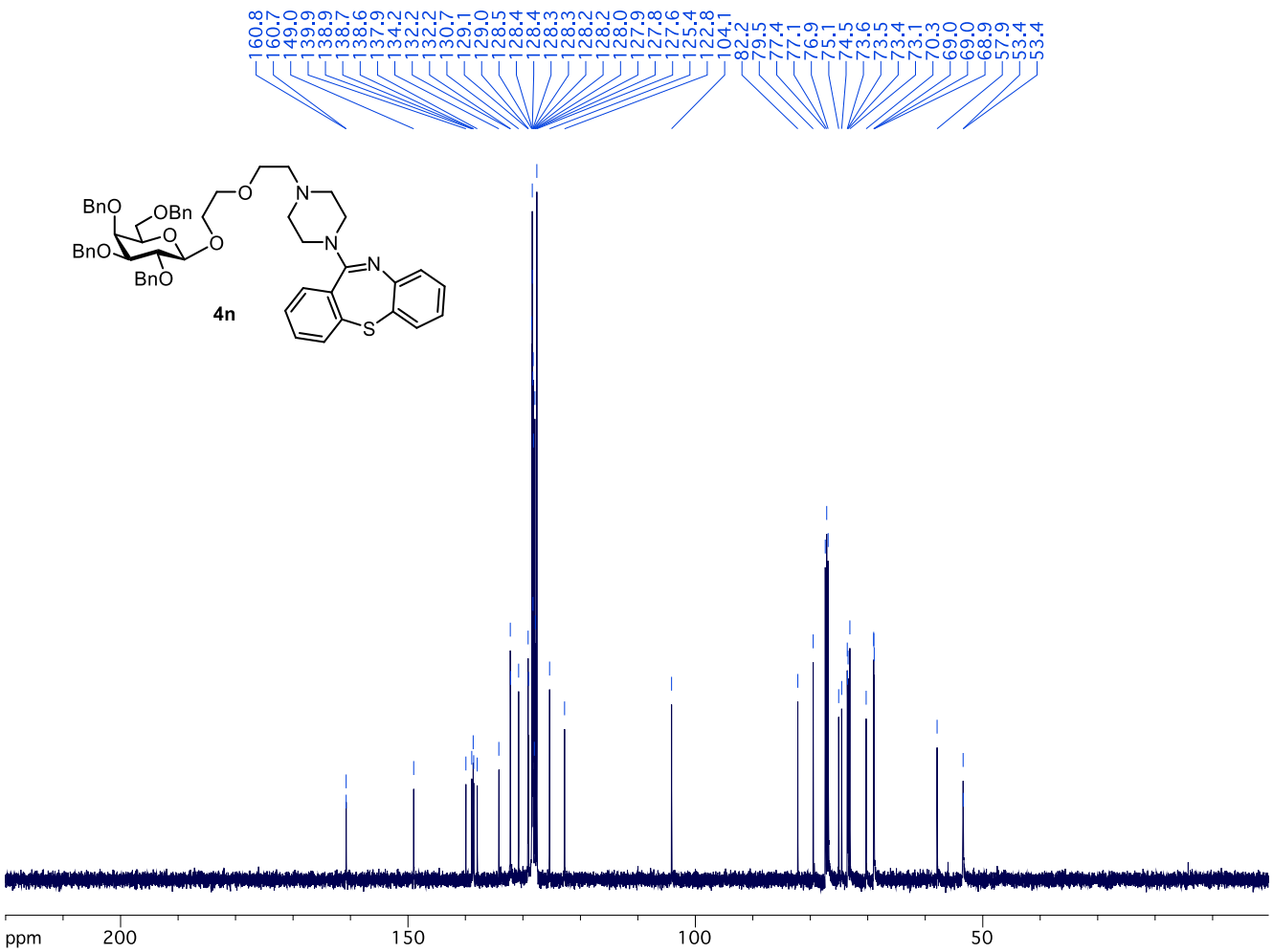

^{13}C NMR (126 MHz) spectrum of **4n** in $CDCl_3$.

Preparation of 3o

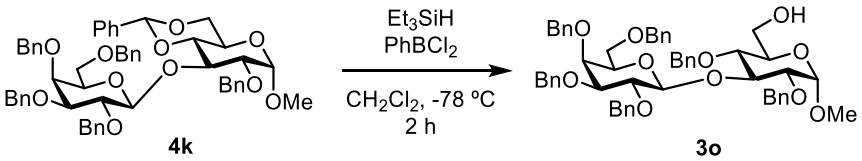

To a flame-dry round bottom flask with a stir bar was charged Gal-β(1,3)-Glu (**4k**) (130 mg, 0.145 mmol), fitted with a septum, and flushed with nitrogen 3-times. Next, 8 mL dry dichloromethane was added to the reaction mixture under nitrogen and cooled to -78 ˚C in a dry ice-acetone bath. When the temperature had equilibrated, triethylsilane (23 µL, 0.29 mmol) and dichlorophenylborane (21 µL, 0.29 mmol) were added sequentially with glass microliter syringes. The mixture was left stirring at -78 ˚C for 2 hours at which point no remaining starting material was observed by TLC analysis. The mixture was concentrated with a stream of nitrogen air and then chromatographed directly without workup on two 25 g SiO_2 using an ether/hexanes gradient on a Biotage MPLC to afford the product (**3o**) in 39% yield (50 mg, 0.056 mmol) as an oil.

^{1}H-NMR (600 MHz, $CDCl_3$): δ 7.40-7.26 (m, 30H), 5.00-4.93 (m, 3H), 4.79 (d, *J* = 11.9 Hz, 1H), 4.73 (d, *J* = 11.9 Hz, 1H), 4.71 (d, *J* = 10.5 Hz, 1H), 4.58 (d, *J* = 11.6 Hz, 1H), 4.55 (d, *J* = 11.6 Hz, 1H), 4.49 (d, *J* = 11.6 Hz, 1H), 4.46 (d, *J* = 11.8 Hz, 1H), 4.40 (d, *J* = 11.8 Hz, 1H), 4.33 (d, *J* = 7.7 Hz, 1H), 4.27 (d, *J* = 4.9 Hz, 1H), 4.21 (dd, *J* = 9.4, 4.9 Hz, 1H), 4.09-4.06 (m,

1H), 4.04 (s, 1H), 4.01 (s, 1H), 3.92-3.90 (m, 1H), 3.86 (d, J = 2.7 Hz, 1H), 3.83 (dd, J = 9.7, 7.8 Hz, 1H), 3.74 (dd, J = 10.9, 6.1 Hz, 1H), 3.56-3.47 (m, 5H), 3.34 (s, 3H).

^{13}C-NMR (126 MHz, $CDCl_3$): δ 138.68, 138.44, 138.38, 138.36, 137.60, 137.58, 137.31, 128.49, 128.43, 128.35, 128.30, 128.08, 128.02, 127.94, 127.82, 127.67, 127.61, 127.55, 108.15, 103.96, 87.37, 82.01, 81.75, 81.64, 78.63, 74.99, 74.64, 73.74, 73.63, 73.21, 72.41, 69.16, 68.42, 64.64, 55.33.

HRMS-ESI (m/z): calculated for $C_{55}H_{60}N_3O_{11}$ [M+H]+: 897.4208, found: 897.4189.

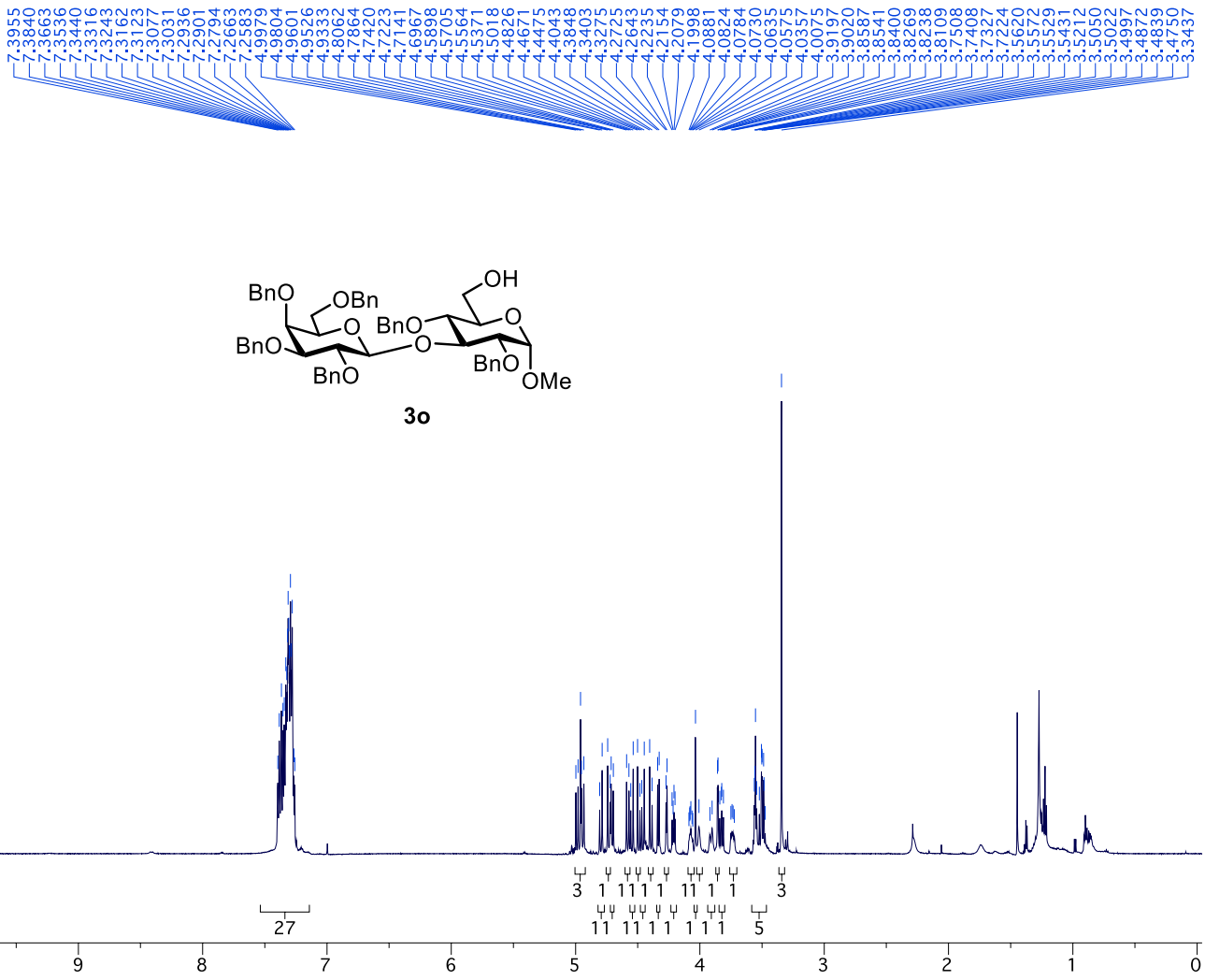

^{1}H NMR (600 MHz) spectrum of **3o** in $CDCl_3$

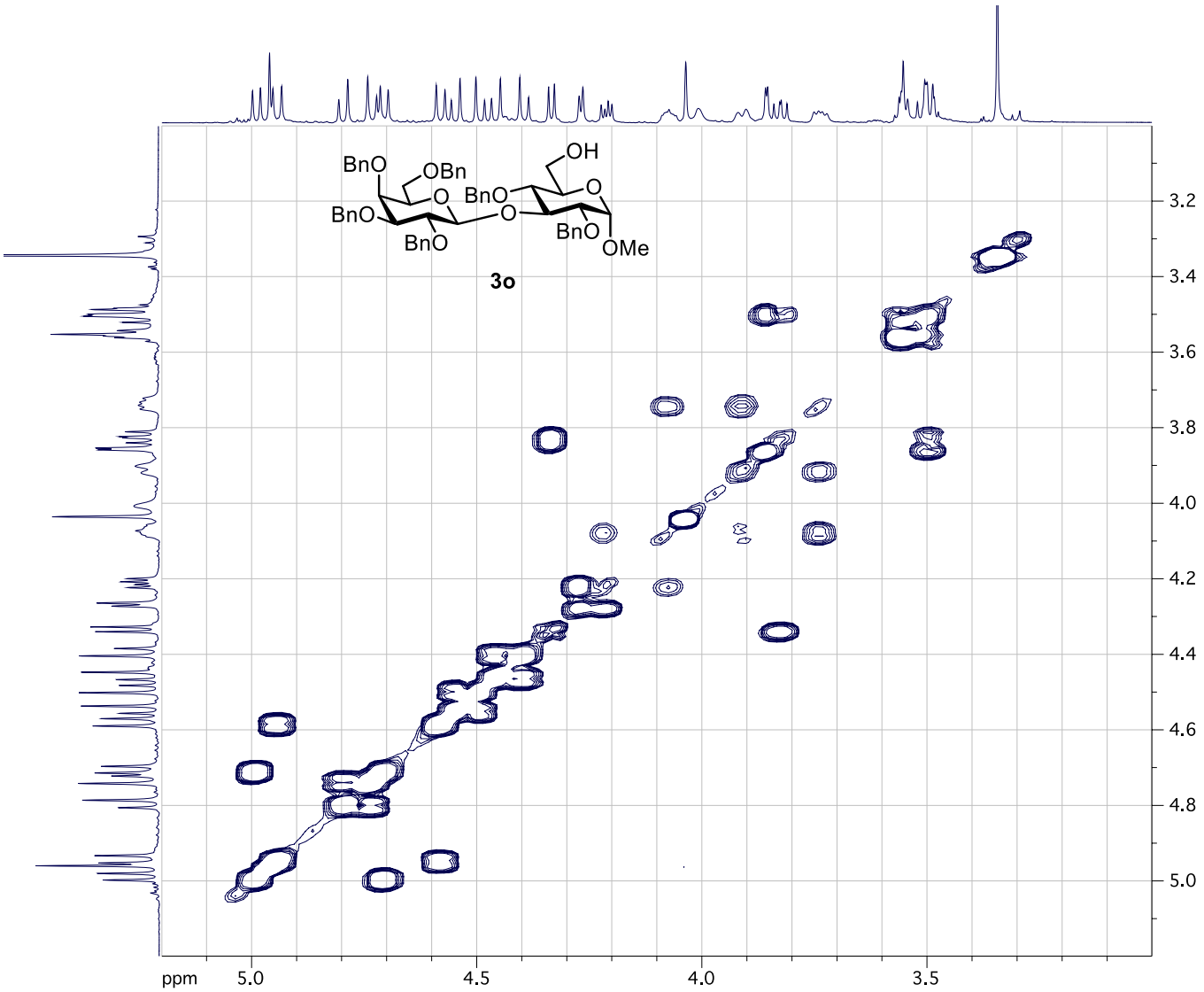

^{1}H-^{1}H COSY NMR (600 MHz) spectrum of **3o** in $CDCl_3$

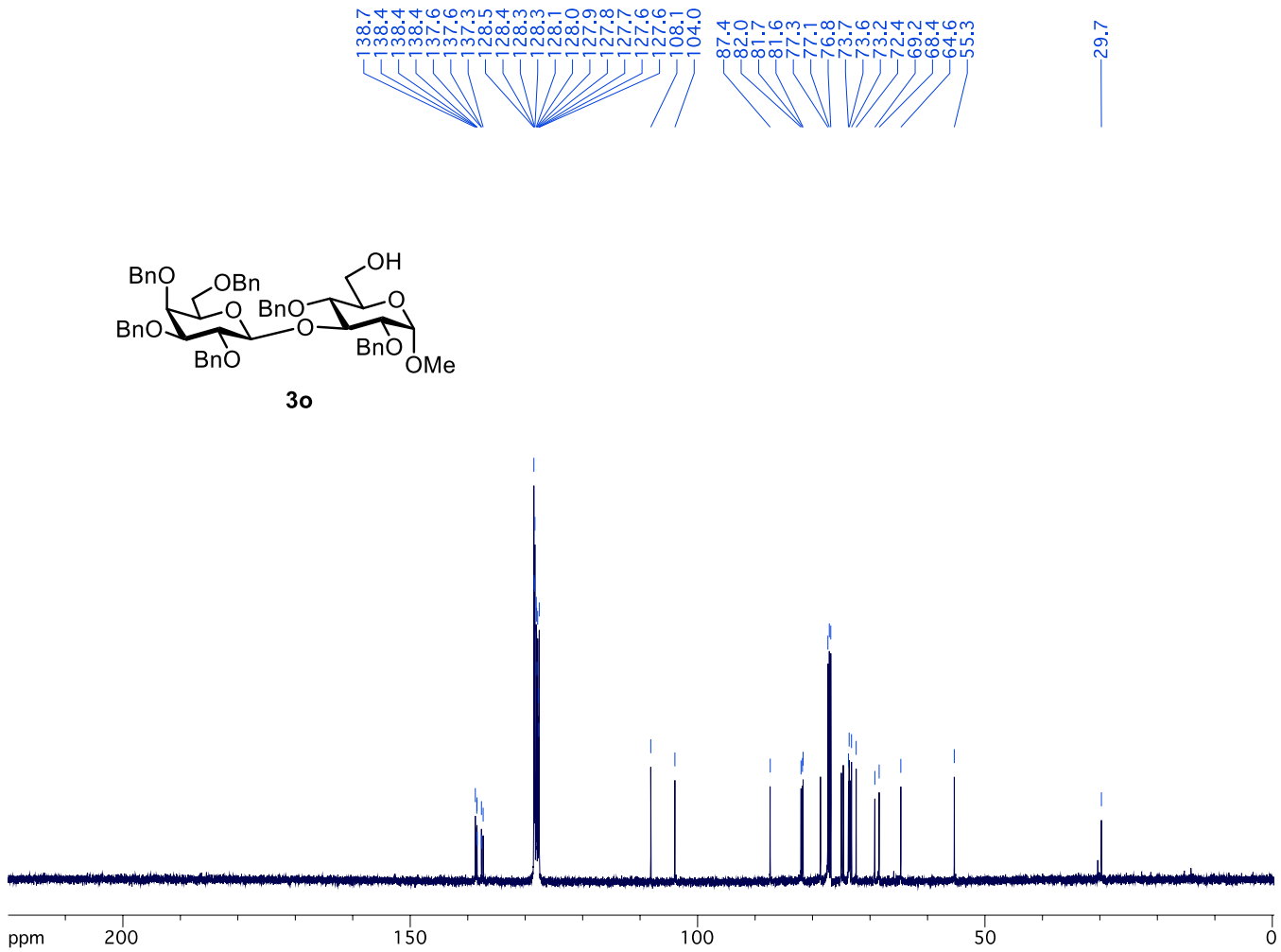

^{13}C NMR (126 MHz) spectrum of **3o** in $CDCl_3$.

Preparation of 4o

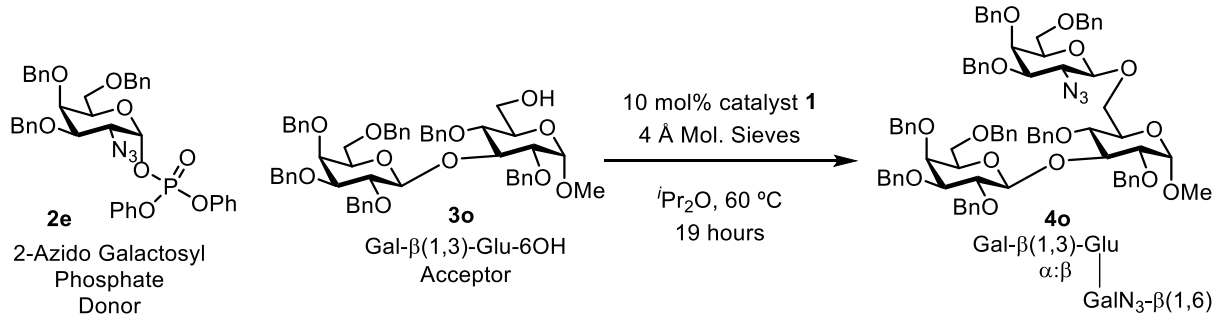

To an oven-dry 0.5-dram vial with a stir bar was charged 40 mg flame-dry 4 Å molecular sieves, 4 mg (4 µmol) catalyst **1**, and 38 mg (42 µmol) Gal-β(1,3)Glu-6OH acceptor (**3o**), and 390 µL of a 0.1 M solution of 2-azido galactosyl phosphate donor (**2e**) was added open to air and the vial was closed with a PTFE cap. The mixture was then heated with efficient stirring at 60 ˚C in an oil bath for 19 hours over which time the mixture thickened. After 19 hours, the mixture is cooled to room temperature and the entire mixture is diluted with diethyl ether and filtered to remove the molecular sieves. This solution is concentrated and ^{1}H NMR analysis on the crude mixture is used to determine the anomeric selectivity (β–only). The mixture was then

chromatographed directly with 50 g SiO_2 using an ether/hexanes gradient on a Biotage MPLC to afford the product (**4o**) in 70% yield (37 mg, 27 μmol) as a single anomer. Fractions before and after the eluted product were also collected, concentrated, and analyzed by NMR and no trace of the α-anomer was observed.

^{1}H-NMR (600 MHz, $CDCl_3$): δ 7.39-7.23 (m, 45H), 4.97 (d, *J* = 10.5 Hz, 1H), 4.92-4.88 (m, 3H), 4.75 (d, *J* = 11.9 Hz, 1H), 4.70-4.64 (m, 4H), 4.56 (dd, *J* = 11.6, 1.1 Hz, 2H), 4.53 (d, *J* = 11.7 Hz, 1H), 4.47 (d, *J* = 11.6 Hz, 1H), 4.44-4.33 (m, 5H), 4.27 (dt, *J* = 13.8, 6.7 Hz, 3H), 4.21-4.17 (m, 2H), 4.01 (s, 1H), 3.91 (dd, *J* = 10.3, 8.1 Hz, 1H), 3.86 (dd, *J* = 13.0, 2.6 Hz, 2H), 3.79 (dd, *J* = 9.8, 7.8 Hz, 1H), 3.71 (dd, *J* = 10.5, 5.7 Hz, 2H), 3.63 (d, *J* = 16.8 Hz, 1H), 3.57 (dd, *J* = 9.2, 5.4 Hz, 1H), 3.53-3.49 (m, 4H), 3.45 (dd, *J* = 9.8, 2.9 Hz, 1H), 3.32 (dd, *J* = 10.5, 2.9 Hz, 1H), 3.29 (s, 3H).

^{13}C-NMR (126 MHz, $CDCl_3$): δ 138.91, 138.68, 138.60, 138.57, 137.98, 137.87, 137.83, 137.54, 128.57, 128.55, 128.48, 128.37, 128.35, 128.30, 128.20, 128.15, 128.09, 128.02, 127.97, 127.95, 127.90, 127.84, 127.70, 127.62, 108.28, 103.72, 103.13, 87.49, 81.94, 81.43, 81.06, 81.01, 78.79, 77.41, 77.37, 77.16, 76.91, 75.09, 74.69, 74.67, 73.77, 73.65, 73.53, 73.20, 72.60, 72.40, 72.38, 71.68, 69.06, 68.59, 68.35, 63.22, 55.35, 29.83.

HRMS-ESI (m/z): calculated for $C_{82}H_{87}N_3O_{15}$ [M+H]+: 1354.621, found: 1354.6173.

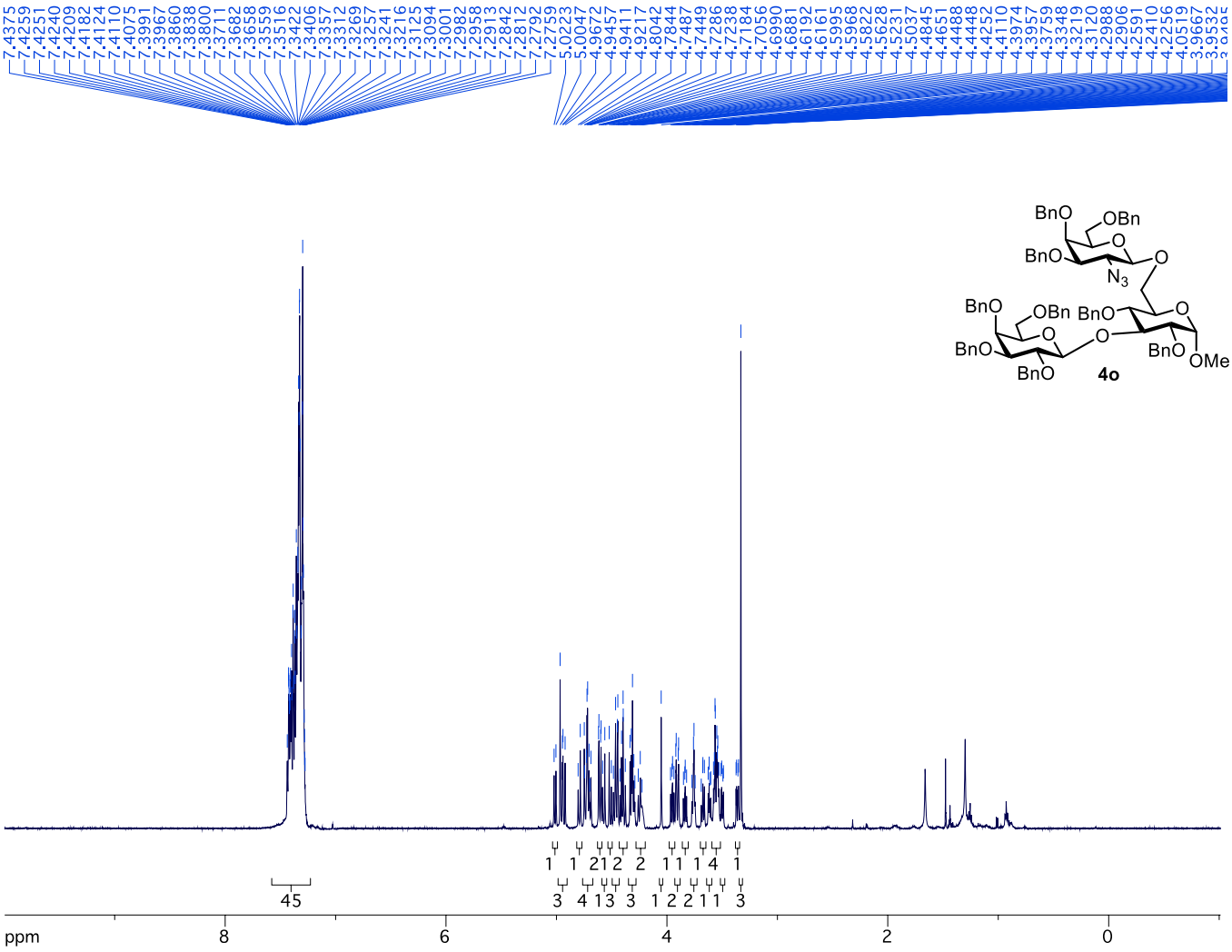

^{1}H NMR (600 MHz) spectrum of **4o** in $CDCl_3$

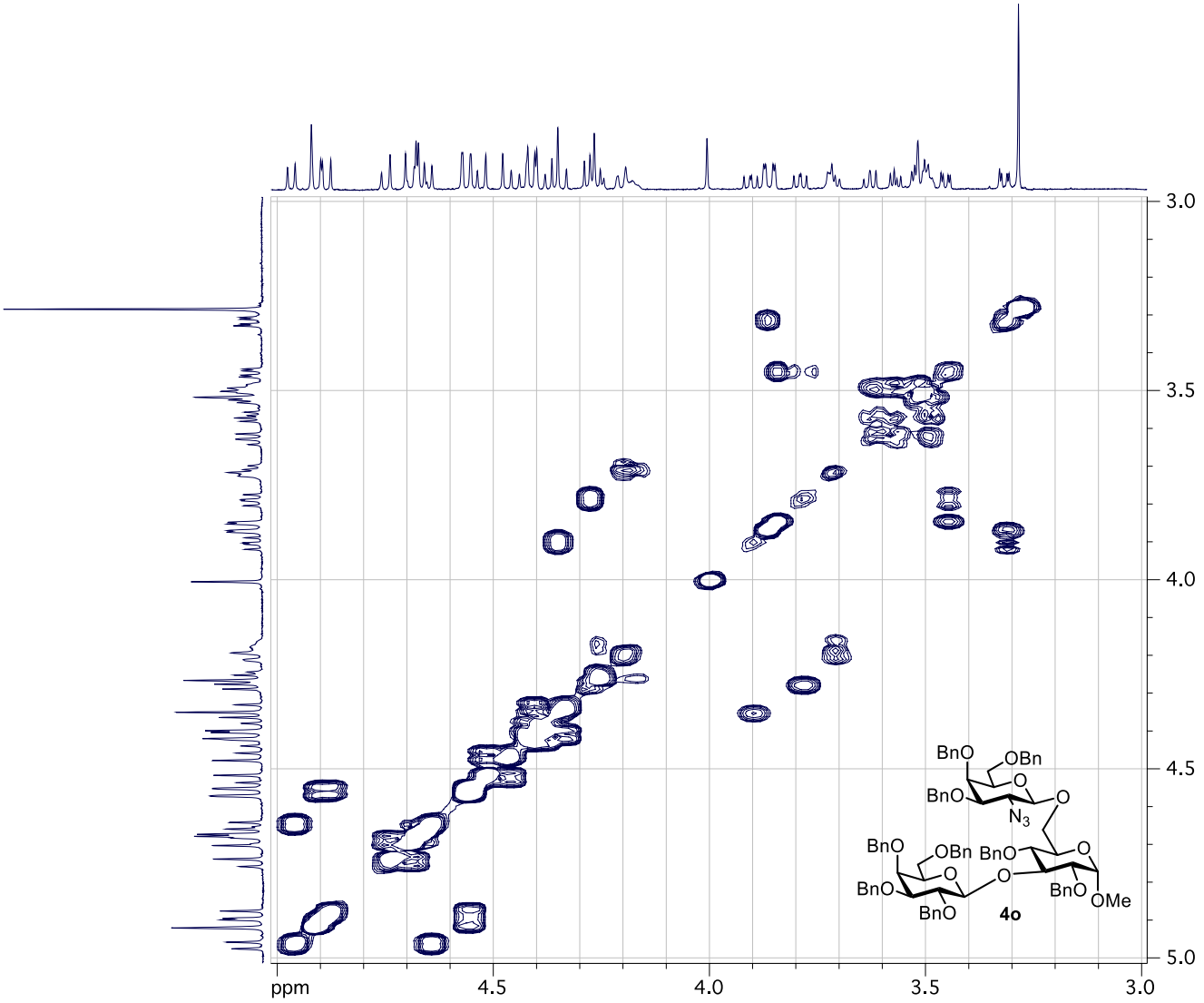

^{1}H-^{1}H COSY NMR (600 MHz) spectrum of **4o** in $CDCl_3$

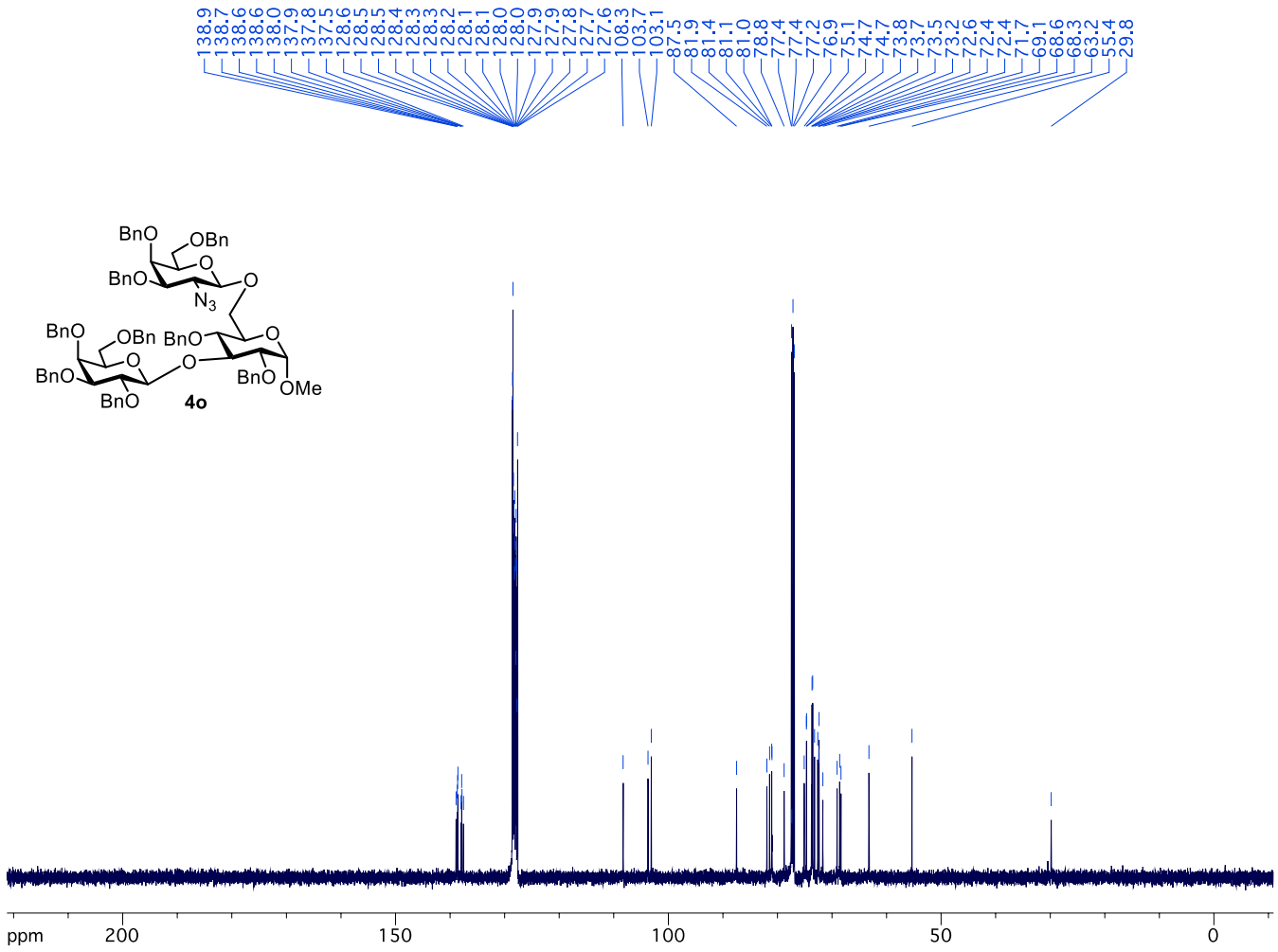

^{13}C NMR (126 MHz) spectrum of **4o** in $CDCl_3$.

Preparation of 2f

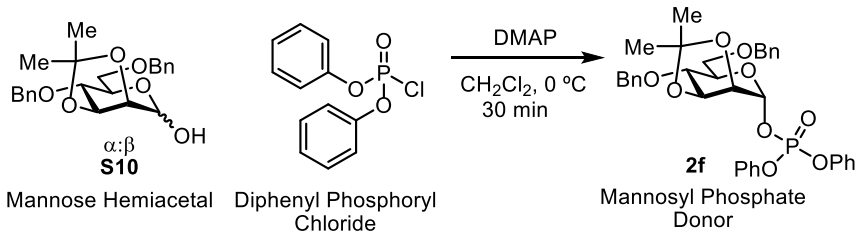

To a flame-dry 25 mL round bottom flask with a stir bar was charged 0.22 g (1.8 mmol, 3.0 equiv.) DMAP. The flask was evacuated and backfilled with nitrogen three times. To the flask was added a solution of 0.240 g (0.6 mmol, 1.0 equiv.) 2,3-Isopropylidene-4,6-O-benzyl mannose hemiacetal (**S10**) in 10 mL dry dichloromethane. The reaction was cooled to 0 °C, and 0.15 mL (0.72 mmol, 1.2 equiv.) diphenyl phosphoryl chloride was added dropwise. The reaction was stirred at 0 °C for 30 minutes. The reaction was concentrated and purified on 25 g SiO_2 using an ether/hexanes gradient on a Biotage MPLC to yield the product (**2f**) in 58% yield (0.220 g, 0.35 mmol).

*Note: the mannosyl donor (**2f**) is best stored as a solution in ethereal solvents. Higher yields of activation are possible by using C2-functionalized reverse phase silica gel with the same mobile phase.*

^{1}H-NMR (600 MHz, $CDCl_3$): δ 7.33-7.15 (m, 20H), 6.18 (d, *J* = 6.5 Hz, 1H), 4.84 (d, *J* = 11.3 Hz, 1H), 4.57 (dd, *J* = 20.6, 11.8 Hz, 2H), 4.47 (d, *J* = 12.2 Hz, 1H), 4.33 (t, *J* = 6.4 Hz, 1H), 4.13 (d, *J* = 5.7 Hz, 1H), 3.86-3.84 (m, 1H), 3.73 (dd, *J* = 10.2, 7.1 Hz, 1H), 3.68 (dd, *J* = 11.1, 3.7 Hz, 1H), 3.50-3.45 (m, 2H), 1.50 (s, 3H), 1.34 (s, 3H).

^{13}C-NMR (126 MHz, $CDCl_3$): δ 150.41, 150.36, 150.31, 138.12, 138.01, 129.57, 128.61, 128.45, 128.43, 128.38, 128.15, 128.04, 127.80, 127.69, 127.54, 125.55, 125.47, 120.22, 120.18, 120.14, 120.07, 120.05, 110.08, 97.40, 97.35, 78.13, 77.23, 77.19, 76.90, 75.45, 75.36, 74.53, 73.47, 73.20, 71.00, 67.99, 27.86, 26.37.

^{31}P-NMR (162 MHz, $CDCl_3$): δ -14.25.

HRMS-ESI (m/z): calculated for $C_{35}H_{37}O_9P$ [M+H]+: 633.2248, found: 633.2239.

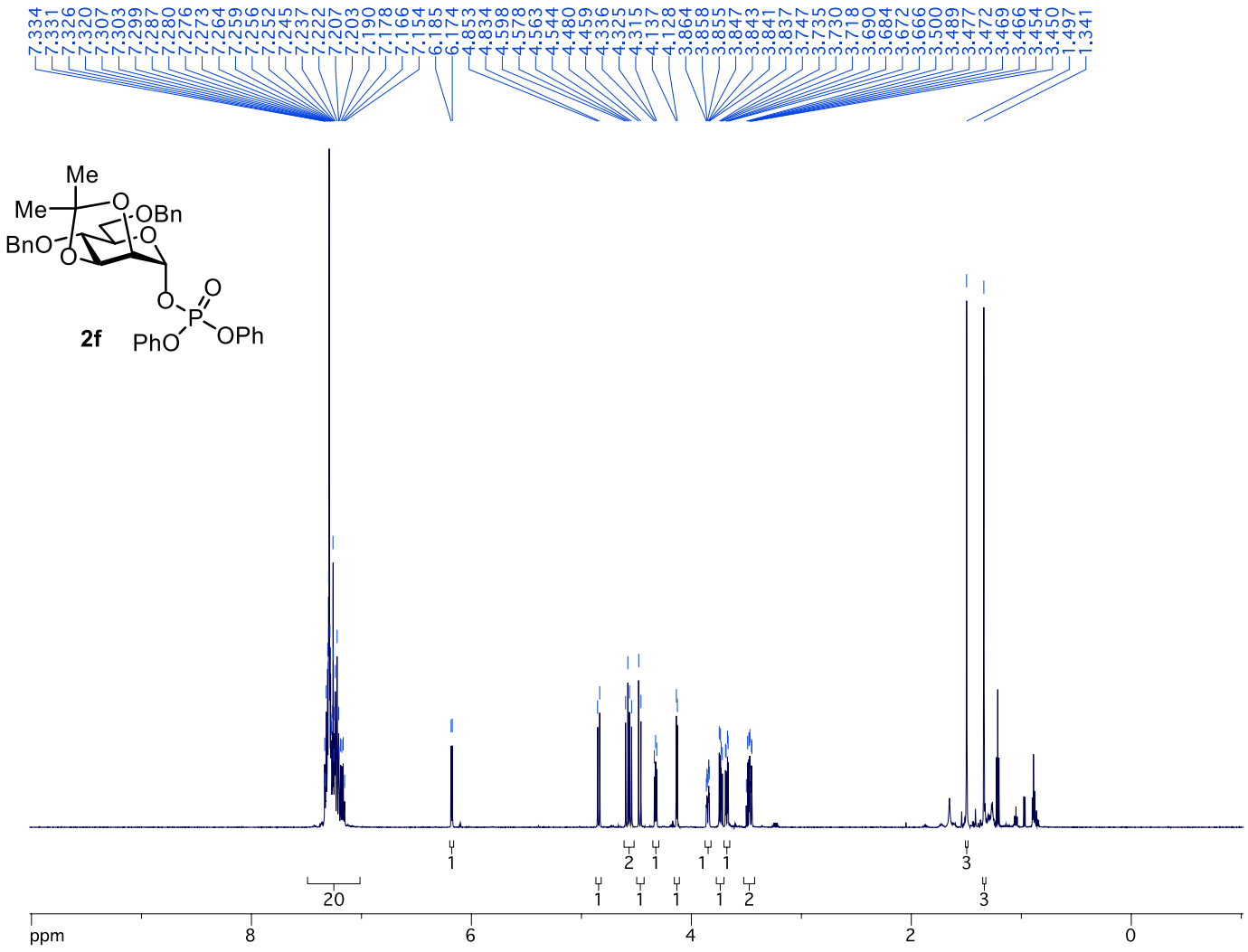

^{1}H NMR (600 MHz) spectrum of **2f** in $CDCl_3$

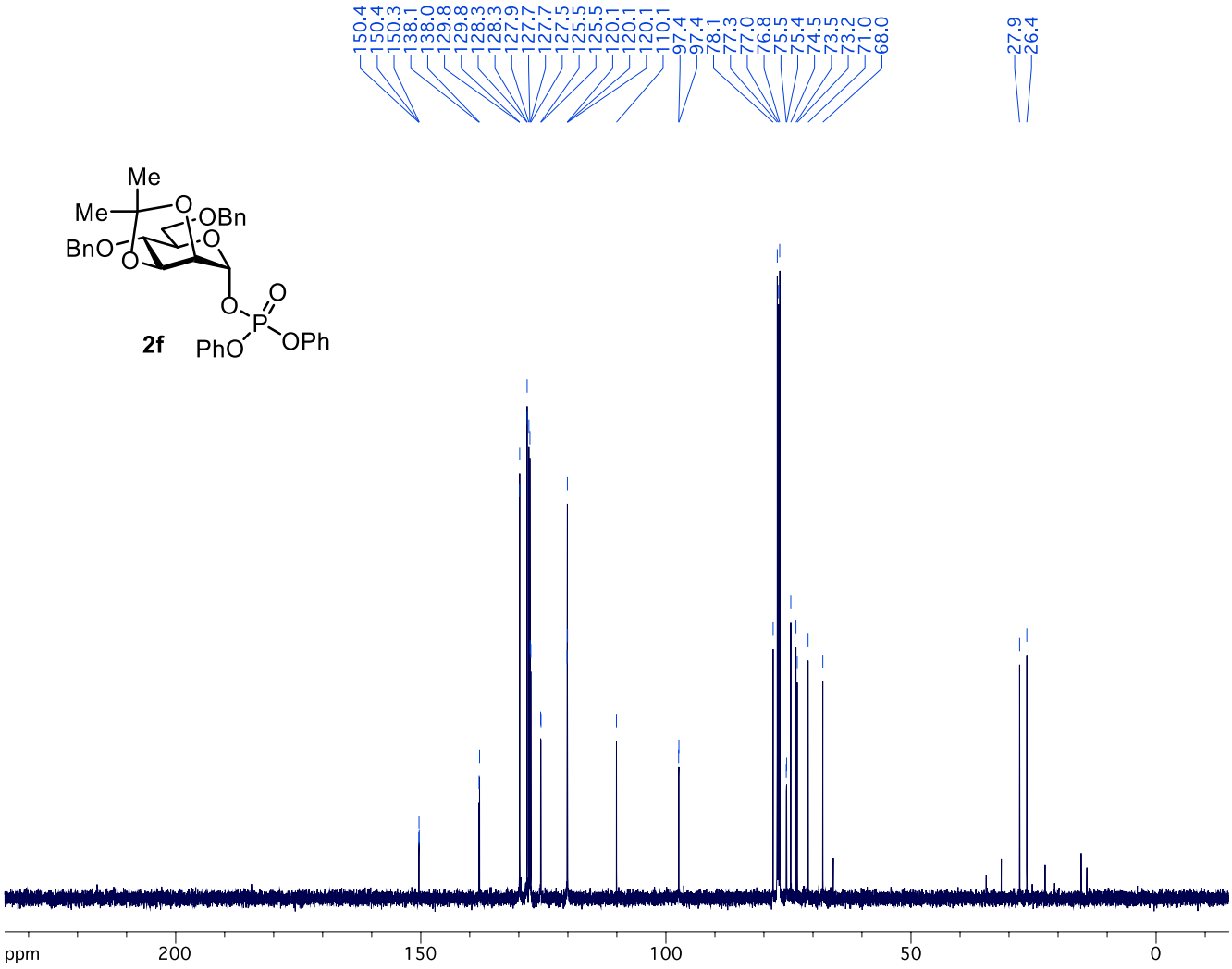

^{13}C NMR (126 MHz) spectrum of **2f** in $CDCl_3$.

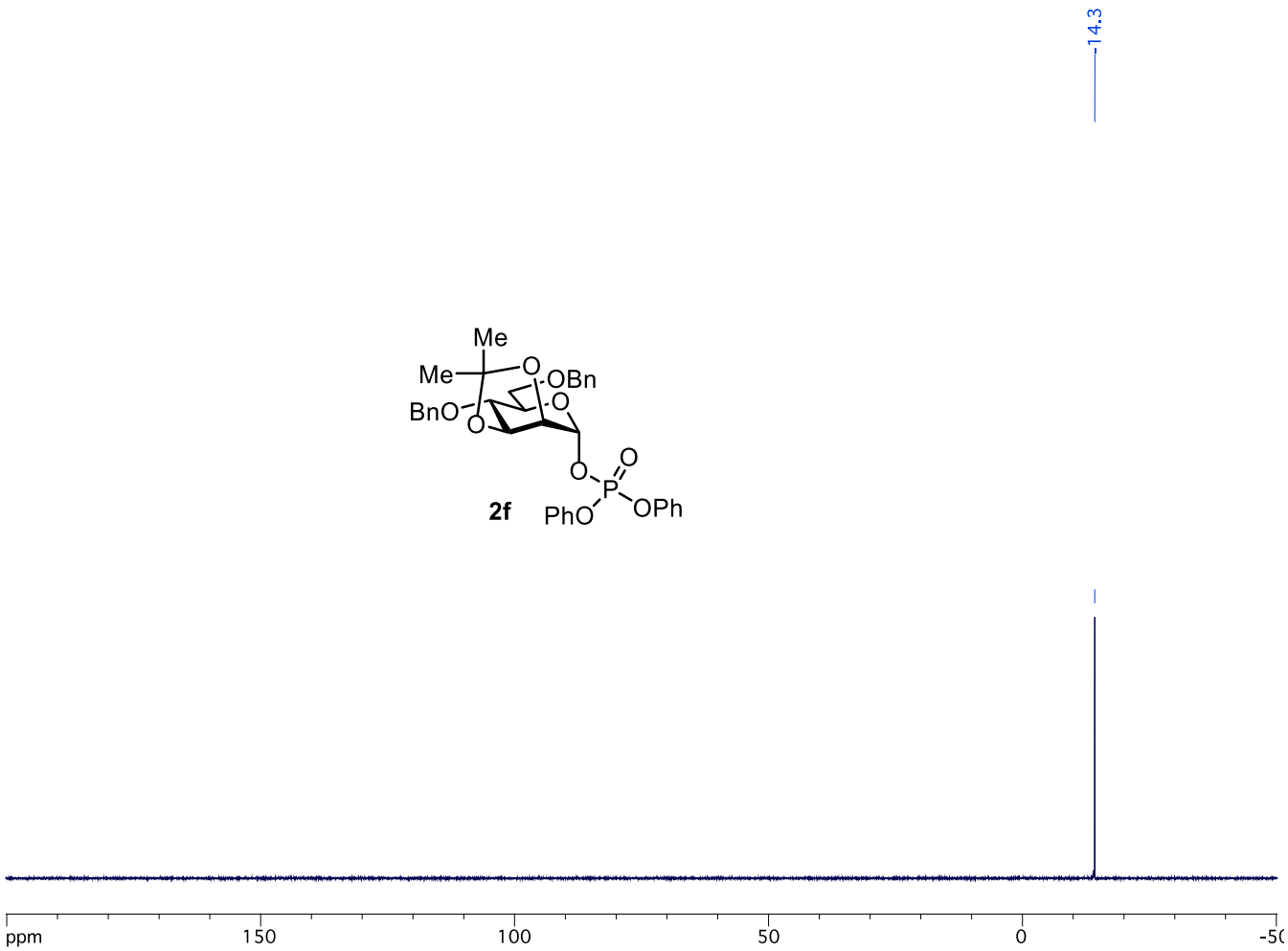

^{31}P NMR (162 MHz) spectrum of **3f** in $CDCl_3$.

Preparation of 4p

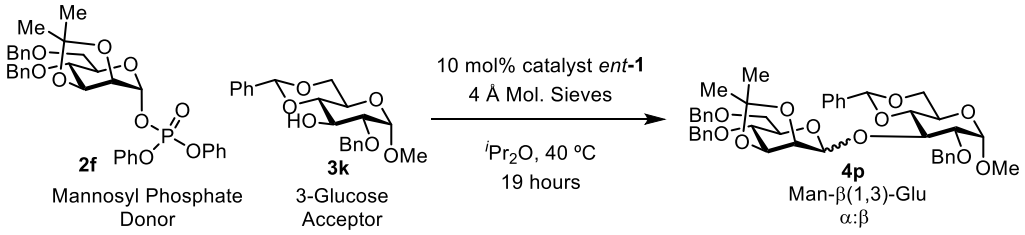

To a flame-dry 5 mL round bottom flask with a stir bar was charged 250 mg flame-dry 4 Å molecular sieves, 28 mg (0.050 mmol) catalyst *ent*-**1**, 186 mg (0.500 mmol) 3-glucose acceptor (**3k**), and the mannosyl phosphate donor (**2f**) (153 mg, 0.24 mmol) open to air. Next, 2.5 mL diisopropyl ether was added and the flask was closed with a plastic cap using parafilm to seal the cap tightly. The mixture was then heated with efficient stirring at 40 ˚C in an oil bath for 19 hours over which time the mixture thickened. After 19 hours, the mixture is cooled to room temperature and 100 µL aliquot is diluted with diethyl ether and filtered to remove the molecular sieves. This solution is concentrated and ^{1}H NMR analysis on the crude mixture is used to determine the anomeric selectivity (92:8 β:α). The mixture was then chromatographed directly with 50 g SiO_2 using an ether/hexanes gradient on a Biotage MPLC to yield the product (**4p**) in 48% yield (87 mg, 0.115 mmol) as a mixture of anomers.

^{1}H-NMR (600 MHz, $CDCl_3$): δ 7.40-7.16 (m, 20H), 5.46 (s, 1H), 5.27 (d, *J* = 2.5 Hz, 1H), 4.84 (d, *J* = 12.0 Hz, 1H), 4.68 (dd, *J* = 11.6, 9.8 Hz, 2H), 4.52 (d, *J* = 3.6 Hz, 1H), 4.42 (q, *J* = 13.5 Hz, 2H), 4.31-4.22 (m, 5H), 3.85-3.79 (m, 2H), 3.66 (t, *J* = 10.3 Hz, 1H), 3.59-3.51 (m, 4H), 3.43-3.41 (m, 4H), 1.59 (s, 3H), 1.39 (s, 3H).

^{13}C-NMR (126 MHz, $CDCl_3$): δ 138.79, 138.21, 138.09, 137.29, 129.02, 128.50, 128.25, 128.19, 128.10, 128.02, 127.68, 127.63, 127.49, 127.23, 126.45, 110.58, 101.97, 99.02, 98.08, 80.20, 80.12, 79.43, 75.68, 75.47, 74.13, 73.66, 73.09, 72.34, 70.74, 69.04, 62.56, 55.39, 27.28, 26.08.

J(C-H) for the anomeric carbon was measured to be 160.7 Hz, consistent with a β-Mannoside.[25-26]

HRMS-ESI (m/z): calculated for $C_{44}H_{50}O_{11}$ [M+H]+: 755.3426, found: 755.3422.

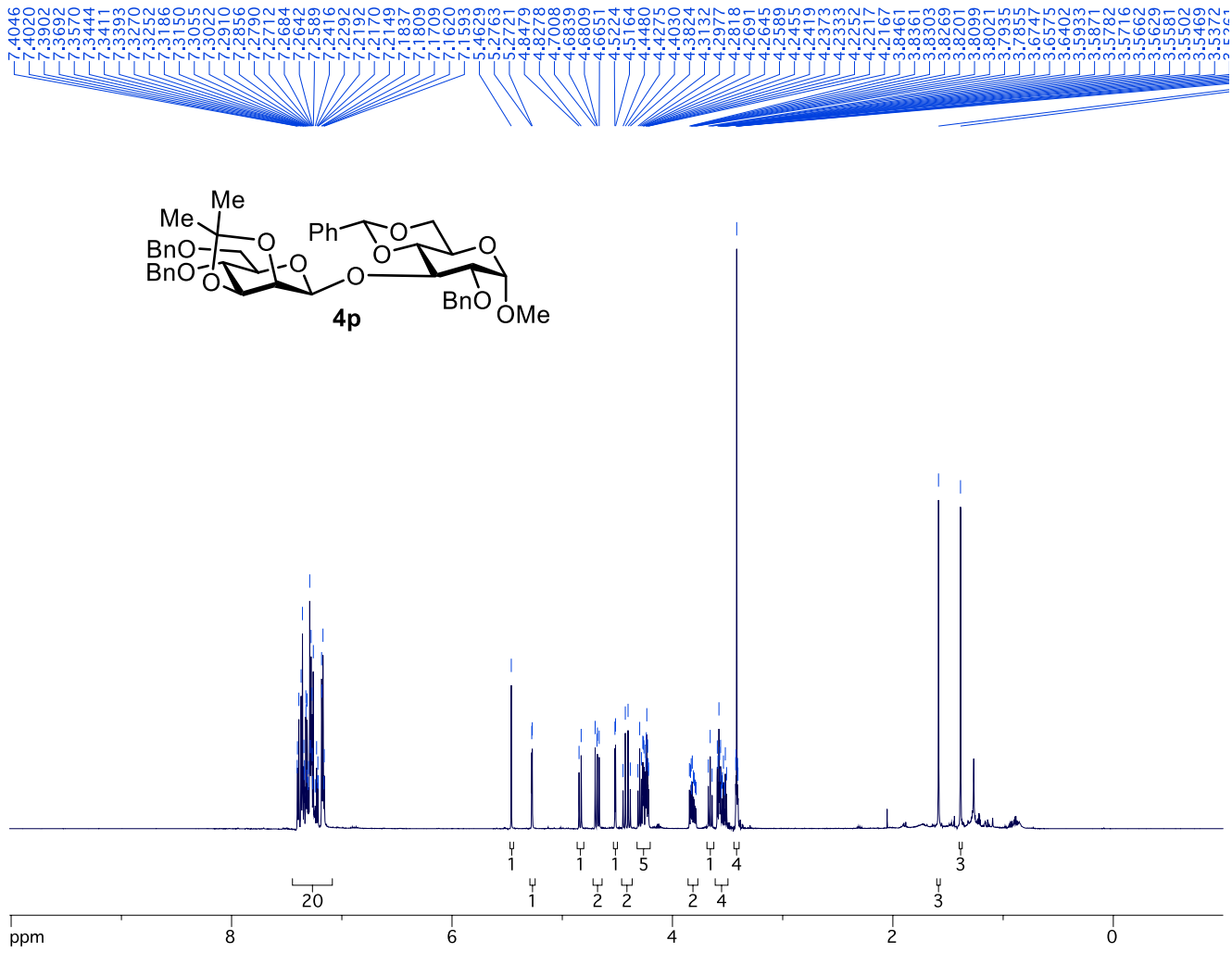

^{1}H NMR (600 MHz) spectrum of **4p** in $CDCl_3$

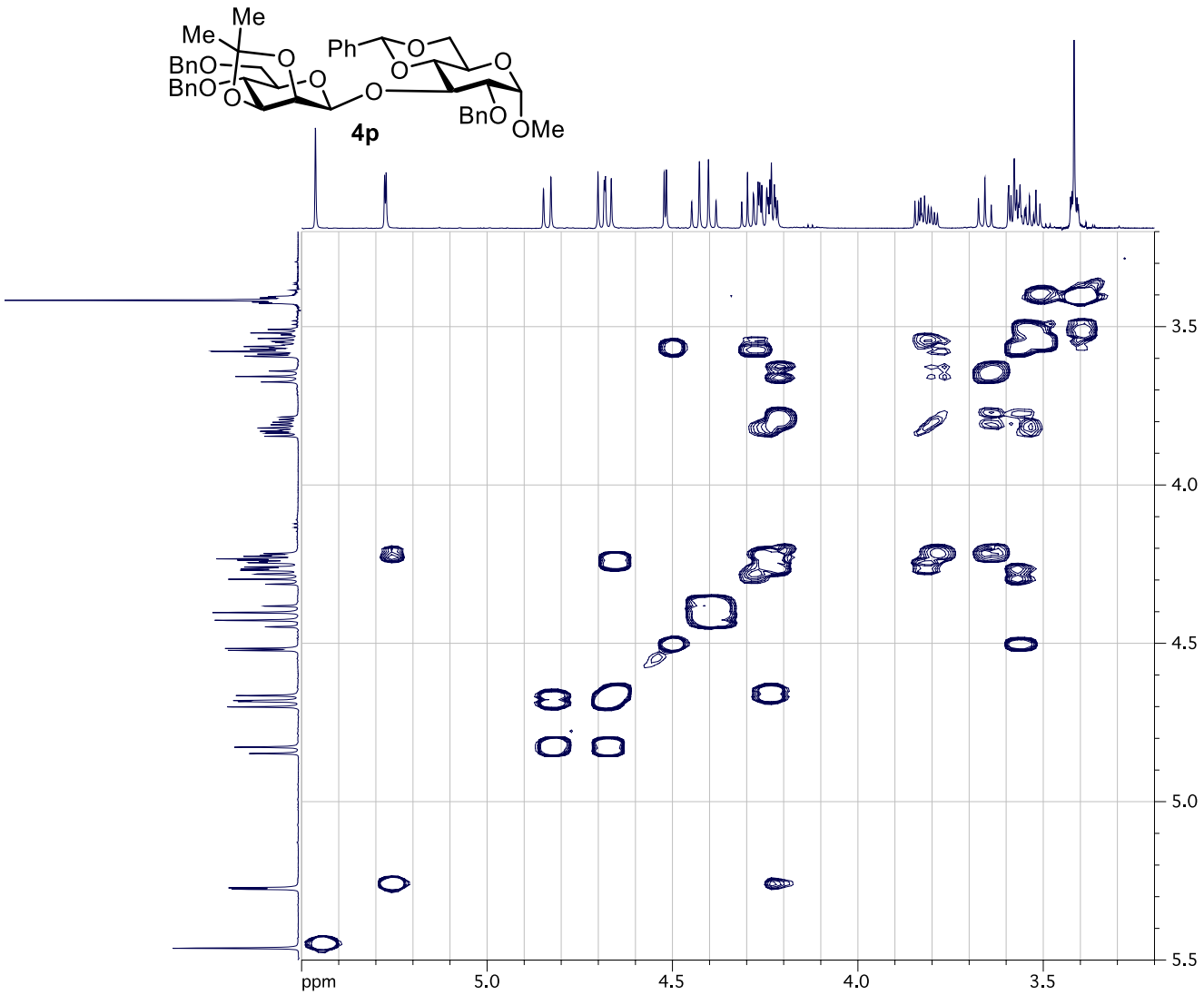

^{1}H-^{1}H COSY NMR (600 MHz) spectrum of **4p** in $CDCl_3$

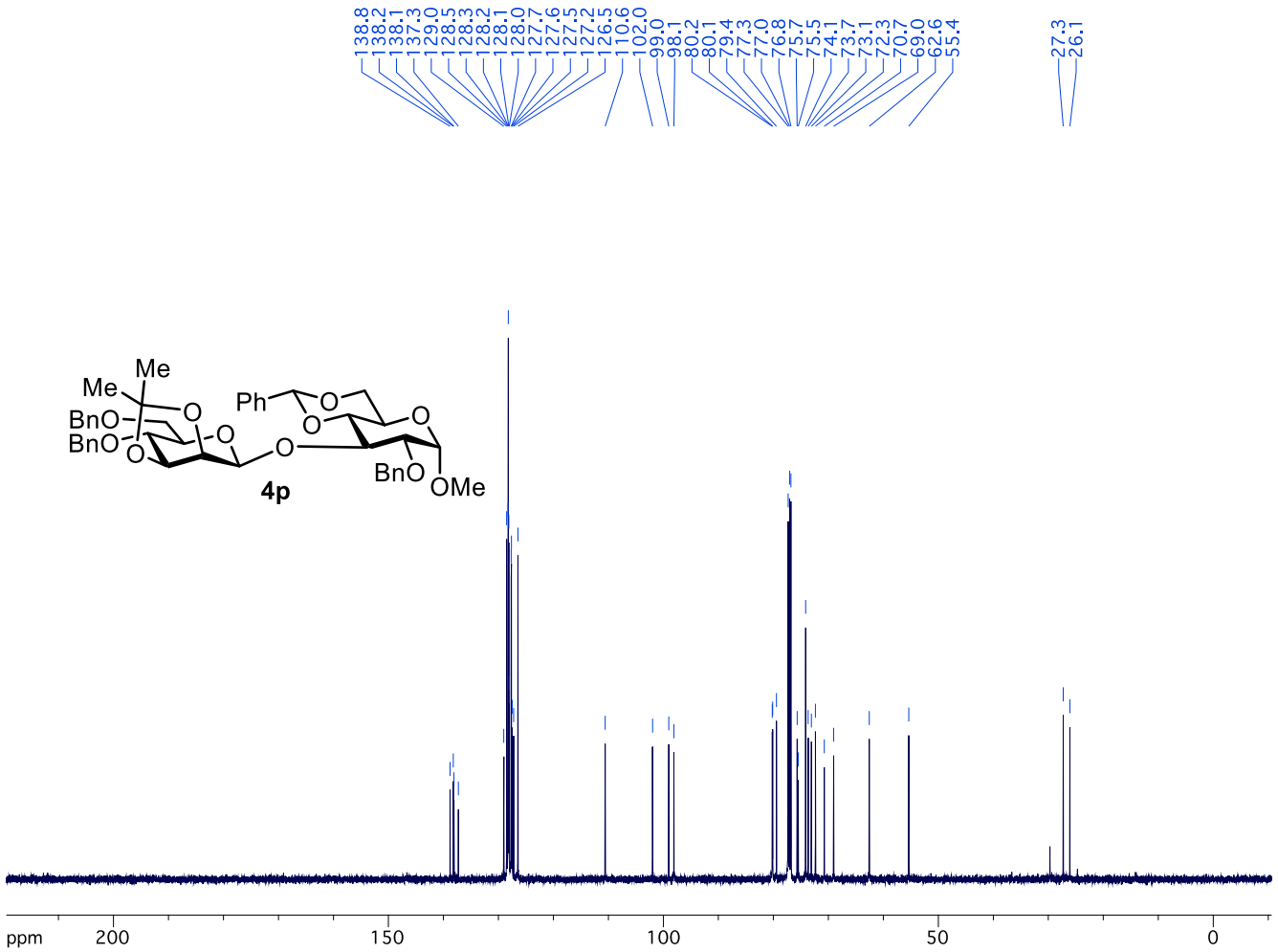

^{13}C NMR (126 MHz) spectrum of **4p** in $CDCl_3$

Preparation of 2g

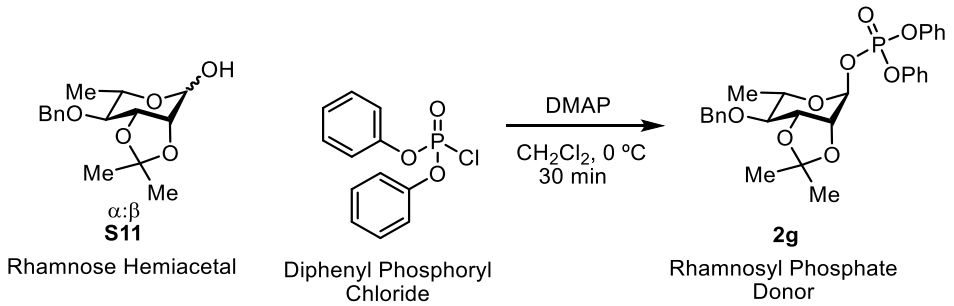

To a flame-dry 25 mL round bottom flask with a stir bar was charged 0.456 g DMAP (3.73 mmol, 3.0 equiv.). The flask was evacuated and backfilled with nitrogen three times. To the flask was added a solution of 0.366 g (1.24 mmol) 2,3-Isopropylidene-4-O-benzyl rhamnose hemiacetal (**S11**) in 12 mL dry dichloromethane. The reaction was cooled to 0 °C, and 0.27 mL diphenyl phosphoryl chloride (1.31 mmol, 1.2 equiv.) was added dropwise. The reaction was stirred at 0 °C for 30 minutes. The reaction was concentrated and purified on 10 g silanized SiO_2 using an ether/hexanes gradient on a Biotage MPLC to yield product (**2g**) in 49% yield (0.32 g, 0.61 mmol).

^{1}H-NMR (600 MHz, $CDCl_3$): δ 7.35-7.16 (m, 15H), 6.07 (d, *J* = 6.4 Hz, 1H), 4.89 (d, *J* = 11.6 Hz, 1H), 4.62 (d, *J* = 11.6 Hz, 1H), 4.28 (t, *J* = 6.4 Hz, 1H), 4.13 (d, *J* = 5.7 Hz, 1H), 3.82 (dq, *J* = 10.5, 5.6 Hz, 1H), 3.23 (dd, *J* = 10.6, 7.2 Hz, 1H), 1.49 (s, 3H), 1.34 (s, 3H), 1.17 (d, *J* = 6.2 Hz, 3H).

^{13}C-NMR (126 MHz, $CDCl_3$): δ 150.59, 150.57, 150.53, 150.47, 138.14, 129.84, 129.71, 128.47, 128.14, 127.90, 125.67, 125.61, 125.49, 120.36, 120.32, 120.28, 120.25, 120.21, 120.19, 120.15, 110.04, 97.38, 97.33, 80.23, 78.14, 75.83, 75.73, 73.29, 67.53, 28.02, 26.46, 17.61.

^{31}P-NMR (162 MHz, $CDCl_3$): δ -14.11.

HRMS-ESI (m/z): calculated for $C_{28}H_{31}O_8P$ [M+H]+: 527.1829, found: 527.1817.

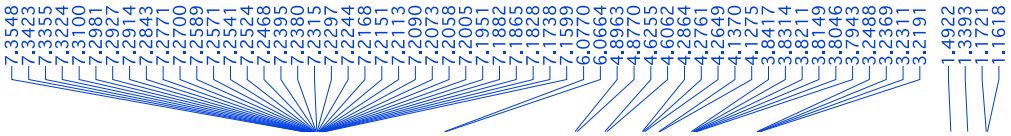

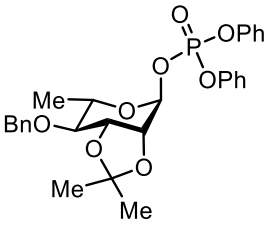

2g

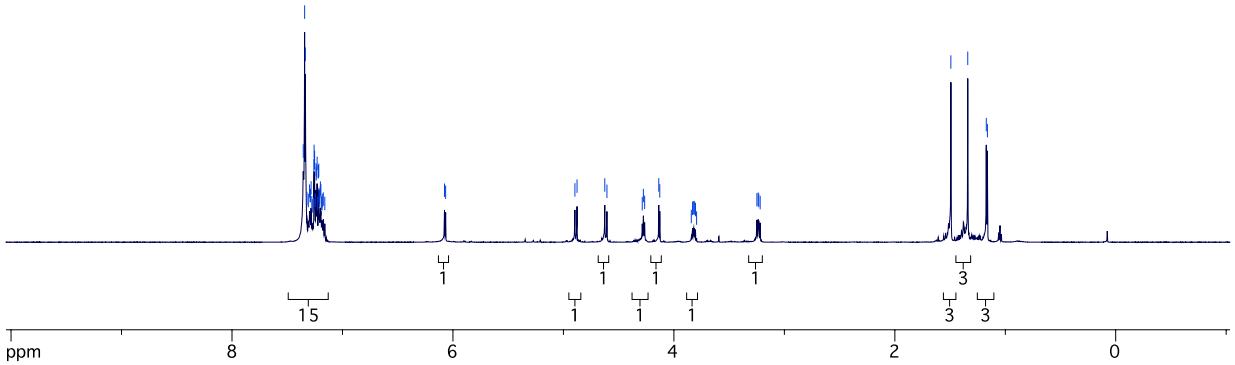

^{1}H NMR (600 MHz) spectrum of **2g** in $CDCl_3$

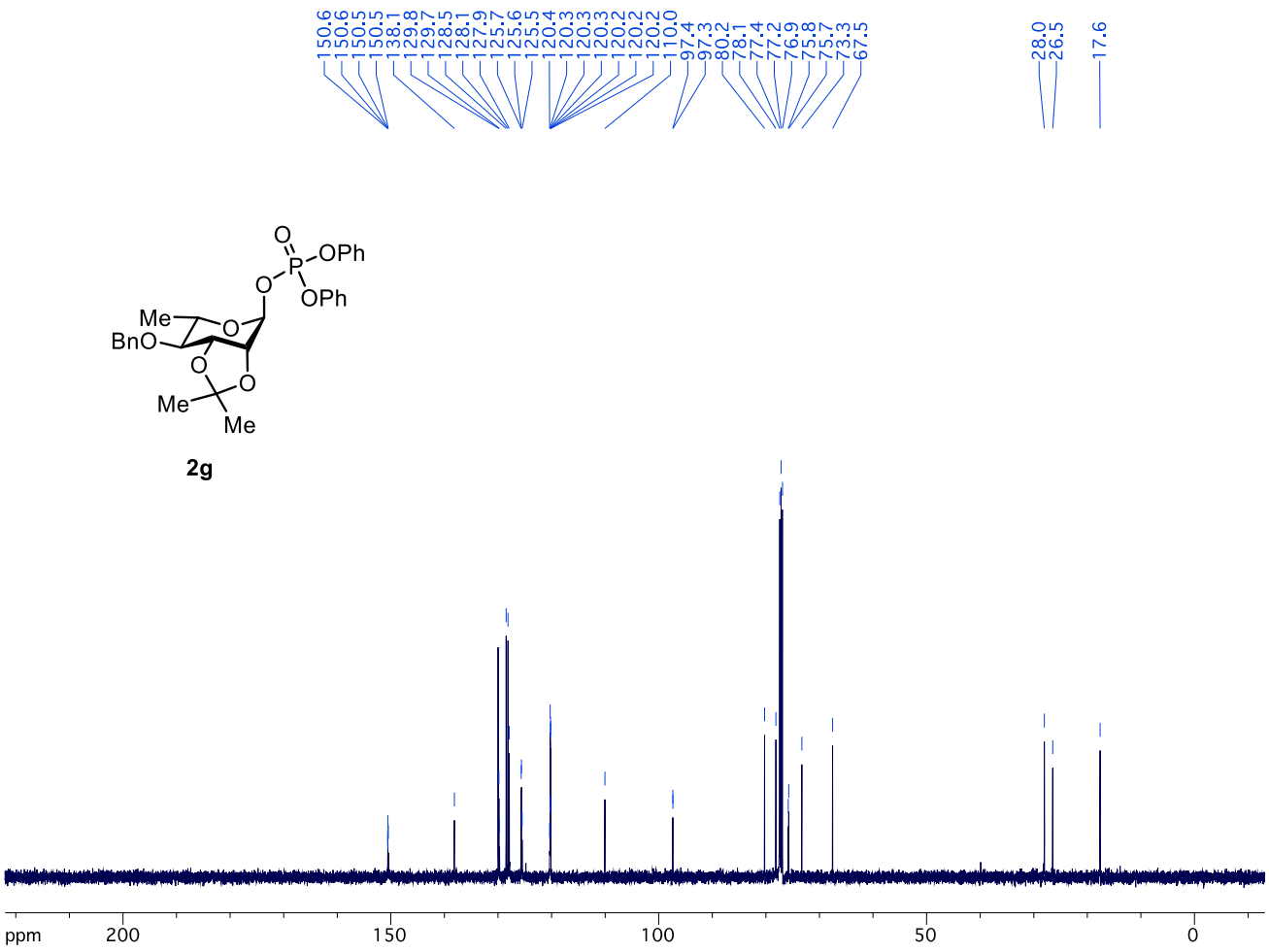

^{13}C NMR (126 MHz) spectrum of **2g** in $CDCl_3$.

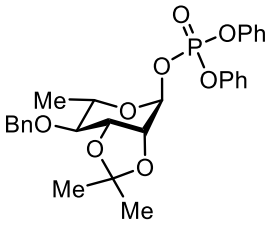

2g

^{31}P NMR (162 MHz) spectrum of **2g** in $CDCl_3$.

Preparation of 4q

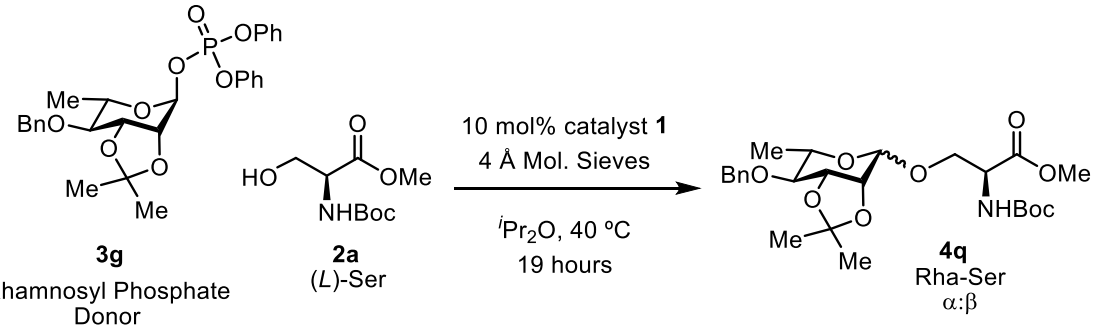

To a flame-dry 1-dram vial with a stir bar was charged 150 mg flame-dry 4 Å molecular sieves, 17 mg (0.015 mmol) catalyst **1**, and 67 mg (0.30 mmol) (*L*)-Boc-Ser-OMe **(3a)**, and 1.5 mL of a 0.1 M solution of 2,3-Isopropylidene-4-O-benzyl rhamnose phosphate donor (**2g**) in diisopropyl ether. Open to air, the flask was closed with a plastic cap and parafilm was used to seal the cap tightly. The mixture was then heated with efficient stirring at 40 ˚C in an oil bath for 19 hours over which time the mixture thickened. After 19 hours, the mixture is cooled to room temperature and 100 µL aliquot is diluted with diethyl ether and filtered to remove the molecular sieves. This solution is concentrated and ^{1}H NMR analysis on the crude mixture is used to determine

the anomeric selectivity (97:3 β:α). The mixture was then chromatographed directly with 25 g SiO_2 using an ether/hexanes gradient on a Biotage MPLC to yield the product **(4q)** in 91% yield (68 mg, 0.137 mmol) as a mixture of anomers.

^{1}H-NMR (500 MHz, $CDCl_3$): δ 7.36-7.27 (m, 5H), 5.60 (d, *J* = 8.7 Hz, 1H), 4.86 (d, *J* = 11.5 Hz, 1H), 4.68 (d, *J* = 2.3 Hz, 1H), 4.61 (d, *J* = 11.5 Hz, 1H), 4.46 (dt, *J* = 8.5, 3.2 Hz, 1H), 4.25-4.22 (m, 1H), 4.19 (dd, *J* = 6.3, 2.4 Hz, 1H), 4.06 (d, *J* = 3.3 Hz, 2H), 3.74 (s, 3H), 3.46-3.41 (m, 2H), 1.51 (s, 3H), 1.44 (s, 9H), 1.37 (s, 3H), 1.33 (d, *J* = 5.7 Hz, 3H).

^{13}C-NMR (126 MHz, $CDCl_3$): δ 171.03, 155.47, 138.17, 128.39, 128.04, 127.79, 110.76, 98.82, 80.62, 79.96, 79.61, 74.24, 72.83, 70.83, 70.05, 53.92, 52.51, 28.41, 28.35, 27.41, 26.14, 18.90.

J(C-H) of the anomeric carbon was measured to be 158.9 Hz, consistent with a β-Rhamnoside.[25-26]

HRMS-ESI (m/z): calculated for $C_{25}H_{37}NO_9$ [M+H]+: 496.2541, found: 527.2537.

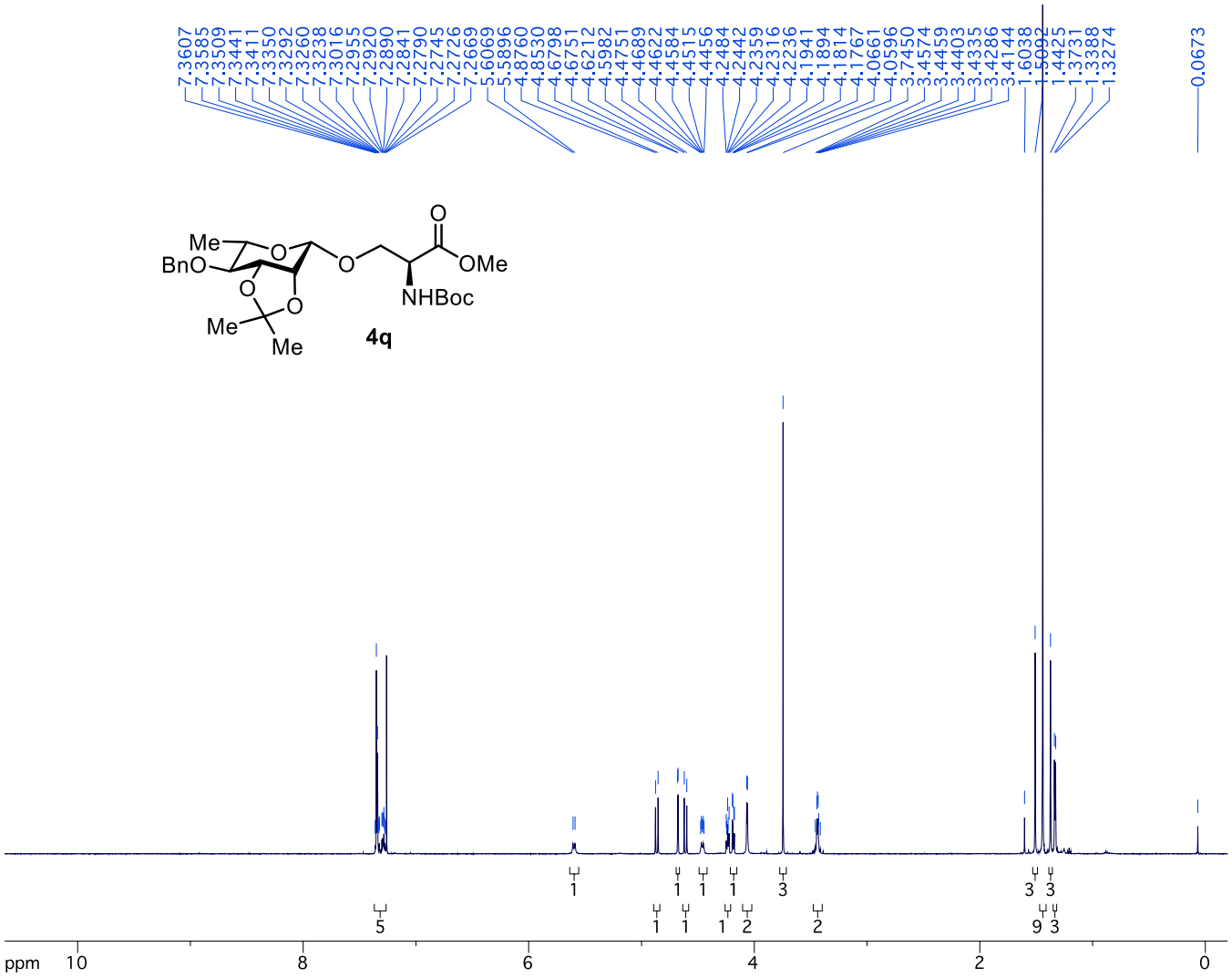

^{1}H NMR (600 MHz) spectrum of **4q** in $CDCl_3$

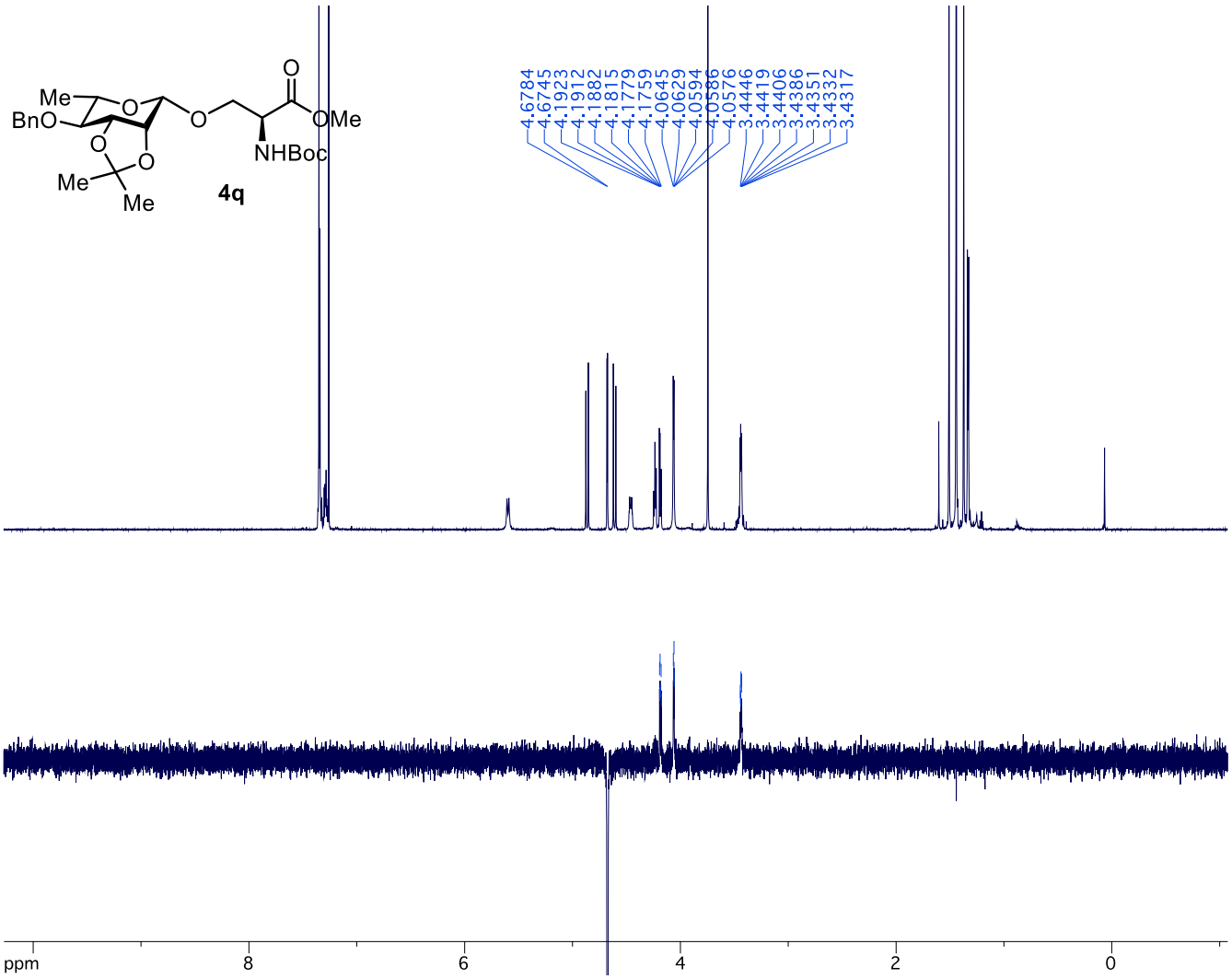

1D NOE irradiating at 4.68 ppm (C1-H) with ^{1}H NMR (600 MHz) spectrum of **4q** in $CDCl_3$

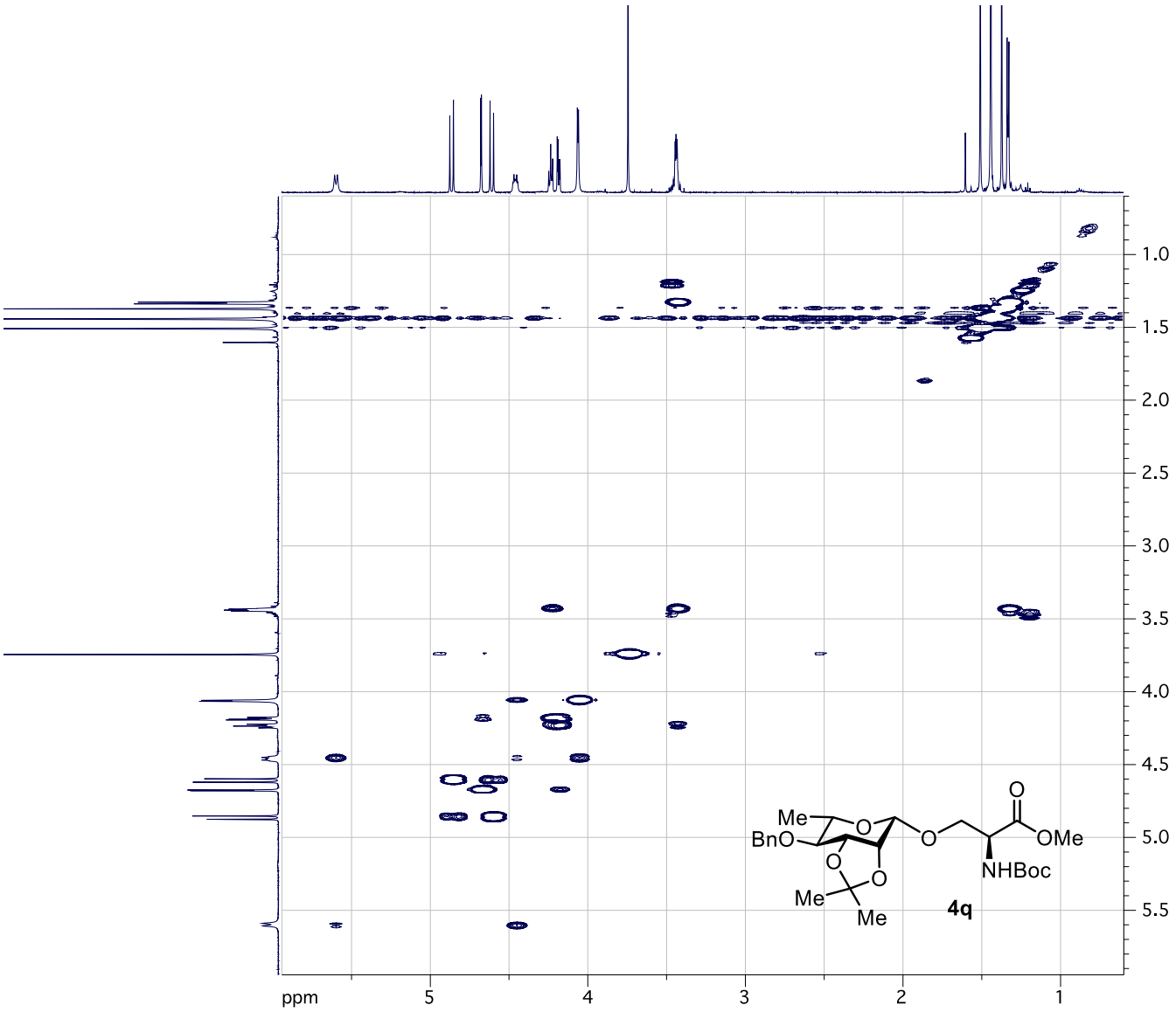

^{1}H-^{1}H COSY NMR (600 MHz) spectrum of **4q** in $CDCl_3$

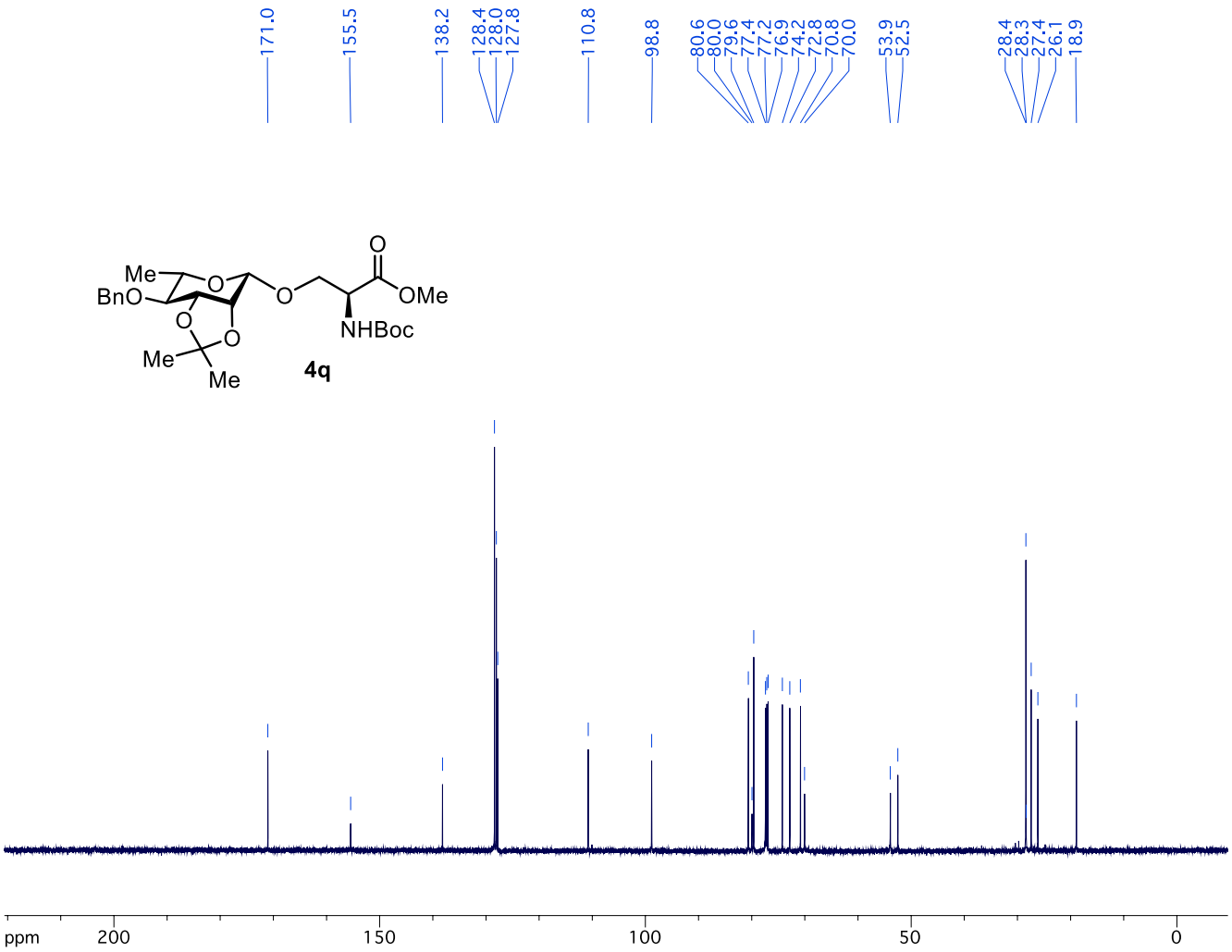

^{13}C NMR (126 MHz) spectrum of **4q** in $CDCl_3$

2.2 Synthetic Procedures and Characterization Data for Previously Reported Compounds

Preparation of 4j

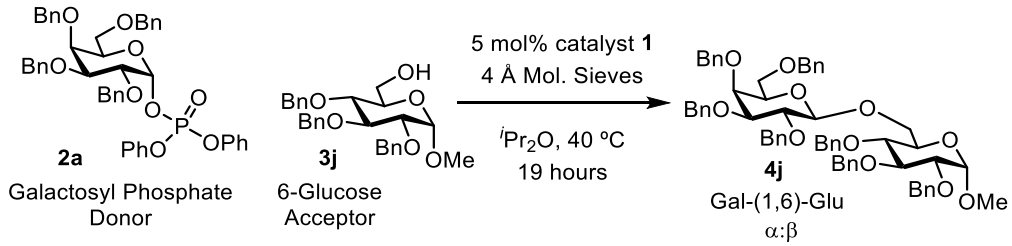

To a flame-dry 5 mL round bottom flask with a stir bar was charged 250 mg flame-dry 4 Å molecular sieves, 14 mg (0.0125 mmol) catalyst **1**, and 232 mg (0.500 mmol) 6-glucose acceptor (**3j**), and 2.5 mL of a 0.1 M solution of galactosyl phosphate donor (**2a**) was added open to air and the flask was closed with a plastic cap and parafilm was used to seal the cap tightly. The mixture was then heated with efficient stirring at 40 ˚C in an oil bath for 19 hours over which time the mixture thickened. After 19 hours, the mixture is cooled to room temperature and 100 µL aliquot is diluted with diethyl ether and filtered to remove the molecular sieves. This solution is concentrated and ^{1}H NMR analysis on the crude mixture is used to determine the anomeric selectivity (β–only). The mixture was then chromatographed directly with 50 g SiO_2 using an ethyl acetate/hexanes gradient on a Biotage MPLC to afford the product (**4j**) in 75% yield (185 mg, 0.187 mmol) as a single anomer. The spectral data matched previous reports of this compound.[11]

Preparation of 4k

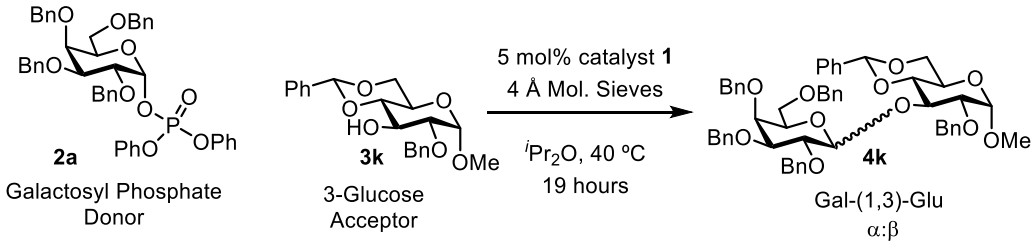

To a flame-dry 5 mL round bottom flask with a stir bar was charged 250 mg flame-dry 4 Å molecular sieves, 14 mg (0.0125 mmol) catalyst **1**, and 186 mg (0.500 mmol) 3-glucose acceptor (**3k**), and 2.5 mL of a 0.1 M solution of galactosyl phosphate donor (**2a**) was added open to air and the flask was closed with a plastic cap and parafilm was used to seal the cap tightly. The mixture was then heated with efficient stirring at 40 ˚C in an oil bath for 19 hours over which time the mixture thickened. After 19 hours, the mixture is cooled to room temperature and 100 µL aliquot is diluted with diethyl ether and filtered to remove the molecular sieves. This solution is concentrated and ^{1}H NMR analysis on the crude mixture is used to determine the anomeric selectivity (96:4 β:α). The mixture was then chromatographed directly with 50 g SiO_2 using an ether/hexanes gradient on a Biotage MPLC to afford the product (**4k**) in 91% yield (203 mg, 0.227 mmol) as a mixture of anomers. The spectral data matched previous reports of this compound.[12]

Preparation of 4l

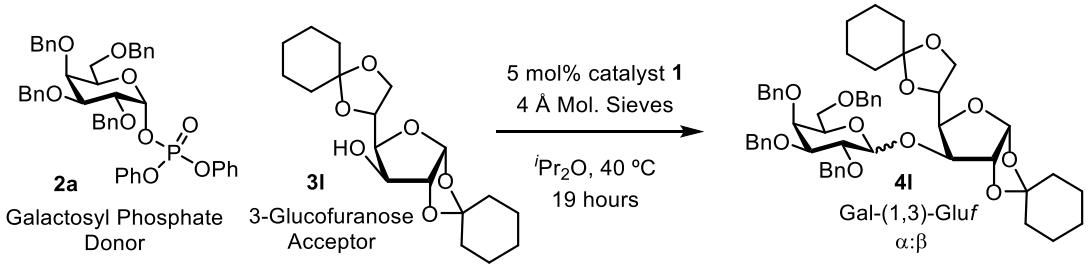

To a flame-dry 5 mL round bottom flask with a stir bar was charged 250 mg flame-dry 4 Å molecular sieves, 14 mg (0.0125 mmol) catalyst **1**, and 170 mg (0.500 mmol) glucofuranose acceptor (**3l**), and 2.5 mL of a 0.1 M solution of galactosyl phosphate donor (**2a**) was added open to air and the flask was closed with a plastic cap and parafilm was used to seal the cap tightly. The mixture was then heated with efficient stirring at 40 ˚C in an oil bath for 19 hours over which time the mixture thickened. After 19 hours, the mixture is cooled to room temperature and 100 µL aliquot is diluted with diethyl ether and filtered to remove the molecular sieves. This solution is concentrated and ^{1}H NMR analysis on the crude mixture is used to determine the anomeric selectivity (96:4 β:α). The mixture was then chromatographed directly with 50 g SiO_2 using an ether/hexanes gradient on a Biotage MPLC to afford the product (**4j**) in 79% yield (170 mg, 0.197 mmol) as a mixture of anomers. The spectral data matched previous reports of this compound.[13]

Preparation of 4r

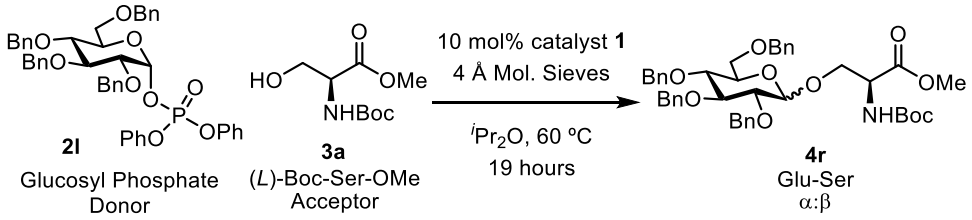

To a flame-dry 10 mL round bottom flask with a stir bar was charged 300 mg flame-dry 4 Å molecular sieves, 11 mg (0.01 mmol) catalyst **1**, and 44 mg (0.200 mmol) serine acceptor (**3a**), and 77 mg (0.100 mmol) glucosyl phosphate donor (**2l**). 3.0 mL diisopropyl ether was added to this mixture (0.033 M in **2l**) open to air and the flask was closed with a plastic cap and parafilm was used to seal the cap tightly. The mixture was then heated with efficient stirring at 60 ˚C in an oil bath for 19 hours over which time the mixture thickened. After 19 hours, the mixture is cooled to room temperature and 300 µL aliquot is diluted with diethyl ether and filtered to remove the molecular sieves. This solution is concentrated and ^{1}H NMR analysis on the crude mixture is used to determine the anomeric selectivity (87:13 β:α). The mixture was then chromatographed directly with 25 g SiO_2 using an ether/hexanes gradient on a Biotage MPLC to afford the product (**4j**) in 85% yield (63 mg, 0.085 mmol) as a mixture of anomers. The spectral data matched previous reports of this compound.

3. X-ray Crystallography Data

3.1 X-ray Data for Catalyst 1

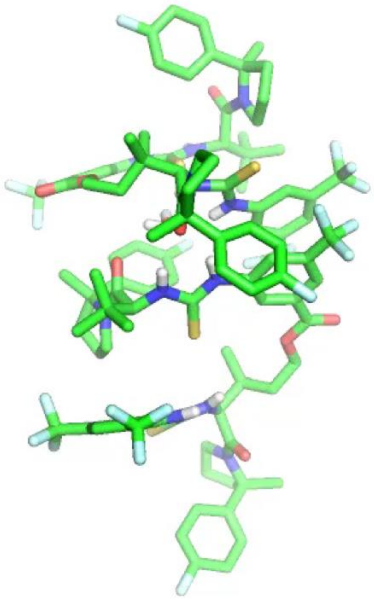

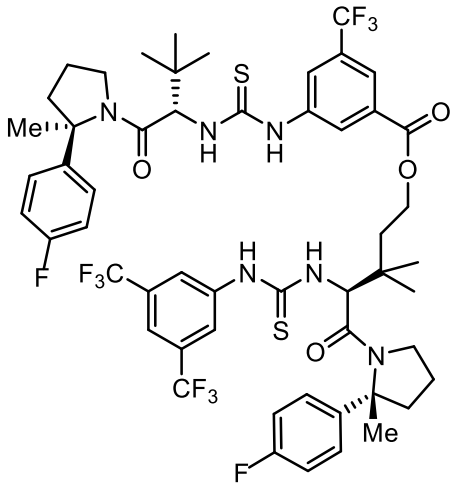

A crystal mounted on a diffractometer was collected data at 100 K. The intensities of the reflections were collected by means of a Bruker APEX II CCD diffractometer ($Mo_{K\alpha}$ radiation, λ=0.71073 Å), and equipped with an Oxford Cryosystems nitrogen flow apparatus. The collection method involved 0.5° scans in ω at 28° in 2θ. Data integration down to 0.84 Å resolution was carried out using SAINT V8.37A (Bruker diffractometer, 2016) with reflection spot size optimization. Absorption corrections were made with the program SADABS (Bruker diffractometer, 2016). The structure was solved by the Intrinsic Phasing methods and refined by least-squares methods again F^2 using SHELXT-2014 (Sheldrick, 2015) and SHELXL-2014 (Sheldrick, 2015) with OLEX 2 interface (Dolomanov, et al., 2009). Non-hydrogen atoms were refined anisotropically, and hydrogen atoms were allowed to ride on the respective atoms. Crystal data as well as details of data collection and refinement are summarized in Table S1, geometric parameters are shown in Table S2 and hydrogen-bond parameters are listed in Table S3. The Ortep plots produced with SHELXL-2014 program, and the other drawings were produced with Accelrys DS Visualizer 2.0 (Accelrys, 2007).

Table S1. Experimental details

	SML-V-FSND
Crystal data	
Chemical formula	$C_{53}H_{59}F_{11}N_6O_5S_2$
M_r	1133.18
Crystal system, space group	Monoclinic, *C*2
Temperature (K)	100
a, *b*, *c* (Å)	33.487 (8), 14.890 (4), 13.878 (3)
β (°)	98.545 (6)
V (Å^3)	6843 (3)
Z	4
Radiation type	Mo *K*α
μ (mm^{-1})	0.15

Crystal size (mm)	0.14 × 0.02 × 0.01
Data collection	
Diffractometer	Bruker D8 goniometer with CCD area detector
Absorption correction	Multi-scan *SADABS*
T_{min}, T_{max}	0.559, 0.745
No. of measured, independent and observed [$I > 2\sigma(I)$] reflections	49271, 11947, 6052
R_{int}	0.165
$(\sin \theta/\lambda)_{max}$ (Å^{-1})	0.597
Refinement	
$R[F^2 > 2\sigma(F^2)]$, $wR(F^2)$, S	0.077, 0.183, 0.96
No. of reflections	11947
No. of parameters	760
No. of restraints	451
H-atom treatment	H-atom parameters constrained
$\Delta\rho_{max}$, $\Delta\rho_{min}$ (e Å^{-3})	0.33, -0.33
Absolute structure	Flack x determined using 2052 quotients [(I+)-(I-)]/[(I+)+(I-)] (Parsons, Flack and Wagner, Acta Cryst. B69 (2013) 249-259).
Absolute structure parameter	-0.06 (9)

Computer programs: *SAINT* 8.37A (Bruker-AXS, 2015), *SHELXT2014* (Sheldrick, 2015), *SHELXL2014* (Sheldrick, 2015), Bruker *SHELXTL* (Sheldrick, 2015).

Table S2. Geometric parameters (Å, º)

S1—C13	1.659 (8)	C28—C29	1.549 (12)
S2—C45	1.621 (8)	C28—H28A	0.9900
F1—C3	1.369 (10)	C28—H28B	0.9900
F6—C52	1.356 (11)	C29—C44	1.514 (11)
F7—C52	1.332 (10)	C29—C30	1.54 (2)
F8—C52	1.378 (10)	C29—C30A	1.542 (16)
O1—C11	1.251 (10)	C30—C35	1.39 (2)
O2—C20	1.339 (9)	C30—C31	1.42 (2)
O2—C21	1.452 (9)	C31—C32	1.38 (2)
O3—C20	1.206 (9)	C31—H31	0.9500
O4—C25	1.236 (10)	C32—C33	1.33 (2)

N1—C11	1.332 (10)	C32—H32	0.9500
N1—C10	1.461 (11)	C33—F5	1.37 (2)
N1—C7	1.477 (11)	C33—C34	1.43 (2)
N2—C13	1.395 (10)	C34—C35	1.39 (2)
N2—C12	1.466 (10)	C34—H34	0.9500
N2—H2	0.8800	C35—H35	0.9500
N3—C13	1.348 (10)	C30A—C35A	1.386 (17)
N3—C14	1.420 (9)	C30A—C31A	1.406 (16)
N3—H3	0.8800	C31A—C32A	1.376 (17)
N4—C25	1.349 (10)	C31A—H31A	0.9500
N4—C26	1.451 (11)	C32A—C33A	1.344 (19)
N4—C29	1.492 (11)	C32A—H32A	0.9500
N5—C45	1.340 (9)	C33A—F5A	1.377 (15)
N5—C24	1.469 (9)	C33A—C34A	1.439 (19)
N5—H5	0.8800	C34A—C35A	1.382 (17)
N6—C45	1.395 (10)	C34A—H34A	0.9500
N6—C46	1.431 (10)	C35A—H35A	0.9500
N6—H6	0.8800	C36—H36A	0.9800
C1—C2	1.381 (12)	C36—H36B	0.9800
C1—C6	1.420 (11)	C36—H36C	0.9800
C1—H1	0.9500	C37—C39	1.504 (11)
C2—C3	1.333 (13)	C37—C38	1.521 (11)
C2—H2A	0.9500	C37—C40	1.539 (11)
C3—C4	1.382 (13)	C38—H38A	0.9800
C4—C5	1.394 (12)	C38—H38B	0.9800
C4—H4	0.9500	C38—H38C	0.9800
C5—C6	1.361 (12)	C39—H39A	0.9800
C5—H5A	0.9500	C39—H39B	0.9800
C6—C7	1.543 (13)	C39—H39C	0.9800
C7—C36	1.525 (13)	C40—H40A	0.9800
C7—C8	1.566 (12)	C40—H40B	0.9800
C8—C9	1.491 (13)	C40—H40C	0.9800
C8—H8A	0.9900	C41—F3	1.338 (15)
C8—H8B	0.9900	C41—F4	1.357 (14)
C9—C10	1.490 (12)	C41—F2	1.373 (14)
C9—H9A	0.9900	C41A—F3A	1.32 (2)
C9—H9B	0.9900	C41A—F2A	1.361 (18)

C10—H10A	0.9900	C41A—F4A	1.379 (19)
C10—H10B	0.9900	C42—H42A	0.9800
C11—C12	1.521 (12)	C42—H42B	0.9800
C12—C37	1.605 (10)	C42—H42C	0.9800
C12—H12	1.0000	C43—H43A	0.9800
C14—C15	1.383 (11)	C43—H43B	0.9800
C14—C19	1.405 (10)	C43—H43C	0.9800
C15—C16	1.429 (11)	C44—H44A	0.9800
C15—H15	0.9500	C44—H44B	0.9800
C16—C17	1.391 (11)	C44—H44C	0.9800
C16—C41A	1.443 (12)	C46—C51	1.360 (11)
C16—C41	1.443 (12)	C46—C47	1.393 (12)
C17—C18	1.383 (10)	C47—C48	1.448 (11)
C17—H17	0.9500	C47—H47	0.9500
C18—C19	1.395 (10)	C48—C49	1.387 (13)
C18—C20	1.479 (11)	C48—C52	1.435 (13)
C19—H19	0.9500	C49—C50	1.331 (12)
C21—C22	1.522 (10)	C49—H49	0.9500
C21—H21A	0.9900	C50—C51	1.423 (11)
C21—H21B	0.9900	C50—C53A	1.48 (2)
C22—C23	1.515 (10)	C50—C53	1.50 (2)
C22—H22A	0.9900	C50—C53B	1.501 (18)
C22—H22B	0.9900	C51—H51	0.9500
C23—C43	1.531 (12)	C53—F11	1.34 (2)
C23—C42	1.554 (10)	C53—F10	1.36 (2)
C23—C24	1.588 (11)	C53—F9	1.40 (2)
C24—C25	1.516 (12)	C53A—F11A	1.33 (2)
C24—H24	1.0000	C53A—F10A	1.35 (2)
C26—C27	1.532 (12)	C53A—F9A	1.38 (2)
C26—H26A	0.9900	C53B—F11B	1.345 (18)
C26—H26B	0.9900	C53B—F10B	1.365 (18)
C27—C28	1.504 (12)	C53B—F9B	1.396 (18)
C27—H27A	0.9900	O1W—H1WA	0.8466
C27—H27B	0.9900	O1W—H1WB	0.9062
C20—O2—C21	117.6 (6)	C30—C29—C28	110 (4)
C11—N1—C10	125.8 (7)	C30A—C29—C28	107 (3)

C11—N1—C7	120.5 (7)	C35—C30—C31	119.1 (19)
C10—N1—C7	112.8 (7)	C35—C30—C29	119 (3)
C13—N2—C12	120.0 (7)	C31—C30—C29	121 (3)
C13—N2—H2	120.0	C32—C31—C30	120 (2)
C12—N2—H2	120.0	C32—C31—H31	119.8
C13—N3—C14	130.2 (7)	C30—C31—H31	119.8
C13—N3—H3	114.9	C33—C32—C31	118 (2)
C14—N3—H3	114.9	C33—C32—H32	120.9
C25—N4—C26	126.0 (8)	C31—C32—H32	120.9
C25—N4—C29	121.6 (7)	C32—C33—F5	121 (2)
C26—N4—C29	112.1 (7)	C32—C33—C34	125 (2)
C45—N5—C24	122.5 (6)	F5—C33—C34	113 (2)
C45—N5—H5	118.8	C35—C34—C33	115 (2)
C24—N5—H5	118.8	C35—C34—H34	122.5
C45—N6—C46	130.4 (7)	C33—C34—H34	122.5
C45—N6—H6	114.8	C34—C35—C30	122 (2)
C46—N6—H6	114.8	C34—C35—H35	119.1
C2—C1—C6	120.3 (9)	C30—C35—H35	119.1
C2—C1—H1	119.9	C35A—C30A—C31A	118.0 (13)
C6—C1—H1	119.9	C35A—C30A—C29	120 (2)
C3—C2—C1	119.8 (9)	C31A—C30A—C29	122 (2)
C3—C2—H2A	120.1	C32A—C31A—C30A	121.5 (15)
C1—C2—H2A	120.1	C32A—C31A—H31A	119.3
C2—C3—F1	120.5 (9)	C30A—C31A—H31A	119.3
C2—C3—C4	122.9 (10)	C33A—C32A—C31A	119.4 (15)
F1—C3—C4	116.6 (9)	C33A—C32A—H32A	120.3
C3—C4—C5	116.8 (9)	C31A—C32A—H32A	120.3
C3—C4—H4	121.6	C32A—C33A—F5A	121.4 (14)
C5—C4—H4	121.6	C32A—C33A—C34A	122.1 (14)
C6—C5—C4	123.1 (9)	F5A—C33A—C34A	116.5 (15)
C6—C5—H5A	118.5	C35A—C34A—C33A	116.7 (15)
C4—C5—H5A	118.5	C35A—C34A—H34A	121.7
C5—C6—C1	117.1 (9)	C33A—C34A—H34A	121.7
C5—C6—C7	123.0 (8)	C34A—C35A—C30A	122.2 (14)
C1—C6—C7	119.9 (8)	C34A—C35A—H35A	118.9
N1—C7—C36	112.2 (8)	C30A—C35A—H35A	118.9
N1—C7—C6	112.1 (7)	C7—C36—H36A	109.5

C36—C7—C6	112.4 (8)	C7—C36—H36B	109.5
N1—C7—C8	101.5 (7)	H36A—C36—H36B	109.5
C36—C7—C8	108.5 (7)	C7—C36—H36C	109.5
C6—C7—C8	109.4 (7)	H36A—C36—H36C	109.5
C9—C8—C7	103.9 (7)	H36B—C36—H36C	109.5
C9—C8—H8A	111.0	C39—C37—C38	111.7 (7)
C7—C8—H8A	111.0	C39—C37—C40	108.6 (6)
C9—C8—H8B	111.0	C38—C37—C40	110.1 (7)
C7—C8—H8B	111.0	C39—C37—C12	112.9 (7)
H8A—C8—H8B	109.0	C38—C37—C12	106.8 (6)
C10—C9—C8	105.9 (8)	C40—C37—C12	106.6 (7)
C10—C9—H9A	110.6	C37—C38—H38A	109.5
C8—C9—H9A	110.6	C37—C38—H38B	109.5
C10—C9—H9B	110.6	H38A—C38—H38B	109.5
C8—C9—H9B	110.6	C37—C38—H38C	109.5
H9A—C9—H9B	108.7	H38A—C38—H38C	109.5
N1—C10—C9	104.0 (7)	H38B—C38—H38C	109.5
N1—C10—H10A	111.0	C37—C39—H39A	109.5
C9—C10—H10A	111.0	C37—C39—H39B	109.5
N1—C10—H10B	111.0	H39A—C39—H39B	109.5
C9—C10—H10B	111.0	C37—C39—H39C	109.5
H10A—C10—H10B	109.0	H39A—C39—H39C	109.5
O1—C11—N1	121.1 (8)	H39B—C39—H39C	109.5
O1—C11—C12	119.4 (8)	C37—C40—H40A	109.5
N1—C11—C12	119.5 (8)	C37—C40—H40B	109.5
N2—C12—C11	107.2 (6)	H40A—C40—H40B	109.5
N2—C12—C37	109.1 (6)	C37—C40—H40C	109.5
C11—C12—C37	114.1 (6)	H40A—C40—H40C	109.5
N2—C12—H12	108.8	H40B—C40—H40C	109.5
C11—C12—H12	108.8	F3—C41—F4	104.9 (16)
C37—C12—H12	108.8	F3—C41—F2	106.3 (12)
N3—C13—N2	111.7 (7)	F4—C41—F2	104.3 (11)
N3—C13—S1	127.8 (6)	F3—C41—C16	111.1 (17)
N2—C13—S1	120.5 (6)	F4—C41—C16	118.6 (13)
C15—C14—C19	120.0 (7)	F2—C41—C16	110.7 (12)
C15—C14—N3	116.1 (7)	F3A—C41A—F2A	107.5 (18)
C19—C14—N3	123.9 (7)	F3A—C41A—F4A	105 (2)

C14—C15—C16	119.8 (8)	F2A—C41A—F4A	103.7 (14)
C14—C15—H15	120.1	F3A—C41A—C16	116 (2)
C16—C15—H15	120.1	F2A—C41A—C16	113.1 (18)
C17—C16—C15	120.0 (8)	F4A—C41A—C16	109.9 (17)
C17—C16—C41A	119.0 (8)	C23—C42—H42A	109.5
C15—C16—C41A	120.9 (8)	C23—C42—H42B	109.5
C17—C16—C41	119.0 (8)	H42A—C42—H42B	109.5
C15—C16—C41	120.9 (8)	C23—C42—H42C	109.5
C18—C17—C16	119.0 (7)	H42A—C42—H42C	109.5
C18—C17—H17	120.5	H42B—C42—H42C	109.5
C16—C17—H17	120.5	C23—C43—H43A	109.5
C17—C18—C19	122.0 (7)	C23—C43—H43B	109.5
C17—C18—C20	117.2 (7)	H43A—C43—H43B	109.5
C19—C18—C20	120.7 (7)	C23—C43—H43C	109.5
C18—C19—C14	119.2 (7)	H43A—C43—H43C	109.5
C18—C19—H19	120.4	H43B—C43—H43C	109.5
C14—C19—H19	120.4	C29—C44—H44A	109.5
O3—C20—O2	123.0 (7)	C29—C44—H44B	109.5
O3—C20—C18	124.2 (8)	H44A—C44—H44B	109.5
O2—C20—C18	112.8 (7)	C29—C44—H44C	109.5
O2—C21—C22	108.2 (6)	H44A—C44—H44C	109.5
O2—C21—H21A	110.1	H44B—C44—H44C	109.5
C22—C21—H21A	110.1	N5—C45—N6	108.7 (7)
O2—C21—H21B	110.1	N5—C45—S2	124.1 (6)
C22—C21—H21B	110.1	N6—C45—S2	127.2 (6)
H21A—C21—H21B	108.4	C51—C46—C47	122.7 (8)
C23—C22—C21	116.8 (7)	C51—C46—N6	124.4 (8)
C23—C22—H22A	108.1	C47—C46—N6	112.9 (8)
C21—C22—H22A	108.1	C46—C47—C48	117.7 (9)
C23—C22—H22B	108.1	C46—C47—H47	121.1
C21—C22—H22B	108.1	C48—C47—H47	121.1
H22A—C22—H22B	107.3	C49—C48—C52	121.9 (9)
C22—C23—C43	114.7 (7)	C49—C48—C47	118.9 (9)
C22—C23—C42	109.2 (6)	C52—C48—C47	119.0 (9)
C43—C23—C42	106.7 (7)	C50—C49—C48	120.9 (8)
C22—C23—C24	109.7 (6)	C50—C49—H49	119.6
C43—C23—C24	108.4 (6)	C48—C49—H49	119.6

C42—C23—C24	108.0 (6)	C49—C50—C51	122.3 (8)
N5—C24—C25	107.7 (7)	C49—C50—C53A	118.5 (14)
N5—C24—C23	108.6 (6)	C51—C50—C53A	119.2 (14)
C25—C24—C23	115.1 (6)	C49—C50—C53	119.6 (14)
N5—C24—H24	108.4	C51—C50—C53	118.0 (14)
C25—C24—H24	108.4	C49—C50—C53B	123.7 (11)
C23—C24—H24	108.4	C51—C50—C53B	113.9 (12)
O4—C25—N4	122.1 (8)	C46—C51—C50	117.6 (8)
O4—C25—C24	119.6 (8)	C46—C51—H51	121.2
N4—C25—C24	118.2 (8)	C50—C51—H51	121.2
N4—C26—C27	104.2 (8)	F7—C52—F6	106.3 (9)
N4—C26—H26A	110.9	F7—C52—F8	104.9 (8)
C27—C26—H26A	110.9	F6—C52—F8	103.2 (8)
N4—C26—H26B	110.9	F7—C52—C48	115.2 (9)
C27—C26—H26B	110.9	F6—C52—C48	114.9 (8)
H26A—C26—H26B	108.9	F8—C52—C48	111.2 (8)
C28—C27—C26	102.6 (7)	F11—C53—F10	111 (2)
C28—C27—H27A	111.3	F11—C53—F9	101 (2)
C26—C27—H27A	111.3	F10—C53—F9	104 (2)
C28—C27—H27B	111.3	F11—C53—C50	114 (2)
C26—C27—H27B	111.3	F10—C53—C50	113 (2)
H27A—C27—H27B	109.2	F9—C53—C50	113 (2)
C27—C28—C29	103.7 (7)	F11A—C53A—F10A	109 (2)
C27—C28—H28A	111.0	F11A—C53A—F9A	109 (2)
C29—C28—H28A	111.0	F10A—C53A—F9A	110 (2)
C27—C28—H28B	111.0	F11A—C53A—C50	113 (2)
C29—C28—H28B	111.0	F10A—C53A—C50	109 (2)
H28A—C28—H28B	109.0	F9A—C53A—C50	108.2 (19)
N4—C29—C44	113.1 (7)	F11B—C53B—F10B	106.2 (16)
N4—C29—C30	107 (2)	F11B—C53B—F9B	103.7 (16)
C44—C29—C30	114 (3)	F10B—C53B—F9B	103.4 (16)
N4—C29—C30A	115.3 (15)	F11B—C53B—C50	117.6 (16)
C44—C29—C30A	109 (2)	F10B—C53B—C50	111.8 (16)
N4—C29—C28	100.8 (7)	F9B—C53B—C50	112.9 (16)
C44—C29—C28	110.8 (7)	H1WA—O1W—H1WB	94.0
C6—C1—C2—C3	2.3 (14)	C27—C28—C29—C44	-155.0 (8)

C1—C2—C3—F1	178.4 (8)	C27—C28—C29—C30	78 (2)
C1—C2—C3—C4	-1.4 (15)	C27—C28—C29—C30A	85.9 (16)
C2—C3—C4—C5	0.8 (14)	N4—C29—C30—C35	-166 (7)
F1—C3—C4—C5	-179.0 (8)	C44—C29—C30—C35	-40 (9)
C3—C4—C5—C6	-1.1 (14)	C28—C29—C30—C35	85 (8)
C4—C5—C6—C1	1.9 (13)	N4—C29—C30—C31	18 (9)
C4—C5—C6—C7	-177.7 (8)	C44—C29—C30—C31	144 (7)
C2—C1—C6—C5	-2.5 (13)	C28—C29—C30—C31	-91 (8)
C2—C1—C6—C7	177.2 (8)	C35—C30—C31—C32	-4 (11)
C11—N1—C7—C36	-63.1 (10)	C29—C30—C31—C32	172 (7)
C10—N1—C7—C36	127.1 (8)	C30—C31—C32—C33	5 (9)
C11—N1—C7—C6	64.6 (9)	C31—C32—C33—F5	177 (5)
C10—N1—C7—C6	-105.2 (8)	C31—C32—C33—C34	-3 (7)
C11—N1—C7—C8	-178.8 (7)	C32—C33—C34—C35	1 (7)
C10—N1—C7—C8	11.4 (8)	F5—C33—C34—C35	-180 (5)
C5—C6—C7—N1	-154.1 (8)	C33—C34—C35—C30	0 (9)
C1—C6—C7—N1	26.2 (11)	C31—C30—C35—C34	2 (11)
C5—C6—C7—C36	-26.6 (12)	C29—C30—C35—C34	-174 (7)
C1—C6—C7—C36	153.8 (8)	N4—C29—C30A—C35A	-168 (4)
C5—C6—C7—C8	94.1 (10)	C44—C29—C30A—C35A	-40 (5)
C1—C6—C7—C8	-85.5 (10)	C28—C29—C30A—C35A	80 (5)
N1—C7—C8—C9	-28.0 (9)	N4—C29—C30A—C31A	13 (6)
C36—C7—C8—C9	-146.4 (9)	C44—C29—C30A—C31A	141 (5)
C6—C7—C8—C9	90.6 (9)	C28—C29—C30A—C31A	-99 (5)
C7—C8—C9—C10	35.4 (10)	C35A—C30A—C31A—C32A	-2 (7)
C11—N1—C10—C9	-159.5 (8)	C29—C30A—C31A—C32A	177 (4)
C7—N1—C10—C9	9.7 (9)	C30A—C31A—C32A—C33A	1 (5)
C8—C9—C10—N1	-28.1 (10)	C31A—C32A—C33A—F5A	-179 (3)
C10—N1—C11—O1	173.3 (7)	C31A—C32A—C33A—C34A	0 (4)
C7—N1—C11—O1	4.9 (11)	C32A—C33A—C34A—C35A	0 (4)
C10—N1—C11—C12	-7.9 (11)	F5A—C33A—C34A—C35A	179 (3)
C7—N1—C11—C12	-176.4 (6)	C33A—C34A—C35A—C30A	-1 (5)

C13—N2—C12—C11	-89.7 (8)	C31A—C30A—C35A—C34A	2 (7)
C13—N2—C12—C37	146.3 (7)	C29—C30A—C35A—C34A	-177 (4)
O1—C11—C12—N2	-41.5 (9)	N2—C12—C37—C39	64.5 (9)
N1—C11—C12—N2	139.8 (7)	C11—C12—C37—C39	-55.4 (10)
O1—C11—C12—C37	79.5 (8)	N2—C12—C37—C38	-58.7 (8)
N1—C11—C12—C37	-99.3 (8)	C11—C12—C37—C38	-178.6 (7)
C14—N3—C13—N2	178.9 (7)	N2—C12—C37—C40	-176.4 (6)
C14—N3—C13—S1	-1.6 (12)	C11—C12—C37—C40	63.7 (9)
C12—N2—C13—N3	174.4 (6)	C17—C16—C41—F3	-77.2 (15)
C12—N2—C13—S1	-5.1 (10)	C15—C16—C41—F3	99.0 (15)
C13—N3—C14—C15	-163.9 (8)	C17—C16—C41—F4	161.2 (15)
C13—N3—C14—C19	15.1 (12)	C15—C16—C41—F4	-22.6 (18)
C19—C14—C15—C16	-0.2 (11)	C17—C16—C41—F2	40.7 (17)
N3—C14—C15—C16	178.9 (7)	C15—C16—C41—F2	-143.0 (14)
C14—C15—C16—C17	-1.0 (12)	C17—C16—C41A—F3A	-54.8 (19)
C14—C15—C16—C41A	-177.3 (8)	C15—C16—C41A—F3A	121.4 (17)
C14—C15—C16—C41	-177.3 (8)	C17—C16—C41A—F2A	70.3 (17)
C15—C16—C17—C18	1.7 (12)	C15—C16—C41A—F2A	-113.5 (16)
C41A—C16—C17—C18	177.9 (8)	C17—C16—C41A—F4A	-174.3 (16)
C41—C16—C17—C18	177.9 (8)	C15—C16—C41A—F4A	1.9 (18)
C16—C17—C18—C19	-1.1 (12)	C24—N5—C45—N6	170.1 (7)
C16—C17—C18—C20	-178.0 (7)	C24—N5—C45—S2	-8.7 (11)
C17—C18—C19—C14	0.0 (11)	C46—N6—C45—N5	170.5 (7)
C20—C18—C19—C14	176.7 (7)	C46—N6—C45—S2	-10.7 (13)

C15—C14—C19—C18	0.7 (11)	C45—N6—C46—C51	-8.4 (13)
N3—C14—C19—C18	-178.2 (7)	C45—N6—C46—C47	174.4 (8)
C21—O2—C20—O3	0.7 (11)	C51—C46—C47—C48	1.1 (12)
C21—O2—C20—C18	-179.3 (6)	N6—C46—C47—C48	178.3 (7)
C17—C18—C20—O3	-7.1 (12)	C46—C47—C48—C49	-0.5 (12)
C19—C18—C20—O3	176.0 (8)	C46—C47—C48—C52	175.6 (8)
C17—C18—C20—O2	172.9 (7)	C52—C48—C49—C50	-176.8 (9)
C19—C18—C20—O2	-4.0 (10)	C47—C48—C49—C50	-0.8 (12)
C20—O2—C21—C22	158.9 (6)	C48—C49—C50—C51	1.5 (13)
O2—C21—C22—C23	78.4 (8)	C48—C49—C50—C53A	-176.8 (15)
C21—C22—C23—C43	-43.5 (9)	C48—C49—C50—C53	-174.9 (15)
C21—C22—C23—C42	76.1 (8)	C48—C49—C50—C53B	-175.2 (12)
C21—C22—C23—C24	-165.7 (6)	C47—C46—C51—C50	-0.4 (13)
C45—N5—C24—C25	-80.9 (9)	N6—C46—C51—C50	-177.3 (7)
C45—N5—C24—C23	153.8 (7)	C49—C50—C51—C46	-0.9 (13)
C22—C23—C24—N5	72.4 (8)	C53A—C50—C51—C46	177.4 (15)
C43—C23—C24—N5	-53.5 (8)	C53—C50—C51—C46	175.5 (15)
C42—C23—C24—N5	-168.7 (7)	C53B—C50—C51—C46	176.1 (12)
C22—C23—C24—C25	-48.4 (9)	C49—C48—C52—F7	79.9 (11)
C43—C23—C24—C25	-174.3 (7)	C47—C48—C52—F7	-96.1 (10)
C42—C23—C24—C25	70.5 (9)	C49—C48—C52—F6	-156.0 (8)
C26—N4—C25—O4	165.4 (7)	C47—C48—C52—F6	28.0 (12)
C29—N4—C25—O4	-8.3 (11)	C49—C48—C52—F8	-39.3 (12)

C26—N4—C25—C24	-18.1 (11)	C47—C48—C52—F8	144.8 (8)
C29—N4—C25—C24	168.3 (6)	C49—C50—C53—F11	-146 (2)
N5—C24—C25—O4	-36.3 (9)	C51—C50—C53—F11	37 (3)
C23—C24—C25—O4	85.0 (9)	C49—C50—C53—F10	-18 (3)
N5—C24—C25—N4	147.1 (7)	C51—C50—C53—F10	165 (2)
C23—C24—C25—N4	-91.7 (8)	C49—C50—C53—F9	100 (3)
C25—N4—C26—C27	-165.5 (7)	C51—C50—C53—F9	-77 (3)
C29—N4—C26—C27	8.7 (9)	C49—C50—C53A—F11A	148 (2)
N4—C26—C27—C28	-30.7 (9)	C51—C50—C53A—F11A	-30 (3)
C26—C27—C28—C29	41.0 (9)	C49—C50—C53A—F10A	-91 (2)
C25—N4—C29—C44	-51.1 (10)	C51—C50—C53A—F10A	91 (2)
C26—N4—C29—C44	134.4 (8)	C49—C50—C53A—F9A	28 (3)
C25—N4—C29—C30	76 (5)	C51—C50—C53A—F9A	-150.2 (19)
C26—N4—C29—C30	-99 (5)	C49—C50—C53B—F11B	-172.4 (18)
C25—N4—C29—C30A	76 (3)	C51—C50—C53B—F11B	11 (2)
C26—N4—C29—C30A	-99 (3)	C49—C50—C53B—F10B	-49 (2)
C25—N4—C29—C28	-169.5 (7)	C51—C50—C53B—F10B	133.8 (18)
C26—N4—C29—C28	16.1 (8)	C49—C50—C53B—F9B	67 (2)
C27—C28—C29—N4	-35.0 (8)	C51—C50—C53B—F9B	-110.1 (18)

Table S3. Hydrogen-bond parameters

D—H···*A*	*D*—H (Å)	H···*A* (Å)	*D*···*A* (Å)	*D*—H···*A* (°)
N2—H2···O4^{i}	0.88	2.08	2.908 (10)	156.3
N3—H3···O4^{i}	0.88	2.19	3.022 (9)	158.4
N5—H5···O1W	0.88	2.08	2.878 (8)	151.0

N6—H6···O1W	0.88	2.02	2.869 (8)	160.8
O1W—H1WA···O1^{ii}	0.85	2.15	2.709 (7)	123.3
O1W—H1WB···S1	0.91	2.36	3.155 (6)	145.7

Symmetry code(s): (i) -*x*+3/2, *y*-1/2, -*z*+1; (ii) -*x*+3/2, *y*+1/2, -*z*+1.

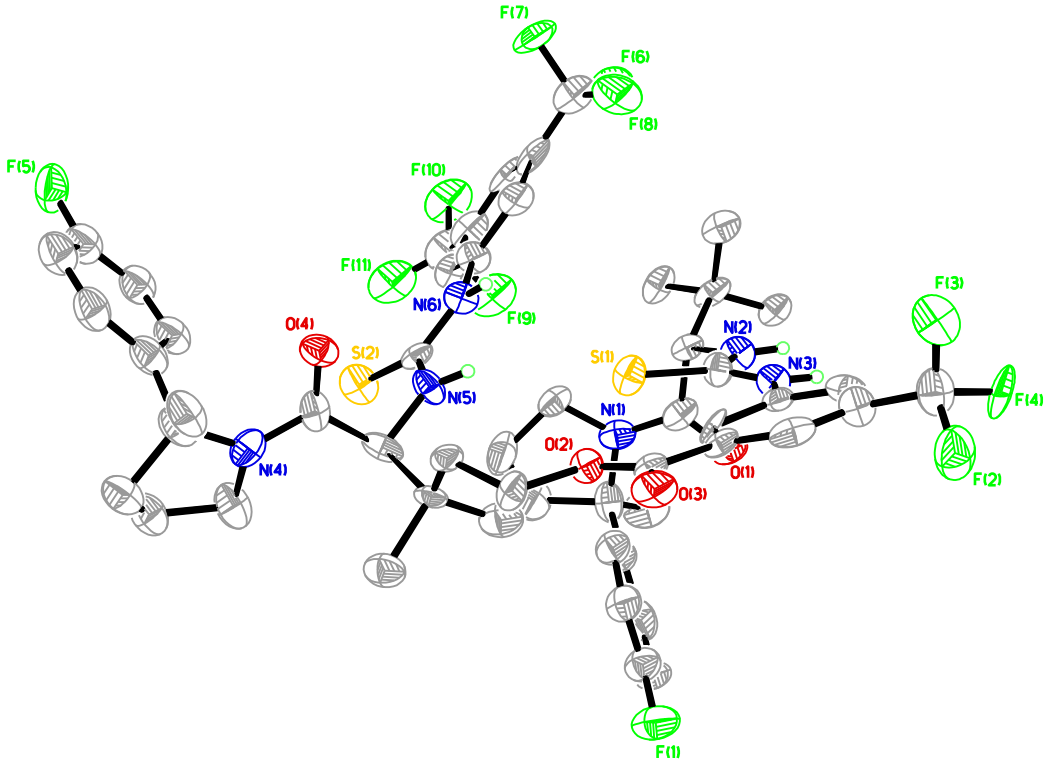

Figure S1. Perspective views showing 50% probability displacement

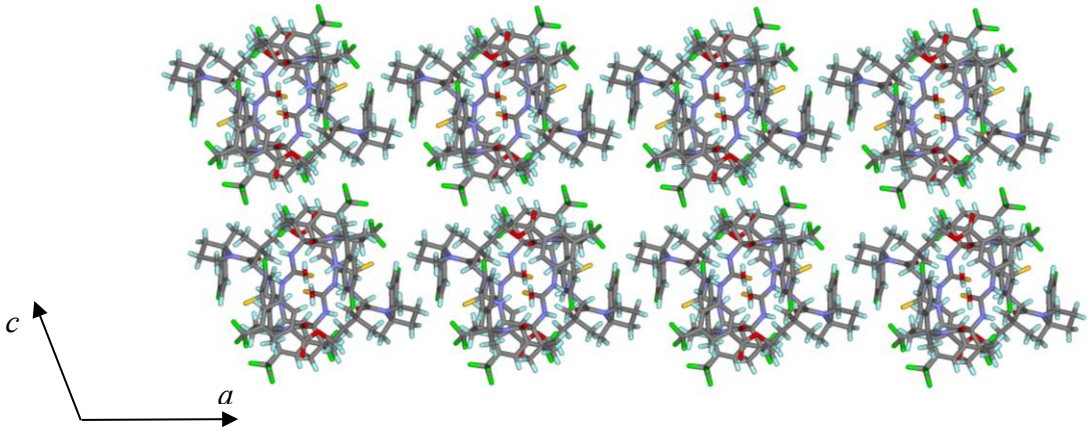

Figure S2. Three-dimensional supramolecular architecture viewed along the *b*-axis direction.

3.2 X-ray Data for Galactosyl Phosphate 2a

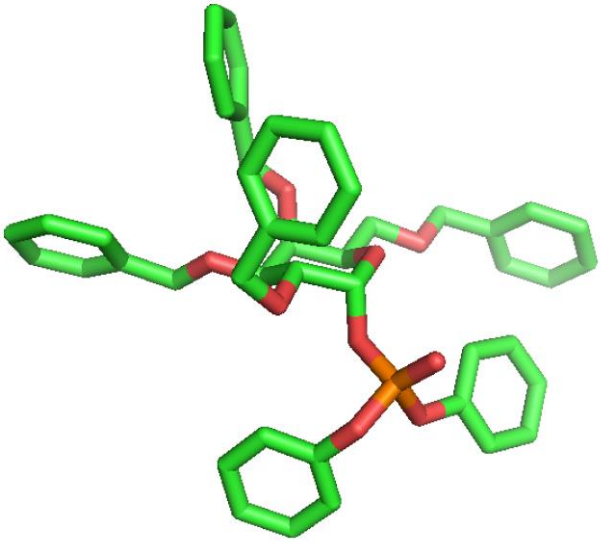

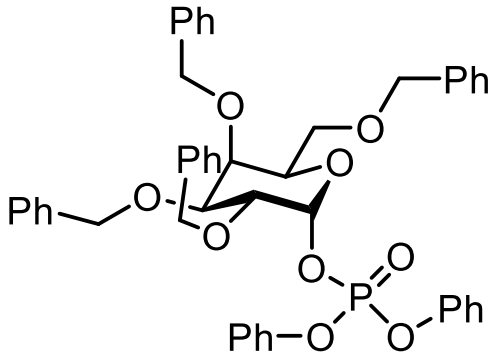

X-ray Crystallography: A crystal mounted on a diffractometer was collected data at 100 K. The intensities of the reflections were collected by means of a Bruker APEX DUO CCD diffractometer ($Cu_{K\alpha}$ radiation, λ=1.54178 Å), and equipped with an Oxford Cryosystems nitrogen flow apparatus. The collection method involved 1.0° scans in ω at -30°, -55°, -80°, 30°, 55°, 80° and 115° in 2θ. Data integration down to 0.84 Å resolution was carried out using SAINT V8.37 A (Bruker diffractometer, 2015) with reflection spot size optimization. Absorption corrections were made with the program SADABS (Bruker diffractometer, 2015). The structure was solved by the Intrinsic Phasing methods and refined by least-squares methods again F^2 using SHELXT-2014 (Sheldrick, 2015) and SHELXL-2014 (Sheldrick, 2015) with OLEX 2 interface (Dolomanov, et al., 2009). Non-hydrogen atoms were refined anisotropically, and hydrogen atoms were allowed to ride on the respective atoms. Crystal data as well as details of data collection and refinement are summarized in Table S4, and geometric parameters are shown in Table S5. The Ortep plots produced with SHELXL-2014 program, and the other drawings were produced with Accelrys DS Visualizer 2.0 (Accelrys, 2007).

Table S4. Experimental details

	SML-VI-99
Crystal data	
Chemical formula	$C_{46}H_{45}O_9P$
M_r	772.79
Crystal system, space group	Orthorhombic, $P2_12_12_1$
Temperature (K)	100
a, b, c (Å)	9.6908 (2), 10.5229 (2), 39.4294 (9)
V (Å^3)	4020.83 (15)
Z	4
Radiation type	Cu $K\alpha$
μ (mm^{-1})	1.07
Crystal size (mm)	0.18 × 0.12 × 0.10

Data collection	
Diffractometer	Bruker D8 goniometer with CCD area detector
Absorption correction	Multi-scan *SADABS*
T_{min}, T_{max}	0.751, 0.806
No. of measured, independent and observed [$I > 2\sigma(I)$] reflections	100800, 7124, 7027
R_{int}	0.033
$(\sin \theta/\lambda)_{max}$ (Å^{-1})	0.596
Refinement	
$R[F^2 > 2\sigma(F^2)]$, $wR(F^2)$, S	0.027, 0.068, 1.06
No. of reflections	7124
No. of parameters	505
H-atom treatment	H-atom parameters constrained
$\Delta\rho_{max}$, $\Delta\rho_{min}$ (e Å^{-3})	0.46, -0.28
Absolute structure	Flack x determined using 2986 quotients [(I+)-(I-)]/[(I+)+(I-)] (Parsons, Flack and Wagner, Acta Cryst. B69 (2013) 249-259).
Absolute structure parameter	0.009 (4)

Computer programs: *APEX3* v2016.9-0 (Bruker-AXS, 2016), *SAINT* 8.37A (Bruker-AXS, 2015), *SHELXT2014* (Sheldrick, 2015), *SHELXL2014* (Sheldrick, 2015), Bruker *SHELXTL* (Sheldrick, 2015).

Table S5. Geometric parameters (Å, º)

P1—O5	1.4556 (15)	C20—C25	1.376 (3)
P1—O2	1.5623 (14)	C20—C21	1.383 (3)
P1—O3	1.5692 (15)	C21—C22	1.390 (3)
P1—O4	1.5829 (15)	C21—H21	0.9500
O1—C1	1.385 (2)	C22—C23	1.383 (4)
O1—C5	1.451 (2)	C22—H22	0.9500
O2—C1	1.465 (2)	C23—C24	1.392 (4)
O3—C14	1.412 (2)	C23—H23	0.9500
O4—C20	1.416 (3)	C24—C25	1.384 (3)
O6—C2	1.423 (2)	C24—H24	0.9500
O6—C26	1.441 (2)	C25—H25	0.9500
O7—C33	1.423 (2)	C26—C27	1.510 (3)
O7—C3	1.427 (2)	C26—H26A	0.9900

O8—C40	1.429 (2)	C26—H26B	0.9900
O8—C4	1.432 (2)	C27—C32	1.384 (3)
O9—C6	1.422 (2)	C27—C28	1.393 (3)
O9—C7	1.430 (3)	C28—C29	1.383 (3)
C1—C2	1.519 (3)	C28—H28	0.9500
C1—H1	1.0000	C29—C30	1.388 (3)
C2—C3	1.520 (3)	C29—H29	0.9500
C2—H2	1.0000	C30—C31	1.390 (3)
C3—C4	1.532 (3)	C30—H30	0.9500
C3—H3	1.0000	C31—C32	1.387 (3)
C4—C5	1.522 (3)	C31—H31	0.9500
C4—H4	1.0000	C32—H32	0.9500
C5—C6	1.508 (3)	C33—C34	1.505 (3)
C5—H5	1.0000	C33—H33A	0.9900
C6—H6A	0.9900	C33—H33B	0.9900
C6—H6B	0.9900	C34—C35	1.386 (3)
C7—C8	1.496 (3)	C34—C39	1.395 (3)
C7—H7A	0.9900	C35—C36	1.391 (3)
C7—H7B	0.9900	C35—H35	0.9500
C8—C9	1.390 (4)	C36—C37	1.380 (3)
C8—C13	1.404 (4)	C36—H36	0.9500
C9—C10	1.382 (4)	C37—C38	1.386 (3)
C9—H9	0.9500	C37—H37	0.9500
C10—C11	1.380 (4)	C38—C39	1.384 (3)
C10—H10	0.9500	C38—H38	0.9500
C11—C12	1.377 (4)	C39—H39	0.9500
C11—H11	0.9500	C40—C41	1.502 (3)
C12—C13	1.388 (4)	C40—H40A	0.9900
C12—H12	0.9500	C40—H40B	0.9900
C13—H13	0.9500	C41—C46	1.382 (3)
C14—C19	1.373 (3)	C41—C42	1.397 (3)
C14—C15	1.374 (3)	C42—C43	1.385 (3)
C15—C16	1.378 (3)	C42—H42	0.9500
C15—H15	0.9500	C43—C44	1.381 (3)
C16—C17	1.365 (4)	C43—H43	0.9500
C16—H16	0.9500	C44—C45	1.382 (3)
C17—C18	1.396 (4)	C44—H44	0.9500

C17—H17	0.9500	C45—C46	1.391 (3)
C18—C19	1.403 (3)	C45—H45	0.9500
C18—H18	0.9500	C46—H46	0.9500
C19—H19	0.9500		
O5—P1—O2	115.98 (8)	C18—C19—H19	121.1
O5—P1—O3	116.95 (9)	C25—C20—C21	122.4 (2)
O2—P1—O3	105.33 (8)	C25—C20—O4	118.26 (19)
O5—P1—O4	111.73 (9)	C21—C20—O4	119.2 (2)
O2—P1—O4	105.97 (8)	C20—C21—C22	118.7 (2)
O3—P1—O4	99.08 (8)	C20—C21—H21	120.7
C1—O1—C5	113.98 (15)	C22—C21—H21	120.7
C1—O2—P1	123.14 (12)	C23—C22—C21	120.0 (2)
C14—O3—P1	127.18 (13)	C23—C22—H22	120.0
C20—O4—P1	123.54 (12)	C21—C22—H22	120.0
C2—O6—C26	113.24 (14)	C22—C23—C24	120.0 (2)
C33—O7—C3	112.67 (14)	C22—C23—H23	120.0
C40—O8—C4	114.44 (15)	C24—C23—H23	120.0
C6—O9—C7	110.60 (17)	C25—C24—C23	120.6 (2)
O1—C1—O2	108.79 (15)	C25—C24—H24	119.7
O1—C1—C2	112.74 (16)	C23—C24—H24	119.7
O2—C1—C2	108.11 (15)	C20—C25—C24	118.3 (2)
O1—C1—H1	109.0	C20—C25—H25	120.9
O2—C1—H1	109.0	C24—C25—H25	120.9
C2—C1—H1	109.0	O6—C26—C27	112.98 (16)
O6—C2—C1	107.64 (15)	O6—C26—H26A	109.0
O6—C2—C3	112.69 (16)	C27—C26—H26A	109.0
C1—C2—C3	110.58 (15)	O6—C26—H26B	109.0
O6—C2—H2	108.6	C27—C26—H26B	109.0
C1—C2—H2	108.6	H26A—C26—H26B	107.8
C3—C2—H2	108.6	C32—C27—C28	119.0 (2)
O7—C3—C2	107.54 (15)	C32—C27—C26	119.86 (18)
O7—C3—C4	111.89 (15)	C28—C27—C26	121.15 (19)
C2—C3—C4	108.28 (16)	C29—C28—C27	120.5 (2)
O7—C3—H3	109.7	C29—C28—H28	119.8
C2—C3—H3	109.7	C27—C28—H28	119.8
C4—C3—H3	109.7	C28—C29—C30	120.2 (2)

O8—C4—C5	108.76 (15)	C28—C29—H29	119.9
O8—C4—C3	109.20 (15)	C30—C29—H29	119.9
C5—C4—C3	110.29 (16)	C29—C30—C31	119.7 (2)
O8—C4—H4	109.5	C29—C30—H30	120.2
C5—C4—H4	109.5	C31—C30—H30	120.2
C3—C4—H4	109.5	C32—C31—C30	119.8 (2)
O1—C5—C6	106.84 (16)	C32—C31—H31	120.1
O1—C5—C4	111.25 (15)	C30—C31—H31	120.1
C6—C5—C4	110.91 (16)	C27—C32—C31	120.87 (19)
O1—C5—H5	109.3	C27—C32—H32	119.6
C6—C5—H5	109.3	C31—C32—H32	119.6
C4—C5—H5	109.3	O7—C33—C34	110.32 (16)
O9—C6—C5	109.39 (17)	O7—C33—H33A	109.6
O9—C6—H6A	109.8	C34—C33—H33A	109.6
C5—C6—H6A	109.8	O7—C33—H33B	109.6
O9—C6—H6B	109.8	C34—C33—H33B	109.6
C5—C6—H6B	109.8	H33A—C33—H33B	108.1
H6A—C6—H6B	108.2	C35—C34—C39	118.45 (18)
O9—C7—C8	108.5 (2)	C35—C34—C33	123.50 (18)
O9—C7—H7A	110.0	C39—C34—C33	117.98 (18)
C8—C7—H7A	110.0	C34—C35—C36	120.59 (19)
O9—C7—H7B	110.0	C34—C35—H35	119.7
C8—C7—H7B	110.0	C36—C35—H35	119.7
H7A—C7—H7B	108.4	C37—C36—C35	120.6 (2)
C9—C8—C13	119.1 (2)	C37—C36—H36	119.7
C9—C8—C7	120.9 (3)	C35—C36—H36	119.7
C13—C8—C7	119.9 (3)	C36—C37—C38	119.1 (2)
C10—C9—C8	120.3 (2)	C36—C37—H37	120.5
C10—C9—H9	119.8	C38—C37—H37	120.5
C8—C9—H9	119.8	C39—C38—C37	120.5 (2)
C11—C10—C9	120.1 (3)	C39—C38—H38	119.7
C11—C10—H10	120.0	C37—C38—H38	119.7
C9—C10—H10	120.0	C38—C39—C34	120.7 (2)
C12—C11—C10	120.6 (2)	C38—C39—H39	119.7
C12—C11—H11	119.7	C34—C39—H39	119.7
C10—C11—H11	119.7	O8—C40—C41	107.99 (17)
C11—C12—C13	119.9 (2)	O8—C40—H40A	110.1

C11—C12—H12	120.0	C41—C40—H40A	110.1
C13—C12—H12	120.0	O8—C40—H40B	110.1
C12—C13—C8	120.0 (3)	C41—C40—H40B	110.1
C12—C13—H13	120.0	H40A—C40—H40B	108.4
C8—C13—H13	120.0	C46—C41—C42	118.70 (19)
C19—C14—C15	123.6 (2)	C46—C41—C40	121.28 (19)
C19—C14—O3	114.00 (19)	C42—C41—C40	119.97 (18)
C15—C14—O3	122.34 (19)	C43—C42—C41	120.61 (19)
C14—C15—C16	117.6 (2)	C43—C42—H42	119.7
C14—C15—H15	121.2	C41—C42—H42	119.7
C16—C15—H15	121.2	C44—C43—C42	120.1 (2)
C17—C16—C15	121.4 (2)	C44—C43—H43	119.9
C17—C16—H16	119.3	C42—C43—H43	119.9
C15—C16—H16	119.3	C43—C44—C45	119.8 (2)
C16—C17—C18	120.4 (2)	C43—C44—H44	120.1
C16—C17—H17	119.8	C45—C44—H44	120.1
C18—C17—H17	119.8	C44—C45—C46	120.1 (2)
C17—C18—C19	119.3 (2)	C44—C45—H45	119.9
C17—C18—H18	120.3	C46—C45—H45	119.9
C19—C18—H18	120.3	C41—C46—C45	120.7 (2)
C14—C19—C18	117.7 (2)	C41—C46—H46	119.7
C14—C19—H19	121.1	C45—C46—H46	119.7
O5—P1—O2—C1	-7.50 (17)	P1—O3—C14—C15	-33.6 (3)
O3—P1—O2—C1	-138.51 (14)	C19—C14—C15—C16	0.8 (3)
O4—P1—O2—C1	117.10 (14)	O3—C14—C15—C16	-177.41 (19)
O5—P1—O3—C14	-48.10 (19)	C14—C15—C16—C17	-0.5 (3)
O2—P1—O3—C14	82.35 (17)	C15—C16—C17—C18	-0.1 (4)
O4—P1—O3—C14	-168.22 (17)	C16—C17—C18—C19	0.4 (4)
O5—P1—O4—C20	-178.69 (15)	C15—C14—C19—C18	-0.5 (3)
O2—P1—O4—C20	54.13 (17)	O3—C14—C19—C18	177.83 (19)
O3—P1—O4—C20	-54.79 (17)	C17—C18—C19—C14	-0.1 (3)
C5—O1—C1—O2	63.81 (18)	P1—O4—C20—C25	-95.9 (2)

C5—O1—C1—C2	-56.1 (2)	P1—O4—C20—C21	88.4 (2)
P1—O2—C1—O1	112.83 (16)	C25—C20—C21—C22	0.2 (3)
P1—O2—C1—C2	-124.44 (15)	O4—C20—C21—C22	175.75 (18)
C26—O6—C2—C1	138.80 (16)	C20—C21—C22—C23	-0.8 (3)
C26—O6—C2—C3	-99.01 (18)	C21—C22—C23—C24	1.0 (4)
O1—C1—C2—O6	179.48 (15)	C22—C23—C24—C25	-0.6 (4)
O2—C1—C2—O6	59.19 (19)	C21—C20—C25—C24	0.2 (3)
O1—C1—C2—C3	56.0 (2)	O4—C20—C25—C24	-175.41 (18)
O2—C1—C2—C3	-64.3 (2)	C23—C24—C25—C20	0.0 (3)
C33—O7—C3—C2	-160.96 (15)	C2—O6—C26—C27	-62.1 (2)
C33—O7—C3—C4	80.26 (19)	O6—C26—C27—C32	125.11 (19)
O6—C2—C3—O7	63.58 (19)	O6—C26—C27—C28	-55.3 (2)
C1—C2—C3—O7	-175.90 (15)	C32—C27—C28—C29	-0.6 (3)
O6—C2—C3—C4	-175.34 (15)	C26—C27—C28—C29	179.77 (18)
C1—C2—C3—C4	-54.8 (2)	C27—C28—C29—C30	0.2 (3)
C40—O8—C4—C5	134.53 (17)	C28—C29—C30—C31	0.4 (3)
C40—O8—C4—C3	-105.07 (19)	C29—C30—C31—C32	-0.7 (3)
O7—C3—C4—O8	54.2 (2)	C28—C27—C32—C31	0.4 (3)
C2—C3—C4—O8	-64.17 (19)	C26—C27—C32—C31	179.99 (18)
O7—C3—C4—C5	173.63 (15)	C30—C31—C32—C27	0.3 (3)
C2—C3—C4—C5	55.29 (19)	C3—O7—C33—C34	-179.03 (15)
C1—O1—C5—C6	177.07 (16)	O7—C33—C34—C35	-15.0 (3)
C1—O1—C5—C4	55.9 (2)	O7—C33—C34—C39	168.04 (17)
O8—C4—C5—O1	64.6 (2)	C39—C34—C35—C36	1.8 (3)
C3—C4—C5—O1	-55.1 (2)	C33—C34—C35—C36	-175.13 (18)

O8—C4—C5—C6	-54.2 (2)	C34—C35—C36—C37	0.1 (3)
C3—C4—C5—C6	-173.92 (17)	C35—C36—C37—C38	-1.2 (3)
C7—O9—C6—C5	176.2 (2)	C36—C37—C38—C39	0.2 (3)
O1—C5—C6—O9	66.2 (2)	C37—C38—C39—C34	1.8 (3)
C4—C5—C6—O9	-172.42 (17)	C35—C34—C39—C38	-2.8 (3)
C6—O9—C7—C8	171.7 (2)	C33—C34—C39—C38	174.34 (19)
O9—C7—C8—C9	95.8 (3)	C4—O8—C40—C41	163.65 (16)
O9—C7—C8—C13	-81.7 (3)	O8—C40—C41—C46	131.7 (2)
C13—C8—C9—C10	1.2 (4)	O8—C40—C41—C42	-50.9 (3)
C7—C8—C9—C10	-176.3 (2)	C46—C41—C42—C43	-0.5 (3)
C8—C9—C10—C11	-0.5 (4)	C40—C41—C42—C43	-178.0 (2)
C9—C10—C11—C12	-0.8 (4)	C41—C42—C43—C44	0.7 (3)
C10—C11—C12—C13	1.3 (4)	C42—C43—C44—C45	-0.4 (3)
C11—C12—C13—C8	-0.6 (3)	C43—C44—C45—C46	-0.1 (3)
C9—C8—C13—C12	-0.7 (3)	C42—C41—C46—C45	0.0 (3)
C7—C8—C13—C12	176.8 (2)	C40—C41—C46—C45	177.4 (2)
P1—O3—C14—C19	148.04 (16)	C44—C45—C46—C41	0.3 (4)

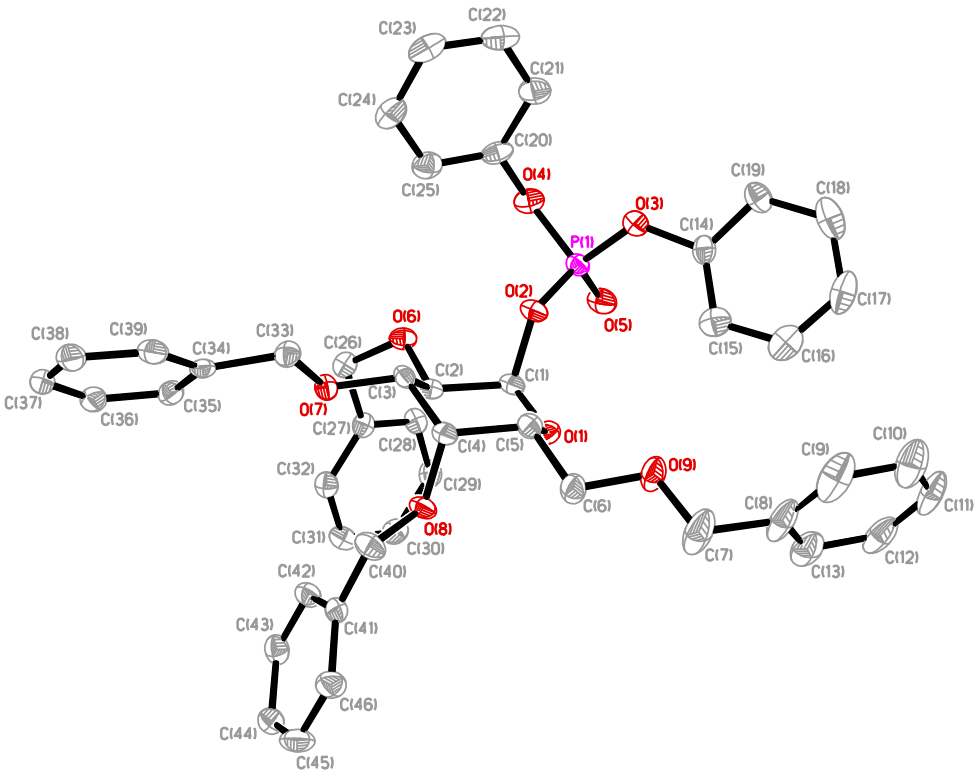

Figure S3. Perspective views showing 50% probability displacement

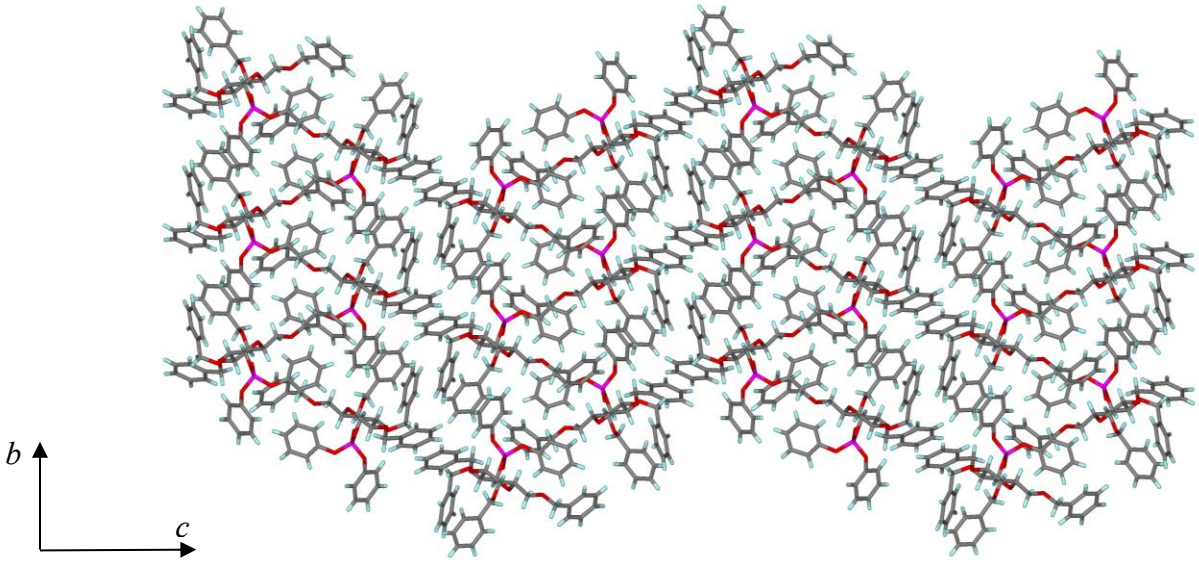

Figure S4. Three-dimensional supramolecular architecture viewed along the *a*-axis direction.

4. Catalyst Evaluation for Glycosyl Phosphate Activation

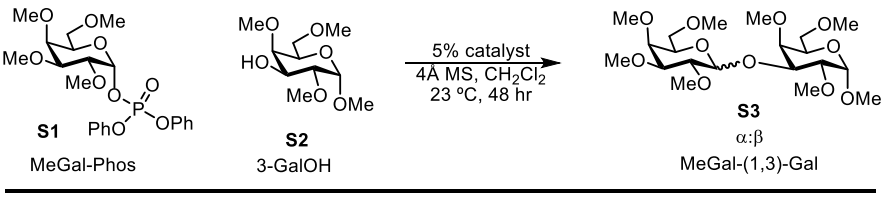

Sieves do not sequester phosphoric acid when used in CH_2Cl_2

*Trace conversion <10%

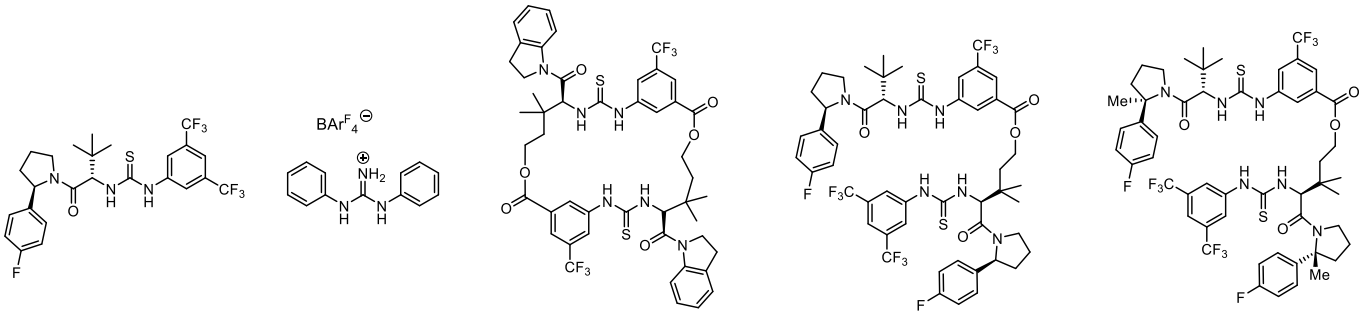

Reisman-Doyle Thiourea
Trace conversion

Diphenyl Guanidinium BArF
Trace conversion

Indocat
Trace Conversion

***epi-* "Naomi Dimer"**
30% conversion
1:20 α:β

Catalyst 1
"Fully Substitued Naomi Dimer"
100% conversion
1:4 α:β

Scheme S1. Preliminary catalyst screen with Galactose-Galactose model system

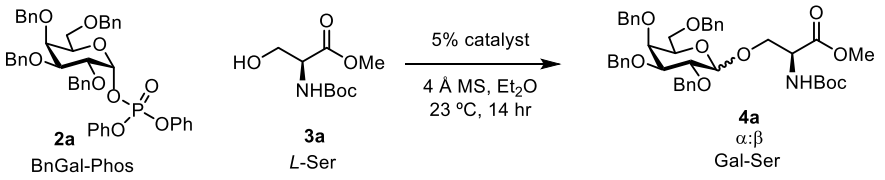

*Trace conversion <10%

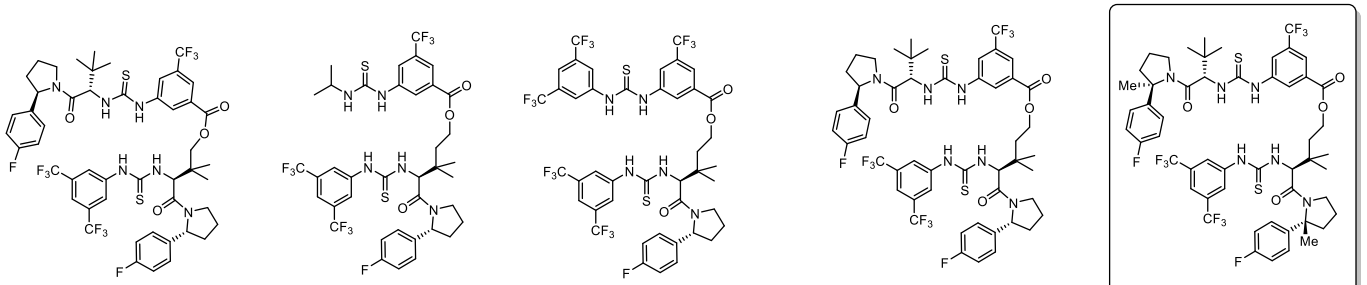

***n*=1 "Naomi Dimer"**
Trace conversion

Northern Isopropyl
Trace conversion

Northern Schreiner
20% conversion
1:2.6 α:β

"Naomi Dimer"
(stereochemistry shown)
85% conversion
1:27 α:β

***ent-* "Naomi Dimer"**
(*ent-* of stereochemistry shown)
14% conversion
1:4 α:β

Catalyst **1**

Catalyst 1 carried forward as optimal catalyst, despite lower reactivity, for improved selectivity and broader donor scope.

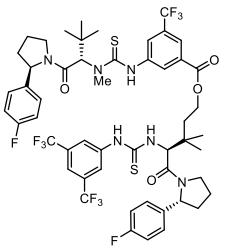

Northern N-Me Thiourea
Trace conversion

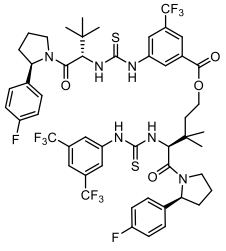

Southern Epimer
41% conversion
1:15 α:β

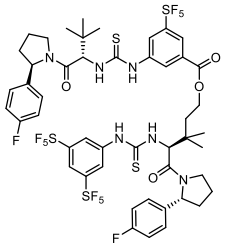

Tri-SF_5
90% conversion
1:42 α:β

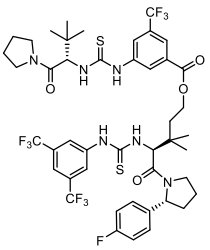

Northern Pyrrolidine
42% conversion
1:15 α:β

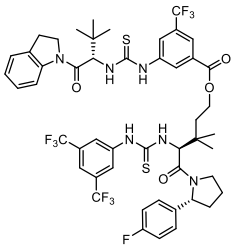

Northern Indoline
52% conversion
1:15 α:β

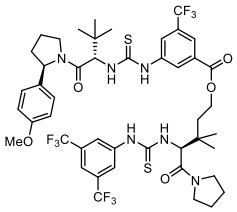

Northern *p*-OMe Phenyl
Southern Pyrrolidine
78% conversion
1:34 α:β

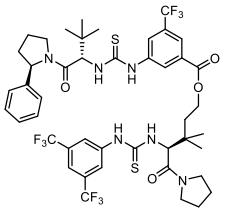

Northern Phenyl Pyrrolidine
Southern Pyrrolidine
77% conversion
1:36 α:β

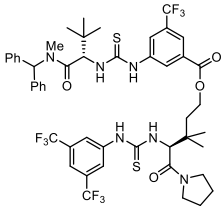

Northern N-Me Benzhydryl
Southern Pyrrolidine
52% conversion
1:24 α:β

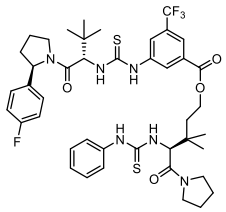

Southern Ph-Thiourea
Southern Pyrrolidine
30% conversion
1:14 α:β

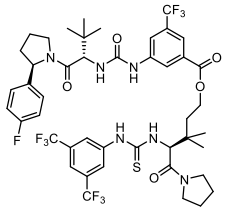

Northern Urea
Southern Pyrrolidine
45% conversion
1:15 α:β

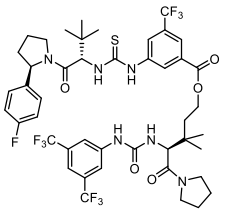

Southern Urea
Southern Pyrrolidine
65% conversion
1:21 α:β

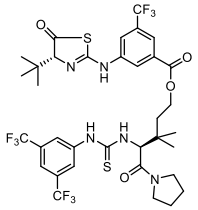

Northern Thiazolone
Southern Pyrrolidine
Trace conversion

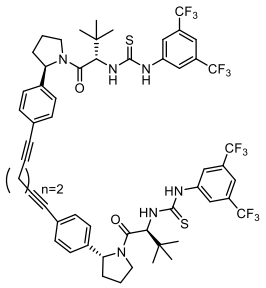

Tail-to-Tail dimer
Trace conversion

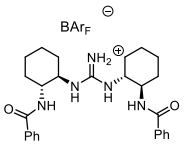

Guanidinium monomer
Trace conversion

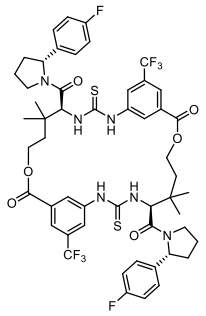

***Macro* Naomi Dimer**
Trace conversion

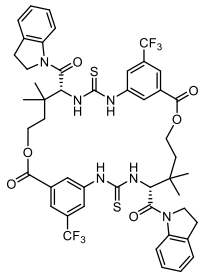

(*R,R*) Indocat
Trace conversion
(*S,S*) Indocat
Trace conversion

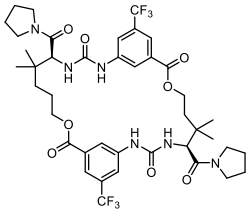

***(2,3)* Pyrrolidine Macrocycle**
Trace conversion

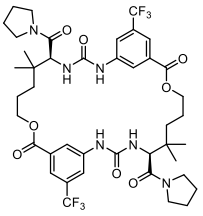

***(3,3)* Pyrrolidine Macrocycle**
Trace conversion

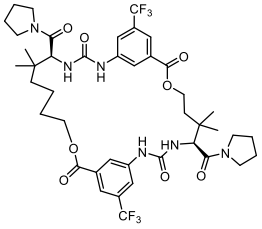

***(2,4)* Pyrrolidine Macrocycle**
Trace conversion

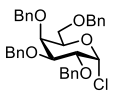

2b
BnGal-Cl

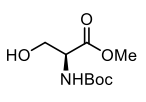

3a
L-Ser

10% **(R,R)-Indocat**

4 Å MS, Toluene

23 ºC, 14 hr

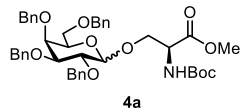

4a
α:β
Gal-Ser

Conditions from *Science* **2017**, *355*, 162.

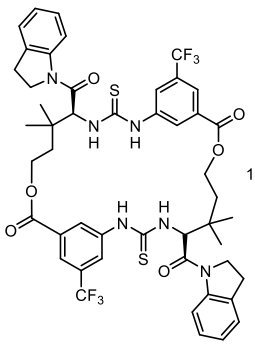

Indocat
16% conversion
25:75 α:β

Scheme S2. Catalyst screen with Galactose-Serine model system

General Procedure: To a 0.5 dram vial was added catalyst, donor, acceptor, and molecular sieves. The vial was charged with a stir-bar and solvent was added (open to air). The mixture was sealed with a PTFE cap and stirred at the indicated temperature. For workup, the mixture was diluted with diethyl ether, filtered, and concentrated. This concentrated mixture was promptly diluted with $CDCl_3$ and analyzed immediately by ^1H NMR analysis using a single scan. Conversion was determined to highly correlate with yield and was calculated by integrating product relative to starting material and hydrolysis byproduct (the only isolable side-product).

Note: *For reactions run in ethereal solvents and aromatic solvents, no phosphoric acid is visible in the NMR spectra. See* ***Section 5*** *for data and discussion.*

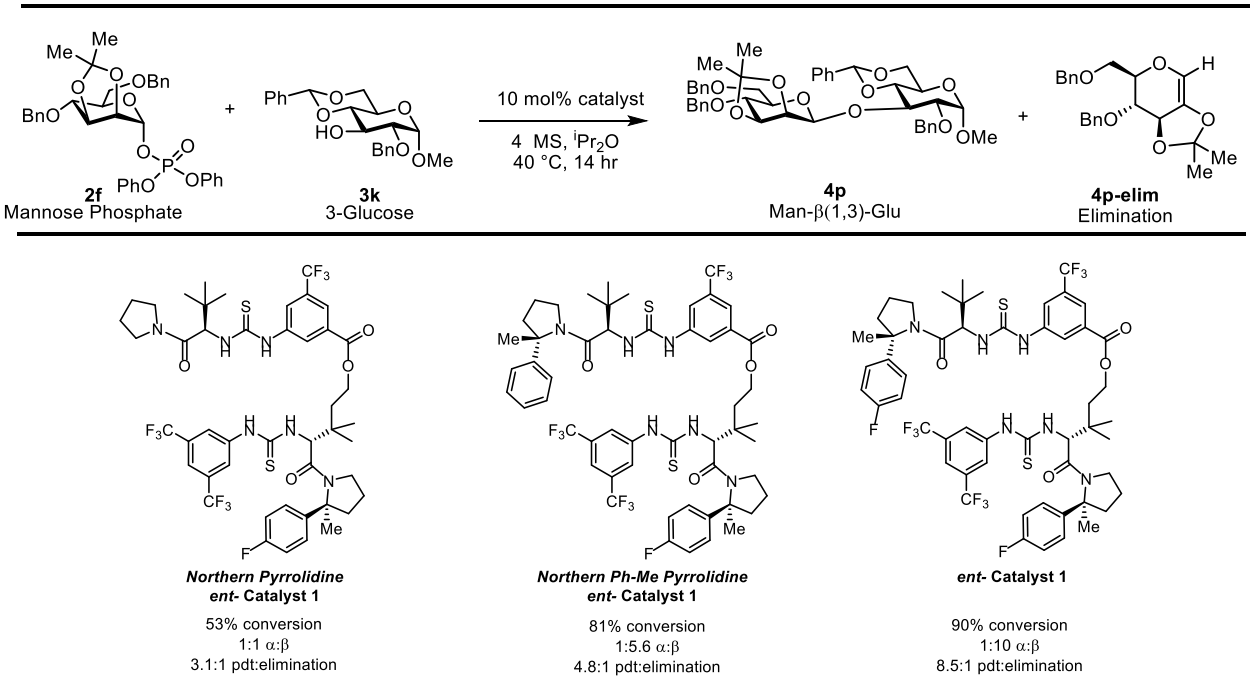

Scheme S3. Catalyst screen with Mannose-Glucose model system

5. Leaving Group Evaluation

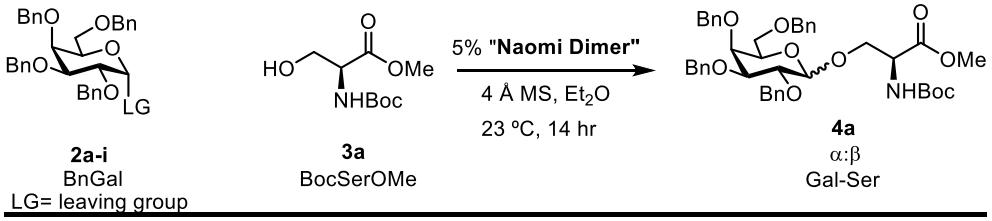

2a-i
BnGal
LG= leaving group

3a
BocSerOMe

4a
α:β
Gal-Ser

Leaving group survey

Leaving group	% Conversion	α:β
-Cl (**2b**)	48%	<1:20
-OP(O)(OPh)$_2$ (2a)	**100%**	**<1:20**
-OAc (**2d**)	0%	N/A
-OC(NH)(CCl$_3$) (**2c**)	0%	N/A
-OMs* (**2h**)	background only	2:1
-ONO$_2$** (**2i**)	0%	N/A

*Performed in CH_2Cl_2 following *in-situ* activation with Ms_2O

**2-Azido Galactose was used due to safety concerns with the nitration of galactose

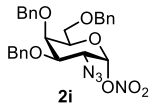

2i
2-Azido Galactose Nitrate

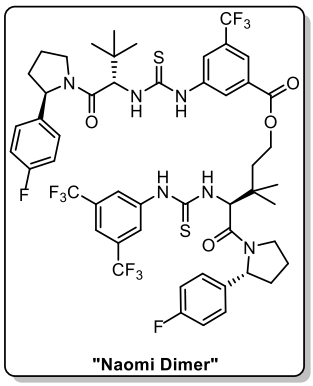

"Naomi Dimer"

Scheme S4. Leaving group evaluation on galactosyl donor **2** with Galactose-Serine model system

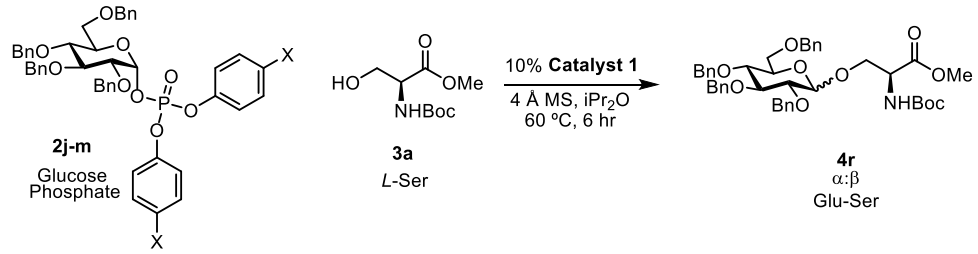

-X	% Conversion	α:β
-Cl (**2j**)	Not soluble	N/A
-Me (**2k**)	42%	1:4.6
-H (**2l**)	61%	1:4.8
-OMe (**2m**)	47%	1:4.8

Run at 0.033 M due to low solubility of several substrates

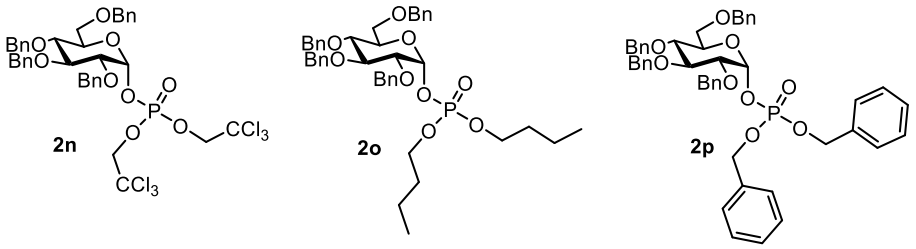

Donors give trace reactivity (<10%) after 24 hr at 23 ºC in Et_2O

Scheme S5. Phosphate leaving group optimization on glucosyl phosphate (**2j-m**)

6. Stereospecificity Experiment

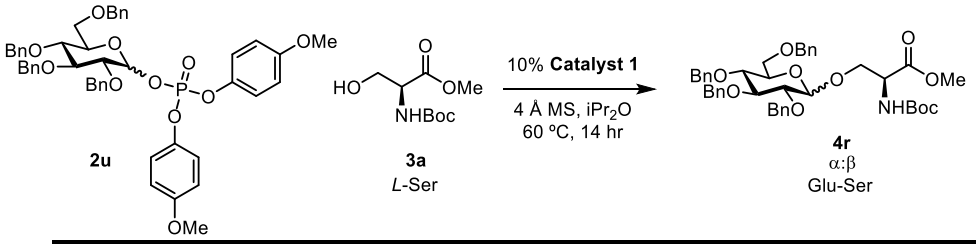

Stereospecificity:

2u (α:β)	% Conversion	**4r** (α:β)
α-only	89%	1:3.8
4.3:1	82%	1:3.8

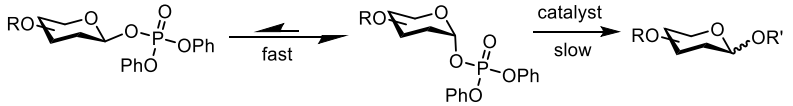

Scheme S6. Phosphate leaving group optimization on glucosyl phosphate (**2j**)

We observe that both anomeric mixtures of glycosyl donor and pure-α glycosyl phosphate donor result in the same product anomeric-selectivity. This has also been observed with 2-azido-galactosyl donor, **2e**, starting with pure-β phosphate donor. Additionally, we observe highly-α enriched starting material (**2u**) after the reaction has been running for 14 hours. We do not observe decomposition of the β-phosphate, suggesting that anomerization of starting material to the thermodynamically favored α-phosphate is fast compared to the glycosylation reaction.

While previous studies with these catalysts and glycosyl chlorides indicated a stereospecific process, the prevalence of α-product from α-glycosyl phosphate is not yet well understood. We and others have hypothesized that these reactions occur within the S_N1-S_N2 continuum, where a highly stereospecific process can arise from a loose, asynchronous-S_N1 mechanism. If this is the case, then α-donor to α-product may be possible from the formation of a (nascent) oxocarbenium species. Further mechanistic elucidation is required to more fully understand this process with glycosyl phosphates.

7. Optimization of Reaction Conditions

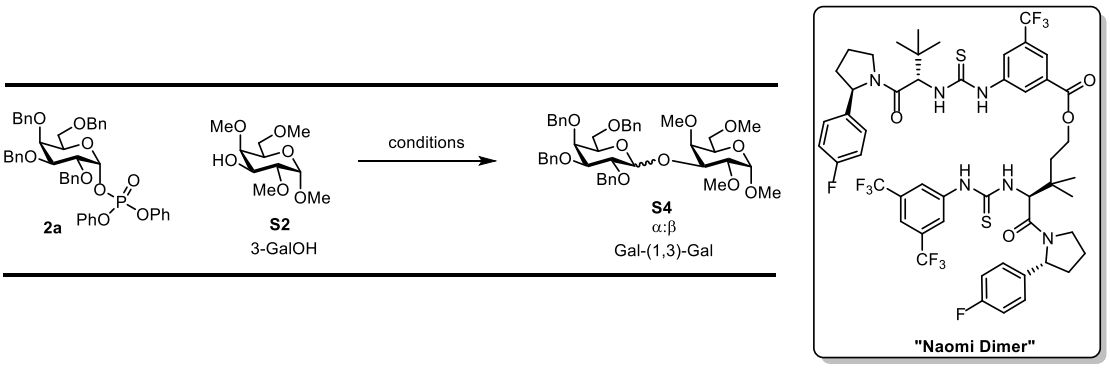

Scheme S7. Galactose (**2a**) and 3-GalOH (**S2**) model system used for optimization of conditions

"Naomi Dimer"	% Conversion	% hydrolysis
N/A	0%	0%
5 mol%	22%	1%
10 mol%	27%	1%
20 mol%	43%	1%

4 Å MS (1.0 g/mL), 0.1 M **2a**, 0.2 M **S2** in Et_2O for 5 hr at 23 ºC

Table S6. Effect of catalyst loading in the reaction mixture

[S2] (M)	% Conversion	% hydrolysis
0.05	9%	1%
0.10	15%	1%
0.20	22%	1%
0.40	14%	1%

10 mol% "**Naomi Dimer**", 4 Å MS (1.0 g/mL), 0.1 M **2a**, 5 hr at 23 ºC

Table S7. Effect of acceptor (**S2**) concentration in the reaction mixture

[2a] (M)	% Conversion	% hydrolysis
0.05	20%	2%
0.10	27%	1%
0.20	26%	2%
0.40	25%	2%

10 mol% "**Naomi Dimer**", 4 Å MS (1.0 g/mL), 0.2 M **S2** in Et_2O for 5 hr at 23 ºC

Table S8. Effect of donor (**2a**) concentration in the reaction mixture

Temp. (ºC)	% Conversion	% hydrolysis	α:β
23	27%	2%	<1:20
40	49%	2%	~1:20
40 (no catalyst)	trace	<1%	2:1**

10 mol% "**Naomi Dimer**", 4 Å MS (1.0 g/mL), 0.1 M **2a** 0.2 M **S2** in $^{i}Pr_2O$ for 5 hr

Note: Higher temperatures resulted in lower selectivity due to increased background.

**19 hours at 40 ºC yields 20% conversion to α+β mixture with 2:1 α:β.

Table S9. Effect of temperature

4 Å MS (g/mL)	% Conversion	% hydrolysis	α:β
0	45%	3%	1:5
0.5	18%	1%	<1:20
1.0	**22%**	**1%**	**<1:20**
2.0	21%	1%	<1:20

10 mol% "**Naomi Dimer**", 0.1 M **2a**, 0.2M **S2,** 5 hr at 23 ºC in Et_2O

Table S10. Effect of molecular sieves in the reaction mixture

Solvent	% Conversion	% hydrolysis	α:β
Dichloromethane*	N/A	N/A	N/A
Acetonitrile	12%	3%	1:1
DMF	19%	5%	4:1
THF	<1%	1%	N/A
Toluene	16%	1%	~1:20
Glyme	N/A	N/A	N/A
MTBE	46%	3%	<1:20
CPME	31%	1%	~1:20
TBEE	75%	1%	<1:20
iPr_2O	**90%**	**2%**	**<1:20**
Et_2O	47%	2%	<1:20
Cyclohexane	80%	1%	<1:20

10 mol% "**Naomi Dimer**", 0.1 M **2a**, 0.2M **S2,** 4 Å MS (1.0 g/mL), 4 hr at 40 ºC

* 14 hr at 23 ºC. No reaction observed by NMR.

Table S11. Optimization of solvent

8. Studies with Phosphoric Acid Byproduct

4 Å MS	"Naomi Dimer"	$(PhO)_2P(O)OH$	% Conversion	% hydrolysis	α:β
N/A	N/A	N/A	0%	0%	N/A
1.0 g/mL	N/A	N/A	0%	0%	N/A
N/A	10 mol%	N/A	45%	3%	1:5
N/A	N/A	50 mol%	59%	2%	1:2
N/A	10 mol%	50 mol%	66%	3%	1:2.5
1.0 g/mL	10 mol%	50 mol%	26%	1%	<1:20
1.0 g/mL	10 mol%	N/A	27%	1%	<1:20

10 mol% "**Naomi Dimer**", 0.05 M **$(PhO)_2P(O)OH$**, 4 Å MS (1.0 g/mL), 0.1 M **2a**, 0.2 M **S2** in Et_2O for 5 hr at 23 ºC

Table S12. The effect of phosphoric acid on reactivity and selectivity with and without catalyst and molecular sieves

These results suggest that:

1) Phosphoric acid is a competent activator of glycosylation reactions involving phosphate leaving groups
2) The phosphoric acid promoted pathway is unselective and competitive with the bis-thiourea catalyzed pathway
3) Molecular sieves do not promote the reaction but can sequester free phosphoric acid in solution. ^{1}H NMR analysis of the crude, filtered, reaction mixtures reveal no phosphoric acid remaining in solution when molecular sieves are added. Zeolites are well known to adsorb phosphate species to their surface. Additionally, **Table S10** demonstrates the molecular sieves are saturating the solution such that increasing or decreasing the concentration of sieves (by a factor of two) does not influence reactivity or anomeric selectivity.
4) Bis-thiourea ("**Naomi Dimer"**) can catalyze highly β-selective glycosylation reactions when phosphoric acid is efficiently removed from the reaction mixture.

The process of sequestering phosphoric acid with molecular sieves has been found to depend on solvent. Specifically, reactions conducted in dichloromethane were found to contain substantial quantities of phosphoric acid with and without the addition of molecular sieves, resulting in drastically reduced β-selectivity.

Additional kinetic studies have shown that selectivity is constant over the course of the reaction when sieves and bis-thiourea catalyst are used together (under optimized reaction conditions).

9. Inhibition Studies with Glycosyl Chlorides and Macrocyclic Bis-Thiourea Catalyst

9.1 Competition Experiment and Data Analysis

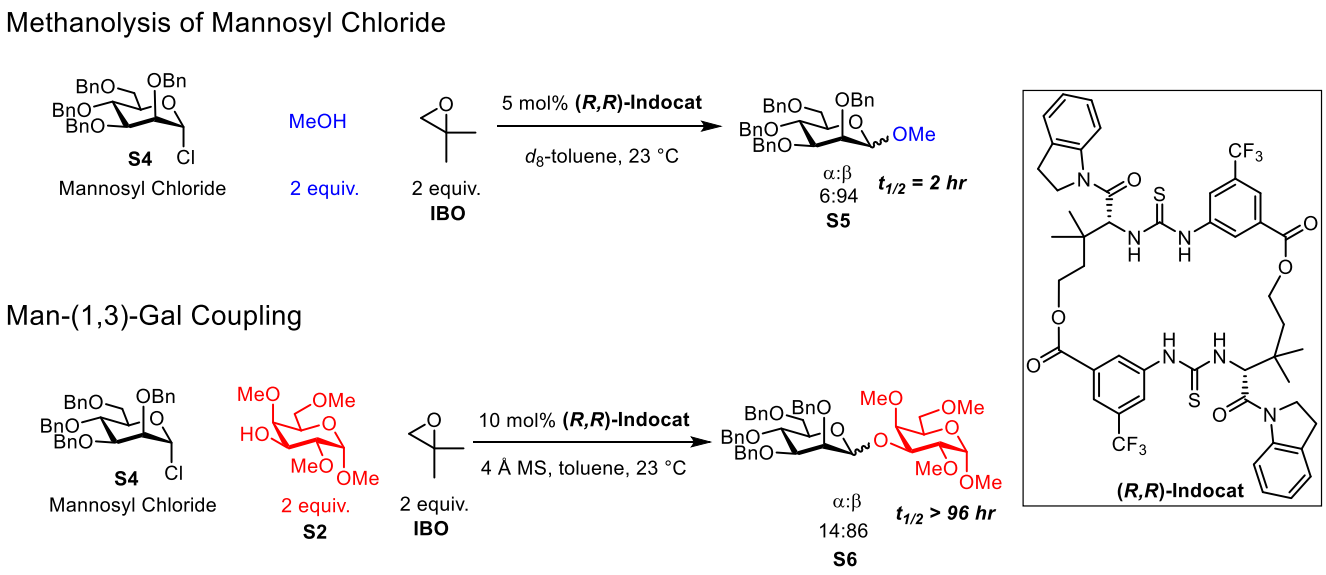

Scheme S8. Glycosylation of Mannosyl chloride prohibitively slow with glycosyl acceptors

In our previously published system with glycosyl chlorides and the catalyst, **Indocat**, we were unable to extend our glycosylation method beyond simple alcohol acceptors. While simple glycosyl acceptors were possible, reduced rates and selectivity were observed.

One example of this limitation is shown in **Scheme S8**. Based on the results summarized above, we hypothesized that rate reduction with **S2** could be due to inhibition of the catalyst by the glycosyl acceptor. To more rigorously test this hypothesis, a competition experiment was conducted between **S2** and methanol. Since the half-life of the methanol reaction with mannosyl chloride (**S4**) was fast on the timescale of the 3-galactose (**S2**) coupling, we would expect to see only methanolysis.

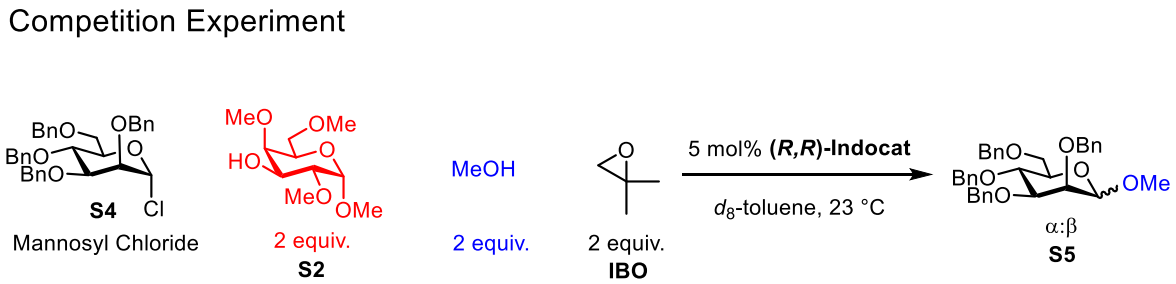

Scheme S9. Competition experiment between methanol and galactose (**S2**) with mannosyl chloride donor (**S4**)

Three experiments were run to test if **S2** inhibits **(*R,R*) Indocat**.

1) The first was reacting **S4** with two-equivalents of methanol, which constitutes the standard reaction conditions.
2) The second experiment used two equivalents of methanol and two equivalents of **S2**.

3) The third experiment reacted four equivalents of methanol with **S4**, to test the effect of doubling the total alcohol concentration in solution.

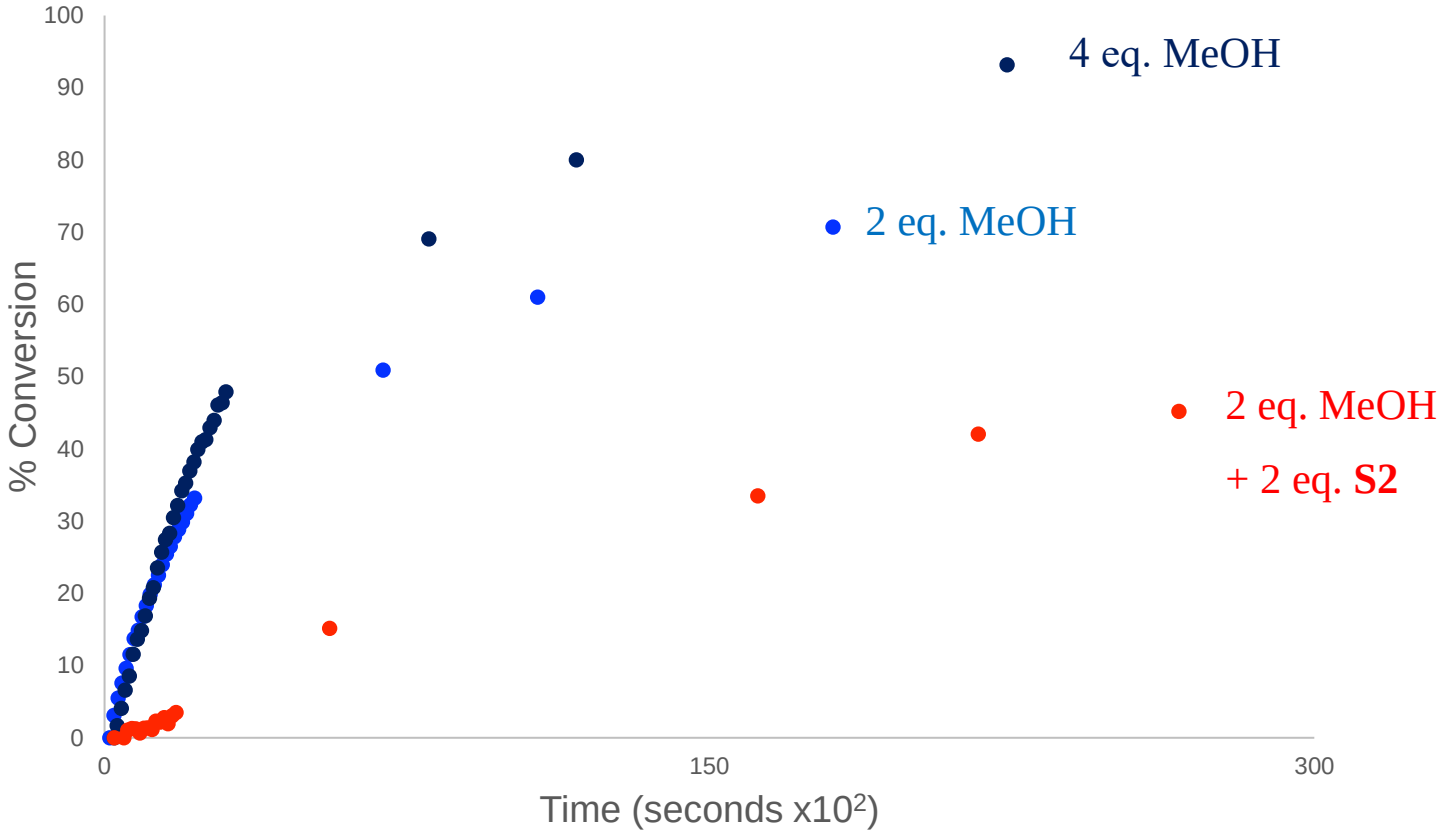

Figure S5. Competition experiment between methanol and galactose (**S2**) with mannosyl chloride donor (**S4**)

The results of the competition experiment clearly demonstrate that **S2** inhibits the catalyst, (*R,R*) Indocat (red points in Figure S5). Using the first 5% conversion measured, the rate is 7.6x slower when **S2** is added to the methanolysis reaction. Additionally, this is not due to the presence of four equivalents of total alcohol in solution since four equivalents of methanol increase the reaction rate (black points in Figure S5).

9.2 Experimental Details for Competition Experiment

Exp. 1: 2 equiv. MeOH

To a dry J. Young NMR tube was added (*R,R*)-Indocat (2.5mg, 0.05 µmol, 5 mol%), 500 µL d_8-toluene, and 4 µL MeOH (2.0 eq., 0.10 mmol, sure/seal, Aldrich). The mixture was shaken until homogeneous and 10 µL isobutylene oxide (IBO, 2.3 eq., 0.11 mmol) and 2.5 µL mesitylene (0.36 eq., 0.02 mmol, internal standard) were added. To the side of the NMR tube (such that it did not contact the solution at the bottom of the tube) was added 28 mg mannosyl chloride, S4 (1.0 eq., 0.05 mmol). The tube was subsequently shaken, and the time was noted. NMR array collection was initiated with 25 sec. delay and single scan for each point.

Exp. 2: 4 equiv. MeOH

To a dry J. Young NMR tube was added (*R,R*)-Indocat (2.5mg, 0.05 μmol, 5 mol%), 500 μL d_8-toluene, and 8 μL MeOH (4.0 eq., 0.20 mmol, sure/seal, Aldrich). The mixture was shaken until homogeneous and 10 μL isobutylene oxide (IBO, 2.3 eq., 0.11 mmol) and 2.5 μL mesitylene (0.36 eq., 0.02 mmol, internal standard) were added. To the side of the NMR tube (such that it did not contact the solution at the bottom of the tube) was added 28 mg mannosyl chloride, **S4** (1.0 eq., 0.05 mmol). The tube was subsequently shaken and the time was noted. NMR array collection was initiated with 25 sec. delay and single scan for each point.

Exp. 3: 2 equiv. MeOH + 2 equiv. 3OH-MeGal (**S2**)

(*R,R*)-Indocat (2.5mg, 0.05 μmol, 5 mol%) and 3OH-MeGal, **S2**, (2 equiv., 24 mg, 0.10 mmol) were mixed and concentrated 3X with benzene and put on high-vacuum overnight. To this mixture was added 500 μL d_8-toluene and the mixture was transferred to a dry J. Young NMR tube. Next, 4 μL MeOH (2.0 eq., 0.10 mmol, sure/seal, Aldrich) was added and the mixture was shaken until homogeneous, followed by 10 μL isobutylene oxide (IBO, 2.3 eq., 0.11 mmol) and 2.5 μL mesitylene (0.36 eq., 0.02 mmol, internal standard). To the side of the NMR tube (such that it did not contact the solution at the bottom of the tube) was added 28 mg mannosyl chloride, **S4** (1.0 eq., 0.05 mmol). The tube was subsequently shaken and the time was noted. NMR array collection was initiated with 25 sec. delay and single scan for each point.

Data analysis:

The arrayed data as well as the subsequent individual time points taken were baseline corrected and analyzed by integration of mesitylene internal standard to the disappearance of the mannosyl chloride (S4) anomeric proton. Appearance of the β-OMe mannose product was also tracked and corresponds to disappearance of mannosyl chloride starting material. Conversion for the graph below was calculated by setting the first spectrum taken equal to 0% conversion. The first spectrum was typically taken 2-4 minutes from the start of the reaction. On the time scale of the reaction ($t_{1/2}$ of ~2 hr), this conversion is small (<10%).

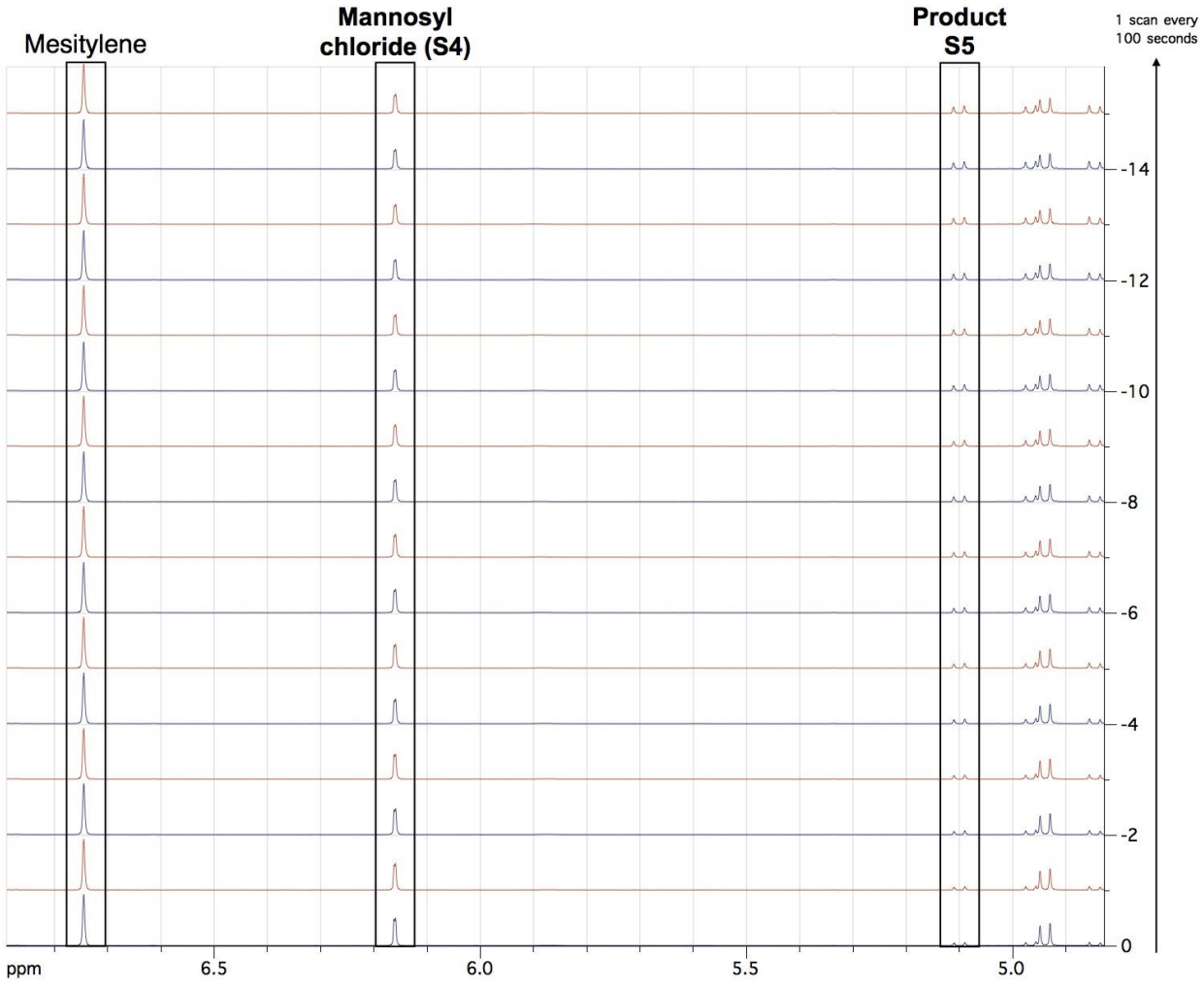

Figure S6. Typical ^{1}H NMR array used for kinetic data analysis

10. Kinetic Analyses of Galactosyl Phosphate (2a) and Galactosyl Chloride (2b)

10.1 . Preparation of Materials for Kinetic Experiments

Note: all stock solutions were prepared using volumetric flasks at 23 ˚C.

28 mg of catalyst **1** and 15 µL of dibenzyl ether (internal standard for HPLC) were added to an oven-dry 1 mL volumetric flask with diisopropyl ether (sure/seal, Aldrich) to generate a solution 0.025 M in catalyst **1** and 0.079 M in dibenzyl ether. It was necessary to store this solution at -80 ˚C to prevent crystallization of the catalyst, which occurs over several days at room temperature.

A 3 M stock solution of (*L*)-Boc-Ser-OMe (**3a**) was prepared and diluted to the desired concentration for each run and stored at 23˚C.

Two stock solutions of galactosyl phosphate (**2a**) in diisopropyl ether were prepared (0.167 M and 0.333 M) and stored at -80˚C. Under these conditions, the substrate crystallizes (see X-ray structure section). For each use, the mixture was slowly warmed to room temperature (23 ˚C) and heated in an oil bath at 40 ˚C until homogeneous. This mixture was then diluted to the desired concentration for each run.

Two stock solutions of galactosyl chloride (**2b**) in diisopropyl ether were prepared (0.167 M and 0.333 M) and stored at -80 ˚C. For each use, the mixture was slowly warmed to room temperature (23 ˚C). This mixture was then diluted to the desired concentration for each run.

A stock solution of galactosyl chloride (**2b**) and galactosyl phosphate (**2a**) in diisopropyl ether was prepared (0.167 M in each glycosyl donor) and stored at -80 ˚C. For each use, the mixture was slowly warmed to room temperature (23 ˚C). This mixture was then diluted to the desired concentration for each run.

10.2 . General Procedure for Kinetic Experiments

To a 0.5 dram vial with stir bar and PTFE cap was charged with 4 Å MS (1 mg/10 µL solvent), glycosyl donor solution, (*L*)-Boc-Ser-OMe (**3a**) solution. This solution was stirred at 40 ˚C for 5 minutes to equilibrate temperature followed by injection of catalyst/internal standard stock solution and the time was noted.

10.3 General Procedure for Sample Collection and HPLC Analysis

The PTFE cap of the 0.5 dram vial stirring at 40˚C was punctured with a 25 µL glass syringe and 10 µL of solution was removed and immediately injected into a new 0.5 dram vial with 500 µL 5% iPrOH/Hexanes. This process efficiently stops the reaction as determined by HPLC analysis the same day and three days after sample collection with no change in product formation. This mixture is pushed through a syringe filter into an HPLC sample vial and capped.

Using 5% iPrOH/Hexanes mobile phase and an AD-H chiral HPLC column, the samples were run for 25 minutes. The β– product was measured relative to the internal standard.

10.4 Reaction Time-Course with Galactosyl Phosphate (2a) and *L*-Ser (3a)

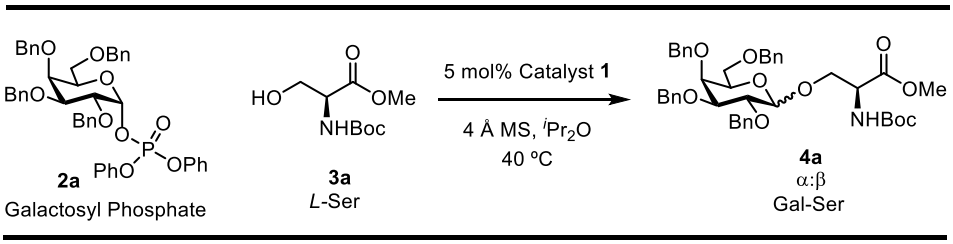

Scheme S10. Galactosyl phosphate and *L*-Serine model system used for kinetic evaluation

A 0.5 dram vial with stir bar and PTFE cap was charged with galactosyl phosphate (**2a**) (0.1 M, 0.05 mmol), (*L*)-BocSerOMe (**3a**) (0.2 M, 0.10 mmol), 4 Å MS (50 mg). This 400 µL solution was stirred at 40 ˚C for 5 minutes to equilibrate temperature followed by injection of catalyst/internal standard stock solution (100 µL) and the time was noted.

HPLC samples were collected according to the above general procedure and analyzed at 254 nm. As shown below, internal standard elutes at 4.3 minutes and product elutes at 20 minutes The Product/Internal standard ratio was normalized to 95% conversion at 6 hours based on ReactIR and NMR data collected on a larger scale (0.15 mmol) of the same reaction. Since the conversion to product is equal to yield (based on isolated yields during scale-up), the concentration of starting glycosyl donor was determined by subtracting product concentration.

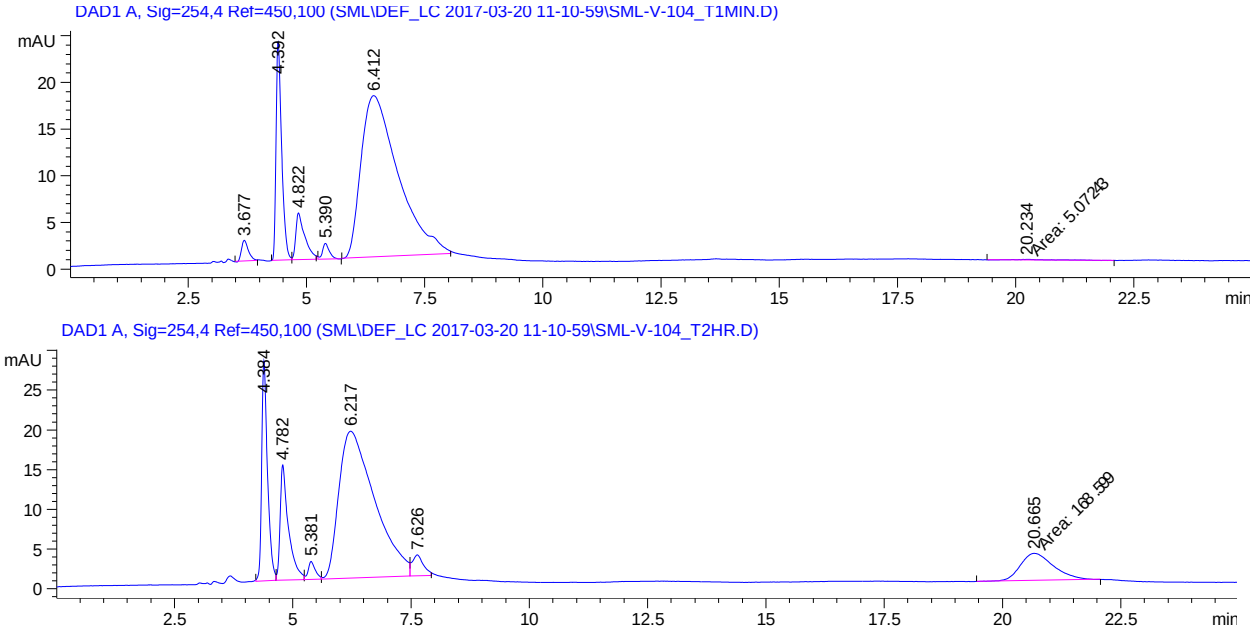

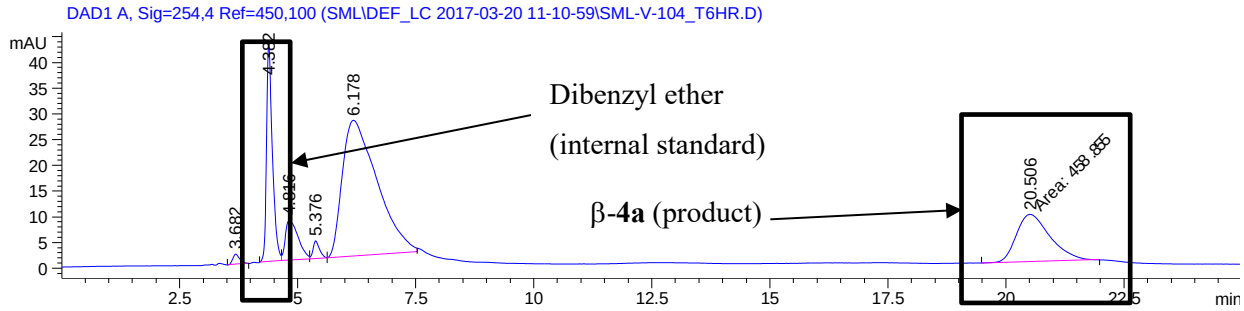

Figure S7. HPLC trace used for kinetic data analysis

Time (hours)	Internal standard (IS)	4a (mAU)	4a:IS	[2a] (M)
0.02	194	N/A	0.000	0.100
0.03	196	N/A	0.000	0.100
0.07	260	6	0.023	0.098
0.10	233	9	0.039	0.097
0.13	197	9	0.046	0.097
0.17	192	12	0.063	0.095
0.20	192	17	0.089	0.093
0.23	213	17	0.080	0.094
0.27	190	20	0.105	0.092
0.30	231	29	0.126	0.090
0.33	217	30	0.138	0.089
0.50	267	53	0.199	0.085
0.67	253	67	0.265	0.080
0.83	310	103	0.332	0.075
1.00	296	115	0.389	0.070
2.00	238	169	0.710	0.046
3.00	279	260	0.932	0.029
4.00	278	296	1.065	0.019
5.00	293	348	1.188	0.010
6.00	**368**	**459**	**1.247**	**0.005**
7.00	521	669	1.284	0.002

Table S13. Raw data from HPLC analysis of reaction between galactosyl phosphate (**2a**) and *L*-Ser (**3a**) over 7 hours.

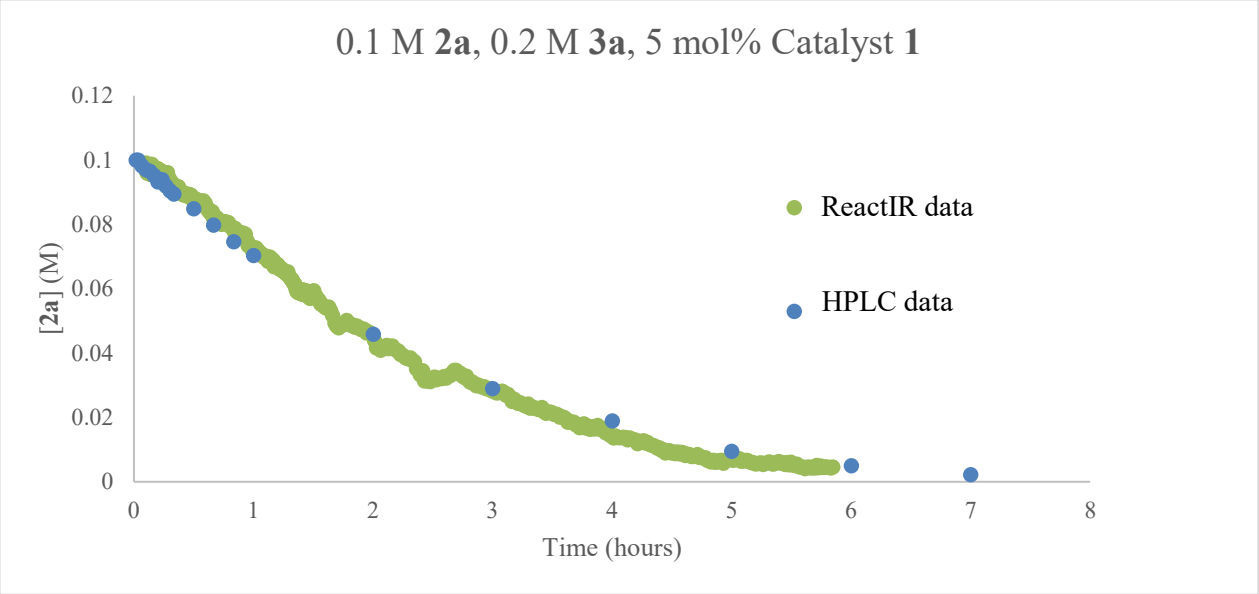

Figure S8. Concentration of galactosyl phosphate (**2a**) versus time in the model coupling reaction with and *L*-Ser (**3a**). HPLC and ReactIR data are overlaid. ReactIR data was obtained using the same general procedure at 0.15 mmol scale.

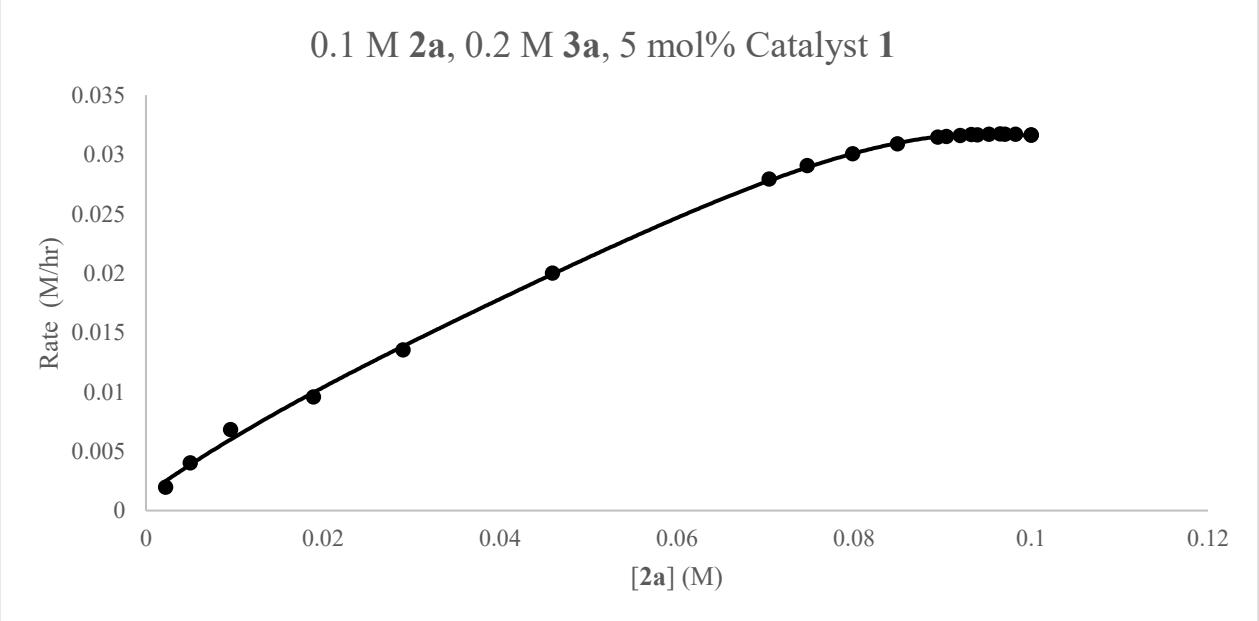

Figure S9. Rate of **3a** consumption as a function of [**2a**] (M) determined by HPLC. 6th-order polynomial was fit to concentration versus time plot and the derivative was used for the above plot.

10.5 Michaelis-Menten kinetic analysis with galactosyl phosphate (2a) and *L*-Ser (3a)

The general procedure described in section 10.2 was followed to setup each sample. Saturation kinetics were done with ***L*-Ser (3a)**, keeping **galactosyl phosphate (2a)** concentration fixed at 0.1 M and catalyst **1** at 5 mol% (0.005 M).

2a (equiv.)	**3a** (equiv.)	Hours	Rate (M/hr)
1.0	0.00	0.17	0.000
1.0	0.00	0.33	0.000
1.0	0.00	0.00	0.000
1.0	0.25	0.17	0.011
1.0	0.25	0.33	0.009
1.0	0.25	0.00	0.000
1.0	0.25	0.50	0.009
1.0	0.50	0.17	0.019
1.0	0.50	0.33	0.017
1.0	0.50	0.00	0.000
1.0	0.50	0.50	0.016
1.0	0.75	0.17	0.024
1.0	0.75	0.33	0.024
1.0	0.75	0.00	0.000
1.0	0.75	0.67	0.018
1.0	1.00	0.17	0.025
1.0	1.00	0.33	0.025
1.0	1.00	0.00	0.000
1.0	1.00	0.67	0.021
1.0	1.50	0.17	0.032
1.0	1.50	0.33	0.030
1.0	1.50	0.00	0.000
1.0	1.50	0.67	0.025
1.0	2.00	0.17	0.032
1.0	2.00	0.33	0.029
1.0	2.00	0.00	0.000
1.0	2.00	0.67	0.023

Table S14. HPLC data for reaction between galactosyl phosphate (**2a**) and *L*-Ser (**3a**), changing concentration in *L*-Ser (**3a**)

Data Analysis: For *L*-Ser (**3a**) at or below 0.50 equivalents, time points were taken at 10, 20, and 30 minutes. For 0.75 equivalents and above, time points were taken at 10, 20, and 40 minutes. For each time point, an initial rate was determined by dividing the product concentration by the time it was taken to generate a M/hr, which was used to fit the saturation curve using the Michaelis-Menten 1-dimensional equation (1).

$$rate = \frac{V_{max}[S]}{K_m + [S]} \quad (1)$$

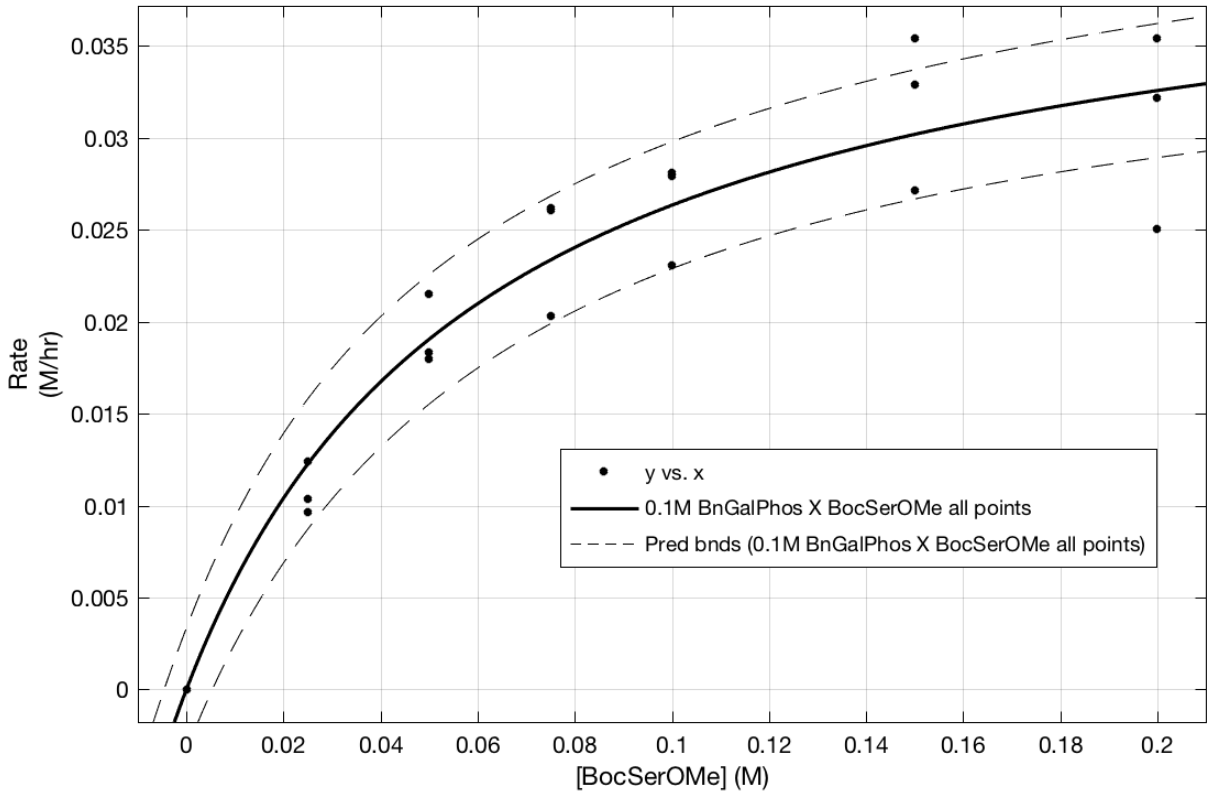

Figure S10. HPLC Saturation curve fit to the Michaelis-Menten equation (1) for **changing [*L*-Ser]** (**3a**) with 95% confidence bounds

General model:

f(x) = Vmax*x/(Km+x)

Coefficients (with 95% confidence bounds):

K_m = 0.06204 (0.04626, 0.07782)

V_{max} = 0.04266 (0.03854, 0.04679)

Goodness of fit:

SSE: 0.0001676

R-square: 0.9799

Adjusted R-square: 0.9796

RMSE: 0.001671

Saturation kinetics were done with **galactosyl phosphate (2a)**, keeping *L*-Ser (**3a**) concentration fixed at 0.2 M and catalyst **1** at 5 mol% (0.005 M).

2a (equiv.)	**3a** (equiv.)	Hours	Rate (M/hr)
0.000	2.00	0.17	0.000
0.000	2.00	0.33	0.000
0.000	2.00	0.00	0.000
0.125	2.00	0.17	0.013
0.125	2.00	0.33	0.010
0.125	2.00	0.00	0.000
0.125	2.00	0.50	0.009
0.250	2.00	0.17	0.021
0.250	2.00	0.33	0.018
0.250	2.00	0.00	0.000
0.250	2.00	0.50	0.016
0.500	2.00	0.17	0.029
0.500	2.00	0.33	0.025
0.500	2.00	0.00	0.0
0.500	2.00	0.50	0.023
0.750	2.00	0.17	0.031
0.750	2.00	0.33	0.025
0.750	2.00	0.00	0.0
0.750	**2.00**	**0.67**	**0.016 (X)**

Table S15-a. HPLC data for reaction between galactosyl phosphate (**2a**) and *L*-Ser (**3a**), changing concentration in galactosyl phosphate (**2a**) from 0.125 M to 0.750 M

2a (equiv.)	**3a** (equiv.)	Hours	Rate (M/hr)
0.0	2.0	0.67	0.000
0.5	2.0	0.67	0.029
1.0	2.0	0.67	0.032
1.5	2.0	0.67	0.032
2.0	2.0	0.67	0.035

Table S15-b. HPLC data for reaction between galactosyl phosphate (**2a**) and *L*-Ser (**3a**), changing concentration in galactosyl phosphate (**2a**) from 0.50 M to 2.00 M

At concentrations above 1.0 equiv galactosyl phosphate (**2a**) (>0.1 M), a separate series of runs were performed using a single time point at 20 minutes using a more concentrated stock solution of glycosyl donor. This was included with the 0-0.75 equiv. series of data.

For 0.75 equiv. galactosyl phosphate (**2a**), the 40-minute time point was discarded from analysis since the initial rate region had passed and deviation from linearity was high (not indicative of initial rate region). Since the initial rate at 20 minutes had been determined previously by NMR, HPLC, and ReactIR, the absolute rate was set at 32 mM/hr at standard conditions (0.2 M **3a**, 0.1 M **2a**, and 0.025 M catalyst **1**).

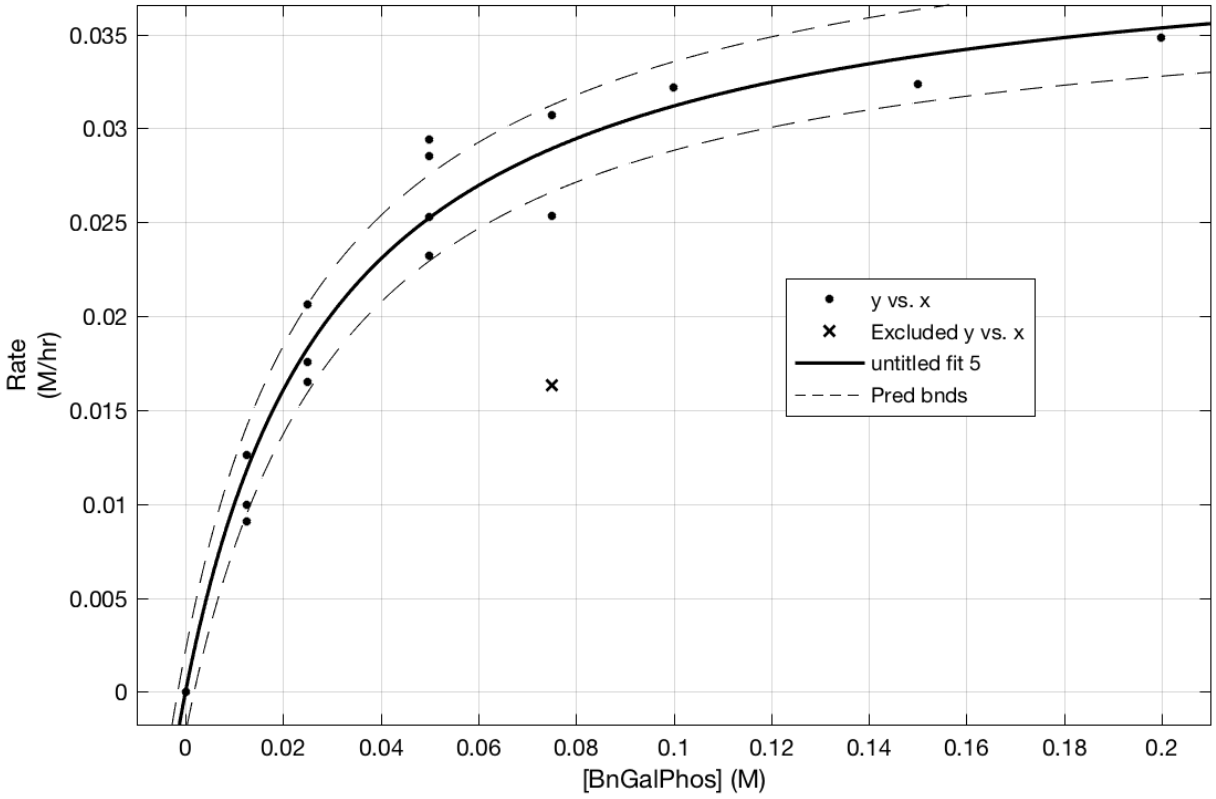

Figure S11. HPLC Saturation curve fit to the Michaelis-Menten equation for **changing [2a]** (**galactosyl phosphate**) with 95% confidence bounds

General model:

f(x) = Vmax*x/(Km+x)

Coefficients (with 95% confidence bounds):

K_m = 0.03081 (0.02605, 0.03556)

V_{max} = 0.04079 (0.03855, 0.04302)

Goodness of fit:

SSE: 7.182e-05

R-square: 0.9899

Adjusted R-square: 0.9897

RMSE: 0.001103

*Note: The data in **Figure 2D** of the main text show the calculated initial rate for each point by fitting a line and plotting the slope (initial rate) versus concentration, rather than three independent initial rates as shown above. The numbers presented reflect the full dataset as described here.*

8.6 Reaction Time-Course with Galactosyl Chloride (2b) and *L*-Ser (3a)

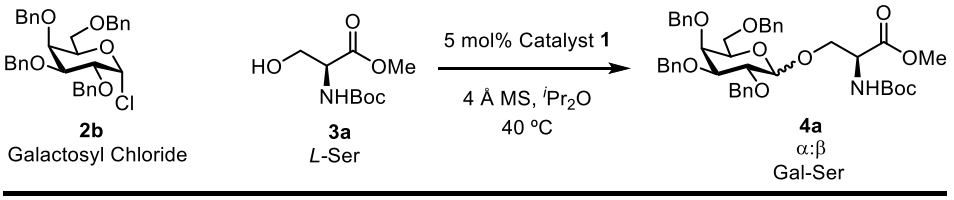

Scheme S11. Galactosyl chloride (**2b**) and *L*-Serine (**3a**) model system used for kinetic evaluation

The same general procedure for the above glycosyl phosphate kinetics (Section 8.4) were followed for the glycosyl chloride (**2b**), using the same catalyst (**1**) and *L*-Serine (**3a**) stock solutions. Given the slow hydrolysis of glycosyl chloride in isopropyl alcohol and the well resolved **2b** peak by HPLC, the concentration was calculated by using product divided by the sum of product and starting material. The data using the same method as for the phosphate reaction profile yielded noisier data, both with similar initial rates. Both analyses of the data are shown below.

Time (hours)	[**2b**] (M)	IS (mAU)	**4a** (mAU)	**4a**:IS	**2b** (mAU)
0	0.100	194	0	0.000	0
0.5	0.095	117	15	0.128	642
1	0.092	153	32	0.209	624
1.5	0.089	183	49	0.268	604
2	0.083	161	69	0.429	634
3.2	0.072	137	95	0.693	560
4.1	0.079	230	122	0.530	538
5.1	0.066	202	172	0.851	587
6.4	0.057	185	200	1.081	527
7.4	0.070	284	210	0.739	482
8.5	0.057	238	253	1.063	491

Table S16. Raw data from HPLC analysis of reaction between galactosyl chloride (**2b**) and *L*-Ser (**3a**) over 8.5 hours.

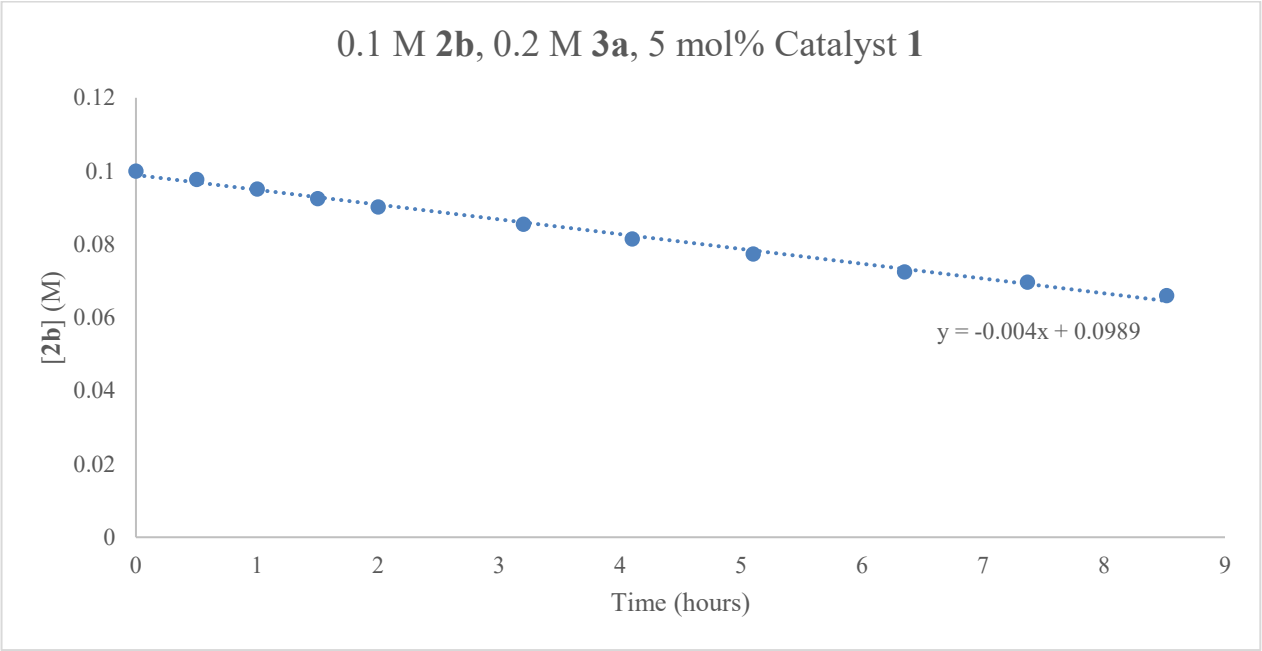

Figure S12-a. HPLC data for reaction between galactosyl chloride (**2b**) and *L*-Ser (**3a**).

Note: *The above plot used the ratio of* ***4a****/(****4a*** *+* ***2b****) to determine concentration of* ***2b****.*

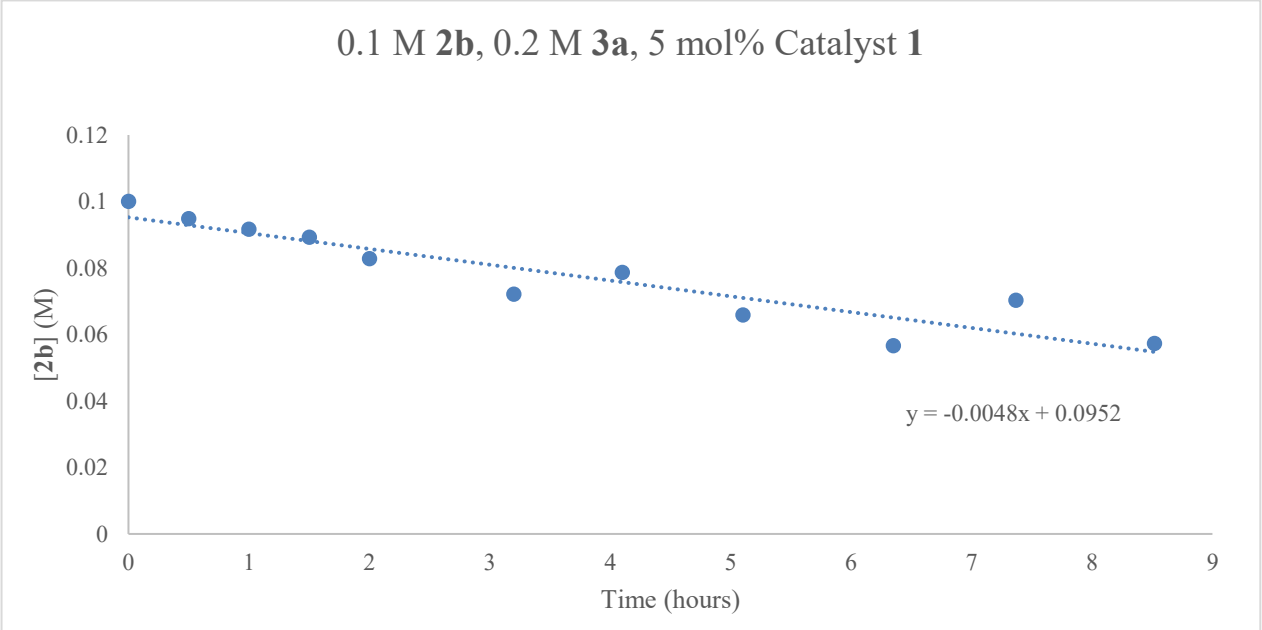

Figure S12-b. HPLC data for reaction between galactosyl chloride (**2b**) and *L*-Ser (**3a**). The above plot measured concentration relative to internal standard (dibenzyl ether).

The initial rate of the phosphate reaction suggests 6- to 8-fold faster reactivity compared to the chloride.

10.7 Michaelis-Menten Kinetic Analysis with Galactosyl Chloride (2b) and *L*-Ser (3a)

Using the general procedure outlined above to setup each sample.

Saturation kinetics were done with ***L*-Ser (3a)**, keeping galactosyl chloride (**2b**) concentration fixed at 0.1 M and catalyst **1** at 5 mol% (0.005M).

[**2b**] (M)	[**3a**] (M)	Time (hr)	Rate (M/hr)
0.100	0.025	1	0.0021
0.100	0.025	2	0.0021
0.100	0.025	3	0.0013
0.100	0.05	0.5	0.0027
0.100	0.05	1	0.0029
0.100	0.05	2	0.0036
0.100	0.05	3	0.0019
0.100	0.075	0.5	0.0030
0.100	0.075	1	0.0040
0.100	0.075	2	0.0046
0.100	0.075	3	0.0023
0.100	0.1	0.5	0.0043
0.100	0.1	1	0.0044
0.100	0.1	2	0.0041
0.100	0.1	3	0.0040
0.100	0.125	0.5	0.0050
0.100	0.125	1	0.0042
0.100	0.125	2	0.0041
0.100	0.125	3	0.0041
0.100	0.15	0.5	0.0042
0.100	0.15	1	0.0041
0.100	0.15	2	0.0045
0.100	0.15	3	0.0043
0.100	0.175	0.5	0.0043
0.100	0.175	1	0.0042
0.100	0.175	2	0.0043
0.100	0.175	3	0.0040
0.100	0.2	0.5	0.0047

0.100	0.2	1	0.0042
0.100	0.2	2	0.0047
0.100	0.2	3	0.0045
0.100	0.25	0.5	0.0058
0.100	0.25	1	0.0042
0.100	0.25	2	0.0046
0.100	0.3	0.5	0.0044
0.100	0.3	1	0.0043
0.100	0.3	2	0.0045
0.100	0.35	0.5	0.0043
0.100	0.35	1	0.0045
0.100	0.35	2	0.0045
0.100	0.35	3	0.0040
0.100	0.4	0.5	0.0039
0.100	0.4	1	0.0045
0.100	0.4	2	0.0042
0.100	0.4	3	0.0037

Table S17. HPLC data for reaction between galactosyl chloride (**2b**) and *L*-Ser (**3a**), changing concentration in *L*-Ser (**3a**)

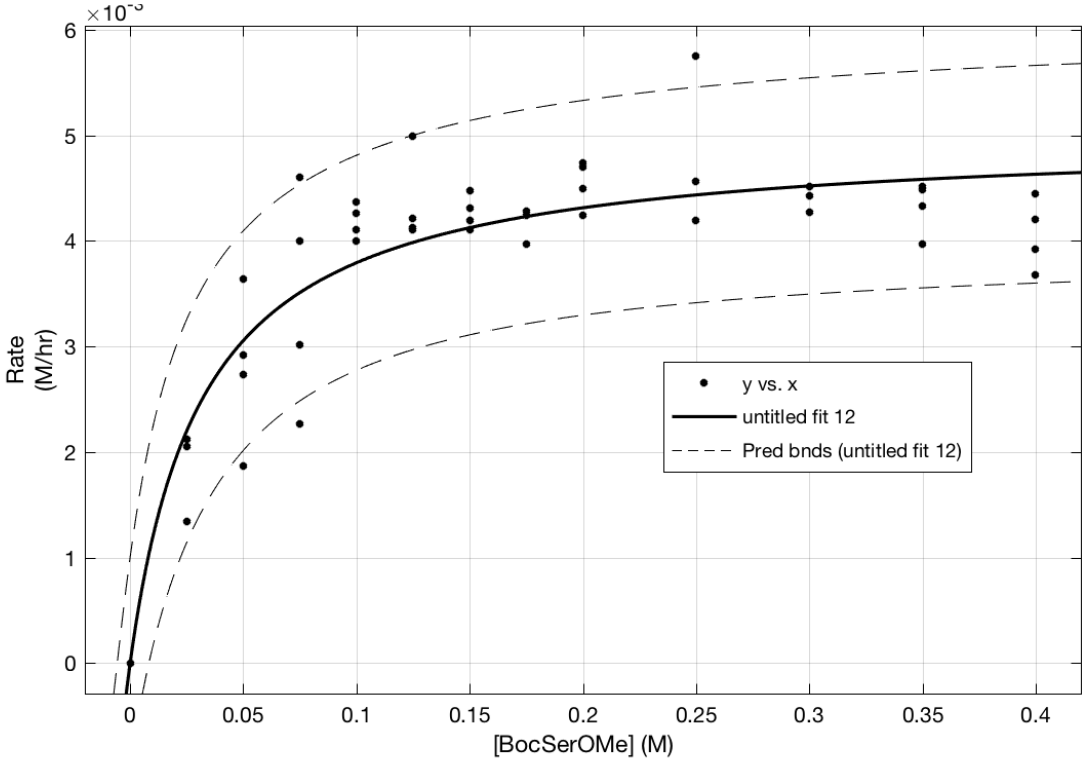

Figure S13. HPLC Saturation curve fit to the Michaelis-Menten equation for **changing [*L*-Ser]** (**3a**) with 95% confidence bounds

General model:

f(x) = Vmax*x/(Km+x)

Coefficients (with 95% confidence bounds):

K_m = 0.03181 (0.01994, 0.04369)

V_{max} = 0.005 (0.004633, 0.005367)

Goodness of fit:

SSE: 1.22e-05

R-square: 0.8957

Adjusted R-square: 0.8936

RMSE: 0.0004991

Saturation at 0.2 M **3a** and possible inhibition of catalyst with nucleophile is observed. While bi-reactant inhibition models do not provide a sufficient level of resolution into the specific mechanism at play, the downward trajectory of the rate versus concentration plot is suggestive of possible inhibition of catalyst with nucleophile. This is consistent with previous observations with glycosyl chlorides (see section 9) and consistent with the hypothesis that strong binding of the glycosyl phosphate could mitigate nucleophile inhibition.

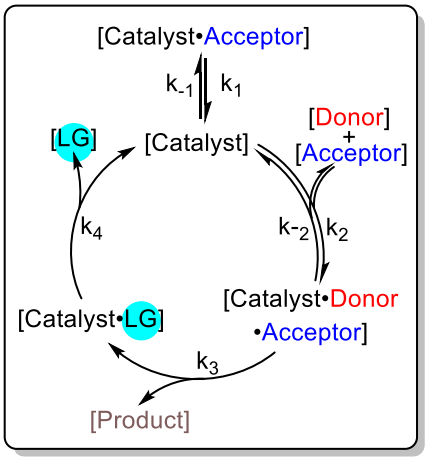

Figure 2E-b: Modified catalytic cycle with off-cycle nucleophile inhibition

Saturation kinetics were done with **galactosyl chloride (2b)**, keeping *L*-Ser (**3a**) concentration fixed at 0.2 M and catalyst **1** at 5 mol% (0.005 M).

[**2b**] (M)	[3**a**] (M)	Time (hr)	Rate (M/hr)
0	0.2	0.5	0.0000
0	0.2	1	0.0000
0	0.2	2	0.0000
0.025	0.2	0.5	0.0012
0.025	0.2	1	0.0016
0.025	0.2	1.5	0.0018
0.05	0.2	0.5	0.0021
0.05	0.2	1	0.0030
0.05	0.2	1.5	0.0029
0.075	0.2	0.5	0.0027
0.075	0.2	1	0.0044
0.075	0.2	1.5	0.0042
0.1	0.2	0.5	0.0031
0.1	0.2	1	0.0058
0.1	0.2	2	0.0045
0.125	0.2	0.5	0.0029
0.125	0.2	1	0.0057
0.125	0.2	2	0.0060
0.15	0.2	0.5	0.0039
0.15	0.2	1	0.0067
0.15	0.2	2	0.0062
0.175	0.2	0.5	0.0047
0.175	0.2	1	0.0070
0.175	0.2	2	0.0062
0.2	0.2	0.5	0.0060
0.2	0.2	1	0.0078
0.2	0.2	2	0.0067

Table S18. HPLC data for reaction between galactosyl chloride (**2b**) and *L*-Ser (**3a**), changing concentration in galactosyl chloride (**2b**)

Note: Time points at 0.5 hours were discarded due to low conversion and unreliable rate calculation. Below is plotted the entire data set with the 0.5 hour time points removed from the fit.

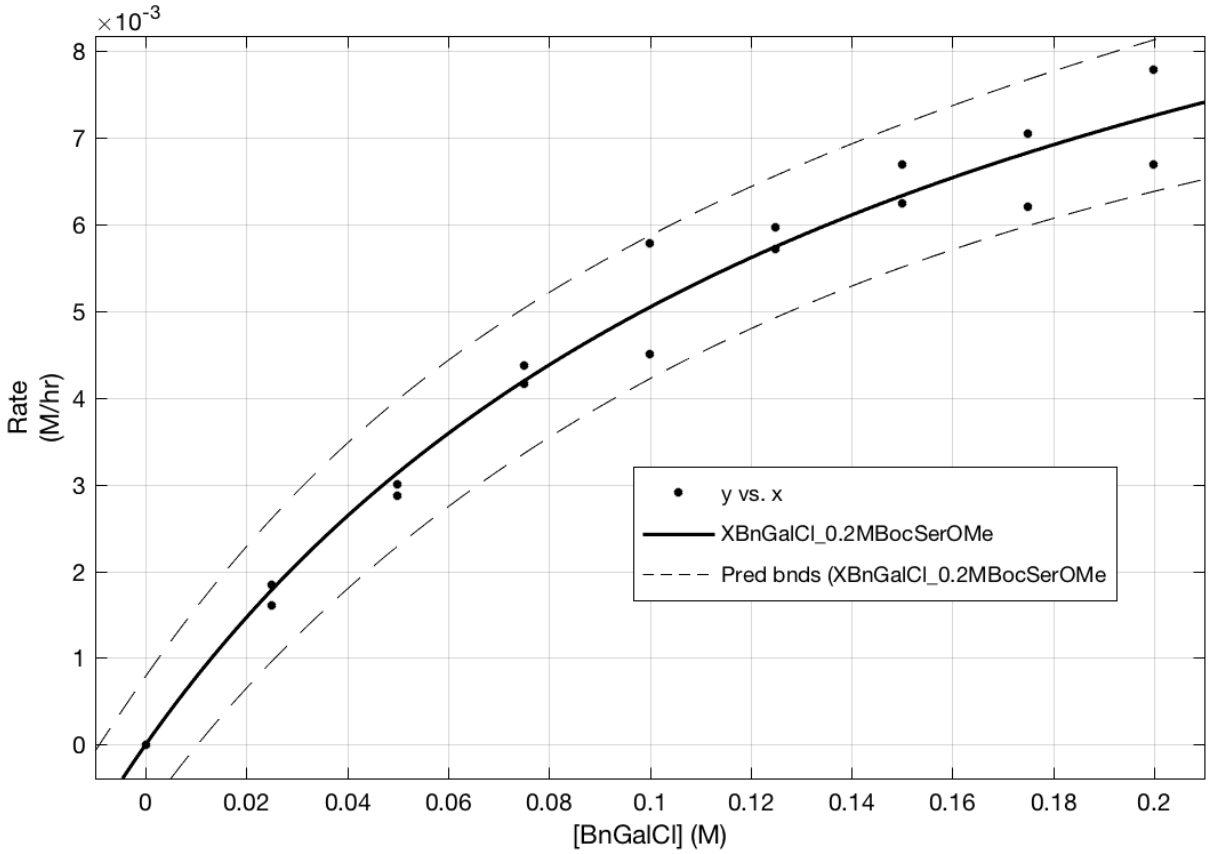

Figure S14. HPLC Saturation curve fit to the Michaelis-Menten equation for **changing [2b]** (**galactosyl chloride**) with 95% confidence bounds

General model:

f(x) = Vmax*x/(Km+x)

Coefficients (with 95% confidence bounds):

K_m = 0.1541 (0.09542, 0.2127)

V_{max} = 0.01284 (0.01021, 0.01546)

Goodness of fit:

SSE: 2.267e-06

R-square: 0.9808

Adjusted R-square: 0.9797

RMSE: 0.0003651

11. Competition Experiment with Galactosyl Chloride (2b) and Galactosyl Phosphate (2a)

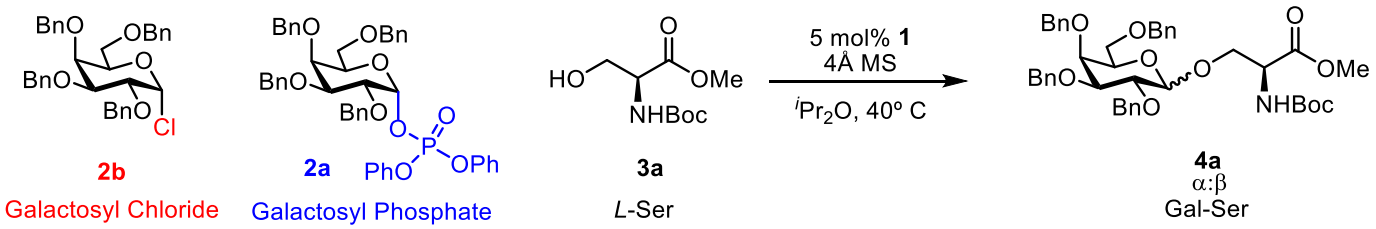

Scheme S12. Competition experiment between galactosyl chloride (**2b**) and galactosyl phosphate (**2a**) with *L*-Ser (**3a**)

NMR of T=0 control sample:

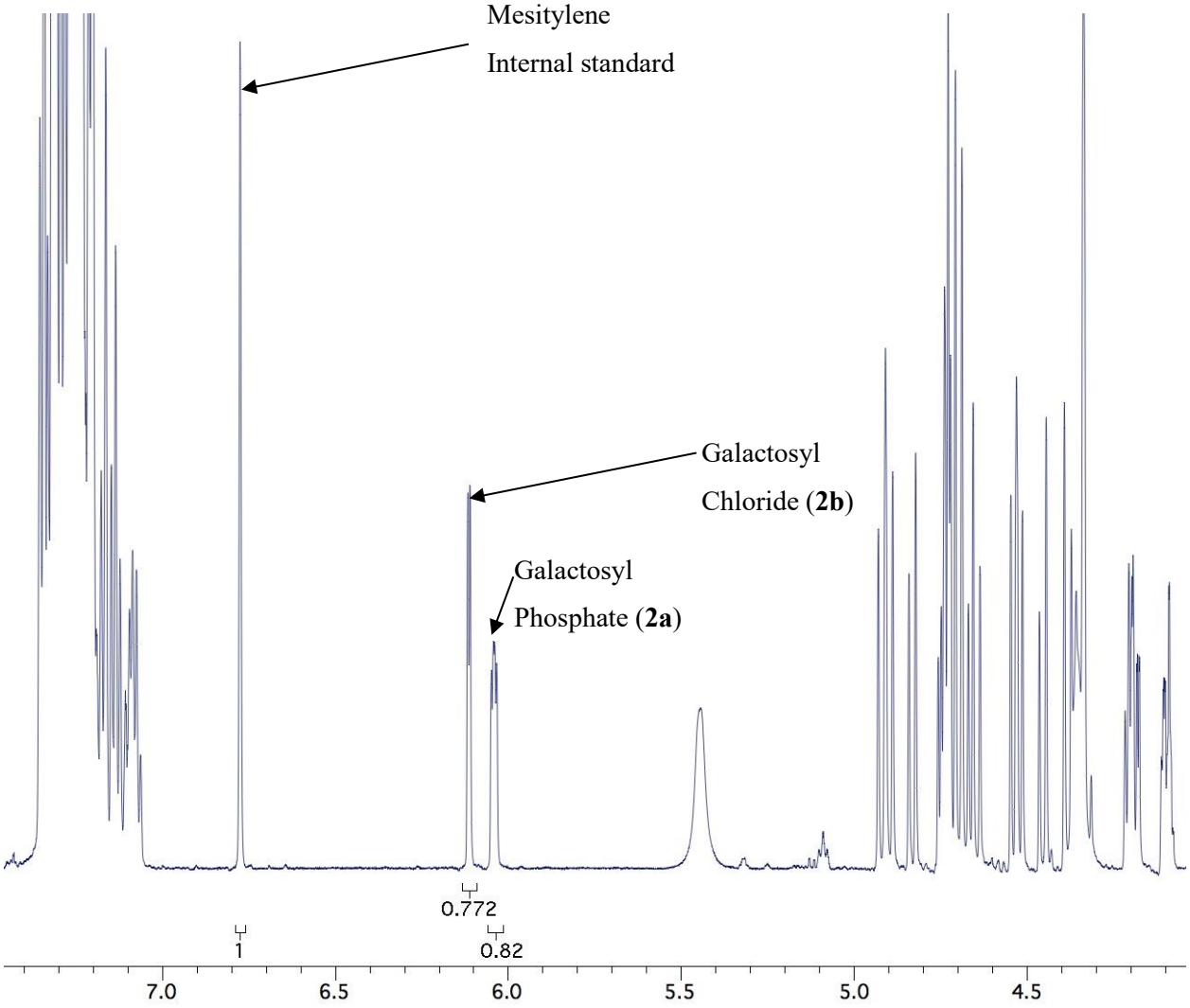

Figure S15. NMR of T=0 sample for competition experiment between galactosyl chloride (**2b**) and galactosyl phosphate (**2a**) with *L*-Ser (**3a**)

General procedure: Two oven-dry 0.5 dram vials were set up according to the general procedure, instead run at 0.02 mmol scale each. The stock solution with a mixture of galactosyl phosphate (**2a**) and galactosyl chloride (**2b**) was used for both reactions containing mesitylene as an NMR internal standard. The reaction was started upon addition of catalyst solution (40 µL, 5 mol%) through the septum to the stirring, equilibrated, reaction mixture in the first vial, while 40 µL diisopropyl ether was added to the second vial as a control.

50 µL aliquots were taken at 0, 10, 20, and 30 minutes from both catalyzed and control vials. These aliquots were diluted into 500 µL $CDCl_3$, which had previously been shown to completely stop the reaction. The diluted aliquots were filtered, and NMR spectra were immediately acquired without removing residual solvent from the reaction. The spectral window was 4 ppm to 8 ppm (to avoid diisopropyl ether signals).

The NMR data were processed with a standard baseline correction in iNMR and integrated. The raw data were reprocessed and integrated two times to provide the following data:

Time (hour)	IS	**2b** (control)	**2a** (control)	**2b** (cat)	**2a** (cat)
0.000	1	0.765	0.811	0.761	0.811
0.167	1	0.764	0.808	0.761	0.761
0.333	1	0.768	0.816	0.764	0.717
0.500	1	0.768	0.816	0.771	0.691

Time (hour)	IS	**2b** (control)	**2a** (control)	**2b** (cat)	**2a** (cat)
0.00	1	0.760	0.804	0.762	0.811
0.167	1	0.760	0.807	0.767	0.765
0.333	1	0.766	0.815	0.769	0.724
0.500	1	0.773	0.817	0.778	0.692

Table S19. NMR of T=0 sample for competition experiment between galactosyl chloride (**2b**) and galactosyl phosphate (**2a**) with *L*-Ser (**3a**)

These data were converted into concentrations by assuming the control starting concentration of galactosyl phosphate (**2a**) = 0.1 M.

The concentration of each glycosyl donor was monitored by subtracting the catalyzed concentration of each reactant from the uncatalyzed reaction concentrations (at each time point).

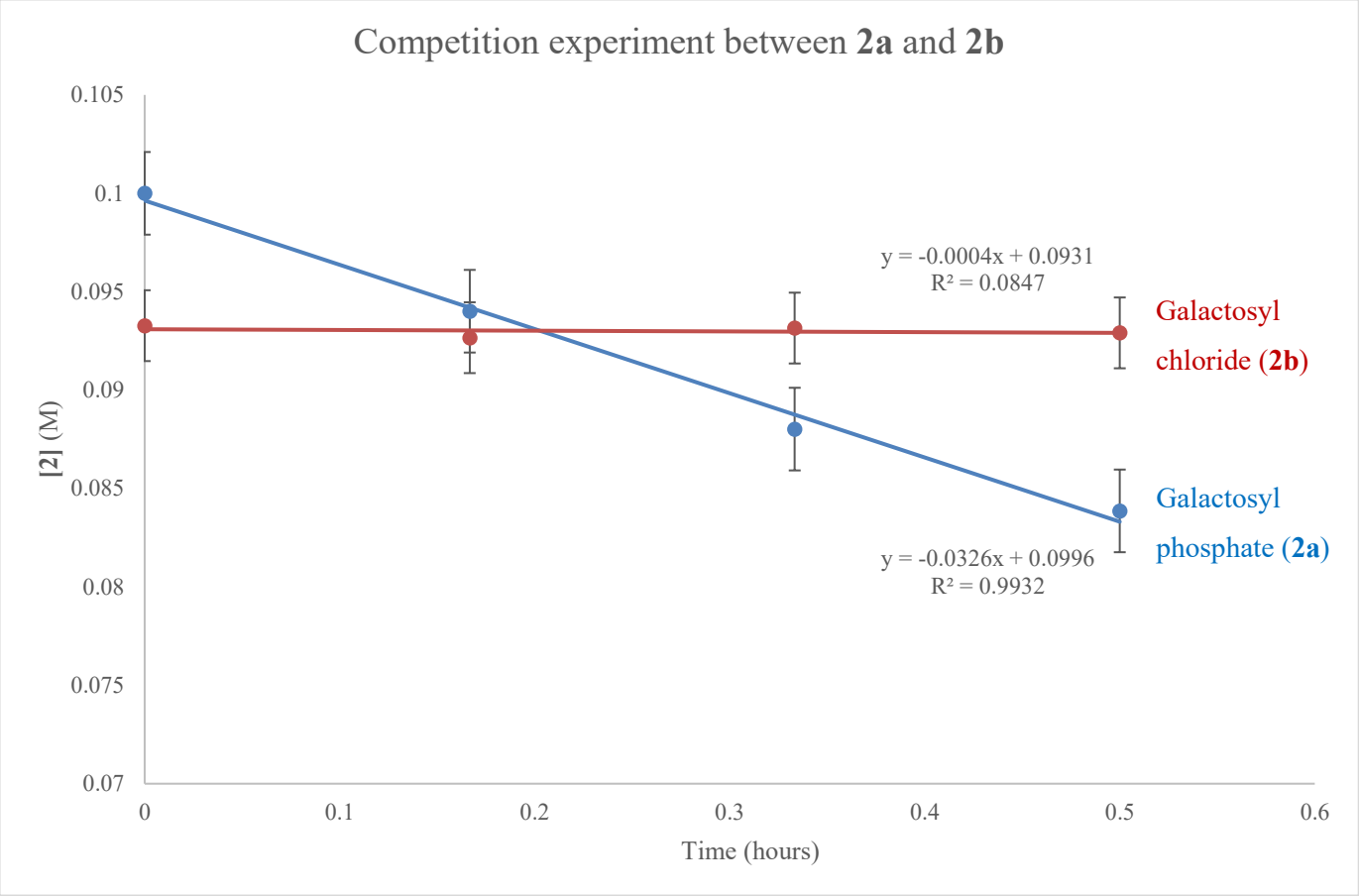

Figure S16. Concentration versus time plot for competition experiment between galactosyl phosphate (**2a**) and galactosyl chloride (**2b**) with *L*-Ser (**3a**)

The [**2b**] does not change relative to the background reaction (within the error of the experiment). However, over the course of 30 minutes **2a** reacts to 15% conversion.

By overlaying the competitive phosphate concentration versus time with its independently determined rate by HPLC, no noticeable difference in rate is observed between the two.

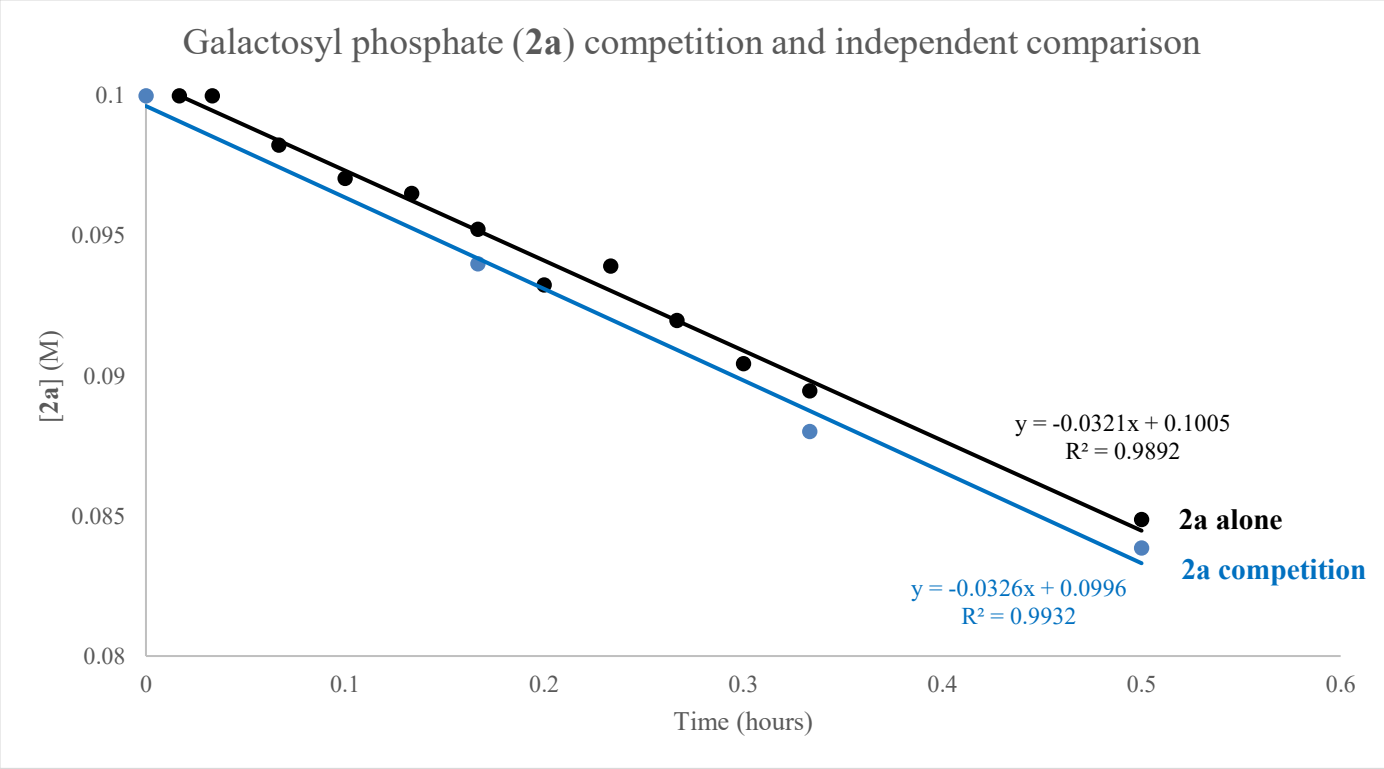

Figure S17. Concentration versus time plot for competition experiment between galactosyl phosphate (**2a**) and galactosyl chloride (**2b**) with *L*-Ser (**3a**) overlaid with standard reaction profile for **2a**

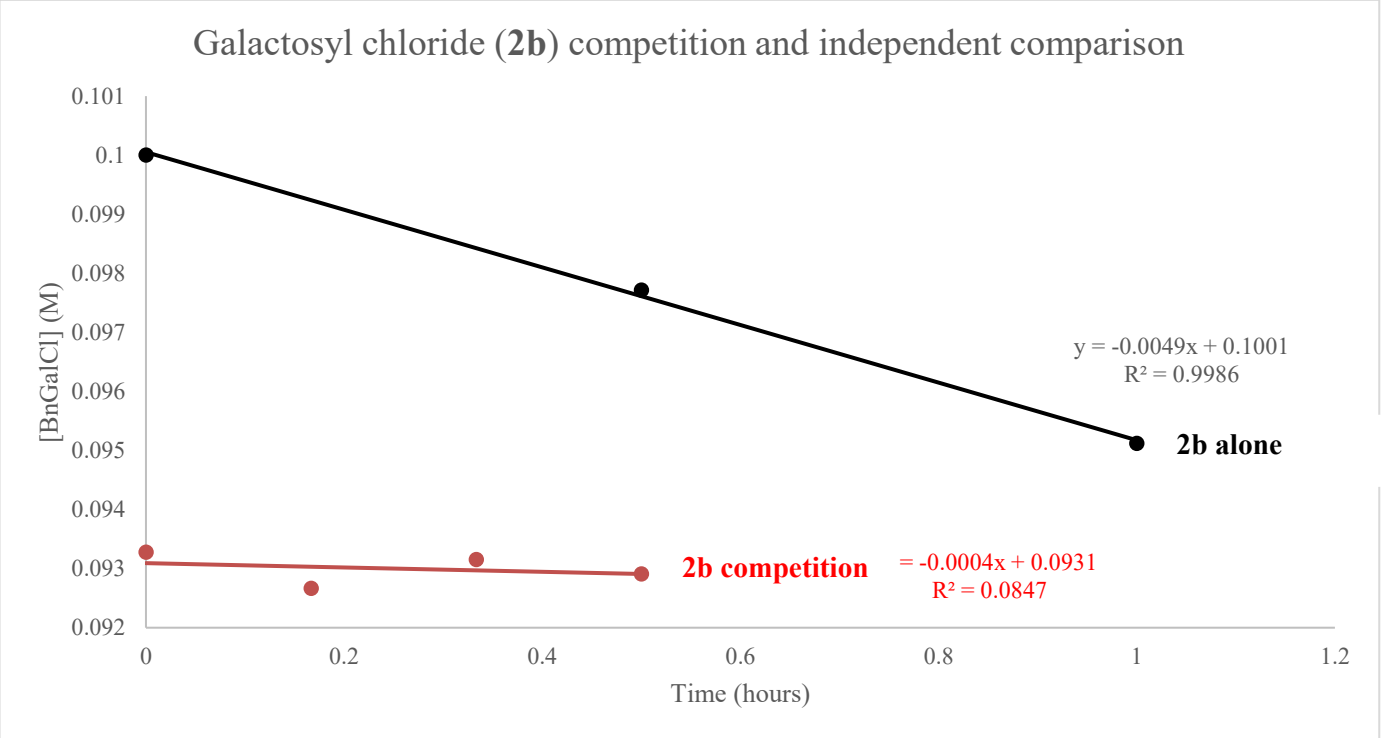

Figure S18. Concentration versus time plot for competition experiment between galactosyl phosphate (**2a**) and galactosyl chloride (**2b**) with *L*-Ser (**3a**) overlaid with standard reaction profile for **2b**

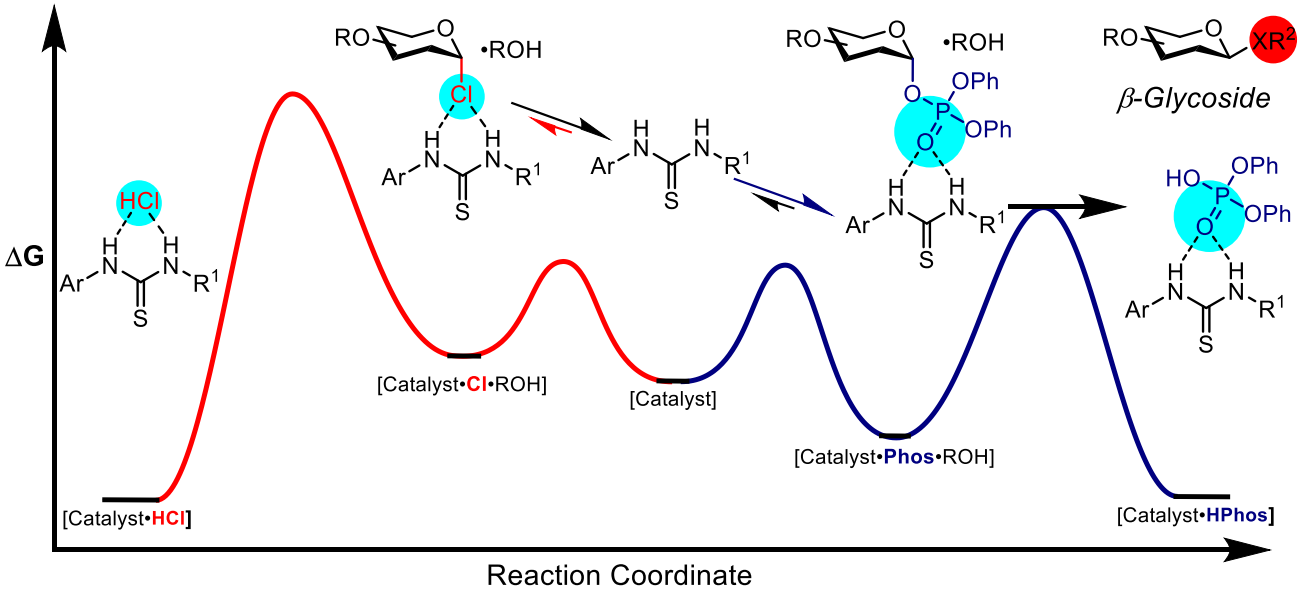

Scheme S13. Reaction coordinate interpretation of competition experiment results

We hypothesize the reduced rate of the chloride in the competitive reaction comes from sequestration of catalyst **1** as the complex with galactosyl phosphate (**2a**) as **Catalyst•Phos**. This effectively inhibits reactivity with galactosyl chloride (**2b**). As shown in Figure S17, the phosphate competitive rate is the same as the normal initial rate, suggesting the galactosyl chloride does not inhibit the galactosyl phosphate.

12. Substrate binding experiments

12.1 Galactosyl Phosphate (2a) Binding with Catalyst 1

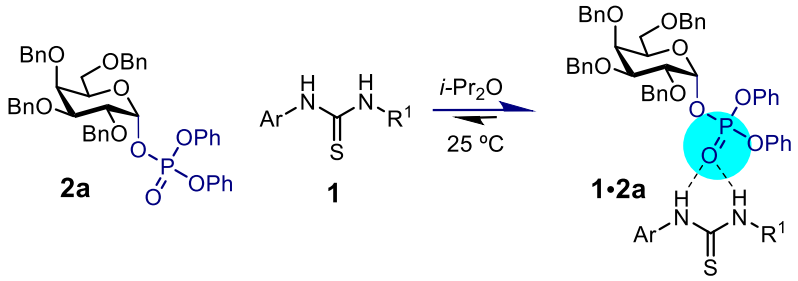

Scheme S14. Equilibrium binding of galactosyl phosphate (**2a**) with catalyst **1**

Note: all stock solutions were prepared using volumetric flasks.

General Procedure: To an NMR tube was added 312.5 µL iPr_2O (sure/seal, Aldrich), 80 µL of a 0.025 M solution of catalyst **1** in iPr_2O. To this was added a sealed capillary insert containing $CDCl_3$ with 1,2-difluorobenzene and triphenylphosphine. At 25 °C, ^{19}F NMR was taken (without any galactosyl phosphate). No shimming was performed prior to acquisition.

To this mixture was titrated a 0.167 M solution of galactosyl phosphate (**2a**). The solution of **2a** was added via syringe followed by vigorous shaking prior to NMR acquisition.

The ^{19}F NMR spectra were referenced to difluorobenzene (DFB), which was arbitrarily set to 0.000 ppm and the corresponding catalyst fluorine peaks were recorded. For galactosyl phosphate (**2a**), the (bis)trifluoromethyl arene fluorine atoms were used to determine the binding constant (see arrows below).

Equiv. **2a**	^{19}F (ppm)	DBF (ppm)	[**1**] (mM)	[**2a**] (mM)	Δ ppm
0	75.397	0.000	6.40	0.00	0.000
0.5	75.439	0.000	6.25	3.13	0.028
1	75.481	0.000	6.11	6.11	0.078
2	75.497	0.000	5.84	11.68	0.114
4	75.534	0.000	5.37	21.48	0.173
8	75.568	0.000	4.62	36.99	0.228
16	75.592	0.000	3.62	57.92	0.272
24	75.605	0.000	2.97	71.38	0.3035
32	75.614	0.000	2.52	80.76	0.315

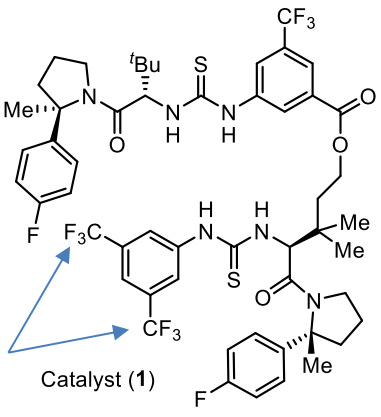

Table S20. ^{19}F chemical shift data of catalyst **1** with titration of **2a**

The following derivation was used for obtaining the association constants from the above chemical shift data.

$$K_a = \frac{[\mathbf{1} \bullet \mathbf{2a}]}{[\mathbf{1}][\mathbf{2a}]} \tag{2}$$

$$[\mathbf{1} \bullet \mathbf{2a}] = K_a[\mathbf{1}][\mathbf{2a}] \tag{3}$$

$$[\mathbf{2a}]_O = [\mathbf{1} \bullet \mathbf{2a}] + [\mathbf{2a}] \tag{4}$$

$$[\mathbf{1}]_O = [\mathbf{1} \bullet \mathbf{2a}] + [\mathbf{1}] \tag{5}$$

$$[\mathbf{1} \bullet \mathbf{2a}] = K_a([\mathbf{1}]_O - [\mathbf{1} \bullet \mathbf{2a}])([\mathbf{2a}]_O - [\mathbf{1} \bullet \mathbf{2a}]) \tag{6}$$

$$[\mathbf{1} \bullet \mathbf{2a}] = \frac{1}{2}\left([\mathbf{1}]_O + [\mathbf{2a}]_O + \frac{1}{K_a}\right) - \sqrt{\left([\mathbf{1}]_O + [\mathbf{2a}]_O + \frac{1}{K_a}\right)^2 + 4[\mathbf{1}]_O[\mathbf{2a}]_O} \tag{7}$$

$$\Delta\delta_{obs} = \delta_{\mathbf{1}}\chi_{\mathbf{1}} + \delta_{\mathbf{1 \bullet 2a}}\chi_{\mathbf{1 \bullet 2a}} \tag{8}$$

$$\Delta\delta_{obs} = \delta_{\mathbf{1}}\left(\frac{[\mathbf{1}]_O - [\mathbf{1} \bullet \mathbf{2a}]}{[\mathbf{1}]_O}\right) + \delta_{\mathbf{1 \bullet 2a}}\left(\frac{[\mathbf{1} \bullet \mathbf{2a}]}{[\mathbf{1}]_O}\right) \tag{9}$$

$$\Delta\delta_{obs} = \delta_{\mathbf{1}}\left(\frac{[\mathbf{1}]_O - \left(\frac{1}{2}\left([\mathbf{1}]_O + [\mathbf{1}]_O + \frac{1}{K_a}\right) - \sqrt{\left([\mathbf{1}]_O + [\mathbf{2a}]_O + \frac{1}{K_a}\right)^2 + 4[\mathbf{1}]_O[\mathbf{2a}]_O}\right)}{[\mathbf{1}]_O}\right) + \delta_{\mathbf{1 \bullet 2a}}\left(\frac{\left(\frac{1}{2}\left([\mathbf{1}]_O + [\mathbf{2a}]_O + \frac{1}{K_a}\right) - \sqrt{\left([\mathbf{1}]_O + [\mathbf{2a}]_O + \frac{1}{K_a}\right)^2 + 4[\mathbf{1}]_O[\mathbf{2a}]_O}\right)}{[\mathbf{1}]_O}\right) \tag{10}$$

Since a solution of galactosyl phosphate (**2a**) is being added to a solution of catalyst (**1**), the concentration of catalyst decreases in the titration while the galactosyl phosphate concentration increases. This equation is used to express galactosyl phosphate concentration in terms of catalyst concentration to solve for the chemical shift of the $\mathbf{1 \bullet 2a}$ complex and the equilibrium constant.

$$[\mathbf{2a}]_O = 133.33 - 20.833[\mathbf{1}]_O \tag{8}$$

The chemical shift of the catalyst without any galactosyl phosphate in solution was measured (above) to be $\delta_{\mathbf{1}} = 75.527\ ppm$.

Using Matlab's curve fitting software to solve for K_a and $\delta_{\mathbf{1 \bullet 2a}}$, catalyst ^{19}F chemical shift and $[\mathbf{1}]_O$ were plotted.

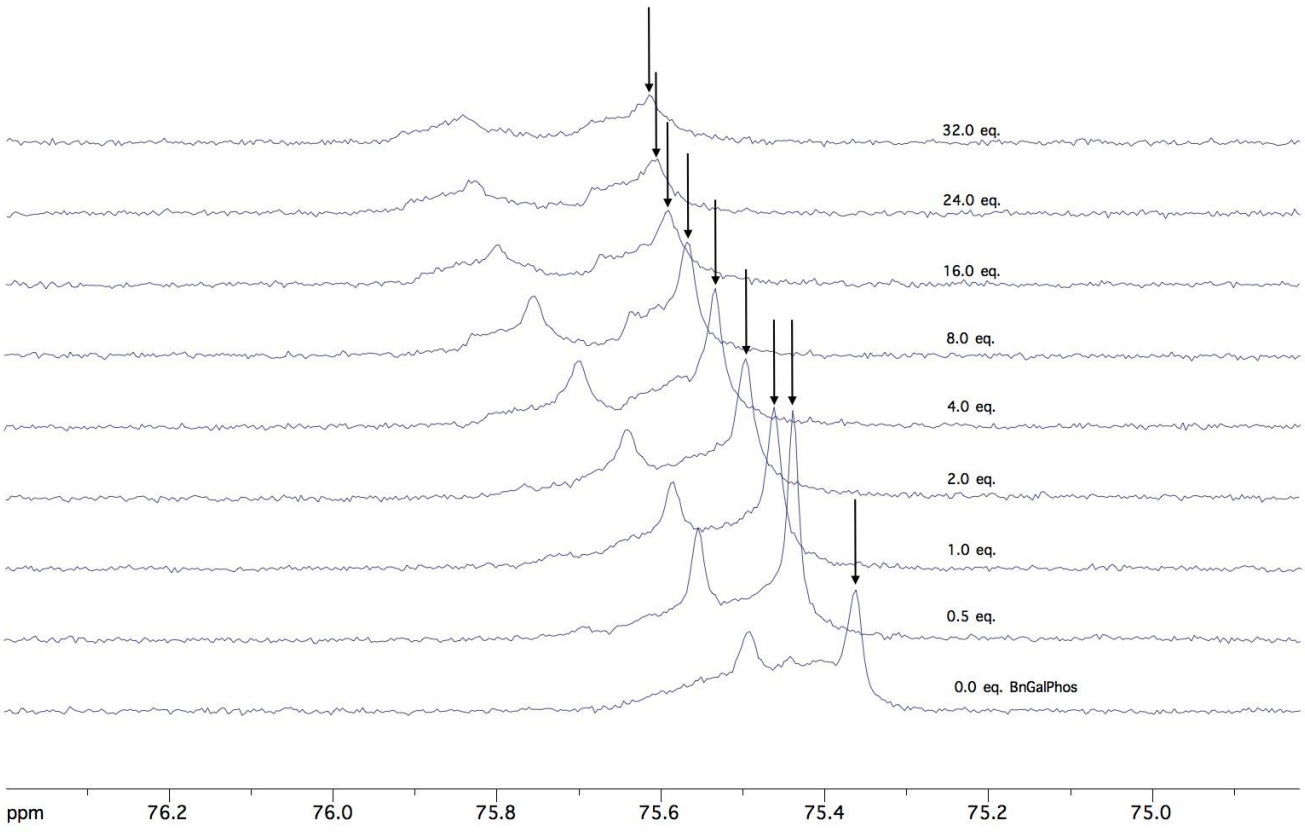

Figure S19. ^{19}F chemical shift data of catalyst **1** with titration of galactosyl phosphate (**2a**)**.** The (bis)-trifluoromethyl peak is shown with increasing equivalents of galactosyl phosphate, ranging from 0.0 eq. to 32.0 eq.

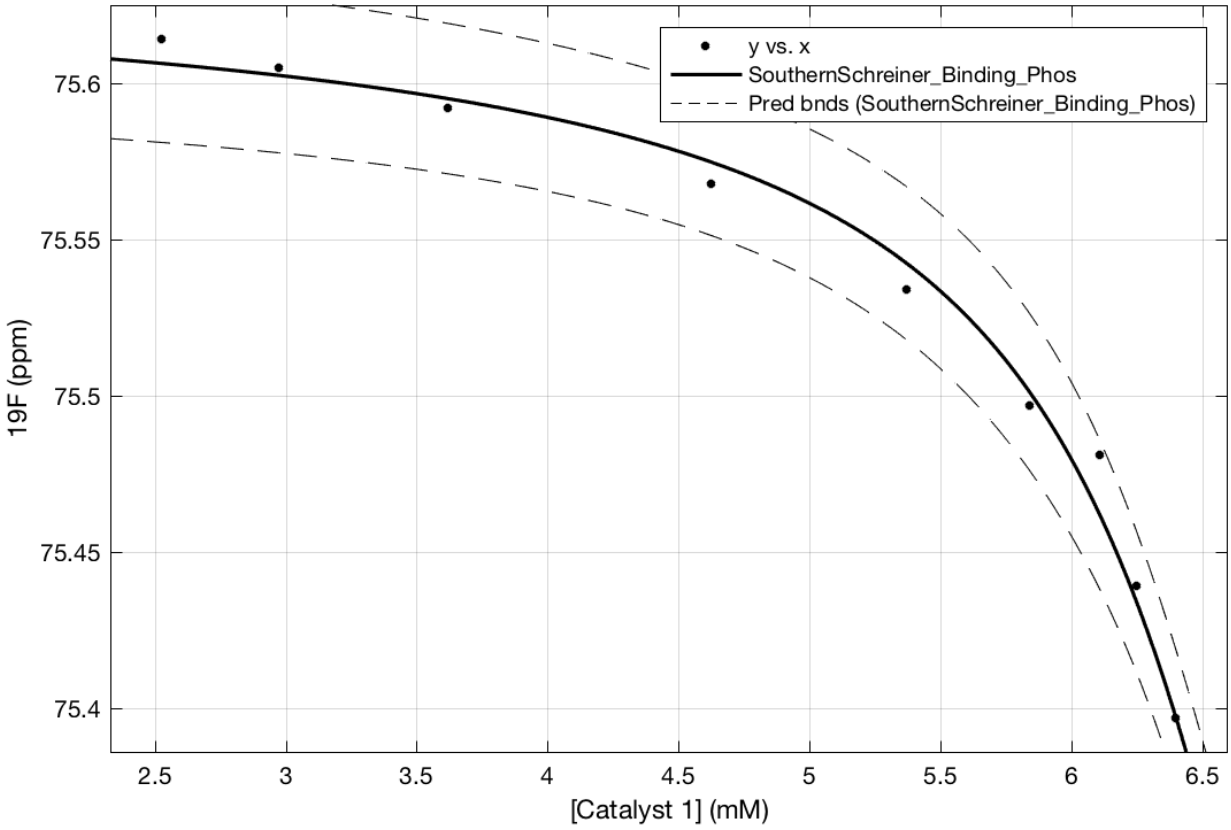

Figure S20. ^{19}F chemical shift data of catalyst **1** plotted against the concentration of galactosyl phosphate (**2a**)

General model:

f(x) = 75.3970*(x-((1/2)*(x+(-20.833*x+133.33)+1/a-((x+(-20.833*x+133.33)
+(1/a))^2-4*(-20.833*x+133.33)*x)^(1/2))))/x+b*((1/2)
*(x+(-20.833*x+133.33)+1/a-((x+(-20.833*x+133.33)+(1/a)
)^2-4*(-20.833*x+133.33)*x)^(1/2)))/x

Coefficients (with 95% confidence bounds):

K_a = 0.08323 mM^{-1} (0.04851, 0.1179)

$\delta_{\mathbf{1}\cdot\mathbf{3}a}$ = 75.64 ppm (75.61, 75.66)

Goodness of fit:

SSE: 0.000588

R-square: 0.9876

Adjusted R-square: 0.9858

RMSE: 0.009165

These data were then used to calculate the percentage of catalyst bound to **2a** under relevant reaction conditions (0.1 M).

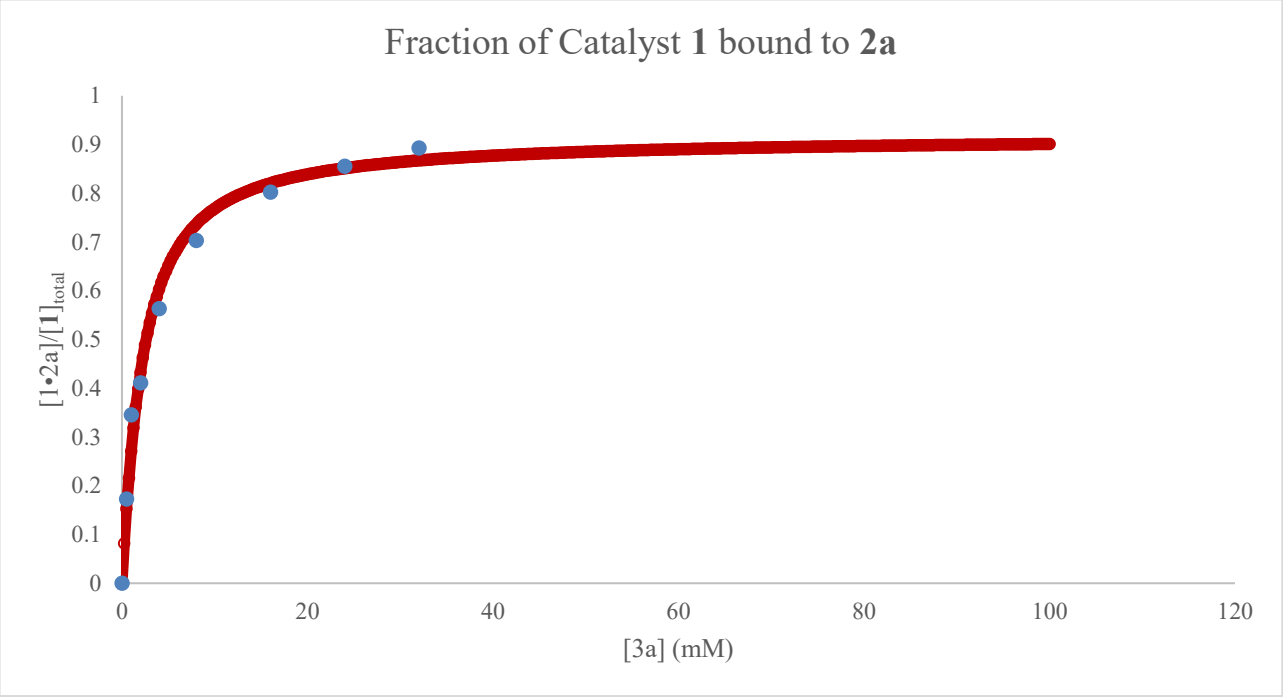

Figure S21. Calculated fraction catalyst **1** bound to galactosyl phosphate (**2a**) as a function of [**2a**]

These data suggest that at 0.1 M in **2a** (standard reaction conditions), the catalyst is 84% bound as the 1•2a complex.

12.2 Galactosyl Chloride (2b) Binding with Catalyst 1

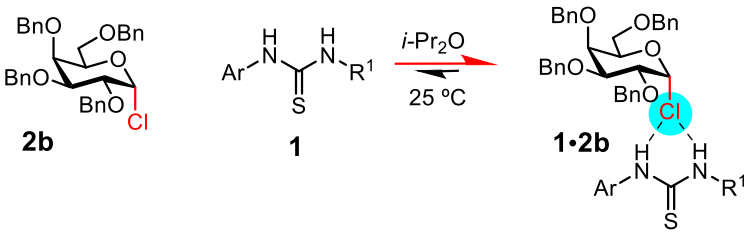

Scheme S15. Equilibrium binding of galactosyl chloride (**2b**) with catalyst **1**

The same procedure and analysis from galactosyl phosphate (**2a**) + catalyst **1** (above) was used for galactosyl chloride (**2b**).

Equiv. **2b**	^{19}F (ppm)	DBF (ppm)	[**1**] (mM)	[**2b**] (mM)	Δ ppm
0	75.291	0.000	6.40	0.00	0.000
0.5	75.302	0.000	6.25	3.13	0.011
1	75.311	0.000	6.11	6.11	0.020
2	75.317	0.000	5.84	11.68	0.026
4	75.345	0.000	5.37	21.48	0.054
8	75.361	0.000	4.62	36.99	0.070
16	75.383	0.000	3.62	57.92	0.092
16	75.416	0.000	3.62	57.92	0.125
24	75.413	0.000	2.97	71.38	0.122
24	75.428	0.000	2.97	71.38	0.137
32	75.448	0.000	2.52	80.76	0.157
48	75.437	0.000	1.94	92.98	0.146
64	75.466	0.000	1.57	100.59	0.175

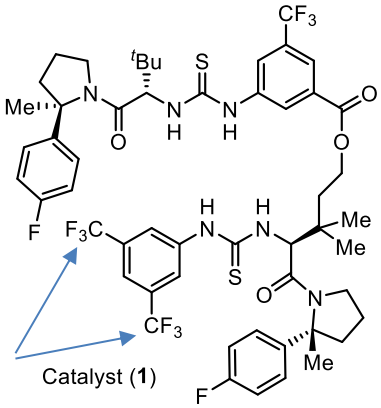

Table S21. ^{19}F chemical shift data of catalyst **1** with titration of **2b**

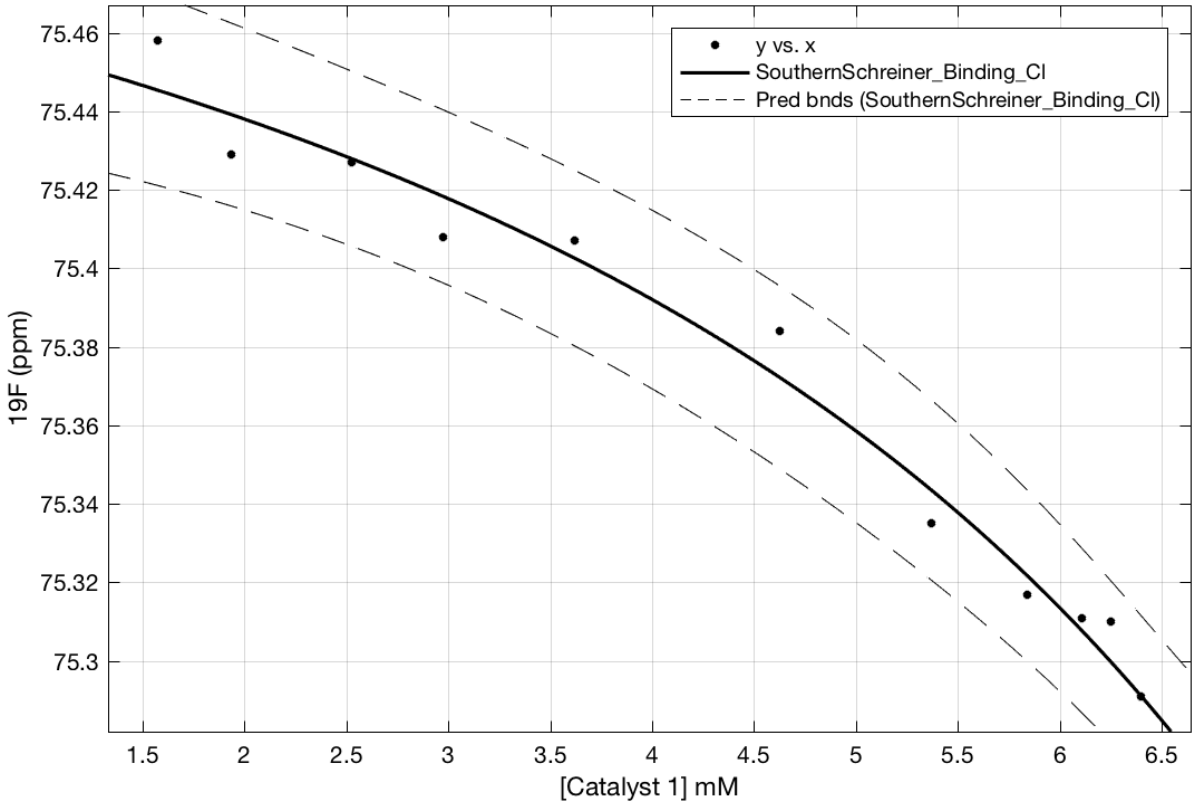

Figure S22. ^{19}F chemical shift data of catalyst **1** plotted against the concentration of galactosyl chloride (**2b**)

General model:

f(x) = 75.291*(x-((1/2)*(x+(-20.833*x+133.33)+1/a-((x+(-20.833*x+133.33)
+(1/a))^2-4*(-20.833*x+133.33)*x)^(1/2))))/x+b*((1/2)
*(x+(-20.833*x+133.33)+1/a-((x+(-20.833*x+133.33)+(1/a)
)^2-4*(-20.833*x+133.33)*x)^(1/2)))/x

Coefficients (with 95% confidence bounds):

K_a = 0.004406 mM^{-1} (-0.001251, 0.01006)

$\delta_{\mathbf{1 \cdot 3}d}$ 75.84 ppm (75.31, 76.37)

Goodness of fit:

SSE: 0.001208

R-square: 0.9727

Adjusted R-square: 0.9702

RMSE: 0.01048

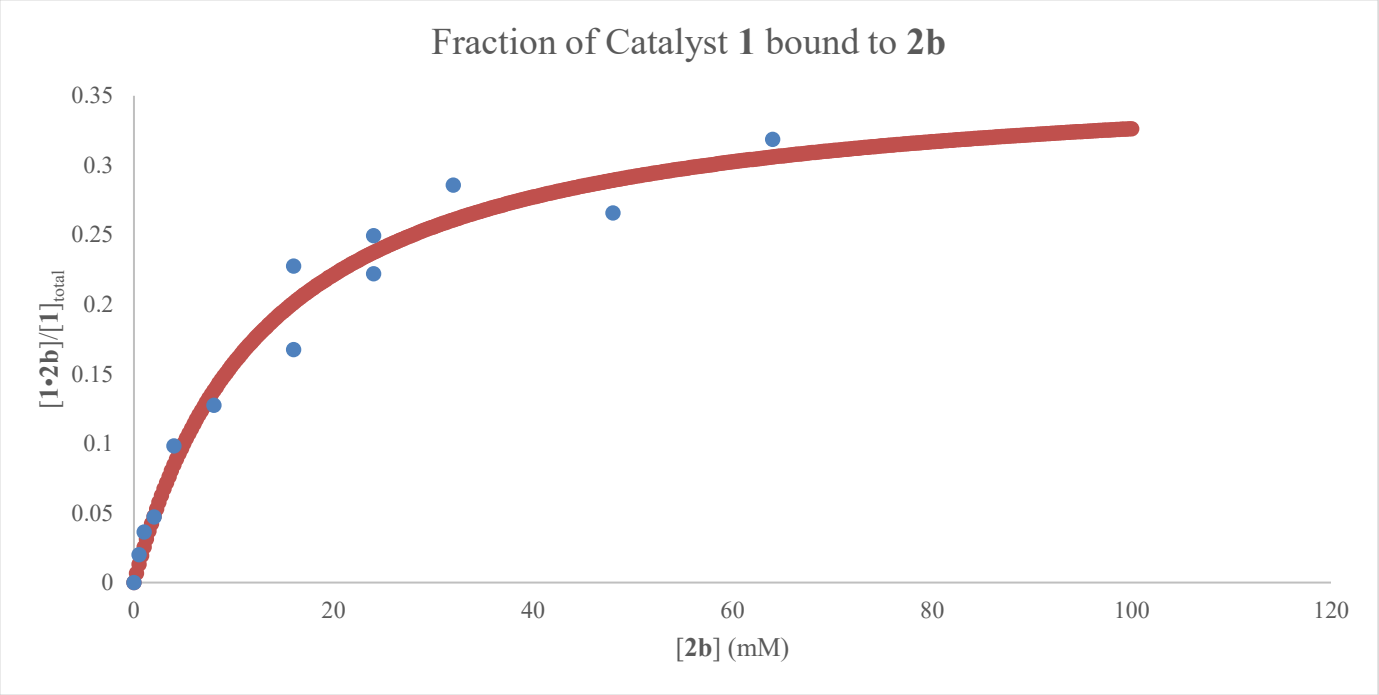

Figure S23. Calculated fraction catalyst **1** bound to galactosyl chloride (**2b**) as a function of [**2b**]

10.3 *L*-Serine (3a) Binding with Catalyst 1

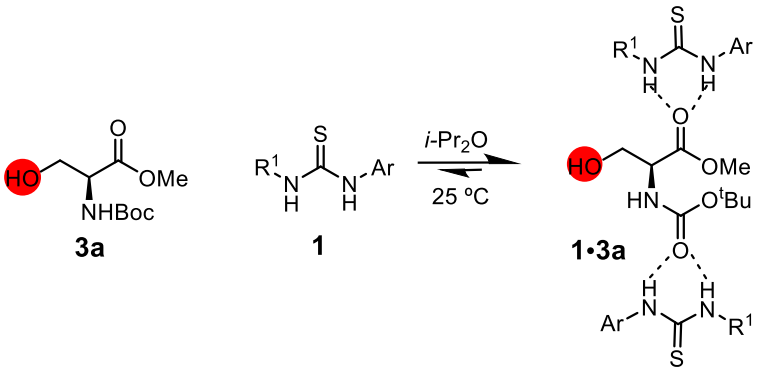

Scheme S16. Equilibrium binding of *L*-Serine (**3a**) with catalyst **1**. Shown are potential binding modes

The same procedure and analysis from galactosyl phosphate (**3a**) + catalyst **1** (above) was used for (*L*)-Serine. Instead of a trifluoromethyl group, a *p*-F phenyl peak was used to track chemical shift. The trifluoromethyl groups did not shift sufficiently over the course of the titration for a reliable binding constant to be extracted.

Equiv. **3a**	^{19}F (ppm)	DFB (ppm)	[**1**] (mM)	[**3a**] (mM)	Δ ppm
4	20.669	0.000	6.40	0.00	0.000
8	20.699	0.000	5.37	21.48	0.031
16	20.730	0.000	4.62	36.99	0.061
16	20.778	0.000	3.62	57.92	0.109
24	20.780	0.000	2.97	71.38	0.111
24	20.790	0.000	2.52	80.76	0.121
32	20.809	0.000	1.94	92.98	0.140
48	20.810	0.000	1.57	100.59	0.141
64	20.820	0.000	1.14	109.56	0.151

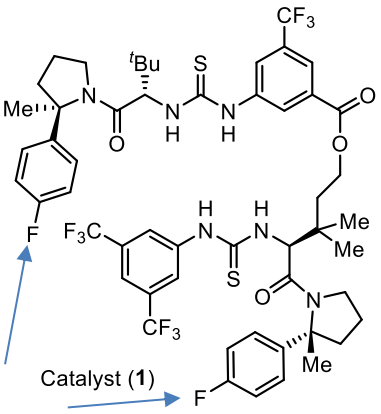

Table S22. ^{19}F chemical shift data of catalyst **1** with titration of **3a**

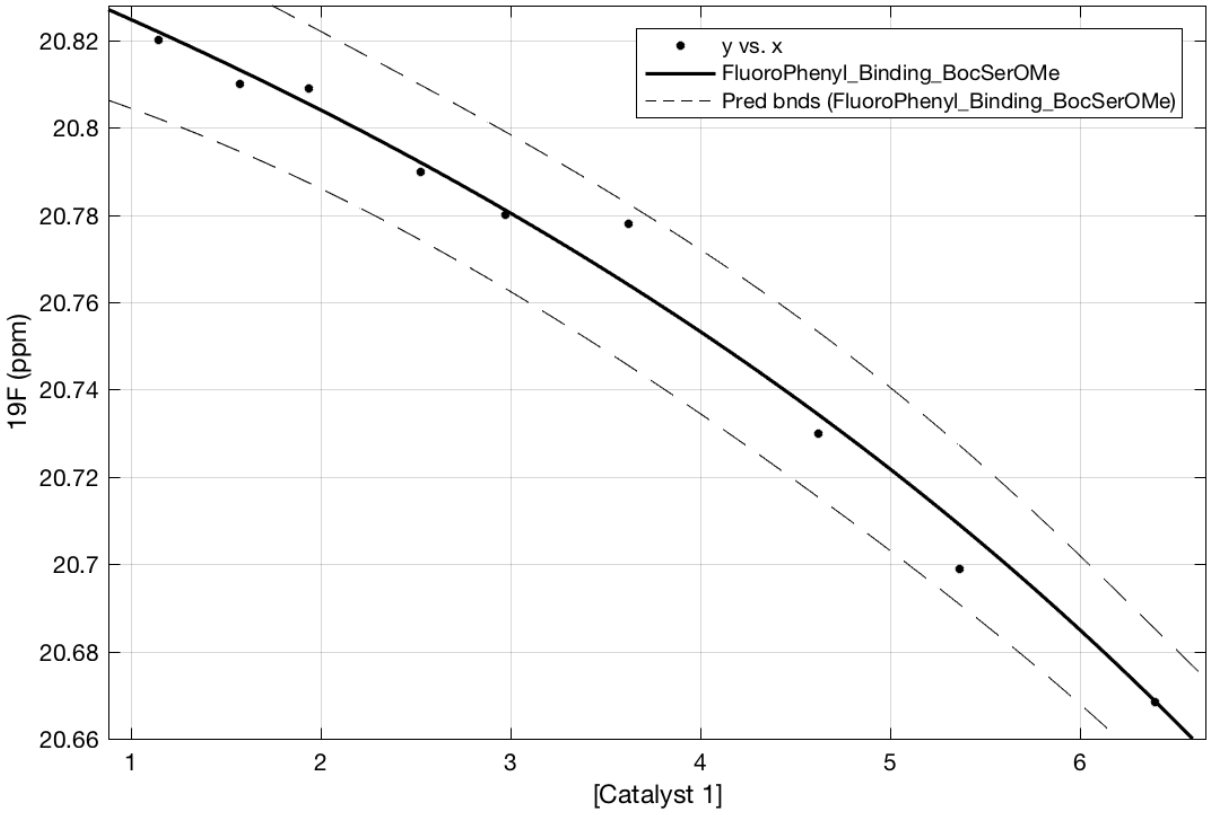

Figure S24. ^{19}F chemical shift data of catalyst **1** plotted against the concentration of *L*-Serine (**3a**)

General model:

f(x) = 20.6685*(x-((1/2)*(x+(-20.833*x+133.33)+1/a-((x+(-20.833*x+133.33)
+(1/a))^2-4*(-20.833*x+133.33)*x)^(1/2))))/x+b*((1/2)
*(x+(-20.833*x+133.33)+1/a-((x+(-20.833*x+133.33)+(1/a)
)^2-4*(-20.833*x+133.33)*x)^(1/2)))/x

Coefficients (with 95% confidence bounds):

K_a = 0.004587 (-3.242e-05, 0.009207)

$\delta_{Cat \bullet Serine}$ = 21.13 (20.8, 21.46)

Goodness of fit:

SSE: 0.0003432

R-square: 0.985

Adjusted R-square: 0.9829

RMSE: 0.007002

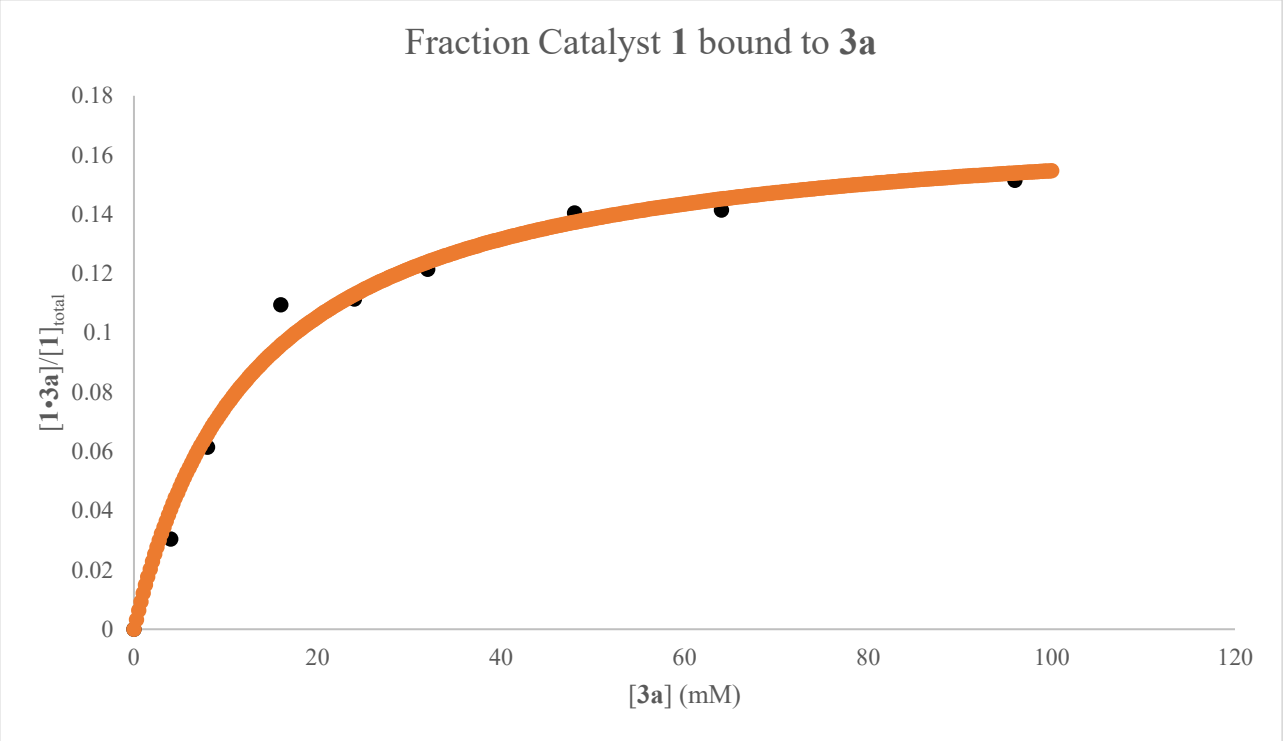

Figure S25. Calculated fraction catalyst **1** bound to *L*-Serine (**3a**) as a function of [**3a**]

12.3 Leaving Group Binding Study

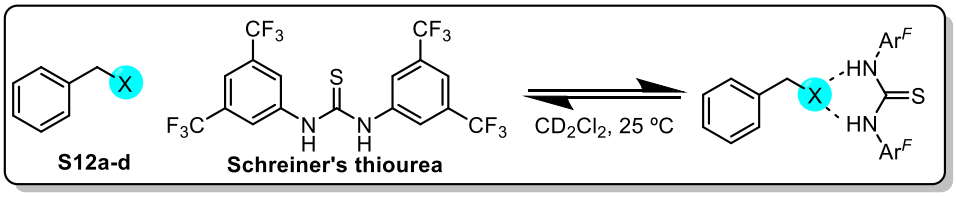

Figure S26. Titration of Various Bn-X derivatives with Schreiner's Thiourea as Quantified by ^{1}H NMR

Bn–	**–OPO(OPh)$_2$**	**–OAc**	**–Cl**	**–ONO$_2$**
equiv	**Dexp (ppm)**	**Dexp (ppm)**	**Dexp (ppm)**	**Dexp (ppm)**
0	0.000	0.000	0.000	0.000
0.1	0.117	0.006	0.003	0.001
0.25	0.247	0.014	0.004	0.001
0.5	0.488	0.025	0.000	0.001
1	0.816	0.051	-0.001	0.002
2.5	1.251	0.120	0.005	0.021
5	1.410	0.217	0.004	0.011
10	1.510	0.359	0.013	0.019
25	1.637	0.620	0.026	0.046
50	1.698	0.987		0.086
100		1.091	0.044	

Table S23. Chemical shift data (^{1}H NMR) for titration of **S12a-d** to 1 equiv. **Schreiner's thiourea**

A modified form of equation 10 was used for the binding study of Schreiner's thiourea with 2a-d and is shown below (11). In every case, Schreiner's thiourea is at 0.01 M.

$$\Delta\delta_{obs} = \delta_{\mathbf{1\bullet 3}\boldsymbol{a}}\left(\frac{\left(\frac{1}{2}\left(0.01 + [\boldsymbol{S12}]_O + \frac{1}{K_a}\right) - \sqrt{\left(0.01 + [\boldsymbol{S12}]_O + \frac{1}{K_a}\right)^2 + 4(0.01)[\boldsymbol{S12}]_O}\right)}{0.01}\right) \quad (11)$$

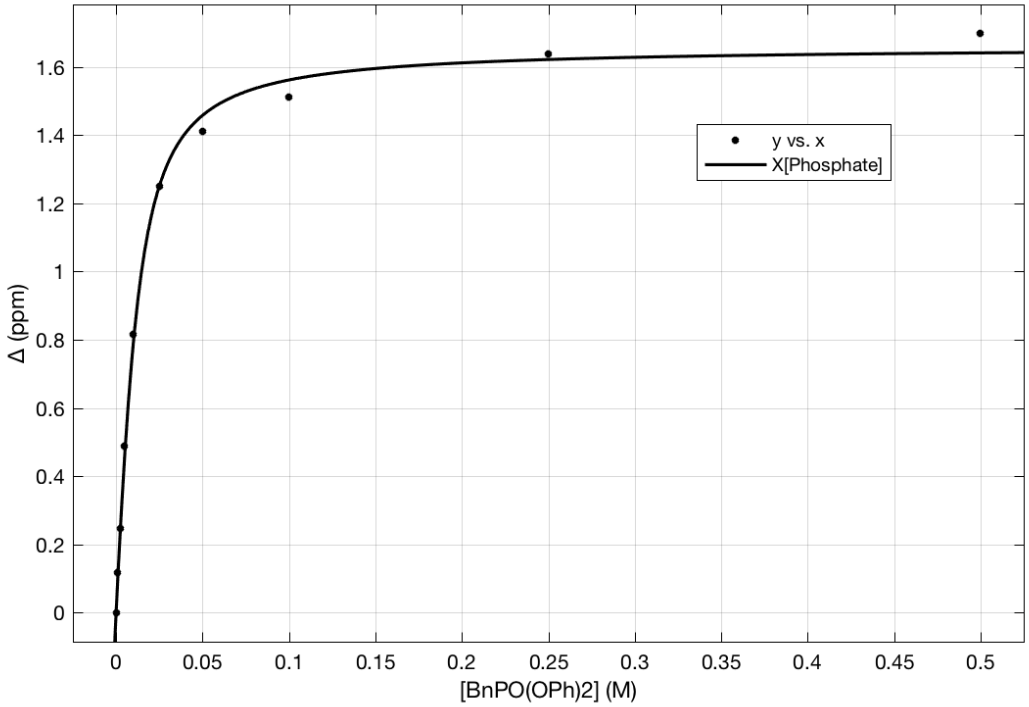

Figure S27. Titration of benzyl diphenyl phosphate (**S12a**) to **Schreiner's thiourea**

General model:

f(x) = d*(((0.01+x+(1/Ka))-((0.01+x+(1/Ka))^2-(4*0.01*x))^(1/2))/(2*0.01))

Coefficients (with 95% confidence bounds):

Ka = 174.9 M^{-1} (135.3, 214.6)

d = 1.66 ppm (1.608, 1.712)

Goodness of fit:

SSE: 0.009806

R-square: 0.9975

Adjusted R-square: 0.9972

RMSE: 0.03501

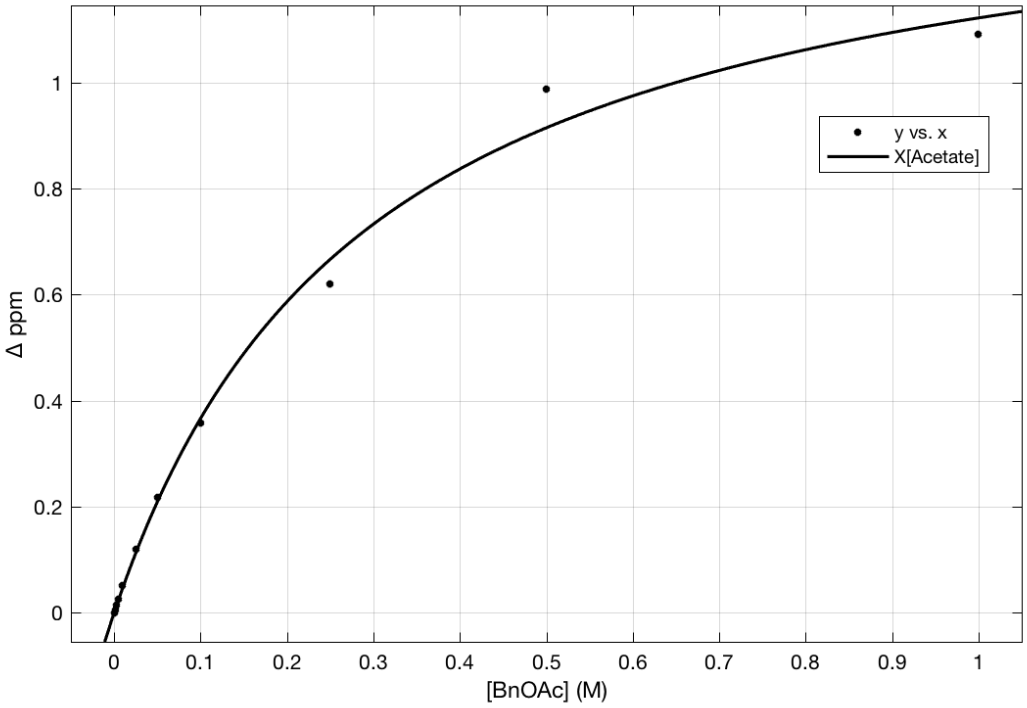

Figure S28. Titration of benzyl acetate (**S12b**) to **Schreiner's thiourea**

General model:

f(x) = b*((1/2)*(x+(0.01)+1/Ka-((x+(0.01)+(1/Ka))^2-4*(0.01)*x)^(1/2)))/0.01

Coefficients (with 95% confidence bounds):

Ka = 3.485 (2.564, 4.405)

b = 1.447 (1.297, 1.596)

Goodness of fit:

SSE: 0.008561

R-square: 0.9948

Adjusted R-square: 0.9942

RMSE: 0.03084

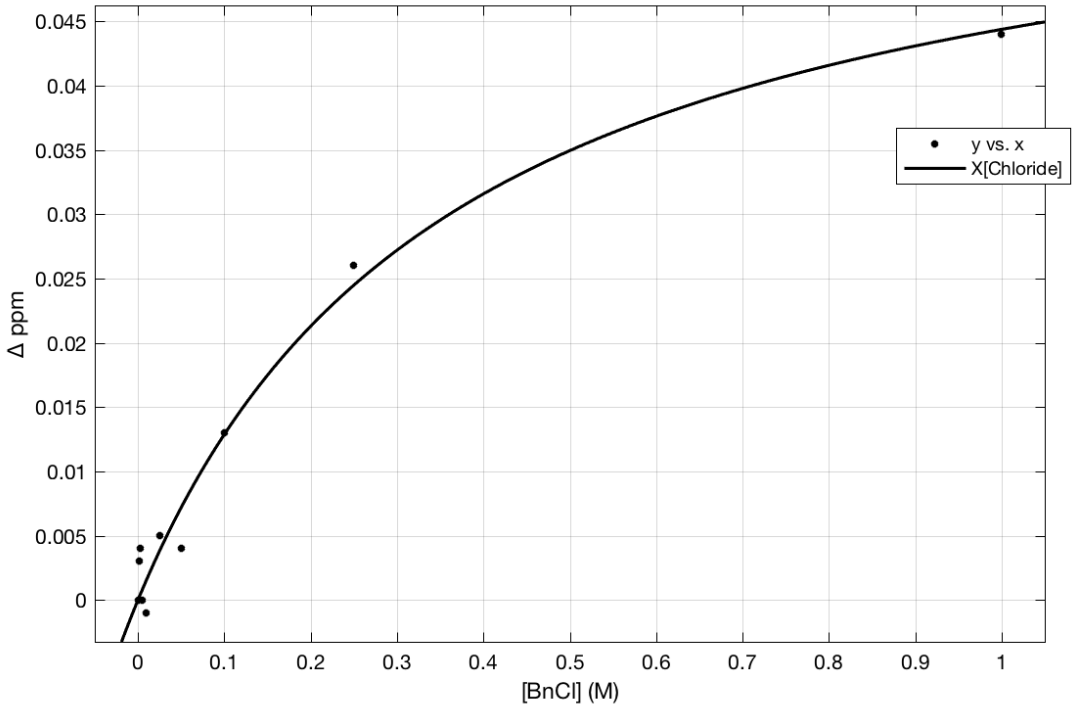

Figure S29. Titration of benzyl chloride (**S12d**) to **Schreiner's thiourea**

General model:

f(x) = d*(((0.01+x+(1/Ka))-((0.01+x+(1/Ka))^2-(4*0.01*x))^(1/2))/(2*0.01))

Coefficients (with 95% confidence bounds):

Ka = 2.759 M^{-1} (1.255, 4.262)

d = 0.06059 ppm (0.04662, 0.07457)

Goodness of fit:

SSE: 4.233e-05

R-square: 0.9776

Adjusted R-square: 0.9748

RMSE: 0.0023

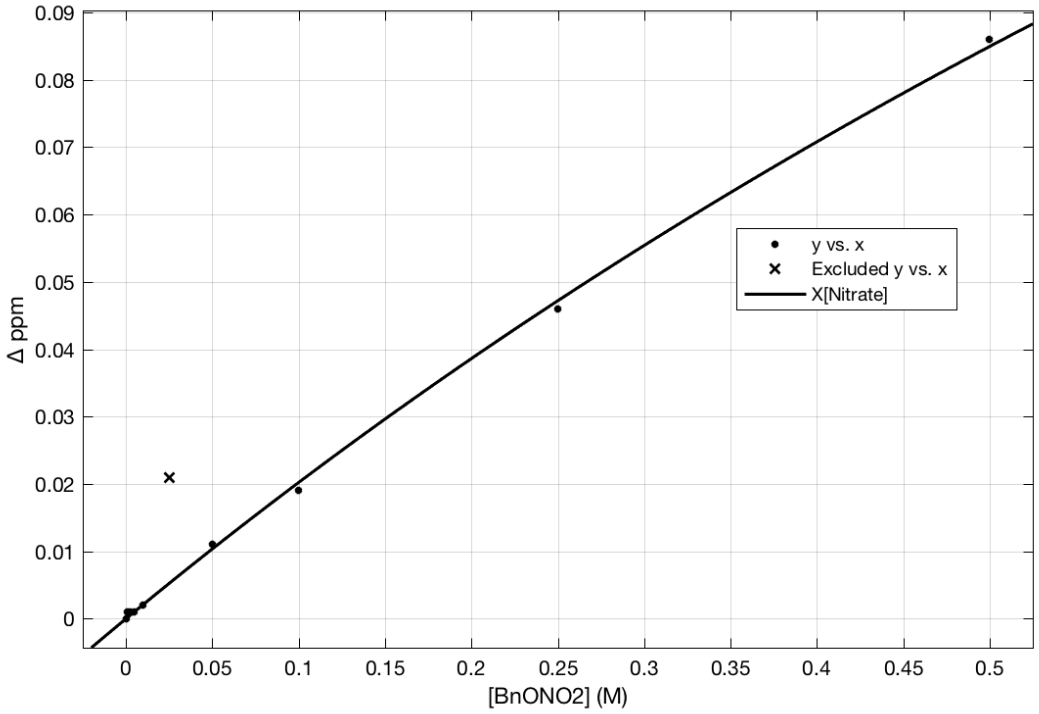

Figure S30. Titration of benzyl nitrate (**S12c**) to **Schreiner's thiourea**

General model:

f(x) = b*((1/2)*(x+(0.01)+1/Ka-((x+(0.01)+(1/Ka))^2-4*(0.01)*x)^(1/2)))/0.01

Coefficients (with 95% confidence bounds):

Ka = 0.5054 M^{-1} (0.2854, 0.7254)

b = 0.4225 ppm (0.2706, 0.5743)

Goodness of fit:

SSE: 5.333e-06

R-square: 0.9992

Adjusted R-square: 0.9991

RMSE: 0.0008729

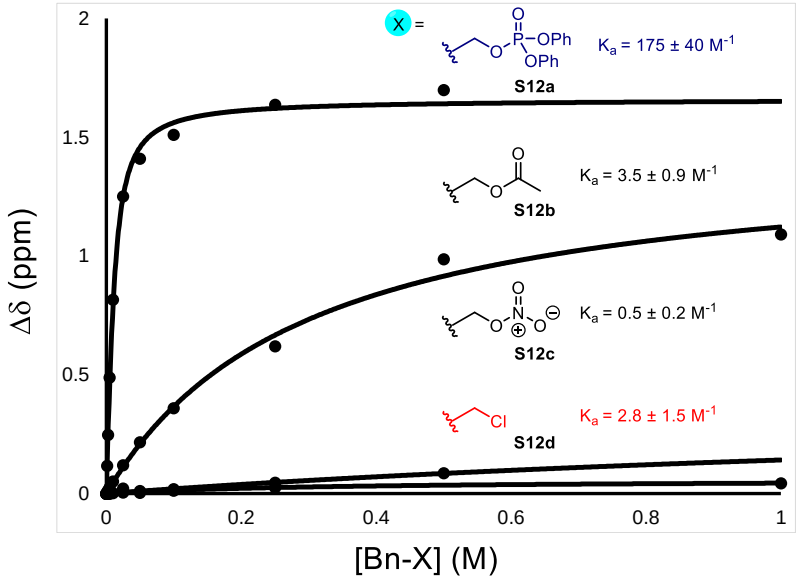

Figure S31. Titration of various Bn-X derivatives with Schreiner's Thiourea as quantified by ^{1}H NMR

Note: These values were collected, analyzed, and reported by Andreas Rötheli and is reported in his thesis.[23]

(1) Pangborn AB, Giardello MA, Grubbs RH, Rosen RK, Timmers FJ (1996) Safe and convenient procedure for solvent purification. *Organometallics* 15:1518–1520.

(2) Kennedy CR, Lehnherr D, Rajapaksa NS, Ford DD, Park Y, Jacobsen EN (2016) Mechanism-guided development of a highly active bis-thiourea catalyst for anion-abstraction catalysis. *J Am Chem Soc* 138:13525–13528.

(3) Sabesan S, Neira S (1992) Synthesis of glycosyl phosphates and azides. *Carbohydr Res* 223:169–185.

(4) Park Y, Harper KC, Kuhl N, Kwan EE, Liu RY, Jacobsen EN (2017) Macrocyclic bis-thioureas catalyze sterespecific glycosylation reactions. *Science* 355:162–166.

(5) Marra A, Shun LKS, Gauffeny F, Sinaÿ P (1990) Anomeric *S*-xanthates of 2-azido-2-deoxy-D-galactopyranosyl derivatives as efficient glycosyl donors. *Synlett* 445–448.

(6) Tsuda T, Nakamura S, Hashimoto S (2004) A highly stereoselective construction of 1,2-*trans*-β-glycosidic linkages capitalizing on 2-azido-2-deoxy-D-glycosyl diphenyl phosphates as glycosyl donors. *Tetrahedron* 60:10711–10737.

(7) Ding W, Zhang J, Yao Z, Lu R, Wu D, Li G, Shen Z, Sun Y, Lin G, Wang C, Zhao M, Peng S (2004) The synthesis, distribution, and anti-hepatic cancer activity of YSL. *Bioorg Med Chem* 12:4989–4994.

(8) Li ZF, Guo ZF, Yan H, Lu ZL, Wu DY (2012) The development and SAR of pyrrolidine carboxamide 11β-HSD1 inhibitors. *Bioorg Med Chem* 20:2897–2902.

(9) Pelletier G, Zwicker A, Allen CL, Schepartz A, Miller SJ (2016) Aqueous glycosylation of unprotected sucrose employing glycosyl fluorides in the presence of calcium ion and triethylamine. *J Am Chem Soc* 138:3175–3182.

(10) Wu J, Liu P, Wang L, Tian H, Wang Q, Zhang S (2011) Synthesis and application of clindamycin succinate as a novel chiral selector for capillary electrophoresis. *J Sep Sci* 34:2455–2462.

(11) He H, Zhu X (2014) Thioperoxide-mediated activation of thioglycoside donors. *Org Lett* 16:3102–3105.

(12) Chu AHA, Minciunescu A, Bennett CS (2015) Aryl(trifluoroethyl)iodonium triflimide and nitrile solvent systems: a combination for the stereoselective synthesis of armed 1,2-*trans*-b-glycosides at noncryogenic temperatures. *Org Lett* 17:6262-6265.

(13) Sakamoto I, Ohrui H (2014) Practical synthesis of the disaccharide epitope, D-galactopyarnosyl-α-1,3-D-galactopyranose, by using 1,2;5,6-di-*O*-cyclohexylidine-α-D-galactofuranose as the glycosyl acceptor. *Bioscience, Biotechnology, and Biochemistry* 64:1974-1977.

(14) Kitowski A, Jimeńez-Moreno E, Salvado M, Mestre J, Castilloń S, Jimeńez-Oseś G, Boutureira O, Bernardes GJL (2017) Oxidative activation of C-S bonds with an electropositive nitrogen promotor enables orthogonal glycosylation of alkyl over phenyl thioglycosides. *Org Lett* 19:5490-5493.
(15) Jiang R, Zong G, Liang X, Jin S, Zhang J, Wang D (2014) Direct 2,3-*O*-isopropylidenation of a-D-mannopyranosides and the preparation of 3,6-branched mannose trisaccharides. *Molecules* 19:6683-6693.
(16) Nguyen HM, Poole JL, Gin DY, *Angew Chem Int Ed* 40:414-417.
(17) Jones S, Selitsianos D, Thompson KJ, Toms SM (2003) An improved method for Lewis acid catalyzed phosphoryl transfer with Ti(*t*-BuO_4). *J Org Chem* 68:5211-5216.
(18) Aellig C, Girard C, Hermans I (2011) Aerobic alcohol oxidations mediated by nitric acid. *Angew Chem Int Ed* 50:12355-12360.
(19) Matlab, Version R2017a (9.2.0556344) maci64, MathWorks, Inc. 2017 (http://www.mathworks.com/).
(20) The PyMOL Molecular Graphics System, PyMOL Version 1.5.0.5 Enhanced for MacOS X, Schrödinger, LLC (http://www.pymol.org).
(21) CYLview, Version 1.0b, C. Y. Legault, Université de Sherbrooke, Sherbrooke QC, 2009 (http://www.cylview.org/).
(22) The PyMOL Molecular Graphics System, PyMOL Version 1.5.0.5 Enhanced for MacOS X, Schrödinger, LLC (http://www.pymol.org).
(23) Rötheli AR (2016) A Mechanistic Approach towards Highly Efficient Anion-Binding Catalysts. Harvard University, Cambridge, MA.
(24) Gottlieb HE, Kotlyar V, Nudelman A (1997) NMR Chemical Shifts of Common Laboratory Solvents as Trace Impurities. *J Org Chem* 62:7512-7515.
(25) Crich D, Smith M (2002) Solid-Phase Synthesis of β-Mannosides. *J Am Chem Soc* 124:8867-8869.
(26) Block K, Pederson C (1974) A Study of ^{13}CH Coupling Constants in Hexopyranoses. *J Chem Soc, Perkin Trans 2* 41:3877-3882.